University of Dundee

MASTER OF SCIENCE

Novel light activated platinum drugs for cancer therapy

Robinson, Kim

Award date:
2012

MASTER OF SCIENCE

Novel light activated platinum drugs for cancer therapy

Kim Robinson

2012

University of Dundee

UNIVERSITY OF DUNDEE

Identification of Novel Molecular Targets for Cutaneous Squamous Cell Carcinoma

Kim Samirah Robinson

A thesis submitted for the degree of Doctorate of Philosophy

Contents

List of Figures

List of Tables

Abbreviations in Text

ADAM	A Disintegrin and Metalloproteinase
AK	Actinic Keratosis
ANK	Ankrin Repeats
AP	Alkaline Phosphatase
BCC	Basal Cell Carcinoma
BDKRB1	Bradykinin Receptor B1
BRDU	5-bromo-2'deoxyuridine
BSA	Bovine Serum Albumin
CD	Cystine rich Domain
cDNA	Complementary Deoxyribonucleic Acid
CDK4	Cyclin Dependant Kinase 4
CDKN	Cyclin Dependant Kinase Inhibitors
CDKN2A	Cyclin Dependant Kinase Inhibitor 2A
CI	Confidence Interval
CPC	Chromosomal Passenger Complex
CPD	Cyclobutane Pyrimidine Dimers
cSCC	Cutaneous Squamous Cell Carcinoma
Ct	Cycling Times
DAPI	4'6-diamidino-2-phenylindole
DDEB	Dominant Dystrophic Epidermolysis Bullosa
DEB	Dominant Epidermolysis Bullosa
dH_2O	Deionised water
DMSO	Dimethyl Sulfoxide
DMBA	7,12-dimethylbenz[a]anthracene
DNA	Deoxyribonucleic Acid
dNTP	Deoxynucleotide Triphosphates
DSL	Delta-Serrate-Lag2
DTT	Dithiothreitol

EB	Epidermolysis Bullosa
EBS	Epidermolysis Bullosa Simplex
ECM	Extracellular Matrix
E.coli	Escherichia Coli
ERK1	Extracellular Signal Regulated Kinases 1
ERK2	Extracellular Signal Regulated Kinases 2
EV	Epidermodysplasia Verruciformis
FBS	Foetal Bovine Serum
FUCA2	Fucosidase alpha-L-1-plasma
GSG2	Germ Cell Associated 2
GSI	Gamma Secretase Inhibitor
H & E	Haematoxylin and Eosin
HPV	Human Papilloma Virus
HCL	Hydrochloric Acid
HER2	Human Epidermal Growth Factor 2
H-ras	Harvey Ras
hTERT	Human Telomerase Reverse Transcriptase
IC	Immunocompetant
ICN1	Intracellular Notch
IRF6	Interferon Regulatory Factor 6
IκB	Inhibitor of Kappa B
IκB Kinase	Inhibitor of Kappa B Kinase
JEB	Junctional Eepidermolysis Bullosaa
K-ras	Kirsten Sarcoma Ras
LB	Lysogeny Broth
LDH	Lactate Dehydrogenase Assay
LOF	Loss Of Function
L2000	Lipofectamine 2000
MAML	Mastermind-Like

MAPK	Mitogen-Activated Protein Kinase
MDM2	Mouse Double Minute 2 Homology
MM	Malignant Melanoma
MMP	Matrix Metaloproteinases
MTS	3-(4,5-dimethylthiazol-2-yl)-5-(3-carboxymethoxyphenyl)-2-(4-Sulfophenyl)-2M-tetrazolium
NaCl	Sodium Chloride
NaOH	Sodium Hydroxide
N^{EC}	Notch Extracellular
NFκB	Nuclear Factor Kappa B
NHF	Normal Human Fibroblast
NHK	Normal Human Keratinocyte
NHS	Normal Human Skin
NMSC	Non-Melanoma Skin Cancer
N^{TM}	Notch Transmembrane
PARP1	Poly[ADP-ribose]polymerase 1
PBS	Phosphate Buffer Saline
PFA	Paraformaldehyde
PLA	Proximity Ligation Assay
Peni/strep	Penicillin/ Streptomycin
PLK1	Polo Like Kinase 1
PRSS21	Protease Serine 21
PSMG	Proteasome Assembly Chaperone 3
pRb	Retinoblastoma Protein
qPCR	Quantitative Polymerase Chain Reaction
RAM	Recombination Signal Binding Protein-1 Association Molecule Domain
RBP-J	Recombination Signal Binding Protein-1
RCA	Rolling Circle Amplification
RCL	Reactive Centre Loop
RDEB	Recessive Dystrophic Epidermolysis Bullosa
RPM	Revolutions Per Minute
RNA	Ribonucleic Acid

RNAi	Interfering Ribonucleic Acid
RT-PCR	Reverse-Transcriptase Polymerase Chain Reaction
SCID	Severe Immunocompromised Deficiency
SCR	Scrambled
SEM	Standard Error of the Mean
SERPIN	Serine Protease Inhibitor
siRNA	Small interfering Ribonuclease Acid
SOC	Super Optimal Broth
T	Transplant
TA	Transit Amplifying
TACE	Tumour Necrosis Factor-α-Converting Enzyme
T-ALL	T-Cell Acute Lymphoblastic Leukaemia/Lymphoma
TM	Transmembrane
TPA	12-O-Tetradecanoylphorbol-13-Acetate
TTBS	Tris Tween Buffer Solution
UK	United Kingdom
uPa	Urokinase-Type Plasminogen Activator
USA	United States of America
UV	Ultraviolet Radiation
UVA	Ultraviolet Radiation A
UVB	Ultraviolet Radiation B
XP	Xeroderma Pigmentosum
7-AAD	7-Amino-Actinomycin D
6-4PP	6-4 Photoproducts

Acknowledgements

I would like to begin by thanking my supervisor, Andy South, not only for his time, encouragement and patience but for being a fantastic supervisor throughout the duration of my PhD. Many thanks are also due to everyone in his lab and Charlotte Proby's lab, for sharing their knowledge and expertise in the subject. It has been a pleasure to work with such intelligent and entertaining individuals. In particular I would like to thank Stephen Watt for being a friend, mentor and superb scientist, and whom without I would have struggled to complete my PhD. Additionally, much appreciation for the support from my friends and family is given, in particular to Ryan for his continual support and for holding my hand throughout.

Declaration

I, Kim Samirah Robinson, hereby confirm that I am the sole author of this thesis; that unless otherwise stated in the text, all referenced cited therein have been personally consulted by me; that the work of which this thesis is a record has been done by me and that it has not been previously accepted for a higher degree.

Kim Samirah Robinson

Certification

I certify that Miss Kim Samirah Robinson has spent the equivalent of three terms in full time research under my supervision and that she has fulfilled the conditions of the Ordinance 32, so that she qualified to submit this thesis for the degree of Doctor of Philosophy.

Andrew Perry South

Abstract

Cutaneous Squamous Cell Carcinoma (cSCC) is the most common human tumour with malignant potential which is responsible for over 1 in 4 skin cancer deaths in the UK. High risk groups exist such as, immunosuppressed patients and those with the genetic condition recessive dystrophic epidermolysis bullosa whom are burdened with increased cSCC incidence, metastasis and mortality. Current clinically available molecular targets for cSCC are limited. Moreover, the key molecular events in cSCC remain poorly defined, presumably including both loss/gain of DNA or through gene silencing by DNA modifications. Understanding the molecular events which lead to cSCC is paramount for developing successful, novel molecular targets for therapeutic purpose. Preceding this thesis, our group used two independent methods to identify potential molecular targets: microarray technology (Watt 2011) and Sanger sequencing (Wang 2011), of which some of the targets identified from these studies, formulate the basis of this thesis.

Using microarray technology, a comparison between gene expression profiles of cultured cSCC and normal keratinocytes, identified a gene signature specific for cSCC. From this signature, five genes were identified as being over-expressed in cSCC compared to normal and whose gene expression was important for cell survival. Subsequently, three of these genes were further explored within this thesis: germ cell associated 2 (GSG2), bradykinin receptor B1 (BDKRB1) and protease serine 21 (PRSS21). To begin, genes were confirmed to be over-expressed at both mRNA and protein level. Following this conformation, several endpoints were monitored using standard assays of cell viability, proliferation and apoptosis, in cSCC keratinocytes using gene specific siRNA. Using this validation method, PRSS21 showed the most promise as a molecular target. Depletion of

PRSS21 resulted in decreased cell viability through an increase in cytotoxicity and apoptosis. Therefore PRSS21 was further validated as a molecular target through stable over-expression in an immortalised normal human cell line with no endogenous PRSS21 expression. Subsequently, using 3D organotypic cultures, it was shown that the expression of PRSS21 clearly transformed these cells into an invasive phenotype, compared to the control. Finally, PRSS21 was shown to interact with the tumour suppressor maspin, potentially negatively regulating maspin dependant apoptosis. This data strongly suggests that both PRSS21 and maspin are potential targets in cSCC.

The second method of identifying molecular targets was direct sequencing of tumour DNA, which identified loss of function *notch* mutations in ~75% of cSCC. It has been postulated that loss of notch function contributes to cSCC through a reduction in differentiation. Using three cSCC cell lines of known *notch* status (wild type/loss of function/notch null), cells were grown in organotypic culture, and the expression of markers associated with differentiation studied. With the aid of a gamma secretase inhibitor to inhibit notch signalling the contribution of notch to the expression of differentiation markers was studied in cSCC cells compared to normal human keratinocytes (NHK). There was a significant reduction in differentiation within the cSCC cell lines compared to NHK, regardless of notch status, and differentiation could be further reduced by the presence of GSI in the cSCC with wild type/loss of function notch expression. Furthermore, over-expression of a gamma secretase regulatable intracellular notch1 (ICN1) construct, showed an induction of involucrin in these cells, compared to cells overexpressing an empty vector control, confirming that notch1 contributes to differentiation.

Overall this work highlights the importance of validating targets before embarking on expensive, time consuming experiments. In doing so, it reveals two potential molecular

targets which could be important for the progression of cSCC, PRSS21 and maspin. Additionally it confirms the potential mechanism of notch loss of function in suppressing differentiation, suggesting that its re-activation would be is a valid approach to cSCC therapy.

Chapter 1: Introduction

1.1 NORMAL HUMAN SKIN

As the outermost layer of the body, the skin acts to protect us from everyday environmental insults. Formed from multiple cell types which undergo continuous self-renewal; where the cells have the ability to go through numerous cell divisions while maintaining the undifferentiated state. Thus, it is a complex system - involving a fine balance between proliferation and differentiation of cells, creating a protective barrier against the environment (Poumay and Coquette 2007). Normal skin structure comprises of two main compartments – the superficial epidermis and the deeper dermis (figure 1.1). Derived from different embryonic components, they retain fundamentally different morphology. Furthermore, they are simultaneously separated, yet connected by the basement membrane, which acts to tightly anchor the epidermis and the dermis together using anchoring fibrils and hemidesmosomes which strengthen the skin structure. The basement membrane also functions as an important epithelial and stromal interface, not only to selectively regulate compounds/molecules but to regulate migration and invasion of normal cells, such as melanocytes and Langerhans cells (Burgeson and Christiano 1997) but also to create a barrier against invasion of malignant cells. (Liotta, Lee et al. 1980). The skin also has other appendages such as hair, sweat and sebaceous glands of epithelial.

Figure 1.1

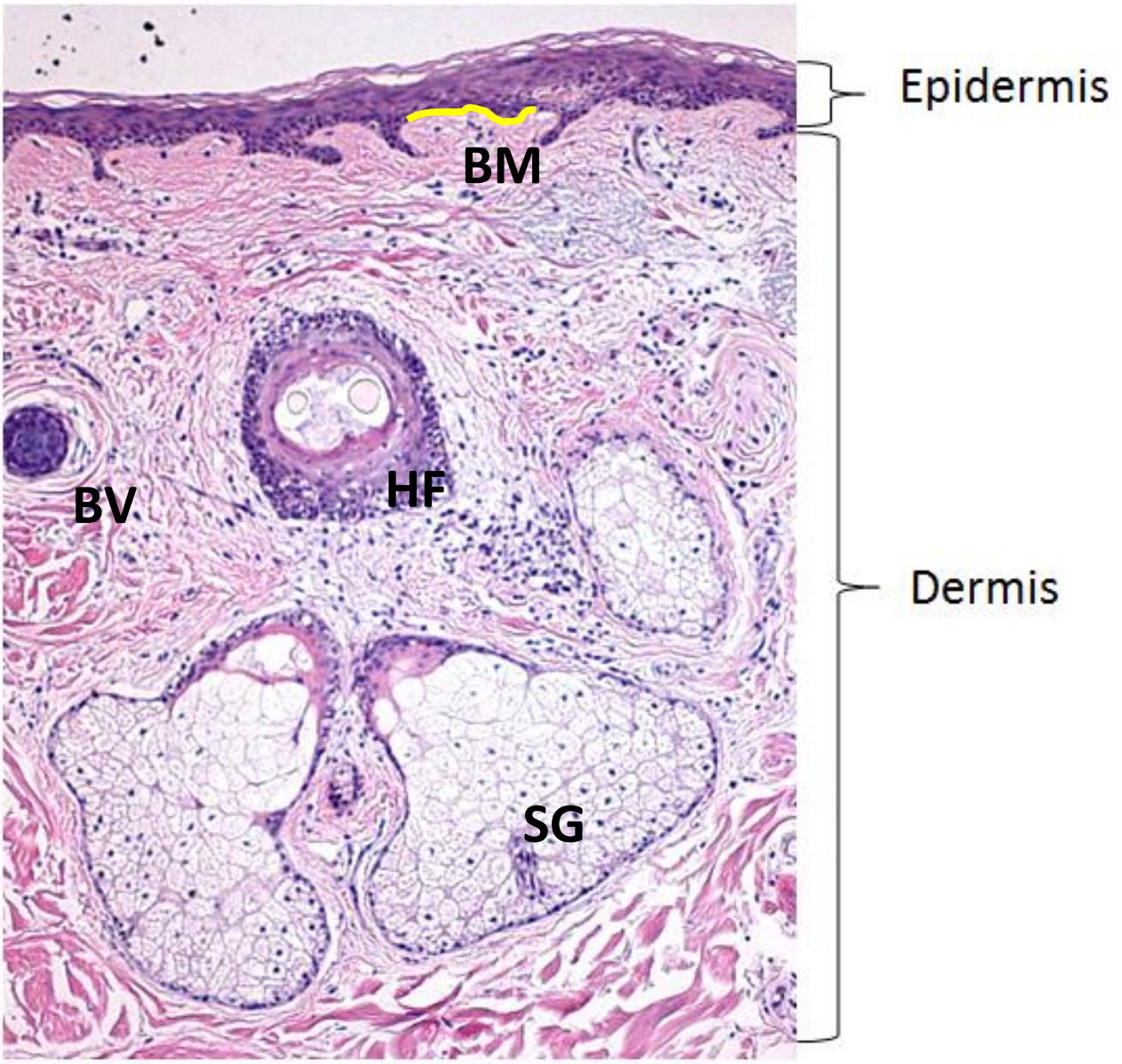

Figure 1.1 Hematoxylin and Eosin (H&E) Staining of the Human Skin

The "yellow line" represents the basement membrane (BM), sebaceous gland (SG), hair follicle (HF), blood vessel (BV) are also noted in this image. The section can also be divided into the epidermis and dermis, which are the two major compartments of the skin. Image taken at 40x magnification.

1.1.1 The Epidermis

The epidermis consists of stratified squamous epithelium and is a highly structural pattern of cell growth required for epidermal renewal, cellular cohesion and barrier formation (Gambardella and Barrandon 2003). Primarily, it is made up of epithelial cells called keratinocytes however; other non-epithelial cells are also embedded within the epidermis such as melanocytes, Langerhans' cells and merkel cells. Melanocytes function to produce melanin – a pigment which helps to protect the skin against ultraviolet (UV) damage and are sparsely situated along the stratum basale (Torrora and Derrickson 2006). Merkel cells which also occur at a low frequency within the epidermis are thought to function as sensory receptors, as some are associated with nerve endings; however their function is of long standing debate (Moll, Roessler et al. 2005). Additionally, the epidermis also gives rise to hair follicles and sebaceous glands (Torrora and Derrickson 2006).

1.1.1.1 Epidermal Differentiation

The cells in the epidermis follow a programmed life cycle beginning at their site of origin in the stratum basale and migrating through to the stratum corneum where they terminate; a process known as differentiation (figure 1.2). Epidermal differentiation, along with cellular proliferation, functions to form a barrier against environmental insults. A lack of regulation of epidermal differentiation can result in fluid imbalance, heat loss and infection (Cartlidge and Rutter 1992) but also neoplastic transformation (Rheinwald and Beckett 1980; Yuspa and Morgan 1981).

The keratinocytes within the epidermis are at different stages of maturation and can be subdivided into 4 layers the stratum basale, the spinous layer, the stratum granulosum and

the stratum corneum (figure 1.2). Immediately above the basement membrane is the first layer, the stratum basale. The keratinocytes in this layer are the keratinocyte progenitor cells also known as epidermal "stem cells". These are considered as a small population of undifferentiated, basal keratinocytes which can produce transit amplifying (TA) cells; it is the TA cells which account for the majority of cells in the basal layer. Epidermal stem cells are capable of a rapid turnover rate, to form a highly organised stratified tissue, required for skin renewal (Potten and Bullock 1983; Morris, Fischer et al. 1985). However, the precise mechanisms of control are not yet clear (Fuchs and Horsley 2008). They are capable of dividing to generate more progenitor cells or alternatively, they differentiate losing contact with the basement membrane to form the spinous layer. As these cells progress into the stratum granulosum and stratum corneum, towards their external environment, they incur a number of genetic and metabolic changes controlled by both extrinsic and intrinsic factors mainly at a genetic level (Schallreuter and Wood 1995). In culture, differentiation can be modulated by the addition of calcium which influences cell-cell interactions and allows stratification through the formation of cellular adhesion molecules - desmosomes. However in 2D culture, since the stratum corneum cannot form, it is impossible to study the stratum granulosum and stratum corneum layers. However, it has been demonstrated that using 3D culture methods, full differentiation is possible (Prunieras, Regnier et al. 1983). Additionally, a number of proteins can be used as biological markers of differentiation which are noted below.

The stratum basale region is composed of a network of keratins 5 and 14. As keratinocytes begin to terminally differentiate they detach from the basement membrane and migrate upwards. Cells in the spinous layer establish intracellular contact through desmosomes and

expression of keratins 1 and 10. These cells also express involucrin which is cross-linked either to its self or to other protein components which contribute to the formation of the cornifed envelope. In the overlying granular layer, cells acquire lipid-containing granules and express fillagrin and loricrin, which also contribute to the outermost cornified layer which helps to provide an effective epidermal barrier to the environment (Watt 1989; Christiano 1997).

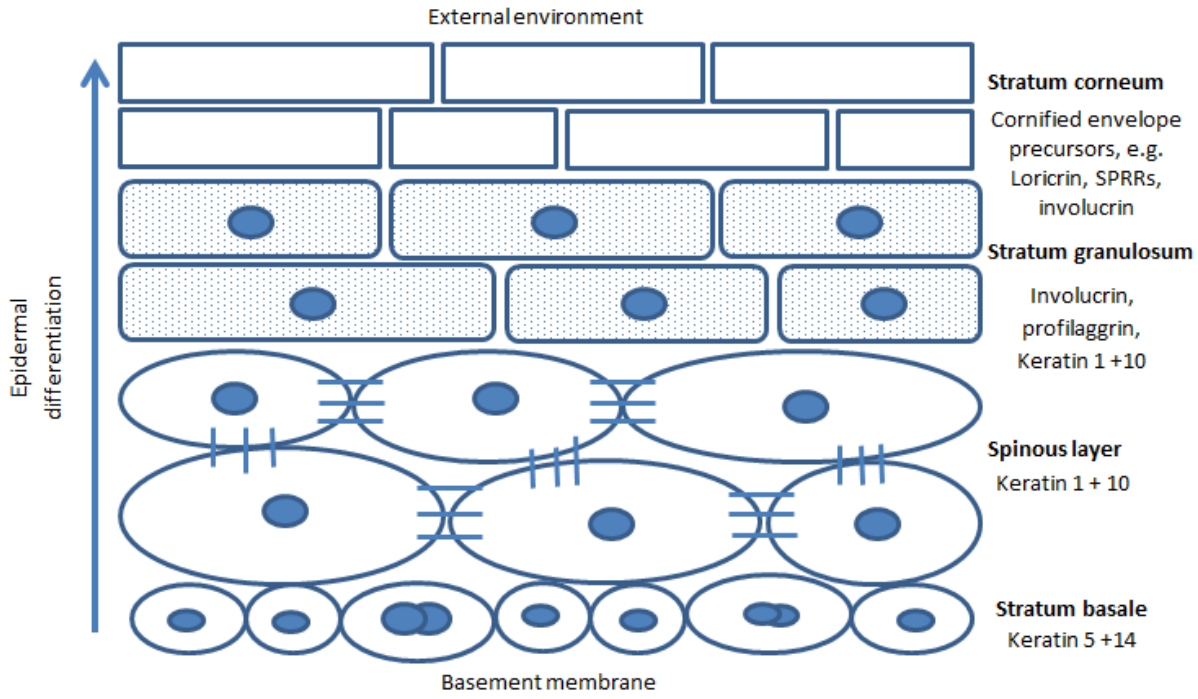

Figure 1.2 Schematic Diagram Showing Keratinocyte Organisation Within the Epidermis.

There are 4 distinct layers within the epidermis which are noted on the right hand side. The keratinocytes within the epidermis are at different stages of maturation, during which they undergo changes in cellular morphology. On the left hand side the arrow indicates the direction of epidermal migration and hence cellular migration to the external environment.

1.1.1.2 Keratin Expression in the Epidermis

The keratin filament proteins play an important role in epithelial differentiation and provide physical resilience for epithelial cells. For instance, mutations in keratin lead to inherited tissue fragility such as epidermolysis bullosa (Lane, Rugg et al. 1992). As evidenced in the section above, keratins are present in various forms throughout the differentiating epidermis. The cells in the stratum corneum form the outermost keratinized layer, where the cells flatten and exocytose lamellar granules containing precursors of lipids and keratin. Eventually these cells die, losing their nuclei and cytoplasmic organelles, leaving a highly structured keratin layer behind. This dense network of keratin helps to keep the skin hydrated by preventing water evaporation and is important for barrier function (Poumay and Coquette 2007).

1.1.2 Signals that regulate skin differentiation

The mechanisms associated with stratification have been well established in terms of morphogenetic changes, however the molecular basis for differentiation are less well established. Multiple signalling pathways have been identified especially those associated with skin barrier function (Blanpain 2007, Blanpain 2006). Important pathways include notch, mitogen-activated protein kinase (MAPK), nuclear factor κβ (NFκβ) and transcriptional regulators p63, AP2 family and CCAAT/enhancer binding protein (C/EBP) and interferon regulatory factor 6 (IRF6). The complex interplay between these complexes has begun to emerge. However central to the process of differentiation is controlled by p63 and canonical notch pathway which contributes to the basal-spinous switch. The notch pathway will be further discussed below.

1.1.2.1 Introduction to the notch signalling pathway

While Drosophila have only one notch receptor and two ligands, mammals possess four notch receptors (Notch 1-4) and five ligands (Jagged1 and 2 and Delta-like 1, 3 and 4) which adds a depth of complexity to the pathway (figure 5.1) (for review see (Kopan and Ilagan 2009). The receptors are synthesised in the endoplasmic reticulum as single trans-membrane polypeptides, before being transported to the cell surface via the trans-Golgi network. During trafficking the receptors are cleaved at an S1 cleavage site which creates ligand-binding and trans-membrane subunits, which are held covalently together. The extracellular domain (N^{EC}) consists of variable numbers of EGF-like repeats that participate in ligand binding. The Notch/LIN domain supersedes these and prevents ligand-independent receptor activation. The transmembrane domain (N^{TM}) of the Notch receptor includes a recombination signal-binding protein 1 for J-κ (RBP-J) association molecule (RAM) domain and ankrin repeats (ANK) which participate in downstream signalling and protein:protein interactions. Additionally, a C-terminal PEST (P) domain is a peptide sequence which acts a signal peptide for protein degradation. Notch signalling is initiated by ligands expressed on neighbouring cells or through secretion into the extracellular space. The ligands are part of the Delta-Serrate-Lag2 (DSL) family of trans-membrane proteins. Mammals have four ligands which activate the notch receptors (JAG1, JAG2, DLL1 and DLL4). They too have variable numbers of EGF repeats, but also the JAG1 and JAG2 have a cystine-rich domain (CD).

Figure 1.3

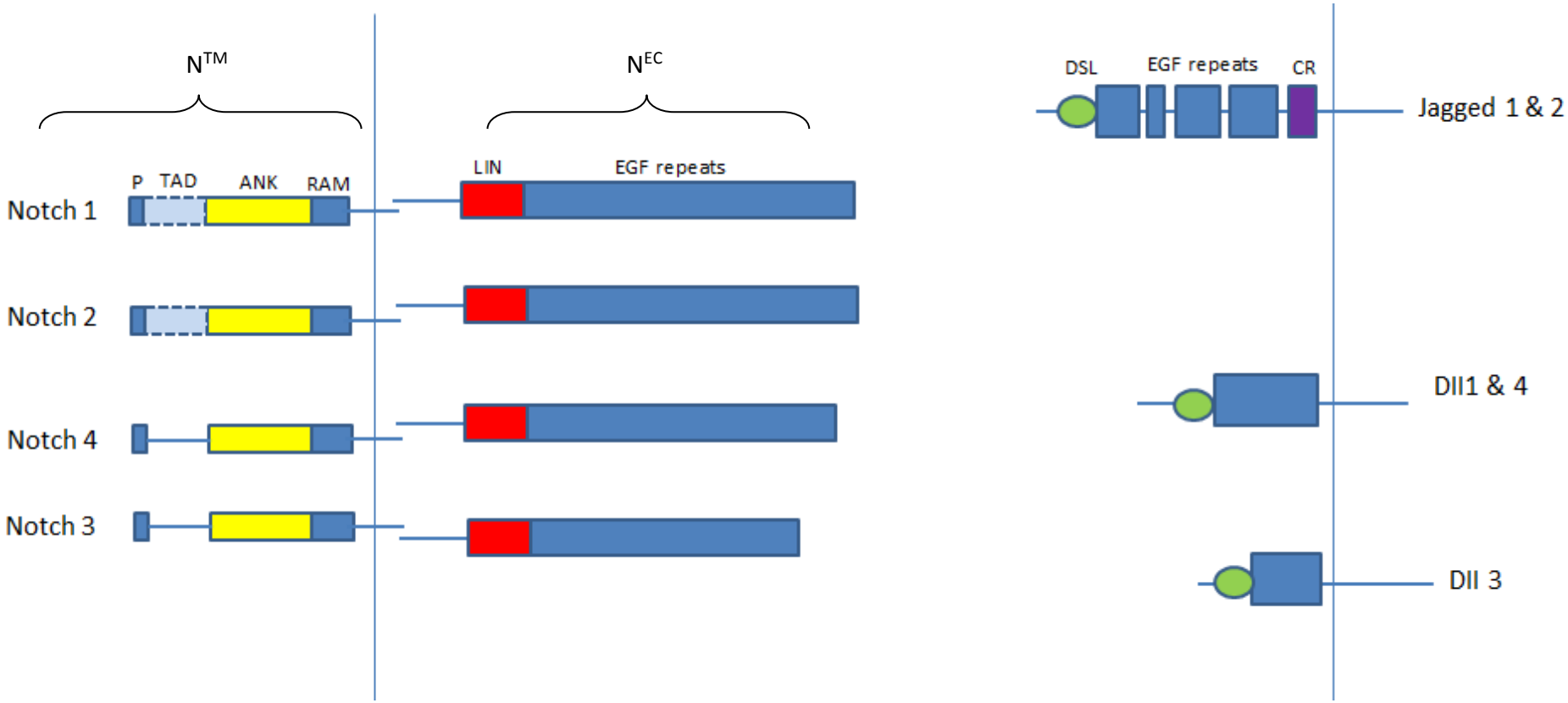

Figure 5.1 The Structure of Notch Ligands and Receptors

Mammals express five notch ligands – Jagged 1 & 2, Delta-like (DLL) 1, 3, 4. Mammals have four notch receptors, notch 1-4 which consist of trans-membrane subunits (N^{TM}) and extracellular (N^{EC}). The N^{TM} is comprised of a RAM domain, ankyrin repeats and a C-terminal PEST domain.The N^{EC} consists of a LIN12/Notch repeat (LNR) and 29-34 EGF repeats. Additionally, the ligands have an N-terminal DSL domain and variable number of epidermal growth factor (EGF) repeats. Jagged 1 & 2 serrate ligands also have a cystine rich domain (CR).

1.1.1 Canonical Pathway

Notch signalling is normally initiated by ligands expressed on neighbouring cells however ligands can also be secreted to activate the notch signalling pathway (figure 5.2, for review see (Kopan and Ilagan 2009). Following notch activation, two successive protolytic cleavages follow. The first is mediated by a metalloprotease of the ADAM family – tumour necrosis factor-α- converting enzyme (TACE), which cleaves the receptor in the extracellular domain, close to the N^{TM} domain. The released extracellular domain is then transendocytosed by the ligand. This then exposes the next cleavage site, which is mediated by γ-secretase, which is a multi-protein complex consisting of presenilin, nicastrin, APH1 and PEN2. Following this final cleavage the intracellular domain is free to translocate to the nucleus where it binds to its downstream transcription factor, the DNA-binding factor RBPJ (also known as CSL) and co-activators of the mastermind-like (MAML) family to create a CSL/ICN/MAML transcription complex. The best characterised targets of this transcription complex activation are the members of the HES and HERP families of bHLH transcriptional repressors (Iso et al 2003). However, a number of other direct targets have been identified which depend on cellular context. Genetic studies suggest that most notch signalling is via this canonical pathway with transactivation of target genes by the CSL/ICN/MAML transcription complex. However recent studies suggest that notch can also function independently of ligand transcription, through post-translational activation of other pathways (for review see Andersson et al 2012). However, depending on dose and cellular context notch signalling can induce a number of cell fate decisions where a number of roles for notch and cancer have emerged (Dotto et al 2008, South et al 2012). The significant involvement of notch signalling in cancer is exemplified by the sequencing of tumours which has revealed a number of somatic

mutations in notch receptor genes (Agrawal, Frederick et al. 1154; Aster, Blacklow et al. 2011; Wang, Sanborn et al. 2011).

Figure 1.4

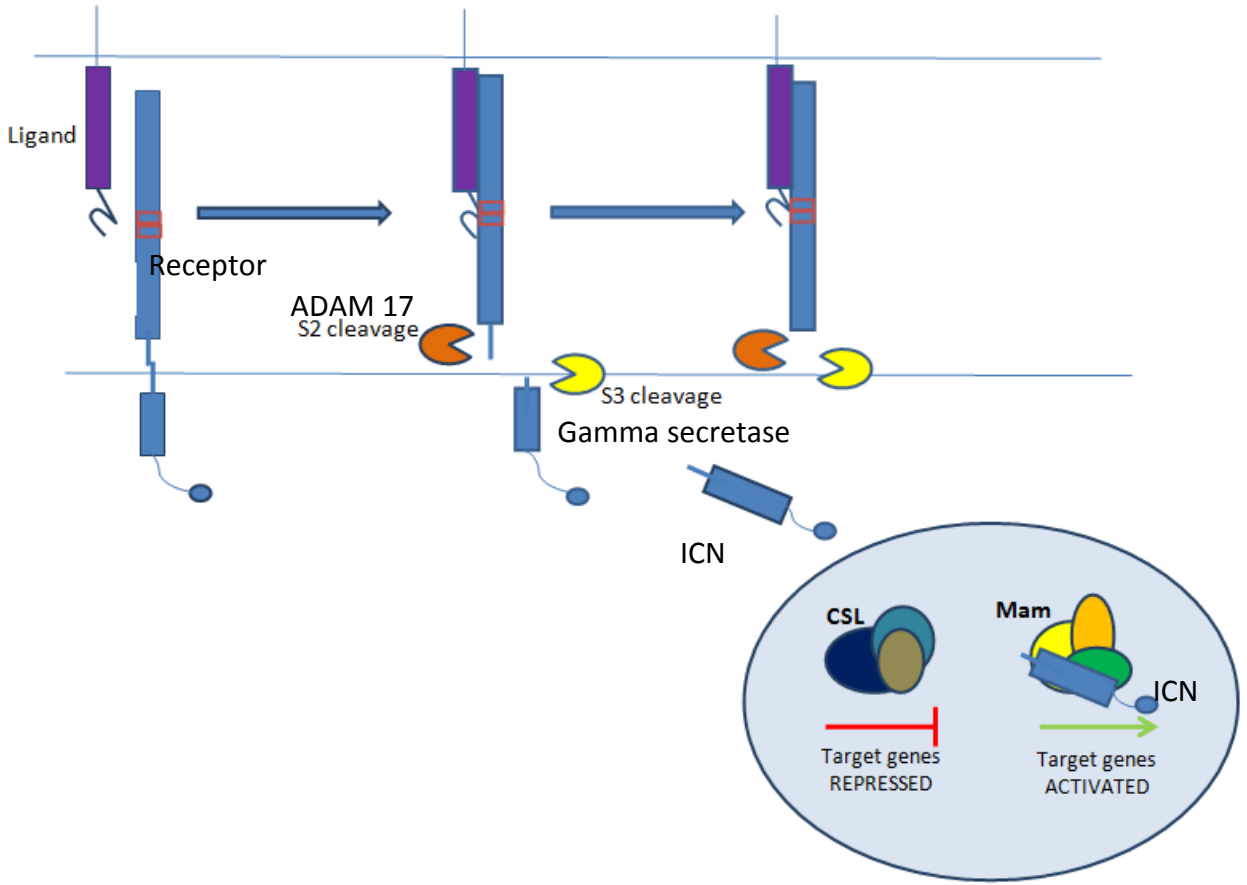

Figure 1.4 Canonical Notch Pathway

Notch signalling is initiated by a ligand on a neighbouring cell which on binding to the receptor induces a proteolytic cascade. The following first cleavage S2 is by ADAM 10 or ADAM-17 metalloproteinase at a site external to the transmembrane domain. The second cleavage S3 is by a gamma secretase complex which allows the release of the intracellular domain of notch (ICN). This ICN then is translocated to the nucleus where allosteric changes may occur in CSL that facilitate displacement of transcriptional repressors. The transcriptional co-activator Mastermind (Mam) then recognises the ICN/CSL complex and recruits co-activators to activate transcription.

1.1.2 The Dermis

The dermis resides directly beneath the epidermis and is divided into two layers the papillary and the reticular layer. The thin upper layer is the papillary dermis composed of elastin and collagen fibres, which lies immediately below and interdigitates with the epidermis above. Anchoring fibrils, composed largely of type VII collagen are responsible for attaching the dermis to the basement membrane (McGrath 2004). In contrast, the reticular dermis is characterised by denser and coarser interwoven collagen and elastin fibres to give this region added strength and elasticity. Both of these regions contain blood and lymph vessels, nerves but also dermal proteins such as collagen and elastin, which are secreted by fibroblast cells. Fibroblasts are important for creating the extracellular matrix, which provide a structural framework (stroma) giving the skin important anatomical and structural function. Indeed, both layers contain different sub-populations of dermal fibroblasts which interact with the epidermis and play an important role in cutaneous wound healing and skin bioengineering (Sorrell and Caplan 2004). Below the dermis is a layer of fat which helps the body to retain heat.

1.2 MALIGNANT CHANGES IN THE EPIDERMIS

The epidermis constantly exposed to various insults, such as ultraviolet (UV) radiation and those mechanical and chemical, often incurs a number of physiological and genetic changes. Hence a number of neoplasms originate from the cutaneous epithelial cells (Owens and Watt 2003). Growths can destroy the organisation of the epidermal and dermal layers, forming a distinctive mass. The most common cutaneous neoplasm is basal cell carcinoma (BCC) followed by cutaneous squamous cell carcinoma (cSCC) and the melanocytic malignancy, malignant melanoma (MM). The focus of this thesis is cSCC which usually

present as a nodular keratinising tumour or as an ulcer, with little evidence of keratinisation. cSCC diagnosis is established histologically in terms of histopathological subtype, degree of differentiation, tumour depth, level of dermal invasion and the presence of vascular or lymphatic invasion (Motley, Preston et al. 2009). A histological image of a well differentiated cSCC can be found in figure 1.3, which shows how invading keratinocytes from the epidermis to the dermis can alter the organisation of the skin.

Figure 1.3 Hematoxylin and Eosin (H&E) Staining of cSCC

The “yellow line” representing the basement membrane is divided by keratinocytes invading into the dermis bellow, as indicated by the arrow. The division between the epidermis and dermis is not as clear as in the normal human skin H&E represented in figure 1.1 Image taken at 40x magnification.

1.2.1 Cutaneous Squamous Cell Carcinoma (cSCC)

cSCC and BCC cancers come under the collective term: non-melanoma skin cancers (NMSC) with cSCC accounting for 20% of all cases (Kwa, Campana et al. 1992; Alam and Ratner 2001). Over 99,000 non-melanoma skin cancers (NMSC) were registered in the UK in 2010, the incidence of which has been rising at an alarming rate over the past two decades. Tayside in Scotland, for instance, has seen a 4-fold increase in all skin cancers in the last 20 years and in 2011 2,982 cSCC were registered in Scotland (ISD Scotland 2011). Additionally, this figure is expected to be underestimated due to the recording of NMSC cases being incomplete.

In addition to the normal population, high risk groups exist. For example the risk of cSCC is increased 100 fold in transplant patients due to immunosuppression during treatment (Penn and Starzl 1972; Jensen, Hansen et al. 1999 Seckin, Barete et al. 2013). Additionally, our lab has a longstanding interest in a particular subtype of the genetic skin blistering disease epidermolysis bullosa (EB) - recessive dystrophic epidermolysis bullosa (RDEB). EB is a rare skin fragility disorder, characterised by chronic blistering of the skin mucosae following minor mechanical trauma. Its incidence in America has been documented as 19.6 per million live births from 1986-1999, with a prevalence of 8.22 per million population (Fine 1999).

1.2.1.1 Epidermolysis Bullosa

EB can be classified into 4 main groups based on the ultra-structural level of blister formation in the basement membrane zone. The 4 main groups are: EB simplex (EBS), junctional EB (JEB), dystrophic EB (DEB) and kindler syndrome. DEB can be referred to as “dominant” or “recessive” as the disorder can be inherited in an autosomal dominant

(DDEB) or autosomal recessive (RDEB) manner, respectively and can be grouped into localised or generalized subtypes based on the extent of blistering. RDEB skin is much more fragile than DDEB skin (Eady, Fine et al. 2004) and includes the most severe subtype, severe generalised (sev-gen) which can lead to disfiguring blistering. The RDEB sev-gen subtype is of particular interest in our lab not only due to it severity, but also as these patients suffer cSCCs as a major complication of the disease (Fine, Johnson et al. 2009). The cumulative risk of developing cSCC in patients with RDEB sev-gen stands at more than 90% by the age of 50 (Fine, Johnson et al. 2009). This remarkably high incidence of cSCC compared to the normal population, suggests that there are~~is~~ likely to be differences in pathogenesis of the disease. Paradoxically, although most cSCC in RDEB patients are histologically differentiated (McGrath, Eady et al. 2004), they are biologically aggressive with the propensity to recur and metastasise to different sites. RDEB patients develop multiple cSCCs 3-3.5 per patient despite excision. This is a devastating disease. Moreover, RDEB patients have a 90% life time risk of developing metastatic cSCC which is main cause of death in this group (Fine, Johnson et al. 2009).

1.2.1.2 Metastatic Potential and Recurrence

Despite BCCs forming the majority of NMSC (80% of all NMSC), BCC rarely metastasise whereas cSCC can. In the normal population, cSCC tumours with high metastatic risk include those that are greater than 2cm, poorly differentiated tumour grade and invasive tumours infiltrating beyond the dermis (Kwa, Campana et al. 1992; Rowe, Carroll et al. 1992). Of particular note, is the tumour grade, which is a broad description of a tumour, in which tumour differentiation is an important feature. For instance, low grade tumours can be defined as showing substantial cellular differentiation, uniform cell size, infrequent cellular mitoses and infrequent nuclear irregularity. Intact intercellular bridges are also present.

However, high-grade tumours are described as showing poor differentiation, frequent spindle cell characteristics, necrosis and high mitotic activity. In general a well differentiated tumour indicates a better prognosis; poorly differentiated tumours have more than double the recurrence rate and triple the metastatic rate of a better differentiated cSCC (Gleason and Mellinger 1974; Motley, Preston et al. 2009). 5 year recurrence rate of primary cutaneous lesions is 8%, and the 5 year metastatic rate is 5%, however regional metastasis to lymph nodes and distant organs leads to a poor survival rate; 5 year survival in this group is 25%- 50% (Rowe, Carroll et al. 1992; Veness, Porceddu et al. 2007). This poor outcome is amplified by the propensity of biologically aggressive cSCC to recur, making disease control difficult. Furthermore, metastasis is the most common cause of death in cancer patients and currently there is no effective treatment for metastatic disease.

1.2.2 Treatment of cSCC

Protection from sun exposure is paramount to the prevention of cSCC. Secondary to this, early detection currently provides the best prognosis. The American Academy of Dermatology and the American Cancer Society have recommended yearly total body examinations for all patients over 40 (Jerant, Johnson et al. 2000). However, implementing a screening program consisting of community and general practitioner education, in addition to, screen clinics for the general population would place a significant burden on health care resources in the UK. For this reason it is advised that self-checking of the skin for any suspicious lesions is carried out regularly. The main treatment available for cSCC is wide local surgical excision which can be followed by dissection of regional lymph nodes and adjuvant radiation therapy (Clayman, Lee et al. 2005). Electrodessication, curettage excision or cryosurgery can eradicate low risk tumours in a cost effective manor (Martinez and Otley 2001) however, if there is a risk of recurrence and metastasis then Mohs surgery or surgical

excision provide the best prognosis at a greater cost (Motley, Preston et al. 2009). Additionally, current treatment for metastatic disease includes both systemic (i.e. high doses of chemotherapy), local therapy (i.e. radiation) or a combination of both however the efficacy of such treatments is limited and there is much need for more effective treatments.

1.2.3 Risk Factors for cSCC

Below is detailed some of the major risk factors in the causation of cSCC.

1.2.3.1 Sun Exposure

Chronic sun exposure is the major risk factor for the development of cSCC. Epidemiological and molecular data strongly suggest that UV radiation is the principal carcinogen implicated in NMSCs (Dazard, Gal et al. 2003). Additionally, the incidence doubles with each 8-10 degree decrement in geographic latitude and is highest at the equator which receives the highest intensity of sunlight. The ultraviolet B (UVB, 290-315nm) portion of UV from the sunlight is principally responsible for DNA damage. Furthermore, UVB is highly immunosuppressive, a key process in malignant transformation (de Gruijl, Longstreth et al. 2003). However, mounting evidence suggests that ultraviolet A (UVA, 315-400nm) adds to the risk (LeVee, Oberhelman et al. 1997; Moyal and Fourtanier 2001). UVA penetrates deeper into the skin and is 20 times more abundant than UVB, which only comprises ~5% of the total UV radiation that reaches the earth. In addition to environmental radiation, exposure to therapeutic radiation such as psoralen and UVA (PUVA), which is used to treat skin disorders, can cause up to a 6 fold increase in cSCC (Chuang, Heinrich et al. 1992). Use of tanning devices such as sun beds which emit UV radiation (mainly UVA) are also associated with increased risk of cSCC, with odds ratios of 2.5 (95% confidence interval [CI] =1.7 -3.8) (Karagas, Stannard et al. 2002).

Lifestyle changes and the increase of “package holidays” have boosted voluntary exposure to sun-light. Those individuals which have fair-skin have the highest risk of developing skin cancer and a history of sunburn during childhood may be a very important risk factor in the development of cSCC (Suchniak, Baer et al. 1997). Although UV radiation is thought to be the main risk factor for the development of skin cancer, there are a large number of other risk factors, some of which are detailed below.

1.2.3.2 Inherited Skin Disorders Associated with cSCC Predisposition

Genetic predisposition to cancer is generally through inherited mutations in tumour suppressor or tumour promoting genes which are important for normal cell function. One of the most prominent examples where patients are genetically predisposed to the development of cSCC is Xeroderma~~e~~ Pigmentosum (XP). This genetic disease is characterised by an extreme sensitivity to UV, and development of lesions at a very young age. UV can cause UV-signature mutations such as cyclobutane pyrimidine dimers (CPD) or 6-4 photoproducts (6-4PP). DNA integrity and stability are essential, so our body has evolved a number of DNA damage detection and repair mechanisms. Failure to repair mutations may result in tumour formation. P~~Incidentally, p~~eople with XP have mutations in the genes involved in nucleotide excision repair (NER) resulting in some cells being unable to repair DNA damage, namely CPDs and 6-4PP. Subsequently, they also have a 2000 fold increased risk of developing skin cancers and these tumours have a high frequency of UV signatures found in the tumour suppressor, tumour protein 53 – (*TP53*) gene (Benhamou and Sarasin 2000). 70% of XP patients develop malignant skin lesions and 50% of these are NMSC (Kraemer, Lee et al. 1994). Interestingly, the incidence of metastasis in this group is comparable to that of the normal population which is around 4% (Kraemer, Lee et al. 1987).

XP is a rare disorder; it is estimated to affect 1 in 1 million people across America and Europe.

In addition to XP, there are a number of other inherited syndromes associated with the predisposition of cSCC these include: multiple self-healing squamous epitheliomata, Albinism, EB, Epidermodysplasia verruciformis (EV), Fanconi anaemia, Dyskeratosis congenita, Rothmund-Thomson syndrome, Bloom syndrome and Werner syndrome (for review see Ng et al 2011). In particular mutations in specific DNA repair genes increase error prone DNA replication and repair in keratinocytes which contributes to the increase in cSCC formation. For instance, Blooms syndrome is caused by a mutation in the BLM gene which is a member of DNA helicase family associated with DNA repair and Fanconi Anaemia is characterised by an increase in the number of chromosome breaks of which 13 genes have been associated with the inheritance of this disease so far.

1.2.3.3 Precursor Lesions and Pre-invasive Skin Conditions

Actinic keratoses (AK) are focal areas of epithelial dysplasia, which can occasionally precede cSCC (Lanssens and Ongenae 2011). They are also known as “solar keratosis”, found prominently on sun-exposed parts of the body, in response to excessive sun exposure over many years (Schwartz 1997). *TP53* mutations are commonly found in AKs; one study found it to be around 70-80% of white patients affected with AK (Park, Lee et al. 1996). In severe combined immunodeficient (SCID) mice, UVB irradiation induced AK (Nomura, Nakajima et al. 1997). However studies show that only 1-10% of AK develop into cSCC (Marks, Foley et al. 1986; Dodson, DeSpain et al. 1991). Other pre-malignant lesions include Kerato-acantoma and Bowen disease (Lanssens and Ongenae 2011).

1.2.3.4 Immunosupression

As mentioned above UVB and to a lesser extent UVA can induce immunosuppression causing multiple effects including: DNA damage, cytokine production and alteration of langerhans' cell function. Immunosuppression has also been shown to contribute to the formation of cSCC. Studies have shown that there is a 65-250 fold increase in the risk of developing cSCC amongst solid-organ transplant patients (Penn and Starzl 1972; Jensen, Hansen et al. 1999). These patients are given immunosuppressive drugs to reduce the chances of allograft rejection however, this also increases their risk of developing cSCC at a younger age and developing lesions that are more biologically aggressive with increased risk of recurrence and metastasis compared to the normal population (Glover, Niranjan et al. 1994; Kaplan and Cook 2005).

This increased risk has been associated with the dose of immunosuppression and UV exposure. For instance, heart transplant patients which receive the highest doses of immunosuppression, have a 2.9 fold increased risk than kidney transplant patients (Jensen, Hansen et al. 1999). This risk also seems to be higher in regions closest to the equator. This is illustrated by Australian kidney transplant patients, which have a 4 fold increased risk of developing cSCC than Dutch transplant patients (Bouwes Bavinck, Euvrard et al. 2007).

1.2.3.5 HPV

Human papilloma virus (HPV) infection has been linked to a small number of skin cancers. Although this link is controversial, one particularly large study analysed the occurrence of HPV in 2,366 patients either with cSCC, BCC or healthy controls. Positivity to at least one β HPV type was associated with an overall odds ratio of 1.3 for cSCC (95% CI 1.04 to 1.61) (Karagas MR et al 2010).HPVs are circular double stranded DNA viruses of which over 100

serotypes exist. The E6 and E7 oncoprotiens can inhibit the human tumour suppressors TP53 and pRb respectively, which is the main cause of carcinogenesis caused by HPV infection (Connolly, Manders et al. 2013). The infection can cause warts, laryngeal papillomas and cancers of the genital and anal areas. Additionally, the inherited disorder EV is characterised by the development of cSCC and these patients have an abnormal susceptibility to widespread HPV infection (Masini, Fuchs et al. 2003).

1.2.3.6 Inflammation and Erythema

Although immunosuppression is considered to be a risk factor for cSCC, inflammation is also paradoxically involved in cSCC establishment. Both UVA and UVB rays can cause inflammation and erythema, DNA damage and gene mutations which are capable of initiating skin cancer. Inflammatory substances play a number of roles in initiation, promotion and progression of a tumour. UV light, in particular UVA, has been demonstrated to increase inflammatory infiltrates which enhances tumour growth. Production of sub-lethal levels of reactive oxygen species and nitric oxide can drive cancer development through induction of DNA damage (Sluyter and Halliday 2001; Fortina, Piaserico et al. 2004). These molecules can further stimulate cancer by increasing cell proliferation which assists tumour establishment (Wiseman and Halliwell 1996; Lonkar and Dedon 1999).

1.3 KNOWN MOLECULAR MECHANISMS OF cCSCC

Over the last 30 years cancer has been revealed to be a disease involving dynamic changes in genetics. The general perception is that cancer develops via a multistep process. In a seminal review, Hanahan and Weinberg discuss how tumorigenesis requires fundamental events to occur, in order to drive transformation of normal human cells into a highly

malignant population. In their original review (Hanahan and Weinberg 2000) six hallmarks were hypothesised: (I) evading apoptosis (II) self-sufficiency in growth signals (III) insensitivity to antigrowth signals (IV) sustained angiogenesis (V) limitless replicative potential (VI) tissue invasion and metastasis. In a follow up review, "re-programming of energy metabolism" and "evading immune destruction" were added to the hallmarks of cancer, in addition to the contribution of "enabling" characteristics such as underlying genetic instability. They also highlight that tumours are complex tissues in which malignant cells are supported by a tumour microenvironment and that our understanding of this support network, is critical to the understanding of the pathogenesis and the development of effective therapies (Hanahan and Weinberg 2011). The tumour microenvironment includes a number of other cells such as blood vessels, immune cells and fibroblasts, in addition to a number of extracellular matrix signals. Work in our lab, has shown that the tumour microenvironment is a key driver of aggressive cSCC in patients with RDEB (Ng, Pourreyron et al. 2012).

Yet, the key molecular events or "driver mutations" in cSCC initiation and progression are poorly defined and are likely to include "signature" changes to both tumour suppressors and oncogenes which control a number of critical cellular hallmarks.

1.3.1 Common Dysfunctional Genes Associated with cSCC Formation

Over the last decade there has been a major effort to understand the molecular pathogenesis of cSCC neoplasms, in the hope of providing new opportunities for molecular based therapeutics. A number of key signalling pathways have been identified to be involved in cSCC. These include genes that act as oncogenes or tumour suppressors, where their gain-of-function or loss-of-function contributes to the formation of a number of

different tumour types. A select few common dysfunctional genes associated with cSCC formation are noted below which are part of key signalling pathways involved in maintaining cellular order, these are summarised in figure 1.4. On their discovery, it was thought that they would be potential molecular targets for cSCC. However current evidence has yet to clinically prove them as targets for cSCC, which exemplifies the need to continue the search for novel molecular targets.

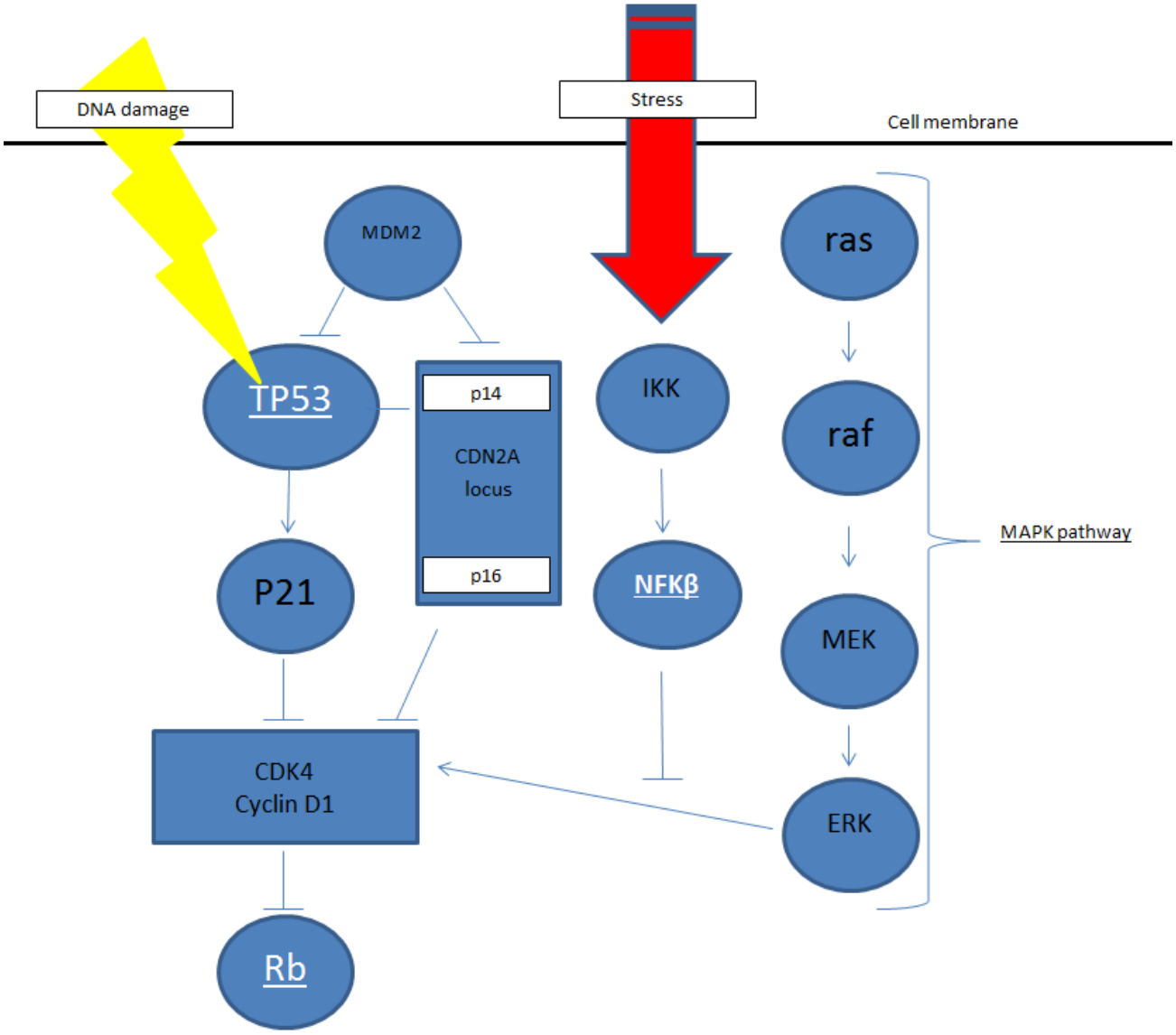

Figure 1.4 Key Signalling Pathways in cSCC

Mutations induced by UV radiation and environmental stress can perturb multiple cellular pathways leading to the contribution of cSCC. Arrows indicate positive relationships whereas T-bars indicate inhibitory relationships. Molecules/pathways that are underlined form subtitled discussions within the text (for review see Ridky and Khavari 2004 or Ratushney et al 2012).

1.3.1.1 Tumour Protein 53 (TP53)

The tumour protein 53 (TP53), is a tumour suppressor which responds to a remarkably large number of DNA damage stresses including hypoxia, heat shock and nutritional. It orchestrates a number of anti-proliferative effector functions, namely; cellular senescence, autophagy, apoptosis and acting at cell cycle checkpoints, which contribute to its tumour suppressor activity. Dubbed as the "guardian of the genome", it results in prevention of genomic instability and protection of tumourogenesis (Lane 1992; Vogelstein, Lane et al. 2000). The contribution of p53 to cancer in general, has been exemplified by a number of observations including families with Li-Fraumeni cancer syndrome, whom are predisposed to the development of cancer - ~60% of these patients have mutations in the *TP53* gene (Malkin 1994). Knockout TP53 mice which develop tumours at a very young age (Donehower, Harvey et al. 1992; Lozano 2010) and 50% of all cancers are shown to contain TP53 mutations in both alleles or exhibit loss of heterozygosity (Olivier, Hollstein et al. 2010; Robles and Harris 2010). Additionally in skin, TP53 has been shown to be mutated at a slightly higher frequency ~60% (South unpublished; Brash 2006) and is the most prominently studied aberration in skin cancer. Of note, TP53 is activated in response to UV DNA damage; hence it protects the skin by maintaining its genetic integrity (Smith and Fornace 1997).

Although there is a vast amount of data which implicate TP53 mutations in the development of cSCC, its involvement in the pathogenesis of the disease is still not clearly understood. For instance TP53 knockout mice display resistance to the development of cSCC through the expression of oncogenes such as v-ras or TGFα in a multistage carcinogenesis model, yet these mice develop cSCC following UV exposure (Greenhalgh, Wang et al. 1996; Jiang,

Ananthaswamy et al. 1999). Additionally, loss of TP53 failed to act as a classical initiator for 12-O-Tetradecanoylphorbol-13-Acetate (TPA) promotion (Greenhalgh, Wang et al. 1995; Greenhalgh, Wang et al. 1996). These data would suggest that a compensatory mechanism for TP53 loss maybe occurring. Functionally, TP53 is complicated by another two related orthologs of TP53~~,~~ which ~~although~~ have been described to be important for developmental function, TP73 (CNS development, Celli et al 1999) and TP63 (epithelial formation, Yang et al 1999), increasing evidence suggests their involvement in cancer (Tan 1001, Yam 2000, Ahomadeghe 2000, Dong 2002). In addition to this, a large number of different functional splice forms of p53, p63 and p73 are under study (Khoury and Bourdon 2010) and chemical modifications resulting from ~~a~~ stress signals can also alter their functions (Meek and Anderson 2009).

A number of studies have been conducted in attempt to "restore" wild-type TP53 function. The role of TP53 inducing apoptosis post chemotherapy drug treatments has been demonstrated (Lowe and Ruley 1993). Additionally, studies have tried to stabilise TP53 protein levels either with an mouse double minute 2 homologue (MDM2) antagonist, to increase genotoxic stress (Ohnstad, Paulsen et al. 2011) or 'stapled' TP53 based peptides that prevent antagonist inhibition (Bernal, Wade et al. 2010) However, although preservation of TP53 function is an attractive possibility for cancer therapy, mutation of TP53 renders cancer cells more resistant to TP53 cancer therapies, due to lack of TP53 mediated apoptosis making targeted therapy difficult.

1.3.1.2 MAPK Pathway

Mitogen-activated protein kinase (MAPK) pathway regulates a diverse set of processes and its activation~~induction~~ is frequently found in cSCC, at both mRNA and protein level (Einspahr, Calvert et al. 1158; Dajee, Lazarov et al. 2003; Zhang, Shen et al. 2007; Hameetman, Commandeur et al. 2013). A number of families of MAPKs have been defined in mammalian cells including, extracellular signal-regulated kinases 1 & 2 (ERK 1, ERK2), Jun N-terminal kinases, p38 kinase isozymes, ERK3/ERK4 and ERK-5. The ERK pathways are the most studied of the mammalian MAPK pathways and a complete pathway from receptor to MAPK has been defined for the ERK1 and ERK2 kinases, which act downstream of the RAS proto-oncoprotein. Activation of the pathway begins with ligands such as hormones or growth factors, which act by binding to the cell-surface receptor tyrosine kinases or G-coupled receptors, leading to activation of ras. Ras-GTP then triggers activation of raf to the plasma membrane followed by phosphorylation of MEK1/2 and ERK1, ERK2. Activation can lead to proliferation or differentiation depending on the strength and timing of the signal (Scholl, Dumesic et al. 2004).

In particular, ras an upstream component of the MAPK pathway has the potential to be an important oncogenic influence in cSCC. There are 3 RAS genes, Harvey sarcoma ras (H-ras), Kirsten sarcoma ras (K-ras) and human neuroblastoma ras (N-ras). Ras was first implicated in cSCC when it was discovered there were H-ras mutations in the papilloma's of the mice treated with 7,12-dimethylbenz[a]anthracene (DMBA), in the chemical carcinogenesis model (Balmain, Ramsden et al. 1984). However, oncogenic ras alone is not sufficient to induce an invasive cSCC in human keratinocytes and it is necessary to co-express it with another oncogene to stimulate cSCC formation (Ridky and Khavari 2004). Khavari and

colleagues, have used ras in combination with cyclin dependant kinase 4 (CDK4) expression (Lazarov, Kubo et al. 2002) or with IκBα-inhibition of NF-κB (Dajee, Lazarov et al. 2003) to efficiently transform human keratinocytes into an invasive SCC.

Variable levels of ras mutations have been found in cSCC and AK (Pierceall, Goldberg et al. 1991). Data from COSMIC indicates 21% of cSCC have activating RAS mutations, which is fairly low (South unpublished; Bamford, Dawson et al. 2004). Disparity between the low frequency of ras mutations and frequent induction of the MAPK pathway suggests that ras may be activated due to upstream events or cross-talk between the PI3K-AKT-mTOR pathways (Ridky and Khavari 2004, Britten 2013). However, activated ras is not required for increased levels of GTP-bound ras which is observed in the majority of cSCC tumours (Dajee, Lazarov et al. 2003).

A new dimension to the ras controversy has arisen from a striking finding; the use of selective RAF inhibitors induces a high frequency of KA and cSCC as well as warty papillomas, developing soon after onset of drug treatment in 25% of patients (Arnault, Wechsler et al. 2009). For instance, BRAF drugs that inhibit MEK/ERK signalling in cells that express oncogenic BRAF, paradoxically induced MEK/ERK signalling in cells that express oncogneic ras. Additionally, Ras inhibitors in the clinic have been largely disappointing (Beeram, Patnaik et al. 2003; Zhu, Hamilton et al. 2003). Although the reason is not entirely clear it is thought to be due to off target effects (Prendergast and Du 1999) or the drugs inability to distinguish from mutant and wild-type forms of ras.

1.3.1.3 Rb Pathway

The retinoblastoma protein (pRb) pathway is a vital controller of the cell cycle. Virtually the entire process involved in the activation of DNA replication and the regulation of the G1/S transition is under the control of the pRb (Weinberg 1995). The Rb pathway consists of five families of proteins – cyclin dependant kinase inhibitors (CDKN), D-type cyclins, cyclin-dependant protein kinases (cdk), Rb, and E2F. In this pathway the CDKN and Rb families of proteins functions as tumour suppressors and the D-cyclins, cdks and E2F promote cell proliferation.

Elements of the Rb pathway are mutated in a wide variety of cancers ~~in a number of cancers~~ including cSCC. Disruption of the pRb pathway leads to increased proliferation, rendering cells insensitive to anti-growth factors which block transition from G1 to S phase of the cell cycle. Disruption can occur in a variety of ways throughout this signalling pathway. For instance, cyclin-dependant kinase inhibitor 2A (CDKN2A, $p16^{ink4a}$) inhibits progression of the G1 phase of the cell cycle by blocking cyclin-dependant kinase 4 (CDK4) from phosphorylating ~~the~~ pRb (Brown et al 1999). Loss of this tumour suppressor results in dysregulated CDK4 and promotion of cell division. Furthermore, CDKN2A is located within the 9p22 chromosomal region. This region is the most frequently deleted in cancer – loss of heterozygosity as well as loss of parts or the entire short arm of chromosome 9 are frequently observed in cSCC (Quinn, Campbell et al. 1994). Additionally CDK4~~4K~~ is frequently over-expressed in cSCC which renders the kinase insensitive to CDKN2A inhibition (Lazarov, Kubo et al. 2002).

The CDKN2A gene generates at least 2 alternatively spliced variants one of which acts to stabilise TP53 by inhibiting MDM2 mediated degradation; $P14^{ARF}$ and $p16^{INK4a}$, a cyclin dependant kinase inhibitor, which regulates pRb (Sherr 2001). Despite being on the same locus, it represents an independent complex signalling network which interconnects both Rb and TP53. Hence therapies targeting the pRb pathway, which prevent the assembly of cyclins with cdks using small molecules, represent a formidable challenge due to the extensive molecular mechanisms involved (Pauletich et al 1999). Cdk inhibitors may prove useful for some tumours, however because certain cdks play non-cell cycle roles, it is important that the inhibitors are specific so to reduce any unanticipated effects (Toogood 2001). Alternatively a complementary approach, based on synthetic lethality may prove useful. For instance, cells that lack pRb manifest defects in E2F regulation are more sensitive than normal cells to cdk2 inhibitors (Chen et al 1999).

1.3.1.4 NF-κB/Rel

Nuclear factor kappa-light-chain-enhancer of activated B cells (NF-κB/Rel) proteins play a key role in regulating immune response to infection; regulating pro-inflammatory and anti-apoptotic genes. NF-κB is also clearly of great importance for skin homeostasis and is strongly linked to cancer. However the pathway is complex involving 5 subunits: RelA (p65), p50, p52, RelB and c-Rel which exist in un-stimulated cells as dimers bound to (nuclear factor kappa-light-chain-enhancer of activated B cells – inhibitor) IκB family of proteins. Binding to IκB prevents the complex from translocating to the nucleus. In the canonical pathway, stimulation leads to activation of the IκB kinase (IKK) complex, which in turn, phosphorylates IκB proteins to allow NF-κB to enter the nucleus and activate response pathways. The different subunits are not all involved in the same signalling pathways, the

canonical pathway involves the p65/p50 subunits but other pathways, induced by different stimuli use other subunits in a highly context dependant mannee~~e~~r. The canonical pathway of IκB inhibitory proteins hold p65/NF-κB inactive until signalling pathways involving IKKs result in release of NF-κB to allow it to enter the nucleus (Dixit and Mak 2002).

Consistent with a role for NF-κB in oncogenesis are observations that inhibition of NF-κB either alone or with cancer therapies, leads to tumour death or growth inhibition however paradoxically, blockade of NF-κB has been shown to promote an anti-proliferative effect which means NF-κB can either promote or oppose tumour development depending on context. Mouse studies show that inhibition of NF-κB increased the susceptibility to cSCC development (van Hogerlinden, Rozell et al. 1999). Additionally when IkB blockade was co-expressed with oncogenic ras it can transform the human keratinocytes through increasing proliferation and creating an invasive neoplasm with features similar to that of cSCC (Dajee, Lazarov et al. 2003). This factor and the signalling pathways involved are an attractive target for cancer prevention and therapy however currently we lack *in-vivo* studies establishing the definitive role of NF-κB signalling in cSCC. In order to appropriately move NF-κB inhibitors in the clinic for other cancers, it is fundamental to determine the molecular mechanisms that dictate the complexity of oncologic and therapeutic outcomes that are controlled by NF-κB.

1.4 TARGETED THERAPIES

Our ability to perform genome-wide gene expression analysis offers opportunities not only to expand our current knowledge of the pathogenesis of cancer, but also to develop new therapies directed at specific molecules. Determining the gene expression of tumours and logically designing targeted anticancer drugs should increase treatment efficacy while decreasing toxicity. Although several mutations contribute to malignancy, not all need to be

corrected to achieve significant therapeutic effects. Most attempts to treat cancers in model systems through replacement of single tumour suppressor genes or inhibition of individual oncogenes have resulted in tumour killing or growth arrest. The success of a number of targeted drugs which have been approved for the treatment of specific types of cancer; transtuzumab (Herceptin, (Cobleigh, Vogel et al. 1999; Druker, Talpaz et al. 2001)) for HER-2 amplified and BRCA- mutated breast cancer and vemurafenib (Zelborafk, (da Rocha Dias, Salmonson et al. 2013; Kudchadkar, Smalley et al. 2013)) for late stage melanoma patients with a BRAF V600E mutation has greatly encouraged the development of targeted therapies. While the appearance of drug resistance has slightly dampened our hopes, it underpins the need for combinational therapies to achieve sustained remission.

This thesis describes follow up functional studies on data generated by Dr AP South's lab using: gene expression profiling and next generation sequencing. These two methods will be further described in chapters 3 and 5 respectively.

1.5 AIMS OF THE THESIS

The aims of the thesis are generally to identify novel molecular targets for cSCC therapy. In order to address this, at the beginning of this thesis the three main areas of investigation were as follows:

1. The gene expression profiling revealed 21 up-regulated potential molecular targets for cSCC which were screened using siRNA knockdown with cell viability as a readout (details in chapter 3, Wwatt *et al.* 2011). The first aim was to repeat this RNAi screen of the 21 genes with cytotoxicity as a readout.
2. The RNAi screen identified five potential molecular targets which were capable of reducing cell viability in cSCC cell lines (which are detailed in chapter 3, Watt *et al*

2011). The second aim was to further validate three of these targets, germ cell associated 2 (GSG2), bradykinin receptor B1 (BDKRB1), protease serine 21 (PRSS21).

3. In a separate project, next generation sequencing identified ~75% loss of function notch1 and notch2 mutations (of which are details in chapter 5, Wang *et al* 2011). The third aim was to further investigate the contribution of notch in cSCC.

Additionally, this thesis aims to understand these potential molecular targets to the contribution and function in cSCC in hope of targeting these pathways for potential preventative and combative therapies for a currently untargeted disease.

Chapter 2: General materials and methods

2.1 CHEMICALS AND MATERIALS

2.1.1 General Reagents

100bp DNA ladder	Invitrogen, UK
IKb DNA ladder	Invitrogen, UK
Alkaline phosphatase (AP)	Roche, Germany
Calcium Chloride	Fluka Biochemika, Switzerland
EDTA-free protease inhibitor cocktail tablets	Roche, Germany
Electrophoresis grade agarose	Invitrogen, UK
Hepes	Fisher Scientific, UK
Isopropanol	Fisher Scientific, UK
Rainbow marker	Invitrogen, UK
RNase-free water	Invitrogen, UK
Set of dNTPs	Invitrogen, UK
Sodium chloride	Fisher Scientific, UK
Tris-Base	Fisher Scientific, UK
Triton X-100	Fisher Scientific, UK

2.1.2 Assay Kits

Cell Titre 96 AQone One solution cell proliferation assay	Promega, USA
ECL advance western blotting detection kit	Amersham, UK

FastStart high fidelity PCR system	Roche, UK
QIAquick gel extraction kit	Qiagen, Germany
QIAquick mini prepgel extraction kit	Qiagen, Germany
QIAquick maxi Prepkit	Qiagen, Germany
TOPO TA cloning kit	Invitrogen, UK
Wizard plus Minipreps DNA purification system	Promega, UK

All chemicals and cell culture reagents were purchased from Sigma-Aldrich Company Ltd. (Dorset, UK) unless otherwise described.

2.2 GENERAL BUFFERS

2.2.1 10x Phosphate Buffered Saline (PBS)

For 1L, 80g sodium chloride (1.37mM), 2g potassium chloride (27mM), 14.4g NaH_2HPO_4(100mM), 2.4g KH_2PO_4 (18mM) were dissolved in 800ml of H_20 and pH to 7.4 before being made up to 1L.

2.2.2 10x TBE

For 1L, 104g Tris Base (1.1M) +55g Boric Acid (900mM) + 40ml 0.5M EDTA (25mM) were dissolved in 800mls of H_2O and adjusted to pH 8.3 before being made up to 1L.

2.2.3 Tris Tween Buffer Solution (TTBS)

For 1L, 6.05gTris/HCL (50mM), 8.76g sodium chloride (150mM), 1ml 0.1% (v/v) tween were dissolved in 800mls of H_2O and adjusted to pH 8.0 before being made up to 1L.

2.2.4 Transfer Buffer

14.4g glycine (192mM) + 3.03g Tris base (25mM) dissolved in 400ml dH_2O then made up to 800ml with dH_2O and add 200ml methanol to give a final volume of 1L.

2.2.5 RIPA Buffer

For 100mls 875mg sodium chloride (150mM) + 1.0% Triton X-100 + 10µl sodium deoxycholate (5%) + 500µl sodium dodecyl sulphate (20%) + 5ml Tris (1M) and filled with H_2O to reach 100ml.

2.2.6 Fixatives

4% (w/v) paraformaldehyde (PFA, Sigma-Aldrich, Poole, UK) was made up in PBS. PFA powder was dissolved in water by stirring at 60°C and adding drops of NaOH until the solution had cleared. The 4% PFA solution was stored at 4°C until required.

Methanol:acetone was made up as a 1:1 ratio of methanol (VWR, France) and acetone (VWR, France).

2.3 TISSUE CULTURE

2.3.1 Keratinocyte Isolation and Growth

All human samples were collected after informed, written consent and in accordance with Helsinki guidelines. Primary keratinocytes were isolated from fresh tumour or normal (non-malignant) skin samples and grown with a 3T3 layer, which had been mitotically inactivated (Rheinwald and Beckett 1981). 3T3 cells are a fibroblast cell line originally established from primary mouse embryonic fibroblast cells (Todaro and Green 1963). Primary keratinocyte isolation was performed by Karin Purdie from the Centre for Cutaneous Research Institute of Cell and Molecular science, Whitechapel, London, UK and Andrew South from the Centre

for Oncology and Molecular Medicine, Division of Medical Sciences, Ninewells Hospital and Medical School, University of Dundee, Dundee, UK. For the isolation and keratinocyte culture method, see Cancer Cell Culture: Methods and Protocols (Purdie, Pourreyron et al. 2011). Briefly, tumour tissue was placed in transport medium (Dulbecco's Modified Eagle's Medium (DMEM), supplemented with 10% FBS, 1x penicillin/Streptomycin (peni/strep), 100x 5,000 unit Penicillin/5,000 µg streptomycine/mL, GIBCO/Invitogen Ltd, Paisley) and 1x fungisone (100x, GIBCO/Invitrogen Ltd Paisley, UK) following excision and transported to the laboratory as quickly as possible. Transport medium can be used to store tissue at 4°C for up to 4-5 days; however cell viability reduces over time. Once in the lab, tumour tissue is washed in PBS before being "minced" into small fragments into a petri dish containing 1x EDTA/Trypsin (GIBCO/Invitrogen Ltd, Paisley, UK). The tumour fragments were then transferred to a tube containing trypsin and incubated at 37°C for an hour and shaken vigorously every 10 minutes throughout this period. Subsequently, an equal volume of (DMEM) with 10% foetal bovine serum (FBS, PAA laboratories Ltd, Somerset, UK) was added and the cells passed through a 100µm cell strainer. The cell suspension was then centrifuged at 500xg for 5 minutes and the recovered cells plated out into 100 mm dishes containing keratinocyte medium with a feeder layer of 3T3 cells before being incubated overnight at 37°C in 5% CO_2. Any undigested pieces of tumour were digested using collagenase D (Roche diagnostics, Burgess Hill, UK) in DMEM/10%FBS and left overnight at 37°C in 5% CO_2. 24hs later this collagenase/tissue suspension was then passed through a 100µm cell strainer and plated out into 100 mm dishes containing keratinocyte media (table 2.1) and feeders and incubated overnight at 37°C in 5% CO_2.'Keratinocyte media' containing 10% serum and growth factors has been previously described by Rheinwald and Beckett and was used as the culture medium used for most cells, unless otherwise stated. Primary keratinocytes are

usually observed after 48h post isolation. All cultures are established on a feeder layer of 3T3 cells however tumour keratinocytes were then subsequently grown in the absence of a 3T3 feeder layer, while normal human keratinocytes (NHK) depended on their presence. Table 2.2 shows a list of cSCC cell lines used within this thesis.

Product name	Company	Amount
Dulbecco's Modified Eagle Medium	Gibco Life Technologies Ltd, Paisley, UK	300ml
Ham's F-12 Nutrient Mixture	Gibco Life Technologies Ltd, Paisley, UK	100ml
Foetal Bovine Serum	PAA, Summerset, UK	10%
Cholera toxin	AbDSerotec (Kidlington,UK)	8.4 ng/ml
Epidermal Growth Factor (EGF)	Sigma-Aldrich (Poole, UK)	5 µg/ml
Hydrocortisone	Sigma-Aldrich (Poole, UK)	0.4 µg/ml
Insulin	Sigma-Aldrich (Poole, UK)	5 µg/ml
Transferrin	Sigma-Aldrich (Poole, UK)	5 µg/ml
3,3',5-Triiodo-L-thyronine sodium salt	Sigma-Aldrich (Poole, UK)	13 ng/ml

Table 2.1: Composition of Keratinocyte Media
This media was originally defined by Rheinwald and Green (Rheinwald and Green 1975) and adapted for culture of tumorigenic lines (Rheinwald and Beckett 1981). All the components listed were mixed together and stored at 4°C and used within a year.

Additional cell lines include:

Phoenix cells which are a retroviral packaging line based on a genetically engineered 293T cell line, (a human embryonic kidney line transformed with adenovirus E1a) which are highly transfectable and are capable of carrying episomes for long term stable production of retrovirus. RHence retroviruses are an efficient means to deliver DNA expression constructs to mammalian cells. These cells were maintained at 37°C, 5% humidified atmosphere with 5% CO_2in media containing only DMEM with 10% FBS (Pear, Nolan et al. 1993).

K1 cells which are normal HPV immortalised keratinocytes. These cells were maintained in the same keratinocyte media as the cSCC cell lines.

Cell line	Patient	Age	Sex	Tumour location	Histology	Metastasis
SCCIC1	Immuno-competent	77	M	Right temple	Mod differentiated	Yes
SCCIC8	Immuno-competent, on PUVA	51	F	Buttock	Poorly differentiated	
SCCIC12	Immuno-competent	87	F	Left calf	Moderately-poorly differentiated	
SCCIC15	Immuno-competent	73	M	Penis	Moderately differentiated	
SCCRDEB2	Col7A1 c.3832-1G>A	54	M	N/A	Poorly differentiated	No
SCCRDEB4	Col7A1 c.8244incC/c.8244insC	32	F	Left forearm	Moderately differentiated	N/A
SCCT1	Renal transplant	61	M	Forearm	Well differentiated	No
SCCT2	Renal transplant	66	M	Hand	Well differentiated	
SCCT8	Renal transplant	67	M	Ear	Poorly differentiated	

Table 2.2: Patient Data from Cell Lines Used Within This Thesis

Cell lines were isolated and established by either Karin Purdie from the Centre for Cutaneous Research Institute of Cell and Molecular science, Whitechapel, London, UK or Andrew South from the Centre for Oncology and Molecular Medicine, Division of Medical Sciences, Ninewells Hospital and Medical School, University of Dundee, Dundee, UK. IC; immunocompetant, REDB; Recessive Dystrophic Epidermolyosis Bullosa, T; transplant

2.3.2 Cell Maintenance

All cells were grown in an antibiotic free environment and incubated at 37°C with 5% CO_2:95% air in a humid atmosphere. All cell culture procedures were conducted in a Class II laminar flow cabinet. Where possible, equipment was autoclaved before use. Cells were routinely split using trypsin (GIBCO/Invitrogen Ltd, Paisley, UK) or trypsin diluted in PBS/versine (GIBCO/Invitrogen Ltd, Paisley, UK) and then centrifuged to remove the trypsin, before being re-suspended in fresh keratinocyte media and passaged 1/5 or 1/10. If cells had a fibroblast contamination, as many fibroblasts as possible were removed using diluted trypsin prior to keratinocyte removal. If cells required counting for experimental purposes, cell number was determined by a CASY®ModelTT cell counter (Roche Diagnostics Ltd, Burgess Hill, UK). This cell counter utilises multiple channel technology to give highly accurate cell counts. When counting cells 100µl of cell suspension was placed into 900µl of CasyTon (Roche Diagnostics Ltd, Burgess Hill, UK). Measuring is performed by suspending cells in CasyTon which is an electrolyte solution. During the measuring process a pulsed voltage is applied to the measuring capillary (which contains multiple channels) via a platinum electrode. The electrolyte filled capillary represents a defined electrical resistance and during the passage of individual cells through the capillary, the volume is the amount of electrolyte solution displaced, which enables the number of cells/ml. Additionally information on viability can be assessed; Intact cells are considered to be insulators and an increased level of resistance is achieved. By contrast, dead cells whose membrane is permeable have reduced resistance. Hence cell viability can be assessed by membrane integrity. An output of viable cells/ml was used unless otherwise stated.

The Casy has a good measuring range, >1:70000 in terms of volume and >1:40 in terms of diameter

2.3.3 Cryostorage of Cells

Cells were re-suspended at a concentration of 1 million cells per ml in freezing medium which is FBS with 10% DMSO. The FBS was always obtained from the same batch, as batch to batch variations can affect cell culture. Additionally, a new batch is always checked for its suitability before use. Cells were then aliquoted into cryovials (Themo Scientific Nunc, NC, USA) into 1ml volumes before being transferred into freezing (CoolCell®, Biocision, CA, USA) containers and placed at -80°C. 24 hours later they were transferred into long term storage in liquid nitrogen.

Thawing of cells from long term storage at -80°C, was carried out as possible under a hot running tap or a water-bath at 37°C for 1-2 minutes. Once thawed, the cells were transferred into 4mls of keratinocyte media before being centrifuged at 260g for 3 minutes. The media was then aspirated off and the cells re-suspended in fresh keratinocyte media without epidermal growth factor (EGF). The keratinocytes adhere to the culture plastic more efficiently in the absence of EGF, and were placed into a T25 flask following re-suspension.

2.3.4 Cell Fixation

Cells were seeded onto sterile glass cover-slips, of which there were 3 per well of a 6 well plate. Cells were then left to adhere overnight in an incubator at 37°C prior to fixation. To fix cells using methanol:acetone, first the media was removed and the cells washed in 1ml PBS. 500µl of ice-cold methanol:acetone was added to each well and placed at -20°C for 20 minutes. Methanol:acetone was then removed and cells washed 3x5 minutes with 1ml PBS. For fixation in PFA, the media was removed and cells washed, as above and cells incubated in 500mls PFA for 20 minutes at room temperature (RT). Fixed cells were then either used immediately or were stored at 4°C in PBS until required.

2.4 SIRNA TRANSFECTIONS

Knockdown of target gene expression was achieved by transfecting cells with the top thee oligonuceotides as ranked by Sigma-Aldrich, Poole, UK. Knockdown was then optimised by firstly transfecting the oligonucleotides individually and as a pool of all three, to see which obtained the biggest knockdown of gene expression. Transfection was performed using lipofectamine 2000 (Invitrogen Ltd, Paisley, UK) according to the manufactures instructions. Briefly, cells were transfected at 90-95% confluency using 5µl lipofectamine diluted in 250µl of Opti-Mem I reduced serum medium (Opti-Mem, Invitrogen Ltd, Paisley, UK) and incubated for 5 minutes, whilst a total of 5µg DNA was diluted in 250µl of Opti-Mem and this too was incubated for 5 minutes. After 5 minutes both mixtures were combined and incubated at room temperature for 20 minutes. Then the combined mix was added to the cells drop-wise, and cells returned to the incubator overnight. The most important aspect of siRNA transfections is to maintain the correct ratio of siRNA ~~DNA~~:lipofectamine. siRNA transfection was carried out for either 24 or 48 hours and duration is indicated in the results section where appropriate.

2.5 RNA/DNA MANIPULATIONS

2.5.1 RNA Extractions – Isolation and Purification

Cells were washed twice with ice cold PBS. In a fume hood, RNABee (Amsbio, Abingdon, UK) which contains phenol and guanidium thiocyanate, was added, to extract RNA. The phenol is water saturated and when used at a pH of 4.5, DNA is soluble in the phenol phase rather than the water phase, allowing the separation of the RNA from the DNA. Additionally, the guanidium thiocyanate in the RNAbee solution helps to lyse the cells and prevent the activity of RNAase enzymes denaturing the sample. Cells were scraped into the RNAbee

solution and the lysed cell suspension transferred to an ice-cold eppendorf. Chloroform was added in a 1:5 ratio to RNAbee, to the eppendorfs and the RNA samples were shaken vigorously for 30 seconds before being left for 15 minutes at 4°C. The samples were then subjected to centrifugal force (12,000g) for 15 minutes at 4°C. Centrifugation separates the sample into different phases; the lower blue phenol-chloroform phase (organic phase), interphase and the upper colourless aqueous phase. The RNA is exclusively in the aqueous phase and the DNA and proteins are in the interphase and organic phase. The aqueous phase is then transferred to a fresh tube and approximately the same volume of isopropanol is added to precipitate the RNA. At this stage the sample can be stored at -20°C until ready to complete the protocol. The sample is then placed in a centrifuge and spun (12,000g; 5mins; 4°C) where RNA is formed as a white pellet at the bottom of the tube. The pellet was then washed with 70% ethanol and the tube flicked until the pellet detaches. Tubes were then centrifuged again for further 5 minutes. The ethanol was then removed and the pellet was allowed to air dry for 5 minutes. Finally, the pellet was re-suspended in 30-50µl of nuclease free water (H_2O) or Tris/EDTA buffer (TE buffer, 10mM tris, 1mM EDTA)

2.5.1.1 cDNA Synthesis

The RNA was then used to generate cDNA which could be used for quantitative PCR analysis. 1µg template RNA was incubated with the Quantitect Reverse Transcription Kit (QIAGEN Ltd, West Sussex, UK), to synthesise cDNA and to remove any contaminating genomic DNA according to the manufacturer's instructions. Briefly, the template RNA was diluted in DNAse free H_20 to give a final concentration of 1µg in 12µl. Then 2µl of gDNA wipe-out buffer was added to give a total volume of 14µl. This was then mixed before incubating at 42° for 2 minutes. This reaction should clear any contaminating genomic DNA in the template RNA. This reaction was then combined with 1µl reverse transcriptase; 4µl

buffer and 1µl primer mix before incubating for 15 minutes at 42° to reverse transcribe the RNA into cDNA. The sample was then incubated at 95° to inactivate the reverse transcriptase. All reactions were prepared on ice.

2.5.1.2 Spectrophotometry

DNA and RNA were both quantified using the Nanodrop (Themo Scientific, Nanodrop 2000, NC, USA). Nucleotides such as RNA and DNA absorb at 260nm, which can be used to measure any molecules absorbing at that wavelength. The ratio of absorbance at 260nm and 280nm is used to assess the purity of the RNA or DNA within the sample. A ratio of ~2.0 is generally accepted as "pure" for RNA whereas DNA has a lower ratio of ~1.8 due to the higher 260/280 ratio of Uracil compared to Thymine. DNAse free H_2O or TE buffer was used as a blank to adjust for any background. TE buffer can be used as an alternative to solubilise RNA while the EDTA in the buffer protects the sample from degradation by nucleases.

2.5.1.3 Primer Design

Primers were manually designed and tested for gene expression unless otherwise stated. Primers are specific sequences designed to amplify a specific DNA sequence. All primers fulfilled the following parameter, in order to design the most efficient primer sets:

1. The 3' portion of each primer (about 15-20 bases) must be complementary to the DNA template. GC content, of around 20-80% range with 50% being the optimal was used to increase the stability of the primer.
2. The 3' portions of primers used in PCR should not be complementary to each other, because this facilitates the formation of primer-dimers. Additionally, long stretches (>4) of identical nucleotides were avoided.

3. Each primer pair was searched in BLASTN (Altschul, Madden et al. 1997) from the NCBI website (http://blast.ncbi.nlm.nih.gov/BLAST.cgi). This was to identify any homologous matches to ensure a single product was amplified.

All primers were obtained from Eurofins MWG Operon (Ebersberg, Germany) and the primers reconstituted in DNAse free H_20 to give a final concentration of 1nm/µl stock concentration according to the data sheet. This was then diluted 1 in 50 to give a 20pMol working solution. Recommended annealing temperatures were also included on the data sheet. However if insufficient amplification occurred, the annealing temperatures can be calculated manually using the following equation:

$$69.3 + (0.41(GC\%)) – 650/\text{Oligo. Length}$$

2.5.1.4 Reverse Transcriptase PCR (RT-PCR)

Reverse transcriptase Polymerase Chain Reaction (RT- PCR) is a variant of the polymerase chain reaction (PCR) which is used to quantitatively detect gene expression in sample cDNA. Generally it is used to check that the PCR primers were amplifying the correct product before quantitating the expression using quantitative PCR (described in section 2.5.1.6). RT-PCR was carried out either in 25 – 50µl volumes. Each 25µl reaction contained all the components listed in the table below (table 2.3).

Product	Volume (µl)	company
10x PCR buffer	2.5	stratagene
Forward primer	1	MWG
Reverse primer	1	MWG
Taq polymerase	0.25	stratagene
cDNA	1.5	N/A
dNTPs	0.5	Qiagen
DNAse free H_2O	18.25	Invitrogen

Table 2.3 RT-PCR reaction mix

All the products listed in the table were mixed together, forming the RT-PCR mix.

When analysing a number of samples a master mix was made up before adding the cDNA. Standard cycling conditions were used which are indicated below, where the annealing temperature is defined by the primer set and extension time can vary depending on the length of amplicon (1Kb products require 1 minute extension) (figure 2.1).

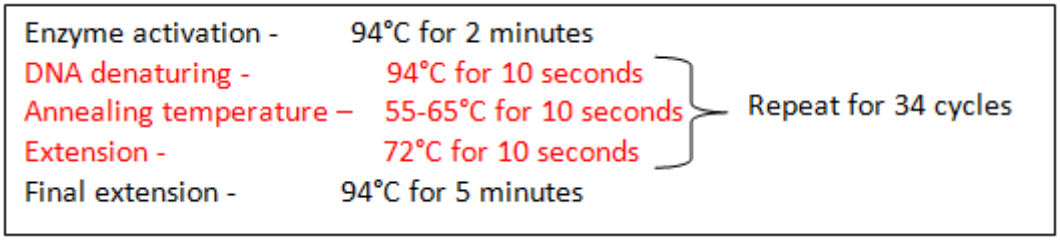

Figure 2.1: Standard PCR Cycling Times.

2.5.1.5 Agarose Gel Electrophoresis

PCR products were resolved on an agarose gel, were the percentage of agarose used in the gel depends on the size of product to be visualised (2% agarose gel for 0.1-1Kb fragments,

0.8-1% for 1-5Kb fragments). DNA fragments are resolved on the basis of size and charge. To begin, a 2% gel was dissolved in the microwave before adding Syber®safe DNA gel stain (Invitrogen 533102, 10µl/100mls) which allows the bands to be visualised using a UV light transilluminator (254nm). Syber®safe is a safer version of ethidium bromide – a DNA intercalating agent. The solution was allowed to cool slightly before pouring into a gel tray with combs and allowing it to set. Once the gel was solidified the PCR products were prepared with a 10x running buffer containing glycerol and bromophenol blue and 5-10µl of sample loaded into each well. The agarose gels were then run at ~100 Volts for approximately 40 minutes before being visualised using the Versadoc (BioRad Laboratories, Hertfordshire, UK).

2.5.1.6 Quantitative PCR

Quantitative PCR (qPCR) allows the user to amplify and simultaneously quantify a targeted DNA molecule. Subsequently the user can then calculate the gene expression relative to an additional housekeeping gene which is expressed at relatively constant levels in a cell. For quantitative measurement of mRNA SYBER Green Master Mix (QIAGEN, Hilden, Germany) was used. SYBER green is a nucleic acid gel stain which intercalates with double stranded DNA. PCR reactions were set up using the Automated PCR workstation QIAgility (QIAGEN, Hilden, Germany) and the Rotor-Gene Q (QIAGEN, Hilden, Germany) was used to detect fluorescence. The fluorescence is dependent on the amount of DNA. The rotor-Gene Q detects the intensity of the florescence and Rotor-gene Q series software (version 1.7) was used to calculate cycle threshold (Ct) values from the intensity of the fluorescence by the ΔΔCT method (Livak and Schmittgen 2001).

Gene	Primer sequence (‘5-‘3)	Tm°C
GSG2	F – ccagcctcaggtcagagttctc R - ctgtgcttgacagacctgga	60.4
BDKRB1	F – ctgaagtgcagtggcacaat R – ctctggttggaggattggag	60.2
PRSS21	F – accctccaggaagttaggt R - ataaggcacagggacacagg	59.4
PR_SAL1	F- ctcgtcgacgaattcggcaccaggccatg R – atggtcgacggctcaggttaggctccag	65.2
Maspin	F – ggtggggattccatagaggt R- aatcggcatccacagaaaag	57.35

Table 2.4 A List of Primer Sequences Used Within This Thesis

2.6 GENE SUB-CLONING

Sub cloning is a basic procedure in molecular biology required to move inserts from one vector to another to gain the desired functionality of insert. For this project the PRSS21 construct purchased from origene which was in a CMV vector, was removed and transferred into a pBABE vector which can be used for mammalian and retroviral expression. This enables PRSS21 to be stably expressed using retroviral transduction in a cell line rather than transiently expressed. Additionally, when expressed in a cell line with no endogenous PRSS21, over-expression can be used to explore the function of PRSS21 in this cell type.

Purified plasma Human cDNA for PRSS21 (transcript variant 1) was obtained from Origene (Origene Technologies Inc, MD, USA). The PRSS21 cDNA purchased was inserted in the vector pCMV6-XL4. The plasmid cDNA was used to transformed *E. Coli* and grown on agar plates (section 2.5.1) before being inoculated (section 2.5.2) and purification of plasmid DNA (section 2.5.3 and 2.5.4), which are noted in the appropriate sections below.

2.6.1 Transformations of Escherichia Coli (*E-coli)*

Electro-competent *E-coli* cells were transformed using electroporation. Electroporation is a method in which foreign DNA is introduced into host cells by applying a high voltage to increase the permeability of the cell membrane. Using this method 0.5µl of DNA was added to 20µl of Top10 electro-competent cells (Life Technologies/Invitrogen, Paisley, UK) in a 2mm electroporation curvette (Peqlab, Hampshire, UK) and kept on ice. The curvette was then electroporated at 20V and curvettes were immediately placed on ice after electroporation and 750µl of Super Optimal Broth (S.O.C) medium added. S.O.C medium is a nutrient rich bacterial medium used for microbiological culture. The contents of the curvette were then transferred to a falcon tube and shook at 37°C for 45 minutes. The transformed *E.coli* was then spread onto agar plates containing 0.1mg/ml ampicillin. Plates were then incubated overnight.

2.6.2 Inoculation of Colonies

Colonies that had grown on the agar plates were inoculated by picking single colonies with a pipette tip and placing in 5mls of Lysogeny broth (LB) containing 0.1mg/ml ampicillin. Cultures were grown at 37°C overnight. Glycerol stocks were created when a new clone had been produced. A glycerol stock was made by adding 800µl of overnight culture to a 2ml cryovial before adding 200µl of 80% glycerol and mixed. The vial was then frozen and stored at -80°C for further use.

2.6.3 Preparation of Plasmid DNA (5ml Plasmid Cultures)

A Wizard® plus Miniprep DNA purification system (Promega, UK) was used to elute the DNA from the overnight culture. 5ml LB broth that had been growing at 37°C overnight was aliquoted into three eppendorfs and a centrifuge used at 10,000 xg for 5 minutes to pellet

the cells. The supernatant was then re-suspended, lysed and neutralised using three different solutions provided in the kit, with centrifugation steps in-between. The supernatant was then purified using a resin and passed through a mini-column which bound the DNA. The DNA was then washed using multiple steps to purify the DNA before elution of the DNA in 30µl nuclease-free water. The DNA was then quantified using the Nanodrop (section 2.5.1.2).

2.6.4 Preparation of Plasmid DNA (100ml plasmid cultures)

Preparations of cultures of 100ml were prepared using a Qiagen plasmid plus kit (QIAGEN, Hilden, Germany), according to manufactures instructions. Briefly, cells were harvested by centrifugal force at 6000xg for 15 minutes at 4°C. The pellets were then re-suspended, lysed and neutralised using solutions in the kit before being passed through a QIAcartriage and high speed maxi tip provided in the kit. The DNA, which is bound to the high speed tip is then washed multiple steps before finally eluting DNA from the maxi tip, of up to 1mg.

2.6.5 Primer Design With Restriction Sites

Following purification of PRSS21 plasmid the PRSS21 gene had to be amplified from the vector DNA by PCR. However as the parent vector for PRSS21 (CMV6-XL4) did not have compatible sites with the destination vector (pBABE); primers were designed to include restriction sites. The primers noted below included SAL1 restriction sites:

PR_SAL1FWD: cgcgtcgcagcattcggcaccaggc (29)
PR_SAL1REV: atggtcgacggctcaggttaggctccag (28)

It must be noted that these restriction sites must not occur with the PRSS21 cDNA otherwise this will affect restriction digest. A RT-PCR was performed (see section 2.5.1.4) as before and products resolved on an agarose gel (2.5.1.5).

2.6.5.1 TOPO Cloning

TOPO cloning is a technique in which DNA fragments can be cloned in to a TOPO vector (Invitrogen Ltd, Paisley, UK) without the requirement of DNA ligases but relies on the biological activity of DNA topoisomerase I. Topoisomerase in a biological setting acts to cleave and re-join super coiled DNA ends to facilitate replication. It is important that fresh PCR amplified PRSS21 product is used for a TOPO reaction. With added restriction sites, a TOPO® reaction was performed using a Taq polymerase that lacks proof reading activity. The following reaction was set up:

1µ fresh PCR product

1µ Salt solution (provided by the manufacture)

5µ ddH2O

1 Topo® vector (provided by the manufacture)

The reaction was then incubated for 5 minutes at room temperature, and placed on ice following reaction incubation. The TOPO® cloning reaction was then used to transform *E. Coli* and grown on agar plates (section 2.5.1) before being inoculated (section 2.5.1) and purification of plasmid DNA (section 2.5.2). An RT-PCR was performed (section 2.5.1.4) and the products resolved on a gel (section 2.5.1.5) to determine if PRSS21 had been successfully inserted into the TOPO® vector.

2.6.6 Restriction Enzyme Digestion

To begin sub-cloning the PRSS21 insert had to be cut out of the TOPO® vector using common restriction enzyme sites to the pBABE destination vector, that are within their multiple cloning sites. Restriction enzyme digestion of PRSS21 TOPO® vector DNA was carried out in 3x 50µl volumes under the following conditions:

5µl plasmid DNA
10µl restriction enzyme SAL1
5µl restriction buffer
5µl BSA (10x)
35µl H_2O

In addition to the PRSS21 TOPO® DNA, pBABE empty vector DNA was also digested in the same manor. These reactions was then incubated at 37°C overnight before being run on a 1% agarose gel using electrophoresis. A 1% agarose gel was made (Standard melting point, Invitrogen, 16500-500) with 10µl Syber® Safe DNA gel stain.

2.6.6.1 Agrose Gel Purification of DNA

After electrophoresis the agarose gel was placed on a UV transilluminator (254nm) to visualise the DNA and the desired bands were excised with a scalpel. Any extra gel was removed to minimise the gel slice. The slice was then transferred to a 1.5ml eppendorf and weighed at ~230mg. QIAquick gel extraction kit was used to extract and purify DNA from the gel.

2.6.6.2 Agarose Digestion

To the gel slice 230µl of Buffer QG (provided by the kit) was added to the gel slice and the slice incubated at 50°C on a heating block for 10 minutes until the gel had completely dissolved. During this time the eppendorf was vortexed every 2-3 minutes to help the gel to dissolve. At this point the colour of the mixture was yellow. Then 230µl of isopropanol was added to increase the yield of DNA. The sample was then placed in a QIAquick spin column in a provided 2 ml collection tube to bind the DNA to the QIAquick column for 1 minute. The flow through was then discarded and the tube placed back into the tube. The column was then washed with 0.75 ml PE buffer (provided by the kit) and subjected to centrifugal force for another minute. The flow through was then discarded and the QIAquick column

centrifuged for an additional 1 minute at 13,000 xg. The QIAquick column was then transferred into a clean 1.5ml microcentrifuge tube and to elute the DNA, 50µl of nuclease free water was added to the centre of the membrane, left to stand for 1 minute and the column centrifuged for a further 1 minute.

2.6.6.3 Ligation of DNA Reaction

DNA ligase facilitates the joining of DNA strands together allowing the joining of the PRSS21 insert into the pBABE vector. A quick DNA ligase kit was used to perform the ligation reaction (Cat. M2200, New England Biolabs Inc., MA, USA). To begin, 50ng of the pBABE vector was combined with a 3-fold molar excess of the insert and the volume adjusted to 10µl with dH_2O. Then 10µl of 2x Quick Ligation Buffer was added along with 1µl of Quick T4 DNA ligase and mixed thoroughly. The reaction was then centrifuged briefly before incubating at room temperature for 5 minutes. The reaction was then chilled on ice and used to transform *E.coli* (section 2.6.1), which were grown on agar plates, colonies chosen (section 2.6.2) and PRSS21 pBABE plasmid DNA prepared (section 2.6.3). Plasmid DNA was then sent for sequencing to identify if the PRSS21 insert had been inserted into pBABE construct and had been inserted in the correct orientation properly.

2.6.7 Retroviral Transductions

Using healthy phoenix cells that have been split once every 2-3 days and not left confluent for any length of time, phoenix cells were seeded at 3.5 x 10^6 in a T25 per each transfection. These were then left overnight in the incubator to adhere. The next day the media was changed on the phoenix cells to 2.5ml of pre-warmed normal media. These cells were then transfected with Lipofectamine 2000 according to manufactures instructions. In another tube 2.5µg of DNA was mixed with 250µl OPTIMEM which was also left for 5 minutes. After

5 minutes these two tubes were mixed together and incubated for 20 minutes at room temperature. Following this time 500µl of this mix was added to the media on the phoenix cells and mixed gently. This was then incubated overnight. The next day the phoenix cells were recovered by replacing the media with fresh media and incubating overnight. 24hs later the cells were split into a larger flask T150 and expanded. Once the transfected phoenix cells had reached confluency the media was changed on the phoenix cells to a small volume (i.e. for a T150, 32mls of media was used) of the target media (normally keratinocyte media). These cells were incubated at 32°C overnight. On the same day the target cells were seeded at 2 x 10^4 cells per well of a 6 well plate and grown overnight at 37°C. The next day the conditioned media from the phoenix cells was collected and replaced with target media and returned to the incubator set at 32°C so that more virus could be collected. The conditioned media was filtered through a 0.45µm non-pyrogenic filter to remove phoenix cells. Polybrene was then added to this to prevent the viral particles from sticking to the plastic at a concentration of 8µg/ml. The media on the target cells was replaced with 2-3mls of filtered virus containing conditioned media. The cells were then spun in a centrifuge at 300g for 1 hour at 32°C. After this time the cells were immediately placed in the incubator at 32°C for another hour before replacing the media with fresh, pre-warmed 37°C media and recovered overnight at 37°C. This infection cycle was then repeated 2 more times to increase transfection efficiency. Then 48 hours following the last infection the cells were selected using 2-10µg/ml puromycin for pBABE-puro.

2.7 3D ORGANOTYPIC CULTURES

2.7.1.1 Collagen Matrigel Invasion Assay

The night before beginning the procedure the Matrigel (VWR ref 734-1100) was placed on ice in the fridge to defrost overnight. Plastic clonal rings (Sigma, ref: C3858-50EA) were sterilised in 70% ethanol for at least 10 minutes before washing them in PBS and putting them into a 6 well plate. Then to seal the ring, 200µl of microwave sterile noble agar (0.5% in PBS, autoclaved) was poured around the base of the ring. Before starting the procedure, all the components required were placed on ice and the pipette, tips and a 50ml falcon tube was placed at 4°C. To begin the procedure NHF were trypsinised and re-suspended in DMEM with 10% FCS at $2x10^6$ cells/ml. Then in an ice cold 50ml falcon tube the following components were added together: 3.5 volumes of collagen (Type 1 rat tail, VWR ref 734-1097), 3.5 volumes of matrigel, 1 volume of 10x DMEM (invitrogen 21430-020). These were then mixed gently and the pH was adjusted by adding Sodium hydroxide (NaOH, 1M) until the mixture became orange/pink (usually after around 100µl of NaOH). Then 1 volume of FCS and if fibroblasts are to be added, 1 volume of fibroblasts were added to the mixture. This was then mixed well before adding 800µl of gel mixture per ring. The gels were then placed in the incubator for 30 minutes to polymerise, before very gently adding 400µl of pre-warmed fibroblast medium with peni/strept on the gel and 1 ml around the ring. The next day keratinocytes were trypsinised and re-suspended in keratinocyte medium with peni/strep at a concentration of $1x10^6$ cells/ 700µl. The fibroblast medium was gently removed using a 1 ml pipette before adding 1 million keratinocytes onto each gel. 1ml of keratinocyte media with peni/strep was added around the ring and gels returned to the incubator overnight. The next day the ring was removed gently using a 200µl tip to detach the gel from the ring. A nylon disk, which had been previously sterilised in 70% ethanol,

washed in PBS and autoclaved, was placed under the gel and used to lift the gel onto a grid in a 6 well plate. Pre-warmed keratinocyte medium with peni/strep was added to reach underneath the gel – this was to lift the gel to provide an air/liquid interface (figure 2.2). The gels were then fixed a minimum of 7 days following lifting onto the grid. The gel on the nylon disk was transferred to 4% parafomaldyhyde in PBS to fix the gel for a minimum of 3 hours (preferentially overnight) before being transferred to 70% ethanol. Once in ethanol the samples were then kept in ethanol for a few days or processed and embedded straight away. Before the sample was processed the section was cut in half and placed into a histology cassette before being processed by an automated tissue processor (Shandon, Citadell 1000, Thermo Scientific) which dehydrates, clears and infiltrates the sample in wax before manually embedding the sample in a wax block which can be clamped into a microtome and sections cut from the sample. When embedding the sample is carefully orientated in molten wax and a cassette is placed on top of the mould, topped up with more wax and the entirety on a cold plate to solidify. When the block is solidified with its attached cassette it can be removed from the mould and is ready to be cut using the microtome (leica, RM2235).

2.7.1.1.1 Invasion Quantification

Sections were cut using the microtome and stained using haematoxylin and eosin stain. The images were then taken using a standard light microscope. The images were first processed using colour deconvolution into an 8-bit image and analysed using Image Pro PLUS® software. The invasion index was calculated based on the total number of invading particles (excluding the surface epithelium) times the total area of the particles for each image.

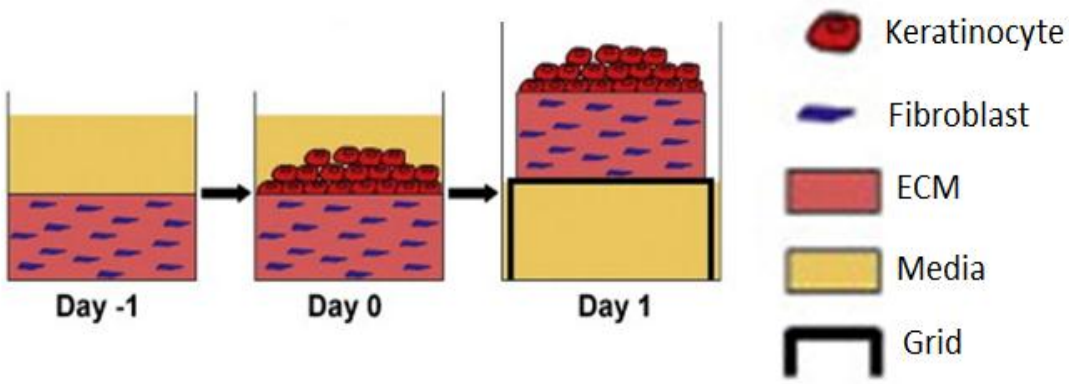

Figure 2.2 Schematic Showing Collagen Matrigel Invasion Assay Principal

A Schematic showing collagen matrigel system, in which a specialised collagen matrigel is used to represent the extracellular matrix (ECM). On day -1 ECM is mixed with fibroblasts and allowed to solidify in a ring before covering with media. The next day (day 0) keratinocytes are seeded onto the gel. Then day 1 is where the gel is raised above the liquid interface, allowing stratification of the keratinocytes. The collagen matrigel also facilitates invasion of keratinocytes into the gel due to its composition. Adapted from (Froeling, F.E. et al 2010).

2.7.1.2 Fibrin Gels

A second 3D organotypic method was also used which involved mixing fibrinogen and thrombin together which coagulate to form a gel. The gels were made firstly by dissolving 5.32ml NaCl (1.1% v/v) to 250mg fibrinogen (F3879, Sigma-Aldrich, Poole, UK). This solution was then agitated on a roller for 20 minutes at room temperature before being transferred into a 15ml falcon tube and placed on ice. Additionally a 5ml aliquot of thrombin (1 KIU of thrombin, T4648, Sigma-Aldrich, Poole, UK) was added to 333.3ml of 2mM~~M~~m $CaCl_2$ to give a stock solution of 3 IU/ml) was thawed and subsequently stored on ice. Before mixing the thrombin and fibrinogen together the fibrinogen was filtered sterilised using a 0.2µM filter. Then 5mls of thrombin was mixed with 5mls of fibrinogen to make the basis of the gel. Once these two components had been mixed together the following steps had to be performed quickly and on ice to prevent the gel from solidifying. Normal human fibroblasts (NHF) were trypsinised and counted to give a 2 million/ml stock solution in DMEM with 10% FBS. Then 750µl of this stock solution was added to the 10mls of the fibrin gel and mixed gently on ice, being cautious not to make any air bubbles within the gel. Then 1ml of this solution was added per well of a 12 well plate. This was left to set at room temperature for 15 minutes. After this time the set gel was covered with NHF medium with 6.3µl/ml stock aprotinin. The stock solution of aprotinin was made by adding 6mls of NHF medium to a vial of aprotinin (sigma-10820) to give a stock solution of 5000 units/ml. The gel was then left overnight at 37°C. The next day the media covering the gel was removed and replaced with 2 million keratinocytes in a total of 3 mls. These were then returned to the incubator and left to adhere overnight before being lifted using the same technique noted in (2.5.1.1) collagen matrigels.

2.8 PROTEIN EXPRESSION

2.8.1 Protein Extractions - Western Blotting

All protein extractions were carried out on ice. The cells were washed with ice cold PBS before being lysed in RIPA buffer (see section 2.2.5 for details) containing protease inhibitors (Roche complete protease inhibitor cocktail, Roche diagnostics, Burgess Hill, UK). Cells were then scraped into the buffer mixture and transferred into cold eppendorfs and left on ice for 30 minutes to allow for cell lysis. Following cell lysis, cell samples were ~~placed in a~~ centrifuged for 15 minutes at 13,000 xg at 4°C and the supernatant stored at -80°C until required for western blot. The total protein concentration of the lysates was measured using the Bradford assay according to the manufactures conditions (Sigma-Aldrich, Poole, UK). For the Bradford assay, serial dilutions of bovine serum albumin (BSA, Sigma-Aldrich, Poole, UK) were used to create a standard curve. The protein concentration of the lysates was then calculated by diluting the sample 1/10, and incubating it with Bradford reagent (Sigma-Aldrich, Poole, UK) and reading the absorbance of the sample of which protein concentrations were extrapolated from the standard curve. Generally protein samples were loaded onto a 4-12% Bis-Tris gel (Novex, Invitrogen Ltd, Paisley, UK) unless otherwise stated. Unless otherwise stated, 20µg~~l~~ of protein was loaded per lane. This was run using a NOVEX gel system (Invitrogen Ltd, Paisley, UK) and MES running buffer (Invitrogen Ltd, Paisley, UK) at 150V for approximately 1 hour. The gel was then transferred onto a Hybond C nitrocellulose membrane (GE healthcare Life Sciences, Buckinghamshire, UK) by wet transfer method. To block the membrane, it was incubated in 5% Marvel milk in PBST (phosphate buffered saline, 0.1% tween) – unless otherwise stated. The primary antibody diluted in block was then added either for an hour at room temperature or overnight at 4°C. Following incubation with the primary antibody the blot was then washed for 3 x 5 minutes in PBST

before adding the secondary antibody and rocking for 1 hour at room temperature (for primary antibody details see figure 2.5). After this time the secondary antibody was then removed and the blot washed for 4 x 5 minutes in PBST before detecting the bands using enhanced chemiluminescence (GE healthcare, Life Sciences, Buckinghamshire, UK) detection method. For this method, blots were incubated in ECL for 5 minutes before being developed in the dark room onto film (GE healthcare, Life Sciences, Buckinghamshire, UK) and the bands produced were compared to the protein molecular weight markers (Full-range Rainbow Molecular Weight Marker, GE healthcare, Life Sciences, Buckinghamshire, UK) to determine the molecular weight of the protein.

Antibody (species)	Dilution and dilutant	Company (Catalogue no.)
PRSS21 (mouse)	1/1000 dilution in 5% Marvel milk in PBST	Abcam (AB68534)
Maspin (mouse)	1/1000 dilution in 5% Marvel milk in PBST	Abcam (Ab95451)
GSG2	1/1000 dilution in 5% Marvel milk in PBST	Bethyl laboratories (A302-241A)
Notch1 (rabbit)	1/3000 dilution in 5% Marvel milk in PBST	Gift from Jon Aster.
Activated notch (rabbit)	1/1000 dilution in 5% BSA in PBST	Cell signalling (2421S)
GAPDH (mouse)	1/1000 dilution in 5% Marvel milk in PBST	Sigma (G8795-200UL)
Actin (mouse)	1/1000 dilution in 5% Marvel milk in PBST	Abcam (ab8226)
c-MYC (mouse)	1/1000 dilution in 5% Marvel milk in PBST	Origene (TA150121)
Involucrin (mouse)	1/10000 dilution in 5% Marvel milk in PBST	Sigma (I9018)
LH1 (mouse)	1/500 dilution in 5% Marvel milk in PBST	Gift from Declan Lunny

Table 2.5: Information on Antibodies Used for Western Blot Within This Thesis

2.8.2 Immunofluorescence of Cells

Cover-slips were cleaned and autoclaved before cells were seeded on them. Following fixation (for method see 2.3.4) cells were then washed 3x in PBS at room temperature and either stored in PBS at 4°C until required or used straight away for staining. Cover-slips were then carefully transferred onto a sheet of parafilm which self-contained any liquid on the cover-slip. Cover-slips were then incubated in PBST (PBS/0.1% triton X-100) for 5 minutes at room temperature. After 5 minutes this was then removed and replaced with a blocking agent (PBST/3% bovine serum albumin (BSA)) for 20 minutes at room temperature. After this time the primary antibody was then added in the blocking agent for 1h at room temperature or overnight at 4°C. Cover-slips were then incubated with a species specific secondary at room temperature for 40 minutes. During this time and steps subsequently after this, the cover-slips were protected from light. Cover-slips were then washed 3 times 5 minutes in PBS at room temperature before adding 10µl of Prolong® Gold anti-fade (Life technologies, Paisley, UK) was added to each cover-slip. This is a mounting medium which contains a DAPI counterstain. The cover-slips can then be immediately mounted onto a cover-slide. Slides were then either visualised after 15 minutes or stored at room temperature before being visualised using a fluorescence microscope.

2.8.2.1 Immunofluorescence of Paraffin Embedded Sections

Parafin embedded tissues were first cut into sections (4µM) using a microtome, before being mounted onto a slide. Slides were then dried overnight at 37°C. Slides were firstly deparaffinised in histoclear three times for 2 minutes. Following these slides were then rehydrated by firstly immersing slides in decreasing concentrations of ethanol (100%, 100%, 95%, 80%) for 2 minutes each. The slides were then immersed in running tap water for 3

minutes. Heat induced antigen retrieval was then used, for which the slides were placed in citrate buffer (10mM sodium citrate, 0.05%, Tween 20, pH 6) and heated in a microwave for 3x 3 minutes on full power. The slides were then cooled in the buffer at room temperature for 30 minutes before proceeding. After this time the slides were then rinsed for 3x 5 minutes in PBS. Sections were then isolated using a wax pen and incubated in PBST for 5 minutes before blocking in 3% BSA in PBST. Slides were then placed in a humidity chamber to prevent the sections from drying out. Primary antibody diluted in block was added to the slides for 1 hour at room temperature. Slides were then rinsed in PBS 3x for 5 minutes before being incubated in a species specific horseradish peroxidase secondary antibody for 40 minutes. During this time and subsequently the slides were kept protected from light. Slides were then washed 3x in PBS before 10µl of a DAPI mount counterstain was added per section and mounted onto a cover-slip.

2.9 FUNCTIONAL ASSAYS

2.9.1 Cell Viability Assay

Water soluble MTS is reduced to an insoluble purple formazin product by dehydrogenases of living cells especially in mitochondria. Following this reaction, solubilisation of the purple formazin product allows spectrophotometric comparison of cell viability in response to toxic insult (Cory et al. 1991). To begin, cells were seeded into 96 well plates at a cell density of 0.5 x 10^4 cells per well, in 200µl of keratinocyte media then allowed to adhere overnight. Where applicable cells were transfected using siRNA targeted to a particular gene and the appropriate controls included (see section 2.4 for siRNA transfection details). Immediately after the addition of the transfection reagent, 20µl of 3-(4,5-dimethylthiazol-2-yl)-5-(3-carboxymethoxyphenyl)-2-(4-sulfophenyl)-2H-tetrazolium (MTS) cell titre 96 aqueous

solution (Promega, Madison, WI) was added and left at 37°C for 3 hours this formed time point zero. Absorbance was read at 490nm using the platereader (M3, SpectraMax, molecular devices, CA, USA). After T0, the plate was returned to the incubator and MTS was added at set time points between 24 and 96 hours after treatment. Each time the MTS was added the plate was incubated for 3h before reading on the plate reader. MTS is toxic to the cells so each time MTS is added the cells in the well are not re-usable for another time point.

2.9.2 Cell Cycle Analysis

Cells were incubated with 30µM 5-bromo-2-deoxyuridine (BrdU, B9285, Sigma-Aldrich Poole, UK) for 30 minutes at 37°C. BrdU was made up in water as a 900µM (30X) stock and stored at -20°C. The media was then removed from the cells and transferred to a falcon tube along with the trypsinised cells. The sample was then centrifuged for 5 minutes at 1,500 RPM at 4°C (Sorvall RT7 plus, DJB labcare Ltd, Buckingshire, UK). Cells were then resuspended in PBS and then ethanol (70%) was added dropwise while vortexing. This was then left to incubate at 4°C overnight. Samples were then subjected to centrifugal force at 13,000 xg for 5 minutes at 4°C before pouring off the supernatant. 2ml per tube of fresh pepsin solution was prepared at 1mg/ml in 20mM HCL (pH 1.5) and pre-warmed to 37°C. 2ml of the pepsin solution was then added to each falcon tube and mixed for 30 minutes at 37°C. The samples were then pelleted by centrifugation (13,000 xg, 5 minutes) before pouring off the supernatant. 1ml 2M HCL was then added to the pellets for 18 minutes at room temperature and then topped up with PBS before centrifugation (13,000 xg, 5 minutes). Pellets were the washed again in PBS and a following time in antibody buffer (100ml PBS, 500µl tween, 0.5g BSA), pelleting cells each time by centrifugation (13,000 xg, 5 minutes). Pellets were then resuspended in 200µl of Becton Dickinson anti-BrdU antibody

diluted 1:50 in antibody buffer and incubated for 1h at room temperature. Following this, the cells are then pelleted and washed in PBS to remove the antibody. Cells are then pelleted again and re-suspended in PBS containing 25µg/ml propidium iodide solution (stock solution 1mg/ml) which acts as a counter stain and can be used to differentiate between apoptotic and normal cells. Samples are then kept on ice in the dark until analysed on the FACScan (LSR Fortessa, Becton Dickinson).

2.9.3 Cytotoxicity Assay

To measure cytotoxicity, the Cytotox 96 assay (Promega, UK) was used which measures the amount of lactate dehydrogenase (LDH) released from the cells into the media. The colour range is proportional to the number of lysed cells. Lysates are collected from all the wells. The lysis buffer is diluted and added to untreated well and left for 45 minutes at 37°C. This is then collected as with the others and is used as the high control, while the UT lysate is low control. All lysates are subjected to centrifugal force (250xg) for five minutes at 4°C. 50µl of lysates are plated per well of a 96 well plate, with media being used as the background. The 50µl of substrate is added to each well and left in the dark to develop for 30 minutes. Finally 50µl of stop solution is added to each well and the colour change is measured using a plate reader at 490nm

2.9.4 Annexin V Staining Method

Cells were seeded at a cell density of $2.5x10^5$cells/well of a 6 well plate, with 3 wells seeded per treatment. The following day, the cells were treated with siRNA targeted to BDKRB1, GSG2 or PRSS21 (following siRNA transfection protocol, see section 2.4). Controls were also included; a positive cell death siRNA (AllStars, Qiagen, Hilden, Germany), no treatment and mock control only. The cells were then left for 48 hours before collecting all the media and

cells following treatment. Cells were then centrifuged to pellet the cells at 2500rpm for 5 minutes, before pouring off the supernatant. Cells were then washed twice with ice cold PBS before being re-suspended in 1x binding buffer at a concentration ~$1x10^6$. 100µl of this solution was then transferred to a 5ml tube. 5µl of FITC Annexin V (Becton Dickinson, NJ, USA) was added to each tube and 10µl of 7-ADD (Becton Dickinson, NJ, USA) was added, the cells gently mixed and incubated for 15 minutes at room temperature in the dark. After 15 minutes 400µl of binding buffer was added to each tube before being analysed on the FACScan (Becton Dickinson, NJ, USA).

2.9.4.1 Cell Death ELISA

Cells were seeded into 24 well plates at a cell density of $1x10^5$ cells per well and transfection was carried out as previously described (section 2.4). For detection of apoptosis the Cell Death ELISA (Roche Diagnostics, IN, USA) was used to determine nucleosomal cleavage and release into cytoplasm upon DNA degradation (this was carried out according to the manufactures instructions). At different time points between 48- 96 hours, 20µl of cell extracts were plated in a streptavidin coated 96 well plate and incubated for 2 hours with 80µl immunoreagent (anti-histone-biotin antibody and anti-DNA-peroxidase antibody) before washing three times with wash buffer and adding 100µl substrate reagent for 20 minutes. The absorbance was then read on the plate reader at 405nm.

2.9.5 Cell Migration Assay

Keratinocyte migration was assessed by an *in-vitro* scratch assay, where cells are grown to confluency and physically scratched using a tip and images taken at the time of the scratch and at a number of time points after to assess the migratory capacity of cells following treatment. Briefly cells were seeded at a cell density of $5x10^5$ per well a 24 well plate.

Confluent cultures were then treated with mitomycin C (10µg/ml) for 3 hours at 37°C to inhibit proliferation. Subsequently a uniform scratch was made using a P200 plastic tip. Cells were then washed 3x 5 minutes in PBS to remove any excess cells and returned to the incubator in media at 37°C. Before returning to the incubator, cultures were photographed to represent the scratch at T0, then again 4 and 18 hours later. To calculate the percentage change in area, the areas were calculated using CS4 Adobe Photoshop and the percentage change in area over time calculated.

2.9.6 Proximity Ligation Assay (PLA)

The proximity ligation assay (PLA) (Duolink, sigma-Aldrich, Poole, UK) is a modified version of immunofluorescence in that it utilises secondary antibodies called PLA probes which have short DNA oligonucleotides attached. The assay principal allows for protein-protein interactions to be detected. To begin, an SCCRDEB2 keratinocyte xenograpft tissue section mounted on a slide was incubated over night at 4°C, with two primary antibodies raised in different species, which recognise both PRSS21 and Maspin. A no primary control was also included. Both antibodies were made at a 1 in 100 dilution and mixed together. The next day, the slide was washed 2x in PBS before adding 50µl of both rabbit and mouse PLA probes to 150µl of block, and adding 40µl of this PLA probe solution per xenograft tissue section. The tissue section was then incubated in a humidified chamber for 2 hours at 37°C. Subsequently a ligation reaction was performed by mixing 40µl of ligase buffer with 155µl H_2O and 5µl of ligase, again adding 40µl of this ligase solution per section. The tissue was incubated in a humidified chamber for a further 30 minutes at 37°C. After this time, the xenograft was washed with buffer A (which was provided by the kit) for 2x 5 minutes before the polymerase step. For the polymerase step, 40µl of stock was added to 155µl of H_2O and 5µl of polymerase. This was mixed together before adding 40µl per section and incubating

at 37°C for 2 hours. The sample was then washed in buffer B (which was provided by the kit) for 2x 10 minutes and a quick wash in 0.1% dilution of buffer B. The sample was then dried in the dark before mounting using DAPI mounting media.

2.10 STATISTICAL ANALYSIS

Unless otherwise stated, the data was reported as the mean ± SD from a representative experiment. The t-test was used for comparing results, and statistical significance was based on $P<0.05$. All experiments were performed at least 3 times each time with 2 or more independent observations.

Chapter 3 Validation of Targets Identified from Gene Expression Array

3.1 INTRODUCTION

3.1.1 Gene Expression Array and Identification of cSCC Gene Signature (Watt 2011)

Previous work published from our lab used microarray technology to elucidate potential molecular targets in cSCC by revealing a cSCC gene signature (Watt 2011). An integrative gene expression analysis was devised comparing gene expression in a range of clinical data sets containing normal skin, cSCC and the hyper-proliferative condition psoriasis. 435 dysregulated genes, which were capable of distinguishing cSCC from normal skin (*in-vivo*) were identified by comparing cell populations isolated from cSCC and normal human keratinocytes (*in-vitro*). These genes were then stratified against three *in-vivo* data sets; one of which was performed by our group comparing RNA isolated from fresh frozen cSCC (n=9) and non-cSCC skin (n=5) while the remaining two were from publically available experiments (GDS2200 (Nindl, Dang et al. 2006) and GSE7553 (Riker et al. 2008)). Of these genes, 154 were expressed in the same way across three independent *in-vivo* data sets.

A comparison between fold change of psoriatic data sets from lesional and non-lesional areas (GSE13355 and GSE14905 (Romanowska, Reilly et al. 2010)), and fold change of cSCC versus normal skin (Watt et al 2011) revealed that the majority of the 154 genes dysregulated *in-vivo* cSCC were also dysregulated in psoriasis. The purpose of this

comparison was to identify cSCC specific genes through comparison with a hyper-proliferative, benign condition. However, 37 genes did not show similar dysregulation and hence were termed 'cSCC specific'. Of the 37 cSCC specific genes, 29 of these genes were concordantly regulated *in-vitro* and *in-vivo* – 8 of which were down regulated and 21 which were up-regulated. The fold change of the 21 up-regulated cSCC genes are detailed in Table 3.1.

3.1.1.1 Microarray Technology

Microarrays have been utilised for a large number of studies to analyse the expression of thousands of genes quickly and efficiently (Southern, Maskos et al. 1992). They have been used to validate a number of hypothesis including: characterising disease states, molecular response to therapeutics, prognosis and typically looking at changes between disease and normal (Meltzer 2001; Mohr, Leikauf et al. 2002). The latter is important when devising customised targets for personalised medicine.

Microarrays are small "chip" like slides made from glass or silicon. Attached to the slides are probe DNA sequences which allow for the hybridisation of complementary DNA strands. The technique is based on hybridization, which uses DNA probes to identify complementary molecules that are able to base-pair with one another. On binding, the substrates are washed to remove any unspecific binding. Hybridised sequences generate a fluorescent signal due to the fluorescently labelled samples. The signal varies depending on the amount of sample bound to the probe. Microarrays use relative quantification, where the intensity of a sample is compared to the intensity of the same gene under a different condition (Shalon, Smith et al. 1996).

Table 3.1 Fold Change of 21 cSCC Up-regulated Targets Identifed Using Microarray Technology

The table shows the *in-vitro* and *in-vivo* fold change of the 21 cSCC specific up-regulated genes. The fold change was determined by comparing *in-vitro* cSCC to NHK and *in-vivo* to normal skin (Watt et al 2011).

GENE	Gene ID (NCBI)	In-vitro cSCC FC	In-vivo cSCC FC
BDKRB1	623	8.4	1.3
BUB1	699	3.3	2.7
C20orf20	55257	2.3	1.3
C6orf150	115004	19.2	3.1
PSMG3	84262	2.4	1.4
CDC25C	995	5.4	1.5
CENPN	55839	4.7	2.2
ELF4	2000	2.6	2.1
FLT3LG	2323	3.8	1.4
FUCA2	2519	4.2	1.6
GSG2	83903	5.8	1.3
LOC152217	152217	2.6	1.3
NUTF2	10204	1.6	1.5
PARP1	142	2.5	1.5
PLK1	5347	3.7	3.1
PRSS21	10942	7.4	1.5
RSRC1	57319	2.5	1.8
SH3TC1	54436	4.3	1.5
SUPT16H	11198	2.3	1.5
WDHD1	11169	2.8	2
WDR67	93594	2.5	1.5

3.1.2 RNAi screening (Watt 2011)

Following identification of 21 up-regulated genes, RNA interference (RNAi) mediated knockdown of each gene individually, using a custom made siRNA library was carried out (Watt 2011). Three individual oligonucleotides per gene, in addition to a pool of all three oligonucleotides, was assessed using cell viability as readout over a time course. Using this siRNA knockdown method, two cSCC keratinocyte populations were screened, SCCRDEB2 and SCCIC1, compared to non-targeting negative control siRNA. All three oligonucleotides targeted to Polo-like-kinase (PLK1) and C20orf20 consistently reduced cell viability. These

two genes are currently under study by other members of Dr AP South's team. In addition to these targets a further three genes were highlighted as potential targets, due to being capable of reducing cell viability *in-vitro* using 2/3 siRNAs and the pool: *PRSS21*, *GSG2* and *BDKRB1*. In follow up of this work performed in the lab, these three genes have been further validated in this thesis as potential targets for cSCC.

3.1.2.1 RNAi Technology (Watt 2011)

RNAi technology has revolutionised studies to determine the role of a gene. Furthermore it has enabled researchers to explore the role of a gene's expression in different disease states such as cancer. Synthetic small interfering RNAs (siRNA) can be easily and inexpensively used to silence gene function in cultured mammalian cells. The phenomenon of specific RNA inactivation was first discovered in plants as a defence mechanism against virus infection (Wassenegger, Heimes et al. 1994; Hamilton and Baulcombe 1999) and later in *Caenorhabditis elegans* (Fire 1999). It was discovered that they produced small double stranded nucleotides that act specifically to down regulate gene expression. The mechanism is driven by a key enzyme, Dicer, which is a cytosolic ribonuclease capable of digesting long double stranded RNAs into short RNA (figure 3.1). These double strands are then un-wound and a single strand associated with the RNA-induced silencing complex that leads to target destruction by cleaving mRNA that is complementary to siRNA (Wall and Shi 2003). A number of transfection methods are available which allow cellular uptake of synthetic siRNA. Broadly speaking they can be divided into biological, chemical and physical, and depending on the nature of the genetic material, can be transient or stable (for a review see (Kim and Eberwine 2010).

Of note siRNA treatments have been developed for a number of diseases, for example BACE1 in Alzheimer's disease or for the BCL/ABL translocation in chronic myloid leukaemia, where siRNA induces apoptosis (Ryther RC et al 2005). However, in cSCC delivery and degradation of siRNA present limitations for use in patients and formulation of small molecular inhibitors/ agonists would have much greater potential.

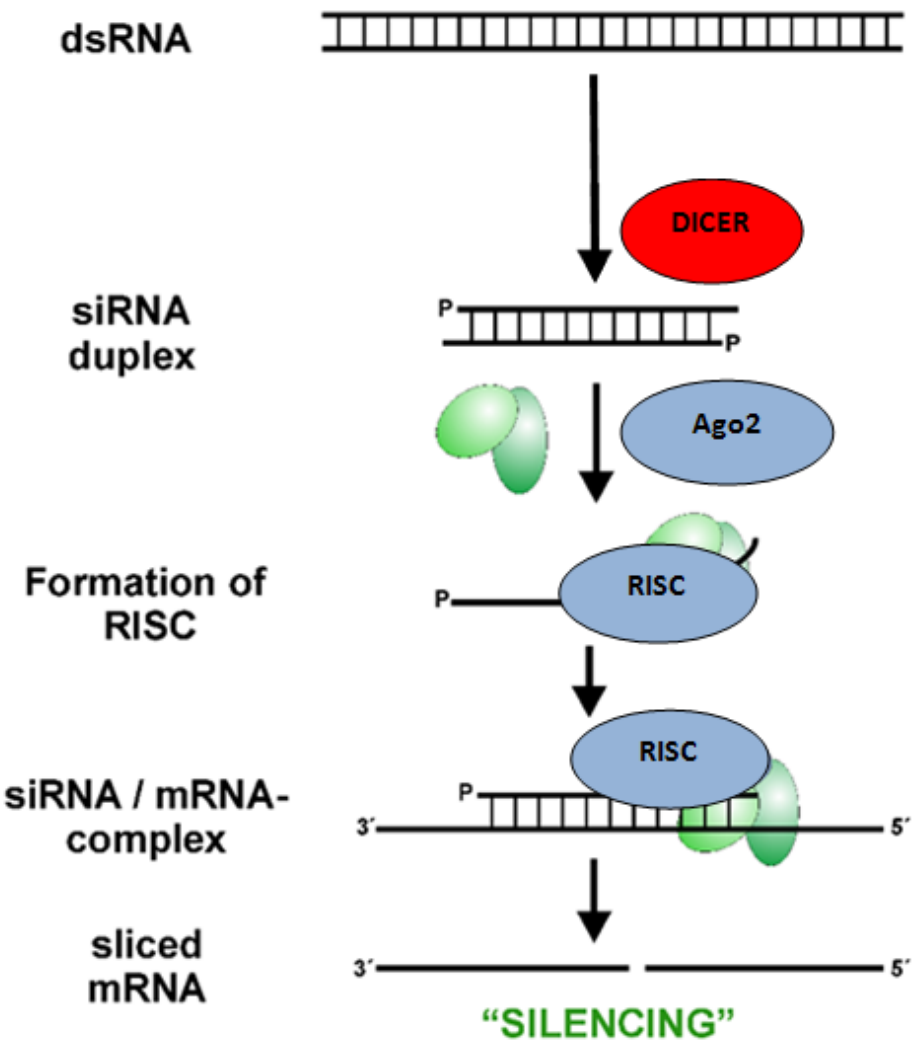

Figure 3.1 Model for RNAi Mediated Degradation

Long double stranded RNA (dsRNA) is cleaved by DICER into short double stranded fragments called small interfering RNA (siRNA) which results in the recruitment of Ago2 and other complexes. Subsequently, Ago2 cleaves the siRNA then associates with the target mRNA allowing association of RNA induced silencing complex (RISC) that leads to target silencing.

3.1.3 Germ Cell Associated 2 (GSG2)

Germ cell associated 2 (GSG2, also referred to as haspin, haploid germ cell-specific nuclear protein kinase) is a serine/threonine kinase, first discovered as a testis specific gene; however Higgins and colleagues have previously detected its mRNA expression, at low levels in other proliferating and differentiated tissues (Higgins 2001). This would suggest that the gene is not exclusively germ cell specific. GSG2 functions to phosphorylate histone H3 at Ser-3 during mitosis which is necessary for cell cycle progression (Dia 2005). Histones play a central role in transcription regulation, DNA repair, DNA replication and chromosomal stability through being essential components of the nucleosome. Histone H3 is one of five main histone proteins involved in structure of chromatin and can undergo several types of post translational modifications including phosphorylation of serine amino acids (Zhang and Reinberg 2001). Additionally, GSG2 regulates the cell cycle of haploid germ cells by positioning and activating aurora B and other components of the chromosomal passenger complex (CPC) at the centromeres. This ensures chromatid cohesion, metaphase alignment and normal progression through the cell cycle. RNAi depletion of GSG2 perturbs chromosome biorientation and sister chromatid cohesion (Dai and Higgins 2005; Dai, Sullivan et al. 2006; Markaki, Christogianni et al. 2009; Higgins 2010). Hence, its importance in mitosis and regulation of other cancer associated proteins and processes, would highlight it as a good potential target for cancer.

There is not a vast amount of literature on GSG2 and its expression in cancer, although it has been shown to be over-expressed in lymphomas (Rosenwald, Alizadeh et al. 2001; Dave, Fu et al. 2006). Despite this there are a number of small molecular inhibitors to GSG2, which

would also further suggest its potential as a therapeutic target. Mitotic kinase inhibitors have been shown by a number of studies, to have fewer side effects than traditional cytotoxic drugs, and some of the inhibitors are in clinical trials such as those targeting, cyclin dependant kinases (Vassilev, Tovar et al. 2006; Malumbres, Pevarello et al. 2008), PlK1 (Gleixner, Ferenc et al. 2010) and aurora kinases (Harrington, Bebbington et al. 2004; Girdler, Gascoigne et al. 2006). Data on CHR-6494, a specific inhibitor of haspin, showed that it causes significant antitumor activity through mitotic catastrophe in apoptosings cells (Huertas, Soler et al. 2012). This would suggest that GSG2 would be a promising target for cancer therapy.

3.1.4 Bradykinin Receptor B1 (BDKRB1)

Bradykinin receptor B1 (BDKRB1), encodes a transmembrane protein which functions as a G-coupled receptor named Bradykinin B(1) receptor (B_1R). Bradykinin, a 9 amino acid peptide, can bind to B_1R to mediate responses to a number of pathologic conditions. B_1R is expressed at low levels in normal tissues however is upregulated during conditions of inflammation, trauma, burns, shock and allergy (Calixto, Medeiros et al. 2004; Leeb-Lundberg, Marceau et al. 2005). Additionally, there have been a number of reports which show it is up-regulated in cancers including breast (Esseghir, Reis-Filho et al. 2006), prostate (Taub, Guo et al. 2003) and lung (Gera, Fortin et al. 2006). Molina and colleagues, demonstrated up-regulation of the B_1R receptor in breast cancer cells both *in-vitro* and *in-vivo.* Additionally, to investigate the consequences of stimulation of the receptor in these cells, they used various concentrations of a B_1R agonist Lys-des[Arg9]-bra-dykinin, the B_2R agonist bradykinin or EGF *in-vitro*. This lead to increased proliferation, through transactivation of EGF and lead to subsequent activation of the ERK1/2 mitogenic pathway. The significance of this as mentioned in chapter 1, is that a number of studies have shown that ERK1/2 signalling plays

a role in cancer progression (section 1.3.1.2). Silencing or antagonism of B_1R is considered to be an effective option to decrease growth in breast cancer. Receptor activation has also been noted in prostate cancer cells to increase migration, cell growth and invasion (Taub, Guo et al. 2003). Additionally, Bradykinin signalling enhances cell migration and expression of integrin through activation of phospholipase C, protein kinase C and NFκB pathways (Yang et al 2010). Both studies would suggest that B_1R inhibition would be an effective therapy for cSCC.

3.1.5 Protease Serine 21 (PRSS21)

Protease, serine 21 (PRSS21), also known as testisin, is a protease which was first reported to be highly expressed in testicular germ cells, but with little expression in normal tissue (Hooper, Nicol et al. 1999; Hooper, Bowen et al. 2000). In the testis it is required for epididymal sperm maturation and fertilizing ability, since mouse sperm lacking PRSS21 display several functional abnormalities in sperm (Yamagishi, Honda et al. ; Netzel-Arnett, Bugge et al. 2009). The C-terminus domains of PRSS21 molecules are post-translationally modified with a glycosylphosphatidylinositol (GSI) anchor which localises it to cholesterol-rich lipid rafts on the cell surface (Hooper, Nicol et al. 1999). Several of the membrane anchored serine proteases are over-expressed by tumour cells and are implicated in the promotion of cancer (Lee et al 2005, List et al 2005). Pericellular proteolysis is an important pathway by which cells can interact with the cell microenvironment, leading to tumour invasion and metastasis. PRSS21 is over-expressed in a number of cancers including: ovarian, cervical, melanoma and lymphoma (Hooper, Nicol et al. 1999; Hooper, Bowen et al. 2000; Honda, Yamagata et al. 2002; Tang, Kmet et al. 2005). Furthermore, PRSS21 promotes transformation when over-expressed in cell culture and mouse xenograft model systems of which it's catalytic; serine protease activity is required for transformation. Additionally,

siRNA depletion of PRSS21 expression increased apoptosis and diminished ability to form colonies in soft agar in ovarian cancer (Tang, Kmet et al. 2005). Another study, by Yeom and colleagues showed that PRSS21 increases invasion using its enzymatic ~~serine~~ activity (Yeom, Jang et al. 2010). They also showed using a yeast two hybrid system that it interacts with the tumour suppressor mammary serine protease inhibitor (maspin) to modulate cell death and invasion in cervical cancer cells. Thus inhibition of PRSS21 may prevent tumour progression in cSCC.

3.2 RESULTS

3.2.1 RNAi Screen Confirms PLK1, C20orf20 and PRSS21 as Important for Cell Survival and Identifies a Further Three Potential Novel Targets for cSCC

In a similar manner to the original screen performed by Watt and colleges, an RNAi screen with cytotoxicity as a readout was used, to further confirm/identify potential targets for cSCC using the microarray data. Using a pool of all 3 oligonucleotides targeted to the 21 cSCC specific genes that were identified in the microarray, a primary cSCC keratinocyte cell line SCCRDEB2 was assessed for cytotoxicity 48 hours following gene depletion (figure 3.2). This method identified C20orf20, PLK1 and PRSS21 to significantly ($P<0.005$) increase cytotoxicity in 4 independent experiments, 48h following transfection compared to a non-targeting siRNA control (SCR). The SCR which was 40% was used as a baseline cytotoxicty which was slightly higher than expected. Additionally, 3 other genes – poly[ADP-ribose]polymerase1 (PARP1), fucosidase, alpha-L-1-plasma (FUCA2) and proteosome assembly chaperone 3 (PSMG3) were also found to significantly ($P<0.05$) increase cytotoxicity, as determined by the students t-test.

Figure 3.2

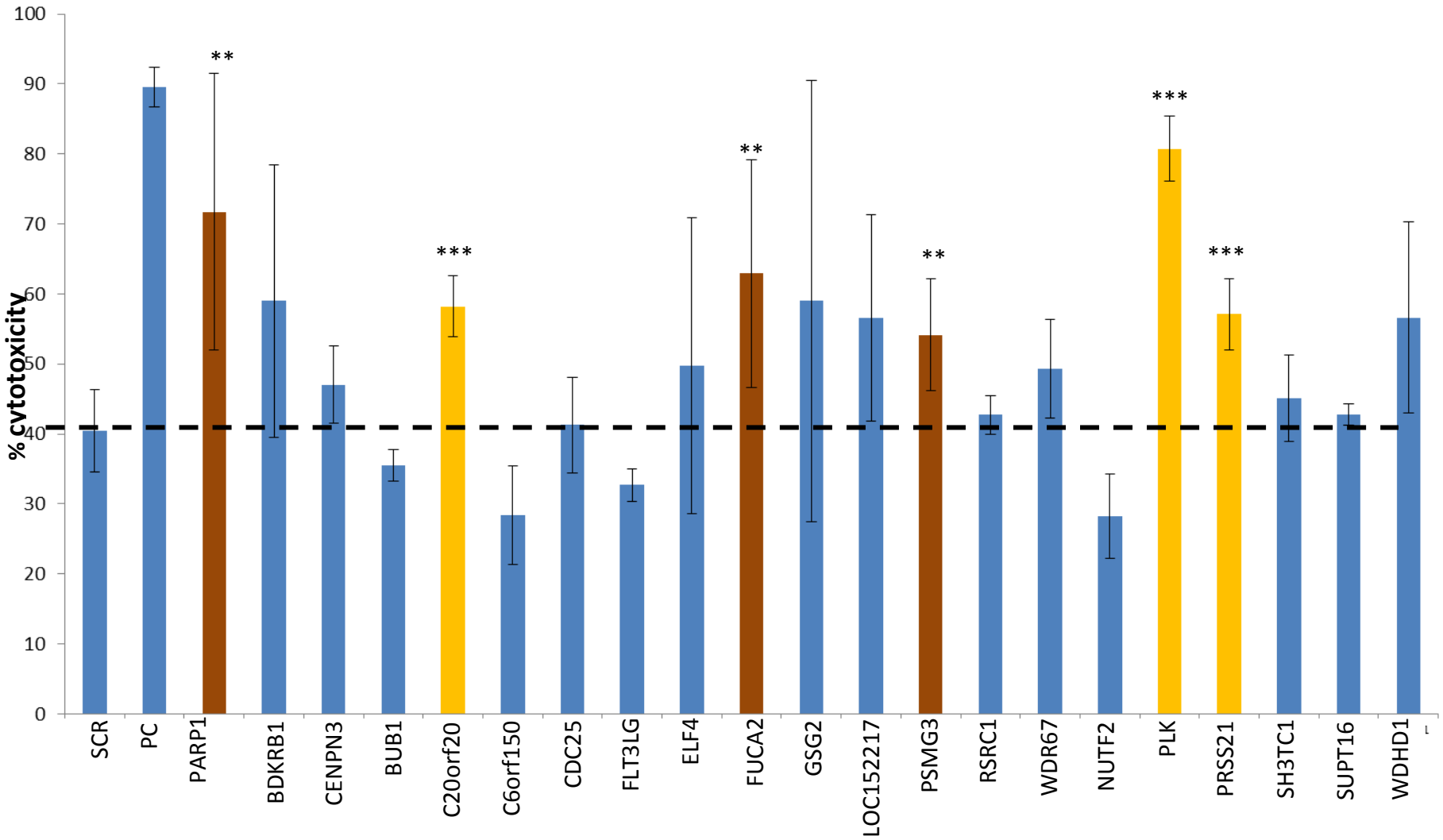

Figure 3.2 Cytotoxicity Screen Confirms C20orf20, PLK1 and PRSS21 as Potential Targets and Further Identifies Novel Targets for cSCC - PARP1, FUCA2 and PSMG3
Results represent the percentage cytotoxicity in SCCRDEB2 cells compared to media only control, using the LDH assay, 48h post-transfection of siRNA targeted to the 21 cSCC specific genes identified in the microarray (Watt et al. 2011, see table 1 for gene IDs). Results show that depletion of C20orf20, PLK1 and PRSS21 highly significantly (***<0.0005, highlighted in yellow) induces cytotoxicity compared to SCR. This screen also revealed depletion of PARP1, FUCA2 and PSMG3 as significantly (**<0.005, highlighted in maroon) able to induced cytotoxicty. Results represent the mean ± SD of 4 independent experiments with the probability calculated using the student's t-test. PC represents the cell death positive control siRNA. Dotted line indicates base line, following normalisation to SCR.

In follow-up, cytotoxicity was explored in 2 cSCC cell lines, SCCIC1 and SCCRDEB2 cells, but also in primary normal human keratinocytes (NHK) using the individual siRNA duplexes to assess the contribution of each duplex to cytotoxicity and to monitor off target effects (figure 3.3). The genes explored were GSG2, PRSS21, PLK1, PSMG2, FUCA2 and PARP1. BDKRB1 was not included knockdown using individual siRNA duplexes had already been performed by a BMSc student in the lab (S.Gaw, University of Dundee, UK). For all the genes explored, knockdown induced no cytotoxicity in the NHK cells which increases their specificity as a molecular target for cSCC without affecting normal cells. Generally, both cSCC cell lines showed similar cytotoxicity following knockdown and are in agreement with the previous results. These results indicate that depletion of *PRSS21* using 2/3 duplexes increases cytotoxicity for PRSS21.

Figure 3.3

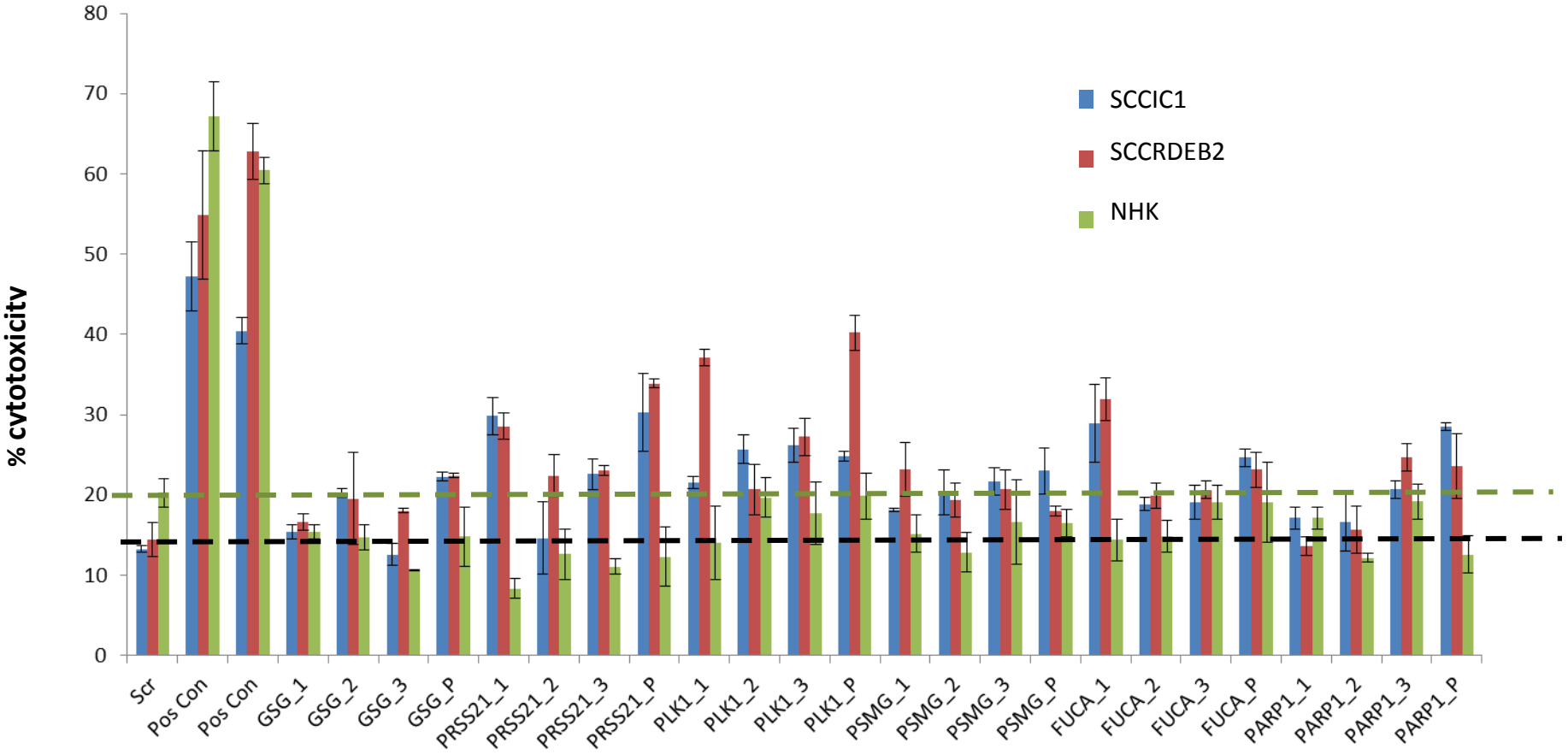

Figure 3.3 Cytotoxicity Screen of GSG2, PRSS21, PLK1, PSMG, FUCA2, PARP1 Using Individual and Pooled Duplexes in Normal Human Keratinocytes, SCCIC1 and SCCRDB2 Keratinocytes

Assessment of cytotoxicity following knockdown using individual (X_1,2,3) and pooled siRNA (X_P)duplexes. Cytotoxicity tested in SCCIC1 (blue) SCCRDEB2 (red) and normal human keratinocytes (NHK, green) cell lines. Results represent the mean ± SEM of two individual experiments. SCR, scrambled, Pos Con; positive control. Black dashed line indicates base line cytotoxicity in the cSCC cells and the green dashed line indicates the base line cytotoxicity in the NHK cells.

3.2.2 Validation of GSG2, BDKRB1 and PRSS21 as Molecular Targets for cSCC

3.2.2.1 Germ Cell Associated 2 (GSG2)

3.2.2.1.1 GSG2 is Over-expressed in cSCC Both at mRNA and Protein Level

GSG2 is over-expressed both *in-vitro* (fold change of 5.8) and *in-vivo* (fold change of 1.2), in cSCC compared to NHK or normal skin, respectively, using microarray technology (Watt et al. 2011). To confirm this, qPCR was used to compare the expression of *GSG2* in SCCRDEB2 keratinocytes and NHK cells. This demonstrated an 11 fold increase in the levels of *GSG2* in these cSCC cells compared to NHK (Figure 3.4A). Figure 3.4B uses immunoblotting to compare the expression levels of GSG2 in SCCRDEB2 to NHK lysates. This data confirms that the over-expression of GSG2 is seen at both protein and mRNA level. Both qPCR (figure 3.4C) and western blot (figure 3.4D) were employed to look at GSG2 expression following knockdown of its expression using siRNA. Knockdown of *GSG2* expression was statistically significant ($p=0.005$) using oligonucleotides – GSG_1 and GSG_3 compared to a non-targeting control. However the knockdown using oligonucleotide GSG_2 was ~30% less effective than the other oligonucleotides at reducing *GSG2* expression. Due to the off target effects of GSG_2, which would in turn dilute the overall effect of the pooled nucleotides (GSG_P), it was not included in any further knockdown experiments for GSG2.

Figure 3.4

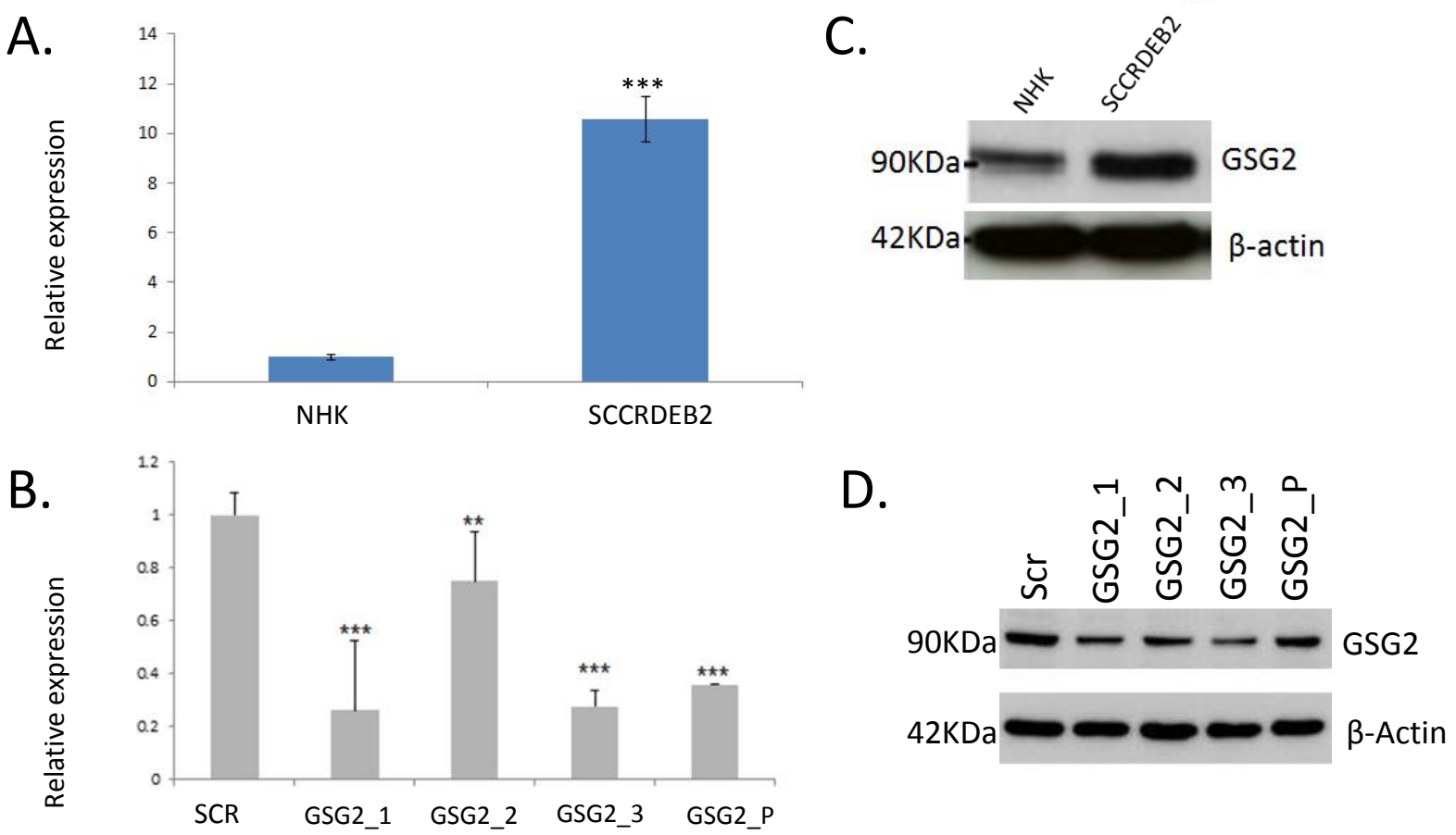

Figure 3.4 GSG2 is Over-expressed at Both mRNA and Protein Level in cSCC Compared to Normal human Keratinocytes (NHK)

(A) mRNA expression levels of GSG2 in NHK versus SCCRDEB2 cells results represent the mean±SD, n=6. (B) Relative expression levels of GSG2 following knockdown with individual siRNA (GSG2_1, 2, 3) / pooled (GSG2_P) oligonucleotides, targeted to GSG2. Results expressed relative to the scrambled control (SCR) and represent the mean±SD, n=6 (C) Western blot showing increased protein expression of GSG2 in SCCRDEB2 cells compared to NHK (D) Western blot showing protein expression following knockdown using individual / pooled oligonucleotides.

3.2.2.1.2 Knockdown of *GSG2* Shows no Significant Increase in Apoptosis or Change in Cell Cycle

Knockdown of *GSG2* did not cause a significant increase in cytotoxicity, 48h following transfection (figure 3.2). Using a time course it was also confirmed not to cause a significant increase in cytotoxicity 24 and 72 hours post-transfection, using pooled siRNA (figure 3.5). Additionally knockdown of *GSG2* did not significantly increase apoptosis compared to the non-targeting control (figure 3.6A).

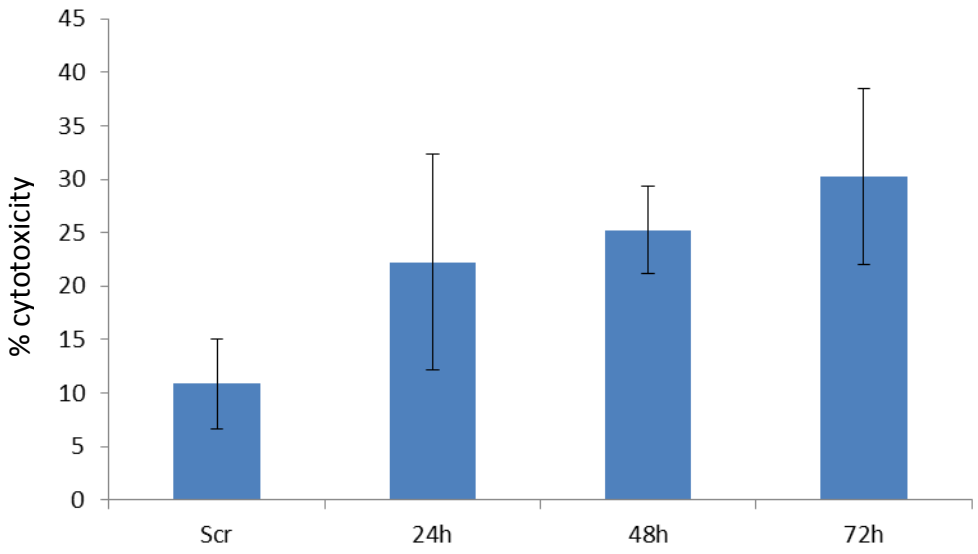

Figure 3.5 No Significant Induction of Cytotoxicity is Observed Following GSG2 Depletion in cSCC Cells

Results show the assessment of cytotoxicity following knockdown of GSG2 24, 48 and 72 hours post-transfection in SCCRDEB2 keratinocytes, indicating no significant induction of cytotoxicity at these time points. Results represent the mean ± SD from 3 independent experiments.

As GSG2 had been shown to cause misalignment of chromosomes following knockdown of its expression, it was hypothesised that knock down of *GSG2* in cSCC cells may result in cell

cycle arrest (Higgins et al 2001a). Fluorescent staining and flow cytometry is a method of quantification of DNA in the cell cycle. BrdU is a synthetic analogue of thymidine that becomes incorporated into the DNA during S phase; subsequently DNA unwinding permits the access of an antibody and addition of a fluorescent secondary. However figure 3.5b shows that using BrdU cell cycle analysis in SCCRDEB2 cells, there is no change in the cell cycle 20h following GSG2 depletion, compared to the non-targeting control.

Figure 3.6

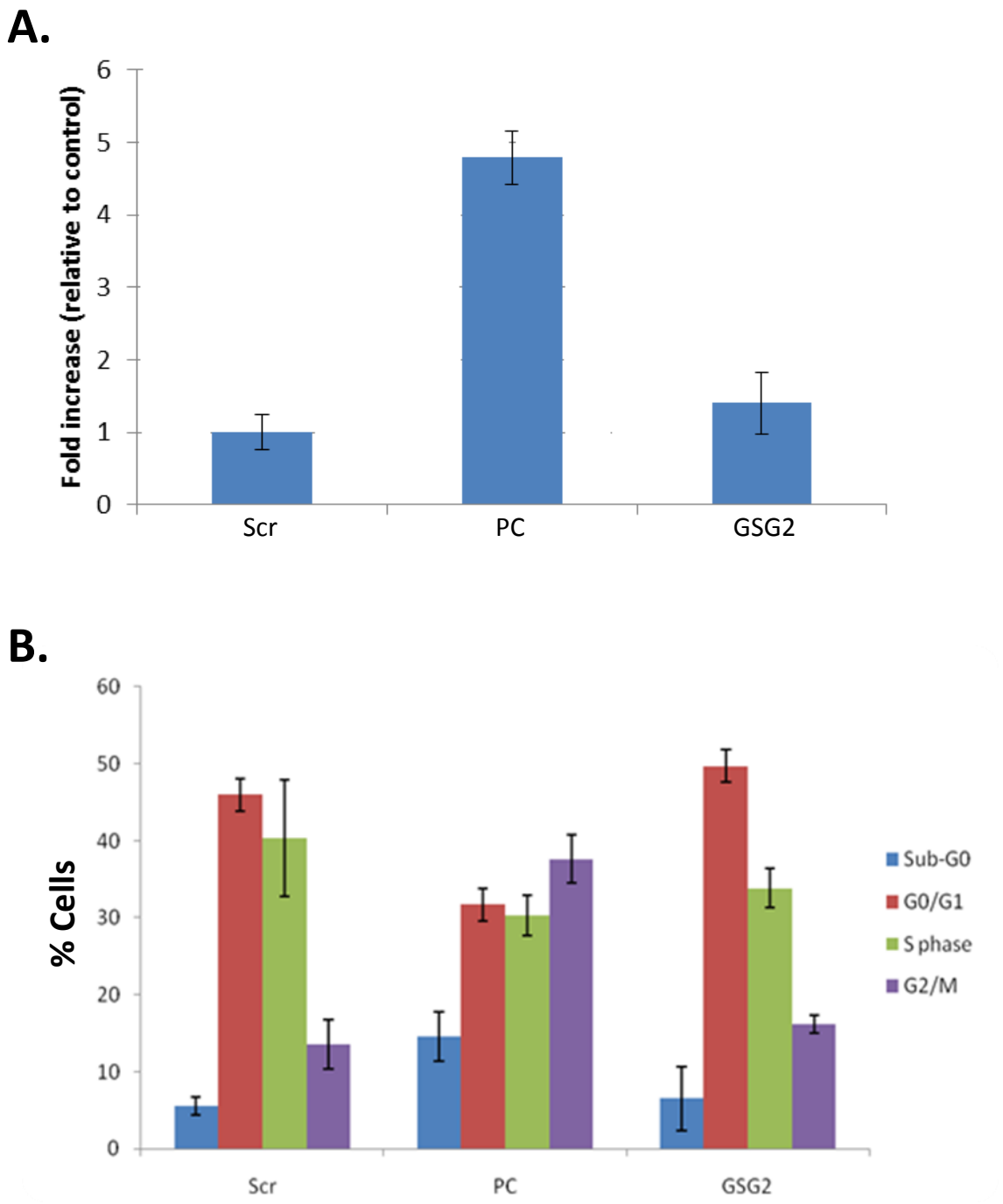

Figure 3.6 Knockdown of GSG2 Does not Induce Cell Cycle Arrest or Apoptosis in cSCC Cells

(A) SCCRDEB2 keratinocytes transfected with a pool of 2 separate siRNAs targeting GSG2 or a cell death positive control siRNA (Sigma, PC) were assessed for induction of apoptosis using Cell Death ELISA assay, 20h after treatment. The results show no significant fold increase in cytoplasmic nucleosomes relative to the scrambled non-targeting control (SCR). (B) Cell cycle analysis in SCCRDEB2 keratinocytes treated with a pool of 2 separate GSG2 targeting siRNA or PLK1, as a positive control (PC) and stained for bromodeoxyuridine (BrdU) and propidium iodide (PI). Results expressed as percentage of cells at the G0/G1, S and G2/M phases of cell cycle and sub-G0 20h following knockdown. Results represent n=4.

3.2.2.2 Bradykinin Receptor B1 (BDKRB1)

3.2.2.2.1 Previous Work on BDKRB1 Performed in Our Lab

Depletion of BDKRB1 using siRNA, resulted in a reduction in cell viability (Watt 2011). Subsequently S.Gaw, a BMSc student in the lab, showed that the reduction in cell viability was attributable to increased cytotoxicity as a consequence of apoptosis. S.Gaw demonstrated that siRNA knockdown of BDKRB1 in the SCCRDEB2 keratinocytes resulted in a 38% increase in cytotoxicity using the LDH assay. Using the apoptosis ELISA she also showed that depletion of BDKRB1 resulted in a 1.8 fold increase in cytoplasmic nucleosomes, indicating an increase in apoptosis 48 hours after transfection. Although S.Gaw was able to demonstrate that BDKRB1 was increased at mRNA level, she was unable to confirm this increase at protein level. In addition to this S.Gaw used agonists and antagonists to stimulate the B_1R, however contrary to predictions they increased proliferation of cSCC cells. In follow up, the sections below attempt to confirm the expression of BDKRB1 at both mRNA level and protein level and to further evaluate the potential of the antagonist and agonists for treatment of cSCC.

3.2.2.2.2 BDKRB1 is Overexpressed at mRNA level but ~~-~~not at the Proteiie~~e~~n Level in cSCC

Using qPCR, the over-expression of *BDKRB1* in cSCC was ~8 fold higher in SCCRDEB keratinocytes than NHK, which confirms its over-expression identified by the microarray (figure 3.7).

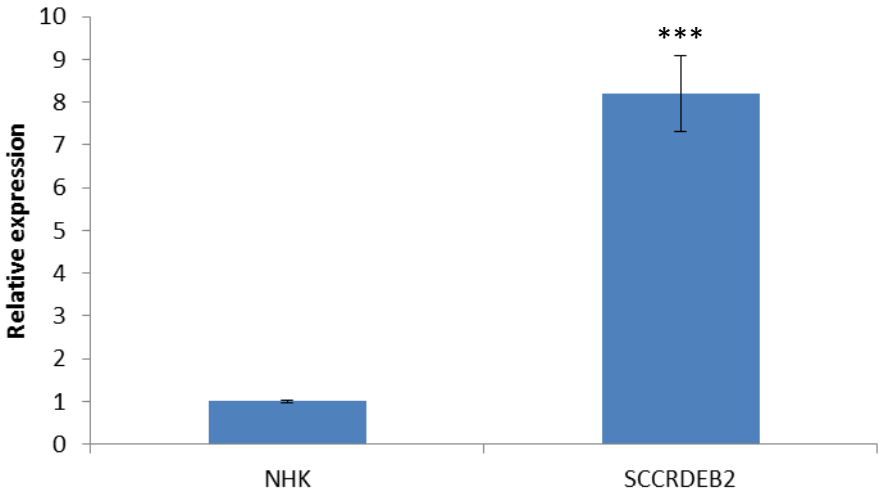

Figure 3.7 *BDKRB1* is Over-expressed in SCCRDEB2 Cells at mRNA Level

The relative expression of *BDKRB1* was assessed in SCCRDEB cells by quantitative PCR. Data shows that expression is ~8 fold higher relative to the NHK. Results are the mean ± SD, n=6. ***p<0.005 compared to control.

Westen blot was used to evaluate the protein expression of BDKRB1 in cSCC versus NHK. The expected band size of BDKRB1 is 40KDa. However, previous work done by S. Gaw, showed that in NHK there is both a band at 40KDa and 80KDa but in SCCRDEB2 cells the majority of the protein expression was at 80KDa. This result indicates that the protien may possibly be dimerising forming a band double of that expected. The problem may have been that the denaturation using our standard conditions was insufficient, and adding different buffers such as dithiothreitol (DTT) or urea may perturb this formation (figure 3.8a). However the 80KDa band still remained even with the use of stronger reducing agents and a recomended positive control K562 – a myloid leukemia cell line did not show the correct size of band either (figure 3.8b). This data would pose the question as to wither the 80KDa band is a dimer. However, the ability to knockdown the expression of *BDKRB1* using targeted siRNA confirms that the 80KDa band is the receptor and not a non-specific band (figure 3.9).

Figure 3.8

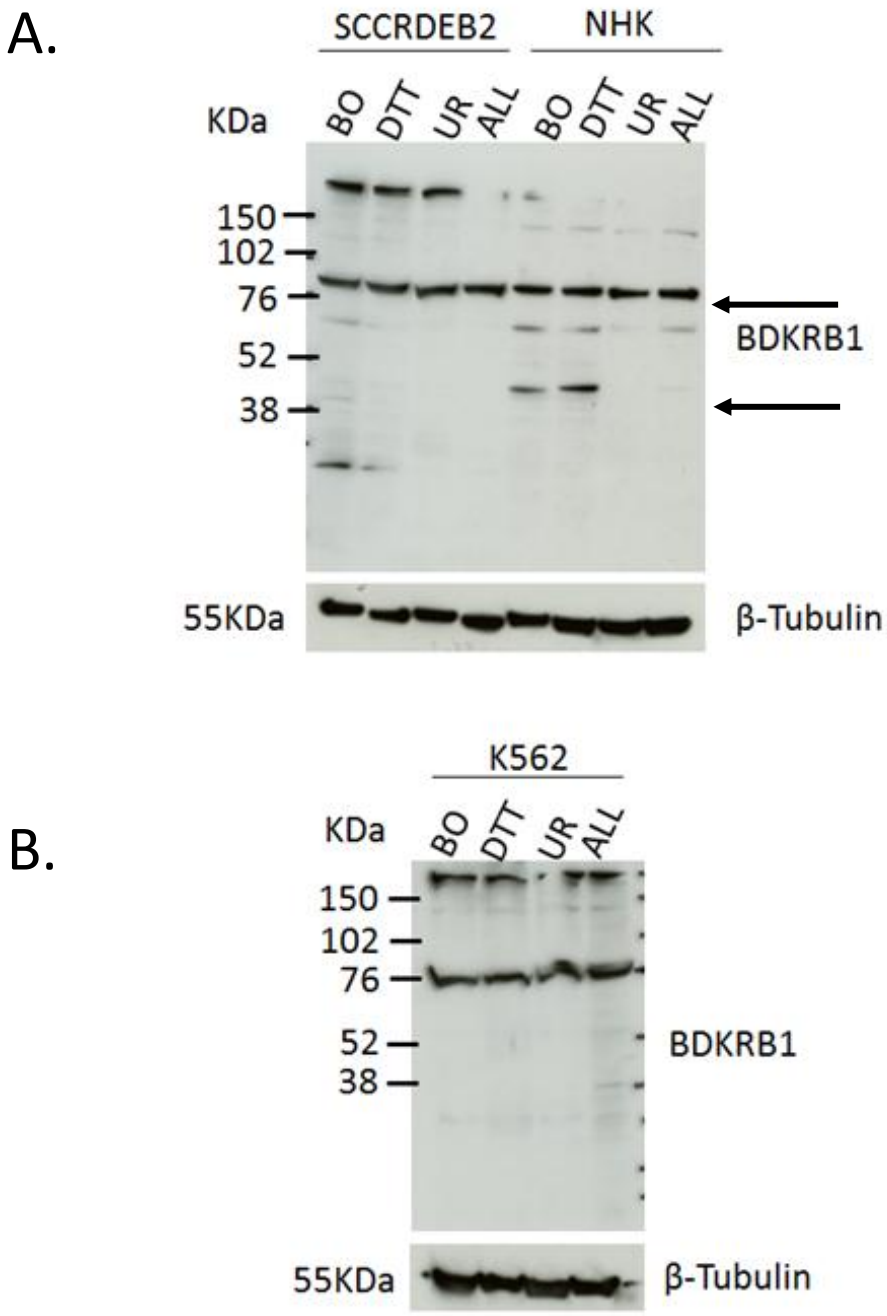

Figure 3.8 BDKRB1 is Expressed at 80KDa Rather than 40KDa in cSCC

(A) Protein expression of BRDKRB1 was assessed using different denaturing buffers, boil only (BO), dithiothreitol (DTT), urea (UR) or BO, DTT and UR (ALL). No expected 40KDa band was seen under any of the treatments in the SCCRDEB2 cells however in the NHK cells a 40KDa band as well as the 80KDa band was detected using BO and DTT buffers. Arrows indicate 80KDa band (upper) and 40KDa (lower) band (B) K562, a myloid leukaemia was used as a positive control lysate in the data sheet provided with antibody. However no band at 40KDa was seen as expected in this cell line either.

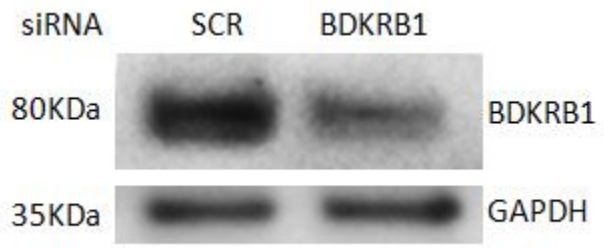

Figure 3.9 Expression of BDKRB1 at 80KDa can be Depleted Using BDKRB1 siRNA

SCCRDEB2 keratinocytes were transfected with a pool of 3 separate siRNA targeting BDKRB1 and BDKRB1 protein expression was determined using western blot. The siRNA targeting BDKRB1 reduces the band at 80KDa. n=1.

3.2.2.3 Agonist Stimulation with R715 Causes a Reduction in Phosphorylation of ERK and Proliferation

B_1R antagonists R892 and R715 and agonists LDBK and DBK were used to target B_1R and could be potentially used as therapies for cSCC. The MAP kinase pathway is known to be stimulated in other cancers, resulting in increased proliferation. As mentioned before in chapter 1 ERK–1 and ERK–2 are part of this pathway and they can be activated by phosphorylation. Looking at phosphorylation levels of ERK (pERK), can help to understand if the agonist and antagonist stimulation of B_1R will have effects on proliferation and pERK. Figure 3.10A illustrates a reduction in pERK levels in SCCRDEB2 stimulated with all the agonists and antagonists tested, with stimulation using LBK and R715 causing the greatest reduction. In comparison, total ERK is equivalent in all cells and is not affected by ligand stimulation. Therefore ligand induced reduction in phosphorylation of ERK may reduce the proliferation in these cells. Subsequently LBK and R715 were used to target B_1R and the effects on proliferation measured using MTS. Serial dilutions of each ligand were used to give a final concentration of 0.1, 1 and 3µM in serum free conditions as previously determined by S.Gaw. After 48h a dose dependant increase in proliferation is observed following SCCRDEB2 stimulation with agonist LDBK (figure 3.10B, upper panel). However

stimulation using antagonist R175 (figure 3.10B, lower panel) showed a reduction in proliferation after T48 hours using a concentration of 0.1µM, with the other concentrations having no effect on proliferation. Therefore this R175 agonist at a concentration of 0.1µM could be used to reduce proliferation in the SCCRDEB2 keratinocytes.

Figure 3.10

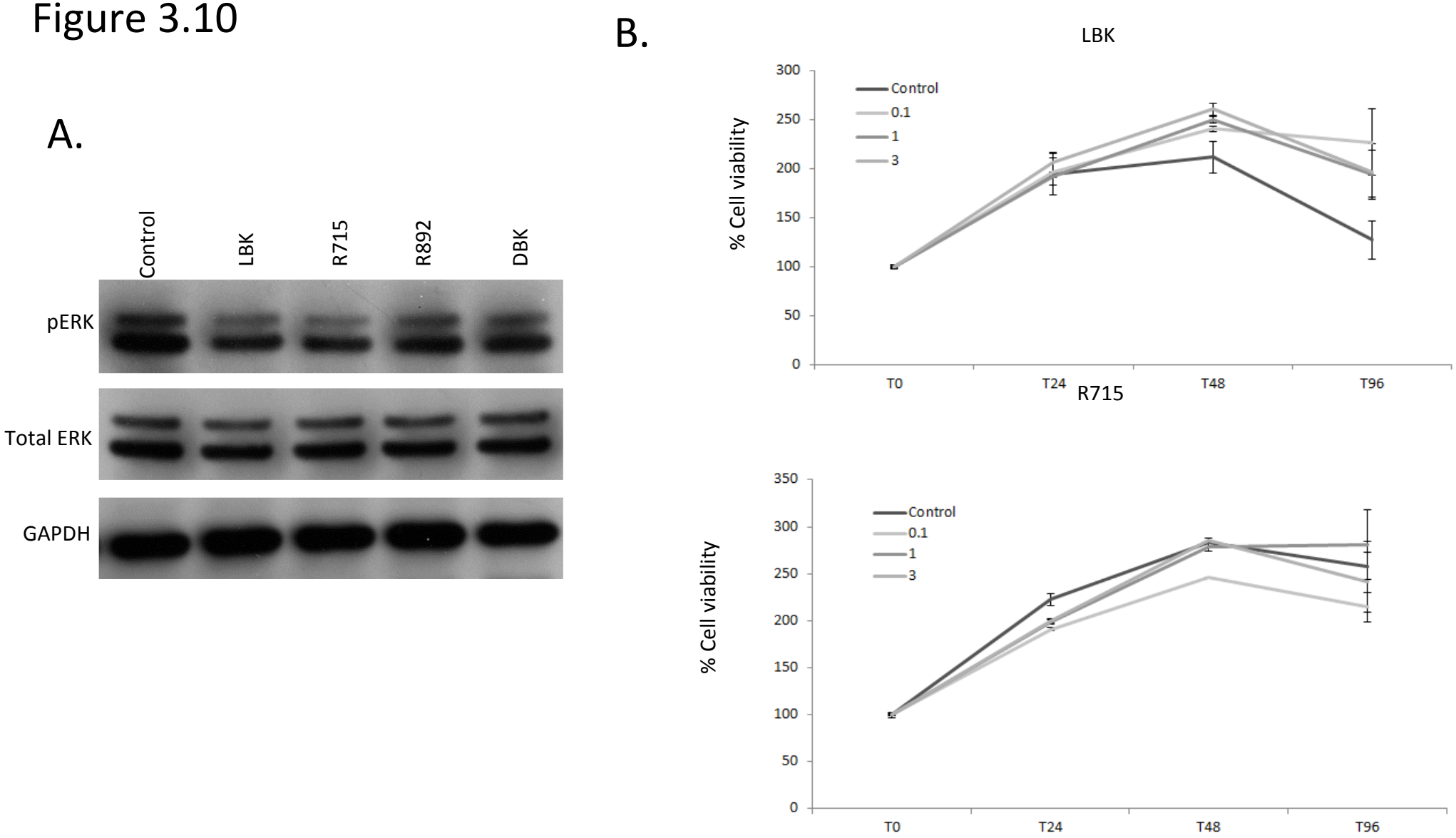

Figure 3.10 Agonist Stimulation with R715 Causes a Reduction in Phosphorylation of ERK and Proliferation in cSCC

(A) SCCRDEB2 cells were stimulated with ligands LBK,R715,R892 and DBK) for 48 hours before collecting lysates for western blot analysis and blotting for phosphorylated-ERK (pERK) and total ERK (n=2). Figure shows a reduction in phosphorylation compared to control (media only). (B) MTS assessing cell viability in SCCRDEB2 cells in serum free conditions (SD±mean, n=3) 24, 48 and 96 hours after ligand stimulation, using 0.1, 1, 3 µM of either LBK (upper panel) or R715 (lower panel). Results show a dose dependant increase in proliferation, 48h following stimulation with LBK, compared to control. However stimulation with R715 shows a reduction in proliferation at all concentrations after 24h, which is maintained after 48 and 96h using a concentration of 0.1µM

3.2.2.4 Protease Serine 21 (PRSS21)

3.2.2.4.1 PRSS21 is Over-expressed at Both mRNA and Protein Level

The serine protease PRSS21 was found to be over-expressed in cSCC versus normal cells/skin (Watt 2011) which was confirmed using qPCR (figure 3.11A). These results show that PRSS21 is over-expressed in both SCCRDEB2 (~10 fold) and SCCIC1 (~18 fold) keratinocytes compared to NHK. PRSS21 is also over-expressed at protein level in the SCCRDEB2 cells compared to the NHK and this expression can be successfully depleted using siRNA targeted to its expression (figure 3.11B).

Figure 3.11

A.

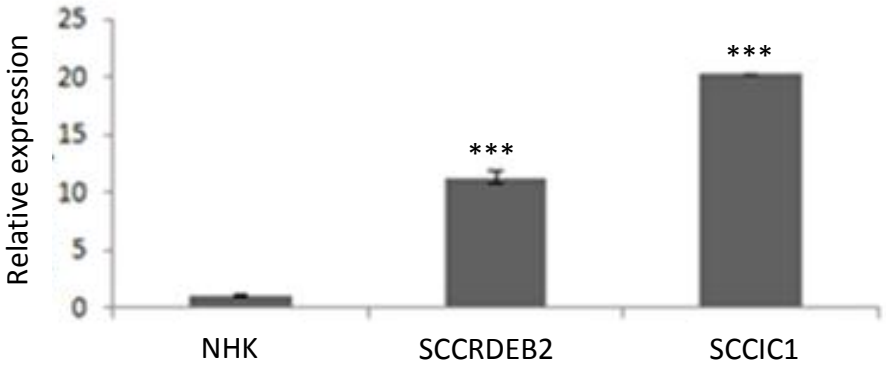

B.

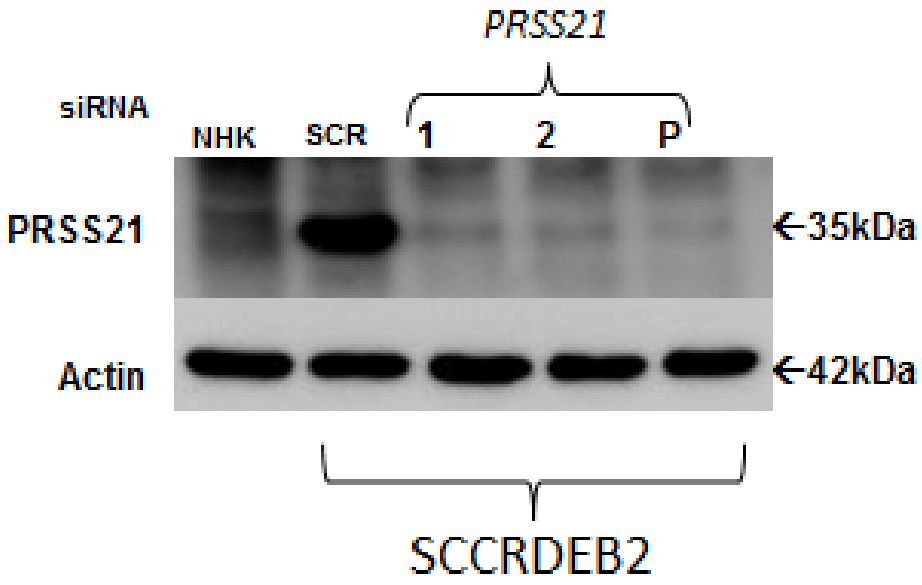

Figure 3.11 PRSS21 is Over-expressed in cSCC at Both mRNA and Protein Level Compared to NHK

(A) Results show mRNA over-expression of *PRSS21* in cSCC SCCRDEB2 and SCCIC1 cells relative to NHK. Results represent the mean±SD, n=2, ***p<0.005, (B) Relative protein expression levels of PRSS21 in normal human keratinocytes (NHK) and in SSCRDEB2 cells following transfection with a non-targeting control (SCR) and with individual oligonucleotides targeted to PRSS21 (PRSS21_1 & PRSS21_2) / pooled oligonucleotides (PRSS21_P) (n=6).

3.2.2.4.2 PRSS21 Depletion Reduces Cell Viability through Increased Apoptosis in cSCC

Using MTS cell viability was assessed in the SCCRDEB2 cells following depletion of PRSS21 using siRNA. This demonstrated that knockdown of PRSS21 reduces cell viability in SCCRDEB2 cells 48 hours post-transfection compared to the scrambled (Scr), non-targeting siRNA control (figure 3.12) by ~20% which was statistically significant.

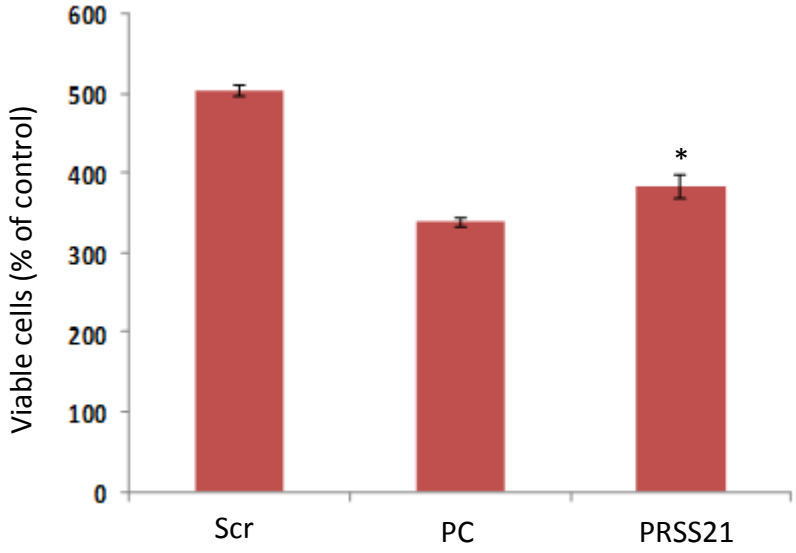

Figure 3.12 Depletion of PRSS21 Expression in cSCC keratinocytes Reduces Cell Viability compaired to Non-targeting control

Cell viability is significantly reduced in SCCRDEB2 keratinocytes using oligonucleotides targeted to PRSS21 compared to non-targeting control (Scr), 48 hours post-transfection. A positive cell death control was also included (PC). Results represent the mean ± SD, n=3, *P<0.01. The percentage viable cell number is shown relative to values at T0.

siRNA knockdown of *PRSS21* resulted in a significant increase in cytotoxicity with no effect on the normal keratinocytes (Figure 3.3). Using the Cell Death Detection ELISA, a 2.3 fold increase in cytoplasmic nucleosomes was detected 48h following depletion of PRSS21, which is significantly different (P<0.05) compared to the non-targeting control (figure 3.13).

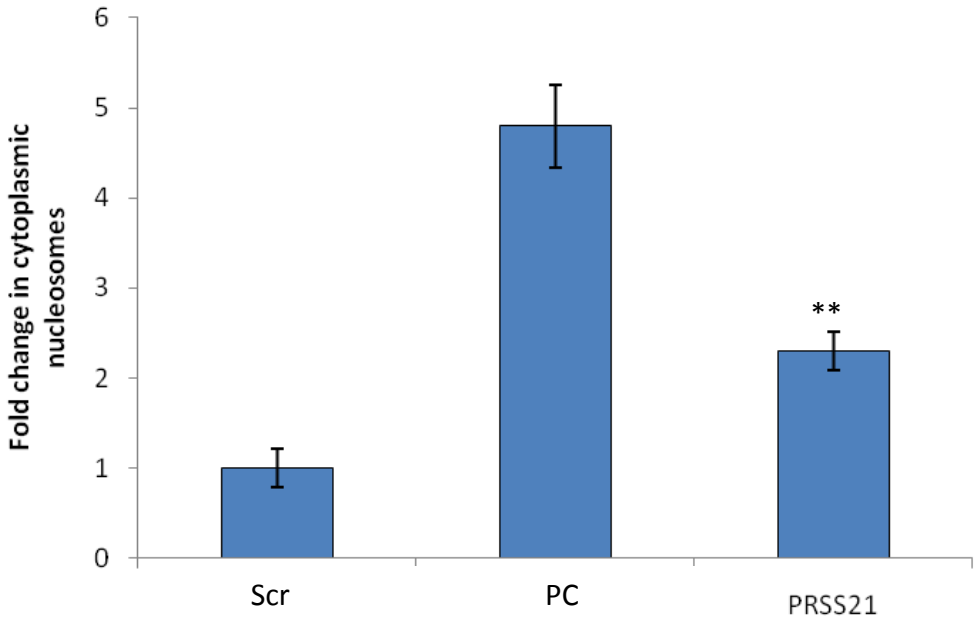

Figure 3.13 Depletion of PRSS21 Increases Apoptosis in cSCC Cells Compared to Non-targeting Control

Using the cell death ELISA kit, results show an increase in cytoplasmic nucleosomes relative to non-targeting siRNA in SCCRDEB2 following depletion of PRSS21. A positive cell death control (PC) is also included. Results are the mean ± SD, n=6. **p<0.001, compared to SCR control.

Analysis of the cell cycle following knockdown of *PRSS21* showed no change in the percentage of cells at the G1/G2 or S phase of the cell cycle however analysis of the sub-G0 population tentatively representing the "dying" population, revealed double the number of cells within this group compared to the control (figure 3.14), reflecting the result from the cell death ELISA assay.

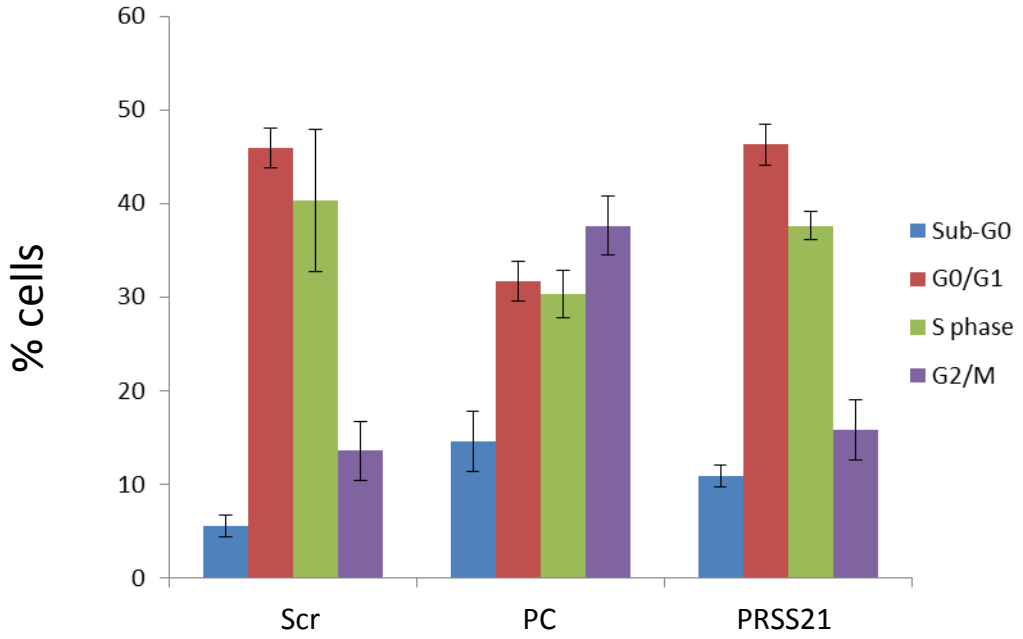

Figure 3.14 BrdU Cell Cycle Analysis Reveals an Increase in Sub-G0 Cell Population Following Depletion of PRSS21 in cSCC Keratinocytes Compared to the Non-targeting Control

Results of cell cycle analysis in SCCRDEB2 -keratinocytes following knockdown using a non-targeting control (Scr), PLK1 (PC) which is known to induce a G2/M arrest and PRSS21 siRNA. Results expressed as percentage of cells at the sub-G0, G0/G1, S and G2/M phases of cell cycle 20h following knockdown, where an increase in the sub-G0 cell population is observed after depletion of PRSS21. Results represent n=4.

3.2.2.4.3 Knockdown of PRSS21 Increases Caspase Activation and Annexin IV Staining in cSCC

To assess the mechanism of cell death, the caspase 3/7 assay was used to assess caspase activity following siRNA depletion of PRSS21. This assay showed a 1.9 fold increase in caspase activity, compared to the non-targeted control, 48h post-transfection (figure 3.15A). Apoptosis was also assessed 48h post-transfection using 7-AAD and Annexin V staining. 48h following transfection the number of live cells was significantly reduced compared to the positive control (figure 3.15B). Additionally there was a ~20% increase in apoptotic cells- comparable to the positive control.

Figure 3.15

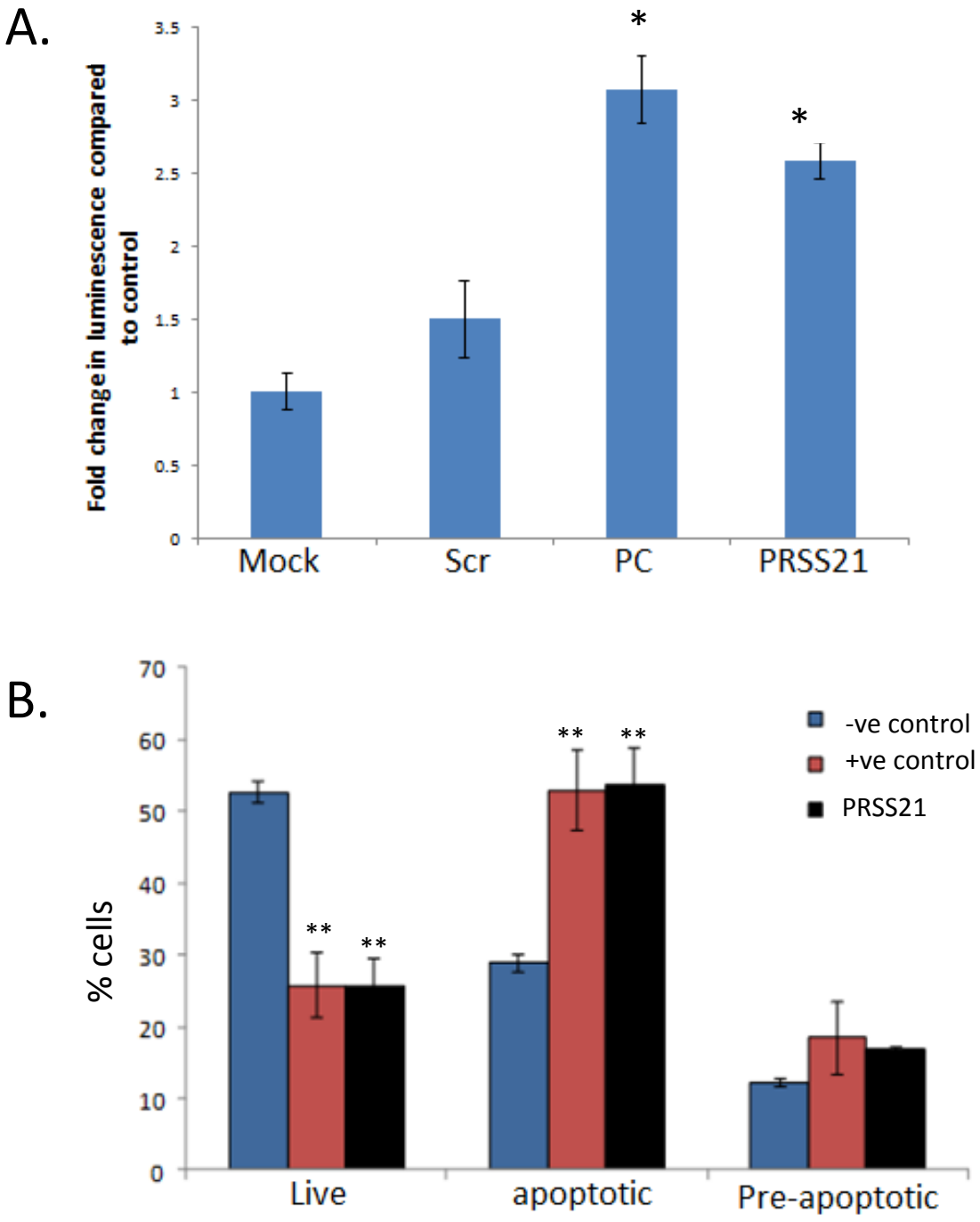

Figure 3.15 Knockdown of PRSS21 Leads to an Increase in caspase Activity and Annexin V Staining in cSCC cells

(A) Caspase activity is significantly increased following KD of PRSS21 in the SCCRDEB2 cells compared to the non targeting control (Scr). Additional controls included are a mock transfection (mock) and positive control (PC). Results represent the mean ± SD, n=3, *P<0.01. (B) Apoptosis was also assessed using FACS and the annexin V/7-AAD staining method. Results represent the mean ± SD, n=4 **P<0.001.

3.3 DISCUSSION

The approach taken by our lab to identify molecular targets for cSCC has already yielded two promising targets, PLK1 and C20orf20 which reduce tumour growth *in-vivo*. In addition to these, three other potential targets from the 21 cSCC signature were highlighted, GSG2, BDKRB1 and PRSS21, depletion of which reduced cSCC viability *in-vitro* (Watt 2011). The aims of this chapter were to:

1. Repeat the original RNAi screen of the 21 cSCC specific genes, performed by Watt and colleagues, however using a different endpoint. The original screen assessed cell viability and thereby using cytotoxicity as an endpoint differentiates between slowing of cell growth and genuine killing. This would essentially re-enforce the potential of the five genes (C20orf20, PLK1, GSG2, BDKRB1 and PRSS21) Watt *et al.* identified to reduce cell viability but also potentially identify novel targets for cSCC (Watt 2011).
2. Further validate 3/5 genes identified by Watt *et al.* to reduce cell viability GSG2, BDKRB1 and PRSS21 as molecular targets for cSCC (Watt 2011).

3.3.1 RNAi screen of 21 up-regulated genes using cytotoxicity as a readout

Using siRNA targeted to the 21 cSCC specific genes with cytotoxicity as readout, confirmed that PLK1 and C20orf20 were important for tumour cSCC survival, as previously shown by Watt and colleagues (Watt 2011). In addition to these, depletion of the serine protease PRSS21, also consistently significantly increased cytotoxicity. A further three targets PARP1, FUCA2 and PSMG3 were also identified to increase cytotoxicity following knockdown and these were further explored in SCCIC1 and NHK cells. Subsequently, siRNA knockdown of

GSG2, PRSS21, PLK1, PSMG, FUCA2 and PARP1 was performed using 3 duplexes or a pool, with cytotoxicity as a readout. BDKRB1 and C20orf20 were not included as these genes were being studied by other members in our lab. The latter is also true of PLK1 however was included as a further positive control. Only PRSS21 and PLK1 showed 'hits' consistently in 2/3 duplexes, furthermore they did so in two cSCC cell lines, SCCRDEB2 and SCCIC1 keratinocytes with little effect on NHK. This was expected from PLK1 as data from our lab would suggest that depletion of PLK1, leads to G2/M arrest increasing mitotic catastrophe, and that PLK1 inhibition significantly reduces tumour volume *in-vivo* (Watt 2011). However although the mechanism of depleted PRSS21 induced cytotoxicty has not been fully explored, data in this chapter would suggest that it leads to a reduction in cell survival and increased apoptosis. This data would suggest that PRSS21 is important for cSCC cell survival. As for the novel targets identified, PSMG, FUCA2 and PARP1 the effect seen in figure 3.3 could have been the result of off target effects. In light of this PSMG2 and FUCA2 were not followed up.

3.3.2 Validation of Germ Cell Associated 2 (GSG2) As a Therapeutic Molecular Target in cSCC

GSG2 would be an interesting molecular target as it plays a role in mitosis and cell cycle control; furthermore small molecular inhibitors are available which would fast track development of a therapeutic target. However, depletion of GSG2 in cSCC did not significantly increase cytotoxicity or apoptosis. To further support the lack of cytotoxicity seen with GSG2 Wang *et al*. show that histone H3 phospho Thr3 generated by haspin contributes to accurate positioning of the chromosomal passenger complex but is not necessarily required (Wang, Dai et al. 2005). As GSG2 is a mitotic kinase, one may assume it to act as an anti-mitotic compound however, using BrdU/PI cell cycle analysis in cSCC

keratinocytes did not show any disruption to the cell cycle following GSG2 depletion. Interestingly, Dai and colleagues showed that GSG2 acts as a mitotic kinase and depletion of GSG2 prevents normal metaphase alignment by assessing the distribution using immunofluorescence. However this group also failed to identify any change in cell cycle parameters. The data presented in this thesis suggest that GSG2 may not be a good target for cSCC.

3.3.3 Validation of Bradykinin receptor B1 (BDKRB1) As a Therapeutic Molecular Target for cSCC

BDKRB1 over-expression was confirmed at mRNA level however at protein level these results seem more complex. Despite the expected molecular weight of BDKRB1 being 40KDa, the only band identified in cSCC cells was an 80KDa band – which is double the expected size. This could be due to receptor dimerisation which has been identified in other cancers – HER positive breast cancer, where the HER2 receptor can form heterodimers with other EGFR tyrosine kinases (Moulder, Yakes et al. 2001). Furthermore dimerisation can switch on signalling pathways and activate downstream events or change agonist affinity (Saltz, Meropol et al. 2004). There is evidence to suggest that B_1R can dimerise with B_2R, another subtype of bradykinin receptor, in prostate cancer cells, which has a molecular weight of 43KDa (Barki-Harrington, Bookout et al. 2003). Ligand labelling studies are required to elucidate BDKRB1 expression at protein level. Studies performed by S.Gaw – a student working in the lab, showed that the siRNA depletion of BDKRB1 lead to a reduction in cell viability due to an increase in cytototoxicty through apoptosis. These results suggest that BDKRB1 may be a good potential target for cSCC. However she also showed that antagonists R715 and R892 induce phosphorylation of ERK and proliferation in cSCC cells, making them not useful as targets in cSCC. However in this thesis it was demonstrated that

these agonists and antagonists actually reduce phosphorylation of ERK, although using MTS to assess proliferation yielded mixed results. This would indicate more work has to be done to elucidate the potential of BDKRB1 as a therapeutic target in cSCC.

3.3.4 Validation of Protease Serine 21 (PRSS21) As a Therapeutic Target in cSCC

siRNA depletion of PRSS21 lead to a reduction in cell viability which has been observed previously and in this chapter. Subsequently it was shown that the reduction in cell viability was due to a significant increase in cytotoxicity through activation of apoptosis. Previous studies have also shown that depletion of PRSS21 expression leads to apoptosis (Tang et al 2005, Yeom et al 2010). Induction of apoptosis in cSCC was shown via two methods the Annexin V staining method and the caspase 3/7 assay, which confirmed that depletion of PRSS21, induces apoptosis through activation of caspases.

In conclusion, from the data in this chapter it was decided to take PRSS21 forward and to undertake further study to determine if it would be a good molecular target for cSCC. PRSS21 will be further discussed in chapter 4.

Chapter 4 Assessment of the Function of PRSS21 in Cutaneous Squamous Cell Carcinoma

4.1 INTRODUCTION

In follow up of the microarray data (Watt *et al* 2011), chapter 3 further validates PRSS21 as a molecular target, showing that it is essential for cSCC survival. Serine proteases, such as PRSS21, control a wide range of proteolytic reactions essential for a diverse set of physiological and pathological functions. Additionally, in living systems, a balance between protease and their anti-proteases occur, and a disturbance of this balance leads to many diseases like cancer (Puente, Sanchez et al. 2003). The function and mechanism behind PRSS21 over-expression in cSCC are currently unknown, which is further explored in this chapter.

4.1.1 Function of Proteases in Normal Tissue

A plethora of proteases exist, which have a diverse range of fundamental functions in key biological processes, including inflammatory control, blood flow and immune regulation (Rawlings, Tolle et al. 2004). Evolutionarily, they derive from a large subset of catalytic enzymes which have the ability to hydrolyse peptide bonds (Puente, Sanchez et al. 2003). It was long considered that proteases sole role, was protein degradation, generally assigned to protein turnover and food digestion (Rawlings, Tolle et al. 2004). However, later work on the trypsinogen activation and blood clotting mechanism, revealed a previously unknown role for proteases in the tight regulation of biological pathways. The blood coagulation cascade, which is one of the most studied proteolytic cascades, involves sequential activation of pro-enzymes or zymogens. The final activation step is thrombin which leads to fibrinogen

activation and blood clot formation (Davie, Fujikawa et al. 1991). By cleaving proteins, proteases are involved in the control of a large number of key biological processes such as cell cycle progression, cell proliferation, cell death, tissue remodelling, coagulation and immune response.

The current identified sets of proteases are classified into five catalytic classes: metallo (194), serine (176), cystine (150), threonine (28) and aspartic proteases (21), the number of members within each class are in brackets. PRSS21 is a serine protease, so this group will be focused on below.

4.1.1.1 Serine Proteases

The serine proteases are the second largest and most conserved proteolytic family found in a number of tissues and biological fluids. For instance, trypsin one of the best characterised serine proteases, is expressed in skin, oesophagus, stomach, small intestine, colon, lung, kidney, liver, spleen and neuronal tissues (Koshikawa, Hasegawa et al. 1998). Serine proteases of the trypsin-like family contain N- or C- terminal domains which tether the catalytic domain to the plasma membrane, which allow proteolysis within the pericellular environment (Neurath and Walsh 1976). The membrane-anchored serine proteases can be divided into sub-groups depending on their structural features. For instance they can be anchored to the membrane by a C-terminal trans-membrane domain through a glycosylphosphatidylinositol (GPI) anchor or via an N-terminal trans-membrane domain with a cytoplasmic extension. PRSS21 is post-translationally modified with GPI anchor, and is subsequently found compartmentalised in lipid rafts of premiotic germ cells (Hooper, Nicol et al. 1999).

Serine proteases (figure 4.1) are characterised by the presence of three critical amino acids – histidine, aspartate and serine in their catalytic site, of which the serine acts as the active site (Davies, Pickard et al. 1998; Di Cera 2009). The catalytic domains are in the extracellular region, exposed to the pericelluar environment, requiring cleavage to become an active protein. The substrate specificities for the serine proteases hepsin, matriptase, prostatin and tryptase have been extensively characterised using peptide libraries however, very little information is available for other serine proteases such as PRSS21 (Herter, Piper et al. 2005; Beliveau, Desilets et al. 2009). The specific substrates targeted by these enzymes are important areas of study.

Figure 4.1

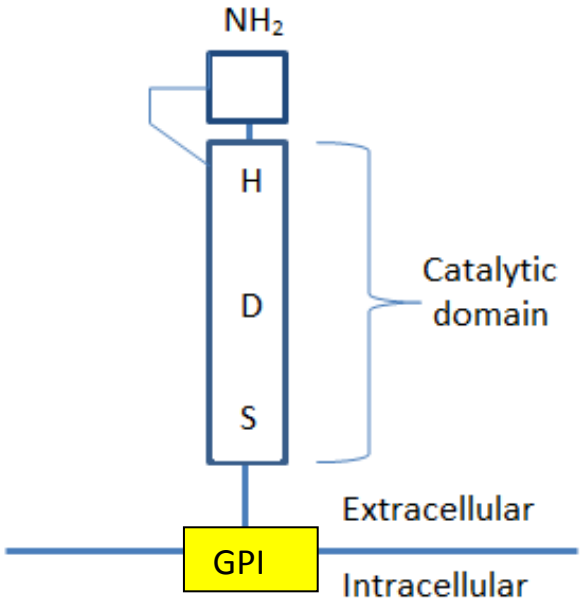

Figure 4.1 Domains and Catatytic Residues of Serine Proteases

Serine proteases are defined by the serine residue (S) in the enzyme active site, which is part of a catalytic triad, also including histidine (H) and aspartate (D). Serine proteases can also contain a C-terminal domain which serves to anchor the serine protease domains directly to the plasma membrane. The example above is an example of a glycosylphosphatidylinositol (GPI) linked Serine Protease.

4.1.2 Function of Proteases in Cancer

Proteases in normal tissue are fundamental in carrying out important biological functions however in cancer they can be the cause of much disruption. Alterations in their expression patterns provide essential processes in cancer – proliferation, cell migration, invasion and angiogenesis (Puente, Sanchez et al. 2003). This would make proteases important at a number of stages in tumour progression and hence a worthy target for cancer therapy.

It has long been recognised that proteolytic enzymes play a significant role in cancer invasion and metastasis (Chambers and Matrisian 1997; Lochter, Galosy et al. 1997; Mook,

Frederiks et al. 2004; Deu, Verdoes et al. 2012). In 1946 Fisher proposed that the tumour associated proteolytic activity could be responsible for the degradation of the cell matrix and subsequent invasion into the surrounding tissue (Fisher A *et al*. 1946). Subsequently, in 1957 Sylven and Malmgren reported the presence of proteases at the leading edge of tumours, where they showed that they were from the live tumour cells, not from leakage of dead cells either from the surrounding tissue or from the centre of the tumour (Sylven and Malmgren 1957). However, cancer cells can induce stromal cells to express proteolytic enzymes which promote cancer cell migration (Zucker, Cao et al. 2000). In the 1970s individual proteases began to be identified and over the next two decades molecular biological studies associated their gain-of function with invasion. By 1993 the general conception was that all 5 classes of proteases; serine, aspartic, threonine, cysteine and metalloproteinases, were involved in extracellular matrix (ECM) degradation. In particular, much of the attention has been given to the urokinase-type plasminogen activator (UPa) system, which is part of the serine protease group and the matrix metalloproteinases (MMPs), which is part of the metalloproteinase group. They have a well-recognised role in tumour invasion and metastasis and their levels and activities were found to be related to growth and distant spread of the tumour (Stetler-Stevenson, Aznavoorian et al. 1993; Dano, Romer et al. 1999). The enzymatic activity of proteases is regulated by levels of protease inhibitors which determine net enzyme activity on the cell surface and affect the extent of ECM degradation and tumour invasion (Puente, Sanchez et al. 2003).

4.1.3 Serine Protease Inhibitors (serpin)

In 1985 Carnell coined the term “serpin” to describe the family of serine protease inhibitors (Carrell and Travis 1985). Serpins, constitute the largest and most broadly distributed family of protease inhibitors which can be found in plants, fungi, bacteria, viruses and mammals of

which 36 have been confirmed in humans (Irving, Steenbakkers et al. 2002). The first serpins were found to tightly regulate blood coagulation (anti-thrombin) and inflammation (anti-trypsin). While most serpins inhibit proteolytic cascades, certain serpins do not inhibit protease functions, but instead control functions such as storage, hormone carriage or have a tumour suppressive role (Getting 2002; Huntington 2011). Serpins can also be divided into extracellular (clade A) and intracellular (clade B) and some have cross class functions (i.e. inhibition of cysteine proteases). Characteristically, serpins have a reactive centre loop (RCL), a peptide stretch that is maintained in a rigid conformation for proteases to bind. The RCL allows for a conformational change which enables the site to provide an optimal state for binding and subsequent inhibition of a protease. Hence, the selectivity of a serpin to its protease is not always evident from its sequence, due to the structural change required to incorporate the protease (Hobson et al 2004). Also in existence, are serpins classed as non-inhibitory, where their RCL is relatively short and unable to undergo a conformational change for protease inhibition- maspin (discussed in the following section) is an example of this subtype (Hopkins and Whisstock 1994; Pemberton, Wong et al. 1995).

4.1.4 Mammary Serine Protease Inhibitor (maspin)

Mammary serpin protease inhibitor (maspin) is a type II tumour suppressor first identified in mammary epithelial cells to inhibit invasion and motility in this cell type (Zou, Anisowicz et al. 1994). Of importance to this thesis, maspin was found to interact with PRSS21 in HeLa cervical cancer cells (Yeom, Jang et al. 2010). Using a yeast two hybrid screening method, DNA sequencing and basic alignment sequences revealed PRSS21 to interact with maspin. To confirm this interaction the authors used co-immunoprecipitation to show that PRSS21 and maspin interact in 293 and HeLa cells and that they co-localise in the cytoplasm of HeLa cells. Furthermore, they show that in cervical cancer cells maspin modulated cell death and

invasion and that these effects could be inhibited by PRSS21, postulating that the ratio of maspin and PRSS21 may be important for tumour progression (Yeom, Jang et al. 2010).

The *maspin* gene is located on chromosome 18q21.3-q23 and is frequently hypomethyalated in cancer (Futscher et al 2002). Its expression has been found to be predominantly down-regulated in a number of tumours – such as breast, gastric –and melanoma however, it has also been shown to be over-expressed in some cancers which suggest that its role may be context dependant (Zou, Anisowicz et al. 1994). This difference may be accounted for due to the observations that maspin can localise to different sub-cellular locations, either cytoplasmic or nuclear or perhaps due to maspin interacting with the surrounding extracellular matrix (Zou, Anisowicz et al. 1994; Chen, Florens et al. 2005; Lockett, Yin et al. 2006; Klasa-Mazurkiewicz, Narkiewicz et al. 2009). Maspin has sequence homology with members of the serpin family of protease inhibitors which ~~re~~acts as a serpin only to membrane bound serine proteases (Schneider, Schick et al. 1995; McGowen, Biliran et al. 2000).

4.1.5 Cellular Function of Maspin

In-vitro studies have revealed that the role of maspin as a tumour suppressor is a combination of increased cellular adhesion and apoptosis but also decreased angiogenesis. Several studies show that maspin increases cellular adhesion (Seftor, Seftor et al. 1998; Cella, Contreras et al. 2006). Furthermore, maspin knockout mice are embryonic lethal, partially due to disrupted visceral endodermal cell adhesion. Restoring the expression of maspin in invasive carcinoma cells alters the expression of proteins regulating cell death and cytoskeltal architecture – resulting in an increased apoptosis and reduced invasive capacity (Chen, Florens et al. 2005). Furthermore; tumour cells biologically induced to re-express

maspin exhibit significantly increased apoptotic responses to a variety of drugs (Jiang, Meng et al. 2002; Liu, Shi et al. 2013).

Maspin is epigenetically regulated and its expression is closely associated with DNA methylation. The promoter methylation of maspin leads to silencing in a number of cancers. Maspin re-expression in breast tumour cells inhibits tumour invasion and metastasis (Zou, Anisowicz et al. 1994). Re-expression studies also confirmed that the inhibitory effect of maspin on tumour motility and invasion is localised on the tumour cell surface associated with increased ECM integrity and correlated with increased stability of cell ECM contacts (Sheng, Carey et al. 1996; Yin, Lockett et al. 2006). Finally of interest to this thesis, the clinical significance of maspin expression in SCC has been well documented in the literature, where re-activation of maspin may be important therapeutically in SCC of the cervix, oral and epithelia (Xia, Lau et al. 2000; Marioni, Staffieri et al. 2009; Liu, Shi et al. 2013; Marioni, Zanoletti et al. 2013).

4.2 RESULTS

4.2.1 PRSS21 is Over-expressed in a Number of cSCC Cell Lines

Before further investigating the function of PRSS21 in cSCC, its expression was quantified both at mRNA and protein level in a panel of cSCC cell lines isolated from a number of different patient types. The patient types investigated include RDEB, immunocompetant (IC) and transplant (T) and PRSS21 expression in these cells was compared to NHK. At mRNA level PRSS21 expression was up-regulated in all seven of the cSCC cell lines tested with the lowest expression seen in SCCRDEB3 and SCCRDEB4 cells (figure 4.2A). There was a good correlation between the mRNA and protein expression data (figure 4.2B), which also showed SCCRDEB3 and SCCRDEB4 to have the lowest expression, compared to NHK. These data would suggest that PRSS21 is over-expressed in a number of cSCC cell lines and hence is worth following up as a functional therapeutic target for the tumour type.

Figure 4.2

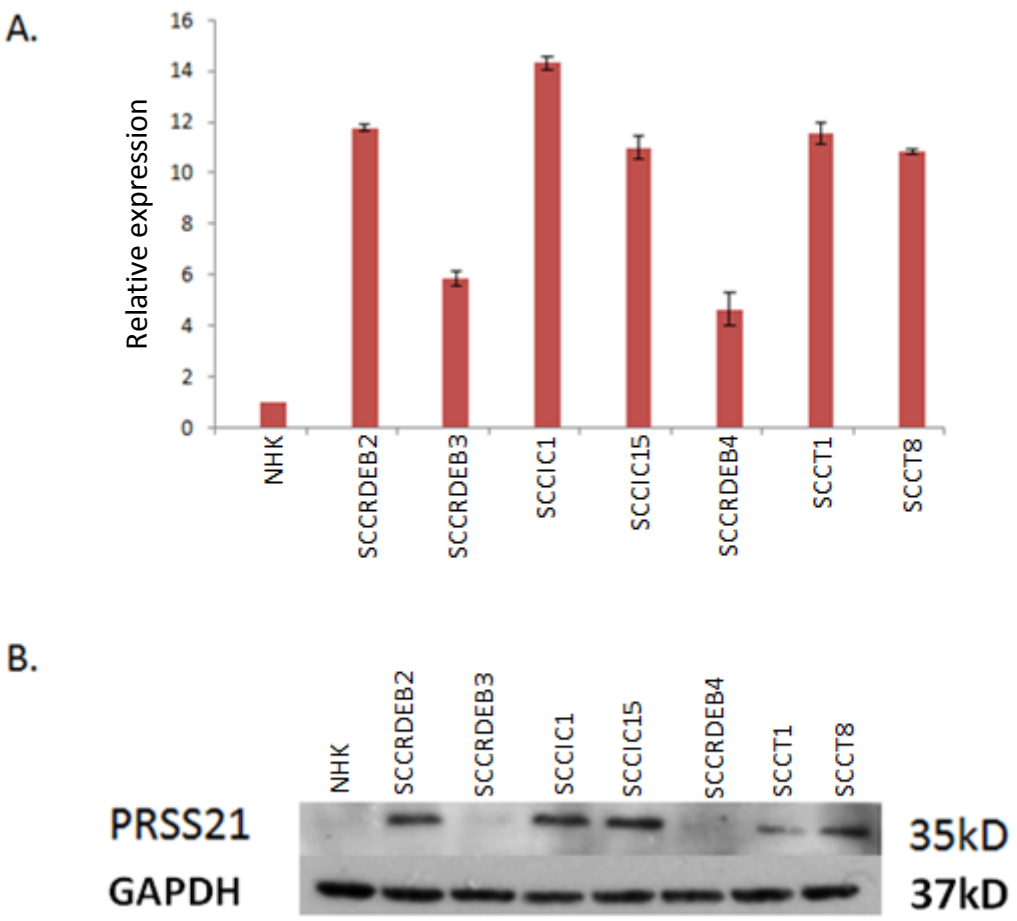

Figure 4.2 PRSS21 is Over-expressed in a Number of cSCC Cell Lines Compared to Normal Human Keratinocytes

(A) qPCR comparing mRNA levels in primary normal human keratinocytes (NHK) to a panel of cSCC cell lines from recessive epidermolysis bullosa (SCCEB2,3 & 4), immunocompetent (SCCIC1 & 15) and transplant (SCCT1 & 2) patients. Results represent the mean±SD, n=2. (B) Protein expression of PRSS21 (35KDa) in a panel of cSCC cell lines (above) as determined by western blot (n=2).

4.2.2 PRSS21 is Localised to the Cytoplasm of cSCC Cells

Immunofluorescence staining of cSCC cells, SCCRDEB2, SCCRDEB4 and SCCT8 show that PRSS21 is localised in the cytoplasm of cSCC cells with marked expression likely in the endoplasmic reticulum (ER). However, double staining with an ER marker would be required to confirm this localisation (figure 4.3). This is surprising as PRSS21 is a GPI linked protein which is supposed to localise it to the cell plasma membrane however other groups have also noted cytoplasmic localisation (Tang, Kmet et al. 2005; Yeom, Jang et al. 2010). Additionally loss of membrane polarity and the epithelial to mesenchymal transition can occur in tumour cells. There two processes have been previously shown to affect the cellular distribution of many of the membrane anchored serine proteases which may explain the misslocalisation observed in PRSS21 in cSCC cells (Lucas, J.M. 2008). Different fixatives did not change the localisation of PRSS21 (data not shown).

Figure 4.3

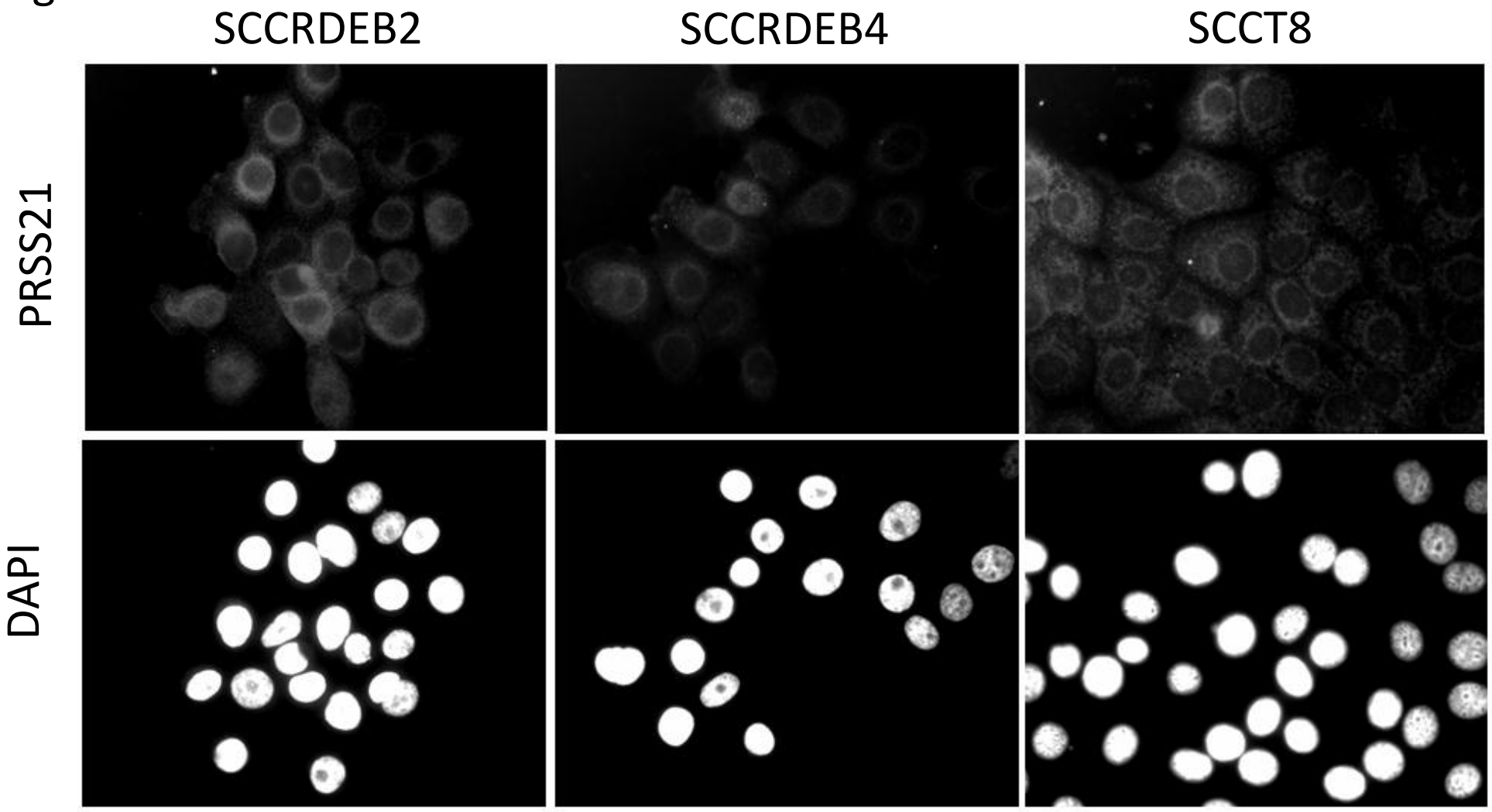

Figure 4.3 Immunofluorescent staining shows that PRSS21 is expressed in the cytoplasm of cSCC cells
Methanol:acetone fixation of SCCRDEB2, SCCRDEB4 and SCCT8 cells followed by immunofluorescent detection for PRSS21 (top panel), shows that PRSS21 is localised in the cytoplasm of these cSCC cell lines. DAPI in the lower panel was used as a nuclear counter stain. Magnification 64x, n=3.

4.2.3 Retroviral Over-expression of PRSS21 Increases Migration and Invasion in K1 Cells

The previous chapter 3, showed that the expression of PRSS21 was important for cSCC tumour cell survival, yet little is known about the function of PRSS21 in this tumour type. Proteases have been shown to function to increase motility and invasive capacity of a tumour. In order to explore this, PRSS21 was retrovirally over-expressed in HPV immortalised, normal human keratinocyte line – K1. Retroviral over-expression is a way to stably express a gene of interest, which is more useful when looking at the long term effects of a gene. By comparison, depletion of a gene using siRNA results in transient knockdown of the gene. K1 cells were chosen as they have very little endogenous levels of PRSS21, which allows the function of PRSS21 to be explored in this cell type. Using a retroviral transduction method (see materials and method section 2.5.7), these cells were transduced with either the empty pBABE vector as a control (K1pB) or with the pBABE vector containing PRSS21 (K1PRSS21). Retroviral over-expression of PRSS21 was then confirmed in these two lines using both qPCR and western blot. qPCR (figure 4.4A) shows that the relative expression of *PRSS21* is ~15 fold higher in the K1PRSS21 cells than the K1pB cells at mRNA level. PRSS21 expression, at protein level was assessed using western blot (figure 4.4B) which shows a significant over-expression of PRSS21 in the K1PRSS21 cells compared to K1pB. Additionally, it confirms that the K1pB cells have no endogenous expression of PRSS21.

Figure 4.4

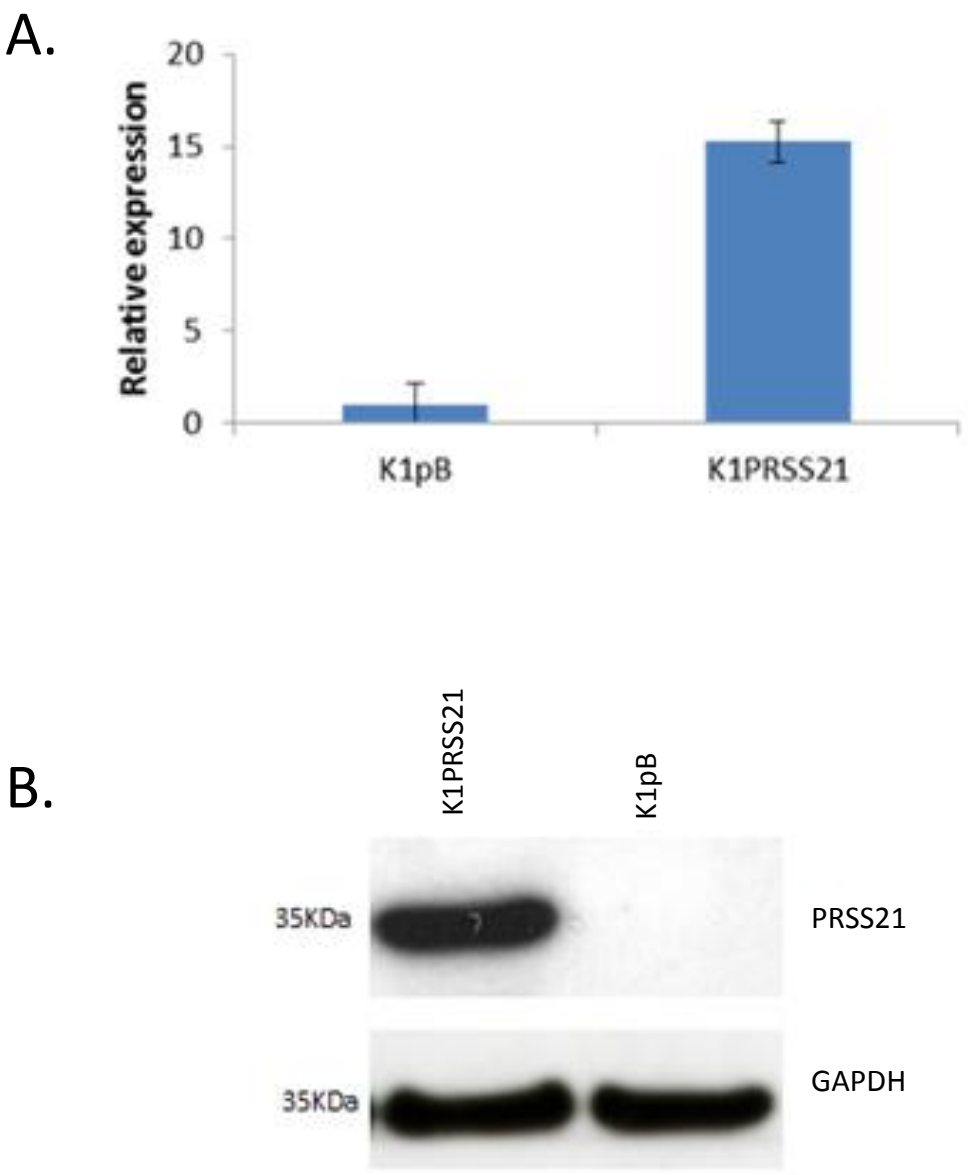

Figure 4.4 Confirmation of Retroviral Over-expression of PRSS21 (K1PRSS21) compared to Empty Vector (KipB) in K1 Cells at the mRNA and Protein Level ~~**Retroviral Over-expression of PRSS21 or Empty Vector in K1 cells (K1PRSS21 and K1pB, respectively) is Confirmed at mRNA and Protein Level**~~

K1 cells were retrovirally transduced with an empty vector pBABE control (K1pB) or PRSS21 vector (K1PRSS21). (A) qPCR showing that the relative mRNA expression of *PRSS21*is ~15 fold higher than in K1pB. (C) Western blot showing the expression of PRSS21 in both the K1pB and K1PRSS21 at protein level, GAPDH acts as a loading control. (n=3)

4.2.4 Over-expression of PRSS21 Increases Cell Migration

Cell migration is required for many important biological processes including tissue remodelling and tumour invasion. Many proteases act at the leading edge to direct cell migration and increase a tumours invasive phenotype. The scratch assay is a cheap effective method to investigate cell migration (Kohn & Liotta 1995)). Confluent cultures are grown and mitotically inactivated, using mitomycin C so that cell proliferation does not interfere with the cells migratory capacity. A scratch is created and representative images taken at 0h, 8h and 18hs (see chapter 2, section 2.8.5 for the methods). Using the *in-vitro* migration assay figure 4.5A shows an increase in migration in the cells expressing K1PRSS21 relative to the empty vector K1pB control, 18h after the scratch was performed. These data suggests that the over-expression of PRSS21 in cSCC may increases cell migration.

Figure 4.5

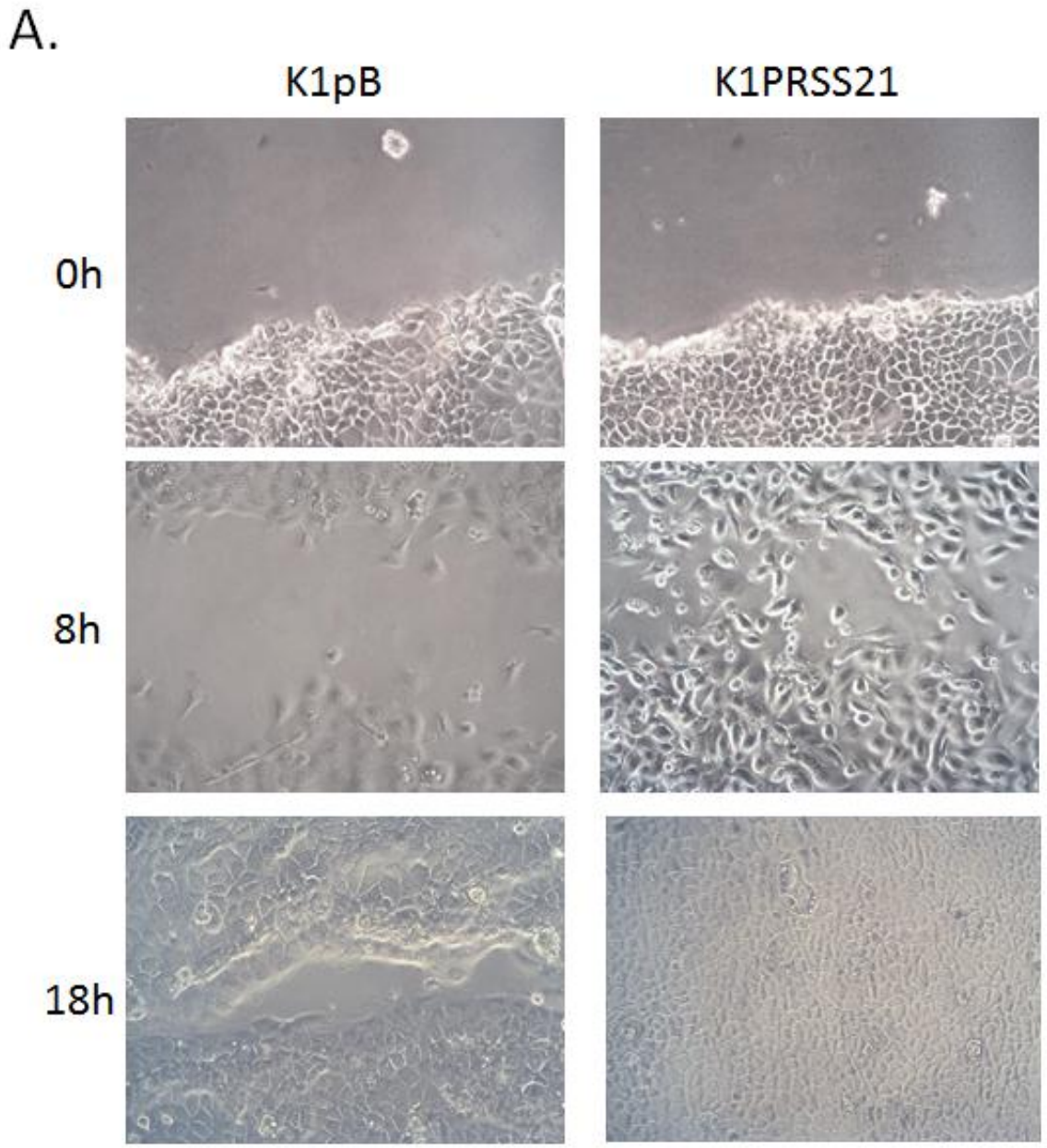

Figure 4.5 K1PRSS21 Cells Migrate Faster Than K1pB Cells

(A) Using the in-vitro migration assay, confluent K1pB or K1PRSS21 cells were scratched and images taken at 0h, 8h and 18h. The images taken at 8h and 18h show that K1PRSS21 cells migrate faster than K1pB cells to close the gap. n=3, images taken at 40x magnification.

4.2.5 PRSS21 Expression in Keratinocytes Increases Invasion in 3D Culture

Over the past decades the ability to mimic human skin *in-vitro* in three dimensional organotypic co-cultures of mesenchymal and epithelial derived cells supported by an extracellular matrix has evolved. A number of three dimensional methods exist such as scaffold-free platforms for spheroid growth, scaffolds, gels, bioreactors and microchips. Here, the collagen matrigel^{TM} system was used as it is routinely used within Dr South's lab. matrigel^{TM} was first documented in 1972 by Hynda Kleinman and is reconstituted BM preparation extracted from Engelbreth-Holm-Swarm mouse Sarcoma, a tumour rich in ECM proteins such as lamina and collagen plus growth factors (for review see Kleinman 2005). The set-up involves stromal fibroblasts either being embedded in collagen I, Matrigel^{TM}. Fibroblast embedded matrices are then used to support the growth of keratinocytes which are induced to stratify by being raised above the air-liquid interface (the assay is detailed in figure 2.1). Organotypic models have been extensively used to help model tumour invasion in the skin (Nystrom et al 2005, Martins et al 2009, Ng et al 2012). Additionally these 3D models with incorporated fibroblasts allow the user to explore stromal-epithelial interactions, which have been previously shown to be important for tumour initiation and progression (Ng, Pourreyron et al. 2012). To examine whether the expression of PRSS21 had an effect on invasion, K1pB or K1PRSS21 transduced cells were cultured on collagen:matrigel gels with incorporated normal fibroblasts (figure 4.6A). Expression of PRSS21 increased invasion of keratinocytes into the gel almost 2 fold. Quantification of invasion showed that after a relatively short period of 7 days there was a 1.5 fold increase in invasion into the gel (figure 4.6B).

Figure 4.6

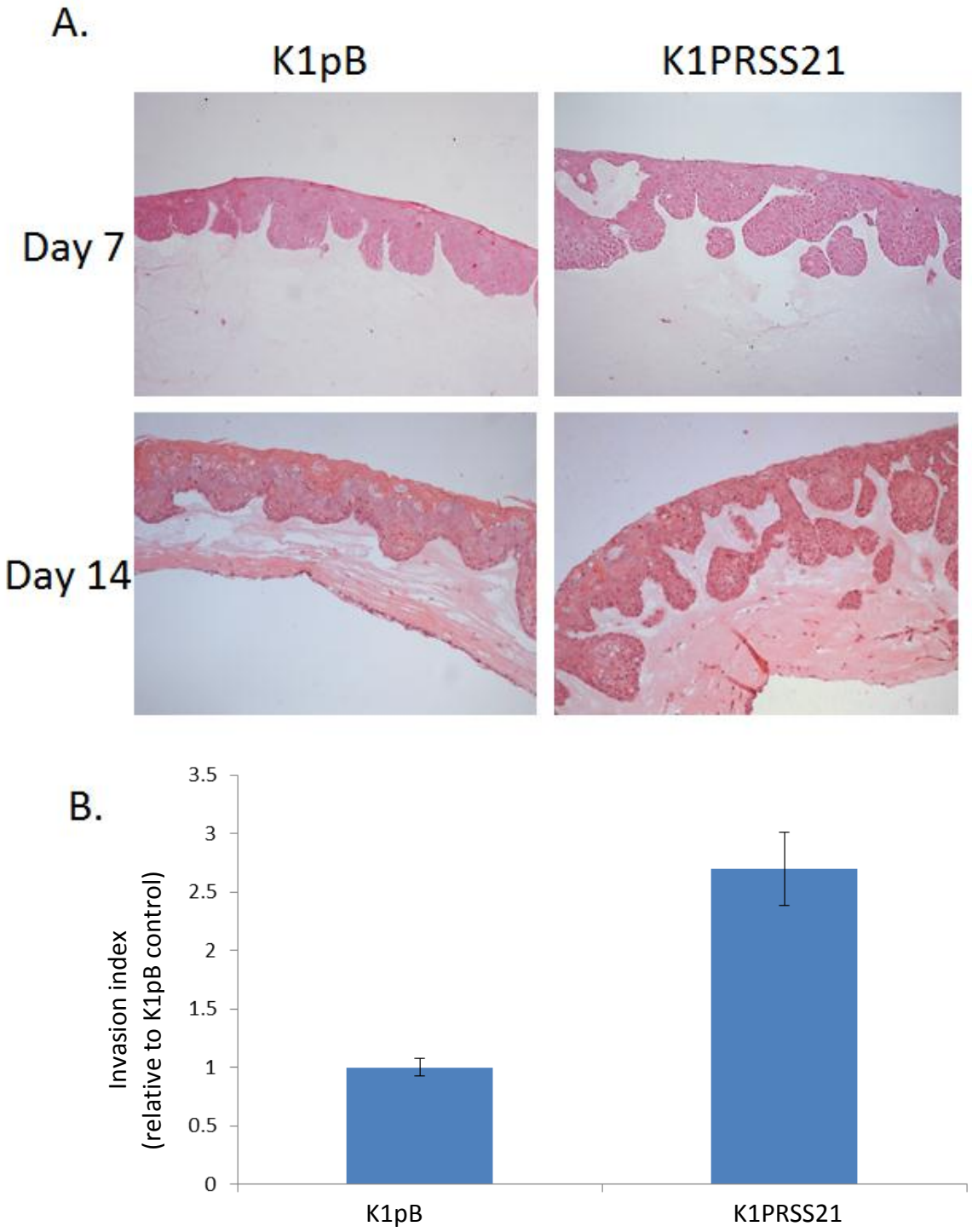

Figure 4.6 Collagen:matrigels Show Increased Invasion in K1PRSS21 Cells Compared to K1pB Transduced Cells.

(A) K1pB or K1PRSS21 cells were seeded onto collagen:matrigels and gels processed after 7 or 14 days. Sections were cut and stained using H&E which shows that the K1PRSS21 cells invade deeper than the K1pB cells. Results are representative of 2 independent experiments, with 8 sections stained from each. Images taken at 40x magnification (B) Depth of invasion was quantified using an invasion index showing that K1PRSS21 invades into the gel after 7days. Results represent the mean ± SD of 8 stained sections across 2 experiments.

4.2.6 PRSS21 and Maspin Interact in cSCC Using the PLA Assay

PRSS21 and maspin have been shown to interact in cervical cancer cells, and their relationship is thought to be important for tumour progression in this cell type (Yeom et al 2010). The proximity ligation assay (PLA) has previously been used to detect protein-protein interactions using antibodies which are not suitable for the standard method of detecting interactions - co-immunoprecipitation. CO-IP was attempted; however the antibody to PRSS21 had a lot of background/non-specific staining using western blot which affected the ability to specifically detect bound proteins which have the ability to maintain stable interactions. The PLA principal is based on two primary antibodies raised in different species being able to recognise the target protein of interest i.e. PRSS21 and maspin (see section 2.8.6). Subsequent incubation with a species specific secondary PLA probes, with short DNA strands attached binds to the respective primary antibody. After addition of the PLA probes, if they are in close proximity then the DNA strands can interact through addition of circle forming DNA which is amplified using phi29 DNA polymerase in rolling circle amplification (RCA). The resulting RCA product indicates~~is~~ a physical interaction between the two proteins. Additionally, an RCA product can be labelled by hybridisation of many fluorophore conjugated DNA oligonucleotides which allow fluorescent visualisation by microscopy. The resulting fluorescent staining indicates an interaction. Using PLA to determine if this interaction occurs in cSCC cells Figure 4.7 shows that PRSS21 and maspin both interact in the cytoplasm *in-vivo* in SCCRDEB2 xenograft tissue. A control with the secondary antibody only, shows that there is a slight background effect. The lower panel of images indicates DAPI counter staining for both images.

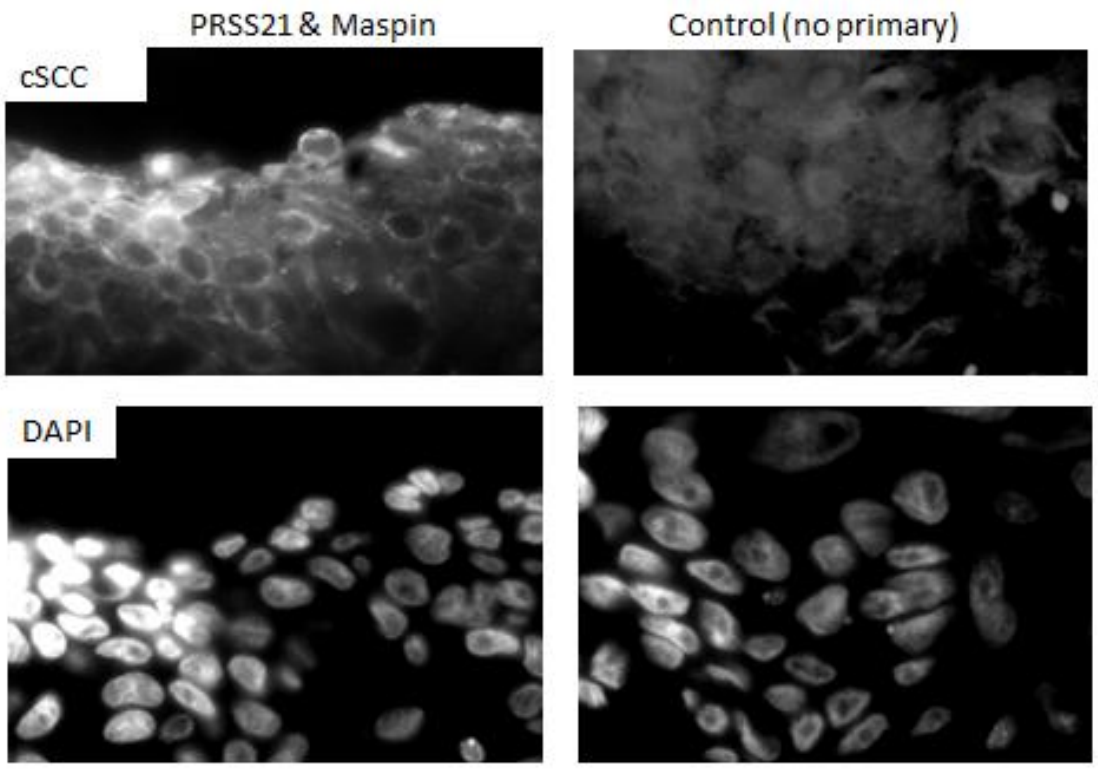

Figure 4.7 PRSS21 and Maspin Interact *in-vivo* in cSCC As Determined By ~~The~~ PLA

Images represent cytoplasmic protein-protein interaction between PRSS21 and maspin in xenograft SCCRDEB2 tissue as detected by the PLA assay. Results represent n=2 experiments.

4.2.7 Depletion of PRSS21 Increases~~Reduces~~ Maspin Expression at mRNA Level and Transient Over-expression of PRSS21 Significantly Reduces the Expression of Maspin in cSCC Keratinocytes

Using siRNA to knockdown the mRNA expression of *PRSS21* in cSCC keratinocytes figure 4.8A shows a 60% increase in the expression of *maspin* using pooled siRNA (PRSS21_P) targeted to *PRSS21* relative to the non-targeting control (SCR). Additionally, over-expression of PRSS21 using cDNA (OriGene, Rockville, MD) in SCCRDEB2 further reduces the expression of maspin at protein level 48 hours after transient transfection (figure 4.8B).

Figure 4.8

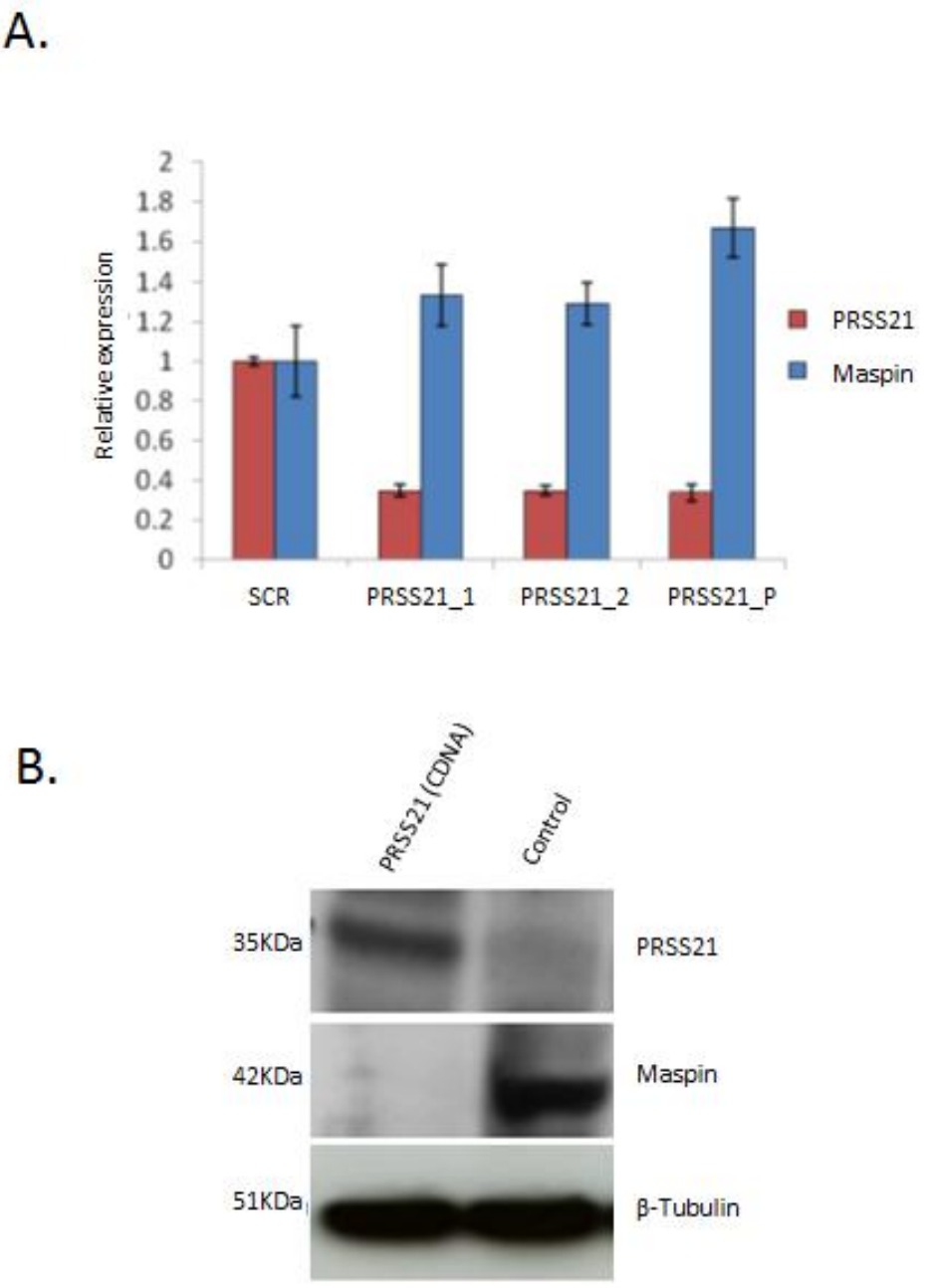

Figure 4.8 Depletion of PRSS21 Increases~~Reduces~~ Maspin Expression at mRNA Level and Over-expression of PRSS21 Reduces the Expression of Maspin in SCCRDEB2 Cells at Protein Level

(A) qPCR following siRNA knockdown of *PRSS21* using individual oligonucleotides (PRSS21_1/2) or pooled oligonucleotides (PRSS21_P) shows a 60% increase in *maspin* expression in SCCRDEB2 cells. Results represent the mean±SD of 3 independent experiments. (B) Western blot showing protein expression of PRSS21 and maspin following transient transfection of SCCRDEB2 cells with PRSS21 cDNA reduces the expression of maspin. β-Tubulin was used as a loading control. immunoblot is representative of 3 independent experiments.

4.2.8 PRSS21 Expression is Reduced in Normal Human Skin Compared to a Panel of cSCC Xenogafts

Immunofluorescence staining of PRSS21 and maspin in normal human skin shows that maspin is strongly expressed throughout the epidermis whereas PRSS21 expression is much lower (figure 4.9). Maspin is also predominantly expressed in the cytoplasm throughout the epidermis.

In 5 out of the 6 tumours stained, PRSS21 expression (figure 4.10A1) is increased compared to maspin expression (figure 4.10A2). However, SCCIC8, which is a well differentiated tumour, is the only tumour to have stronger staining of maspin compared to PRSS21. Maspin is thought to be associated with well differentiated tumour types. Additionally SCCRDEB2 has patches of high maspin expression, which may be associated with an area of differentiation in this tumour type. DAPI was used as a nuclear counter-stain for the staining – these images are in figure 4.10B1, 4.10B2 for PRSS21 and maspin staining, respectively.

Figure 4.9

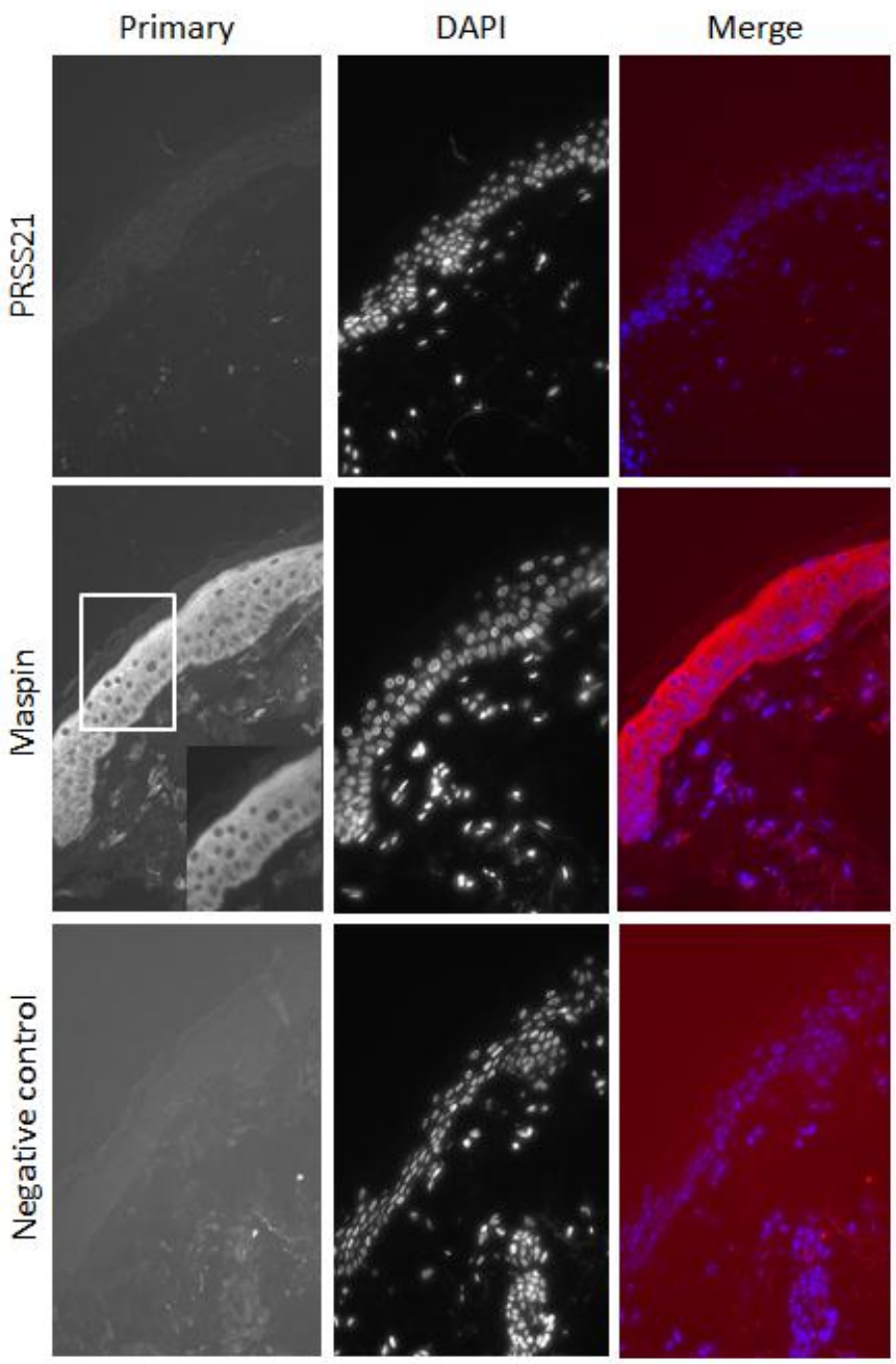

Figure 4.9 Immunofluorescent Staining of Normal Human Skin with Antibodies Raised Against PRSS21 and Maspin.

Top panel shows that normal human skin (NHS) has no positive PRSS21 staining however the middle panel shows that NHS has positive maspin expression throughout the epidermis, with the majority of expression localised in the cytoplasm. The lower panel is a negative control for the secondary antibody. Results are representative of 2 experiments. All images taken at 16 x magnifications apart from inset of primary maspin antibody staining which is at 40x magnification.

Figure 4.10A

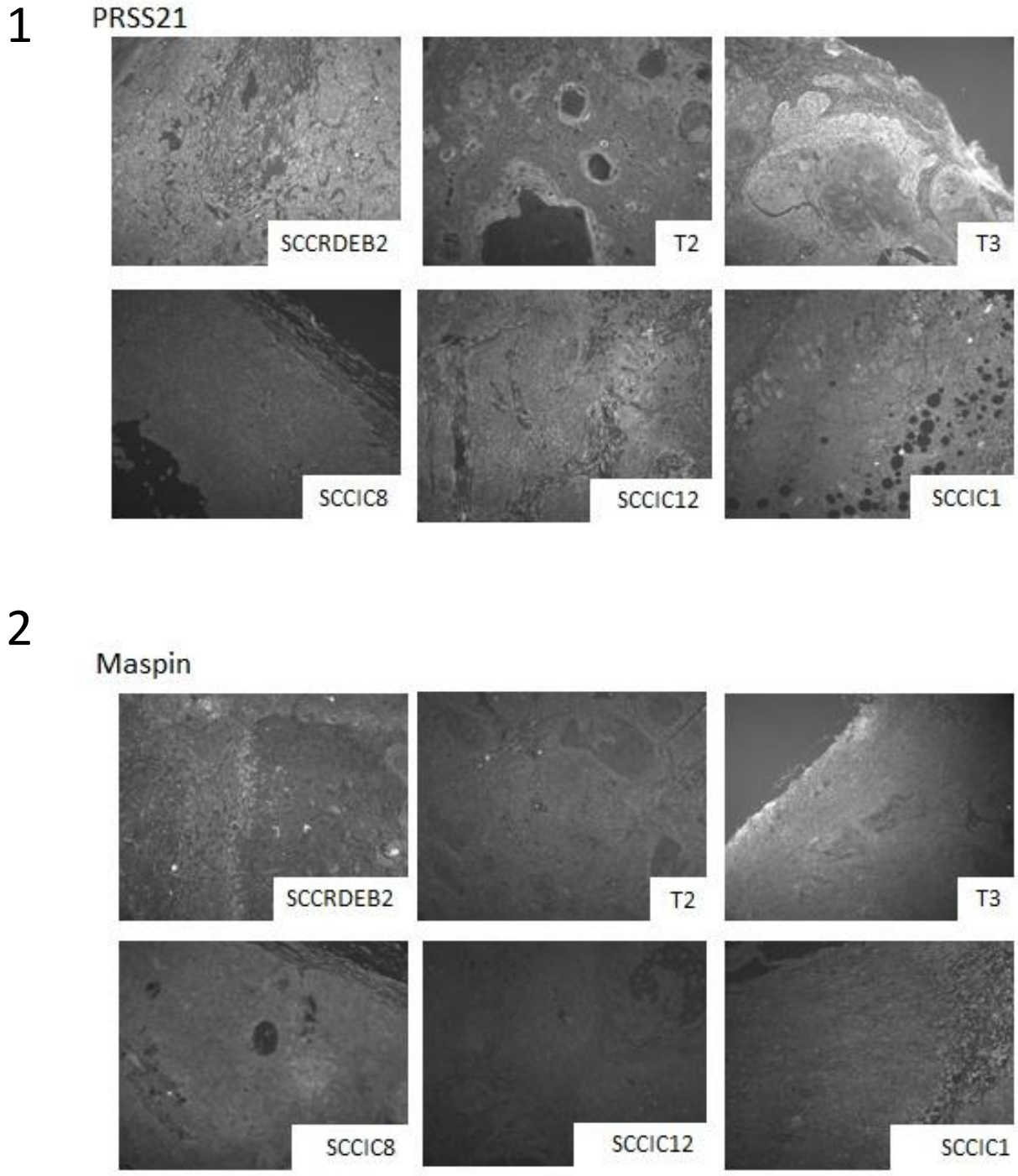

Figure 4.10A Expression of PRSS21 and Maspin in a panel of cSCC Xenograft Tumours

Immunofluorescent staining of PRSS21 (1) or maspin (2) in formalin fixed paraffin embedded xenograft tumours. Tumours are from recessive dystrophic epidermolysis bullosa (RDEB), transplant (T) and immunocompetent patients (for more clinical details see table 2.1). Images taken at 16x magnification. N=2

Figure 4.10B

1

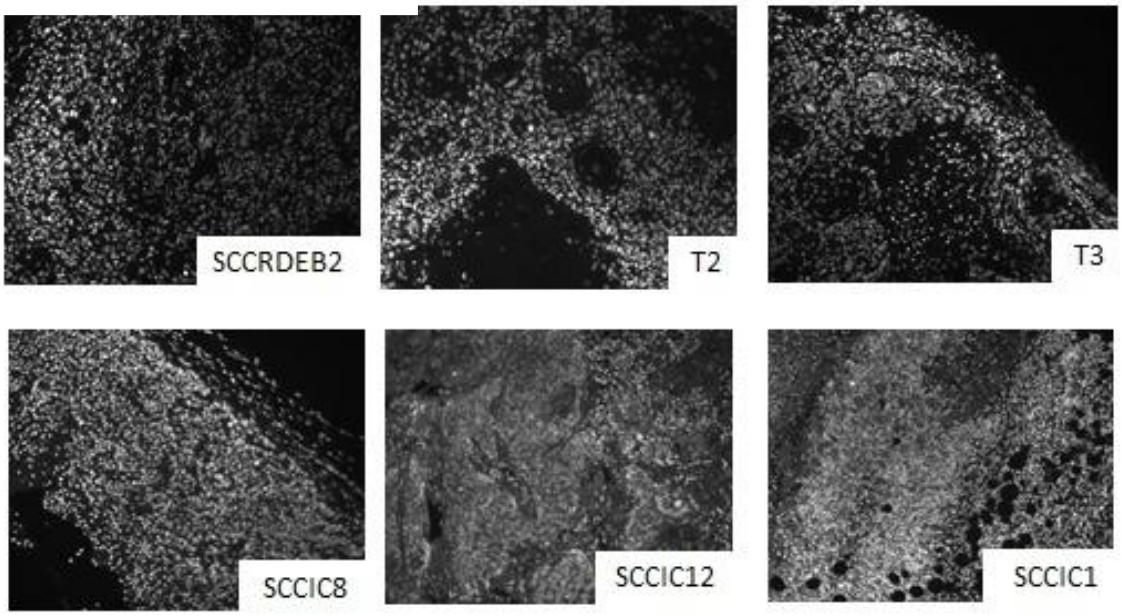

2

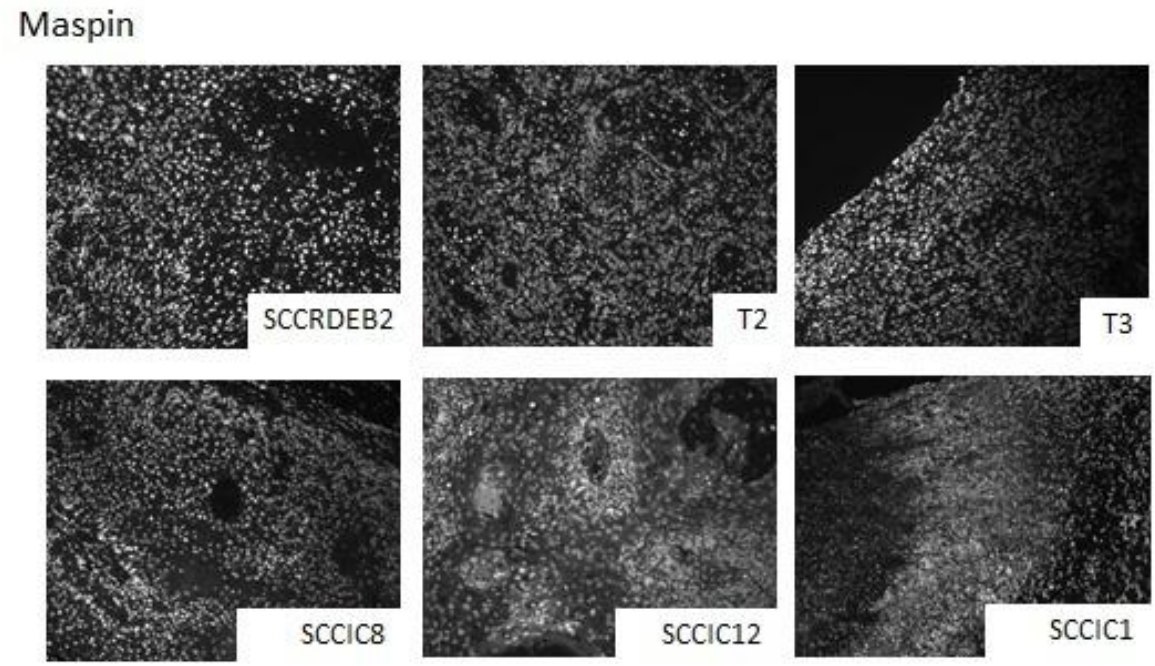

Figure 4.10B DAPI for Xenograph Staining in Figure 4.7A

Immunofluorescent staining of PRSS21 (1) or maspin (2) in formalin fixed paraffin embedded xenograft tumours. Tumours are from recessive dystrophic epidermolysis bullosa (RDEB), transplant (T) and immunocompetent patients (for more clinical details see table 2.1). Images taken at 16x magnification. N=2

4.2.9 Retroviral Over-expression of PRSS21 Reduces Maspin Expression in Organotypic Cultures

Staining of collgan:matrigels with K1pB and K1PRSS21 with antibodies to maspin or PRSS21 confirms there is an increased expression of PRSS21 in the cells transduced with PRSS21 compared to the empty vector control cells (figure 4.11). Additionally, the expression of PRSS21 is more prominent at the leading edge of the invading cells in the gels with K1PRSS21. A concurrent reduction in maspin expression is also seen in these cells; K1pB express significantly more maspin than the K1PRSS21.

Figure 4.11A

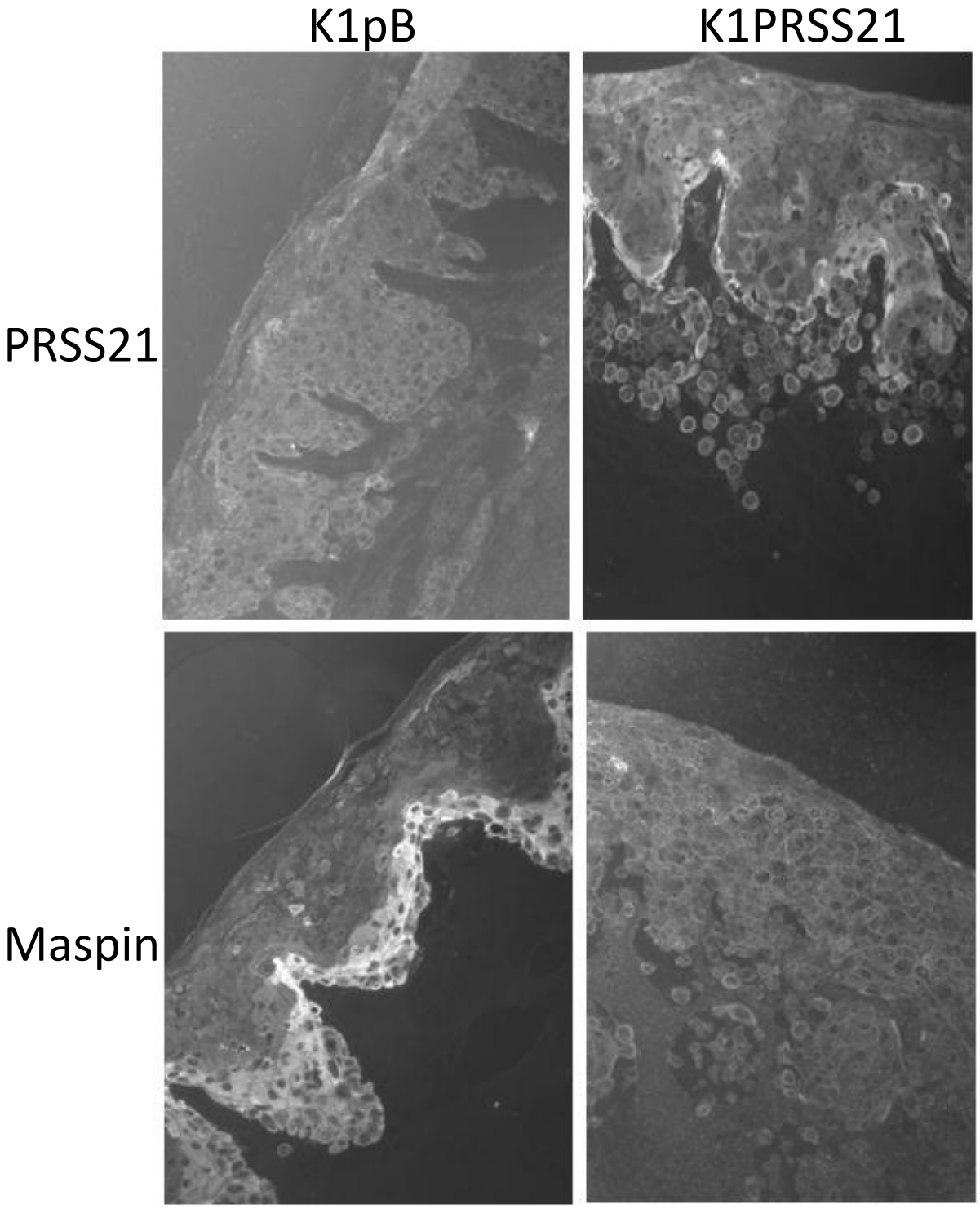

Figure 4.11A Retroviral Over-expression of PRSS21 Reduces Maspin Expression in Organotypic Cultures

The top panel shows PRSS21 staining in K1PRSS21 collagen:matrigel organotypic cultures is over-expressed compared to K1pB. The lower panel shows the opposite is true for maspin expression; which is highly expressed in K1pB cells but not K1PRSS21 organotypics. Images are representative of 2 independent experiments. Images taken at 16x magnification.

Figure 4.11B

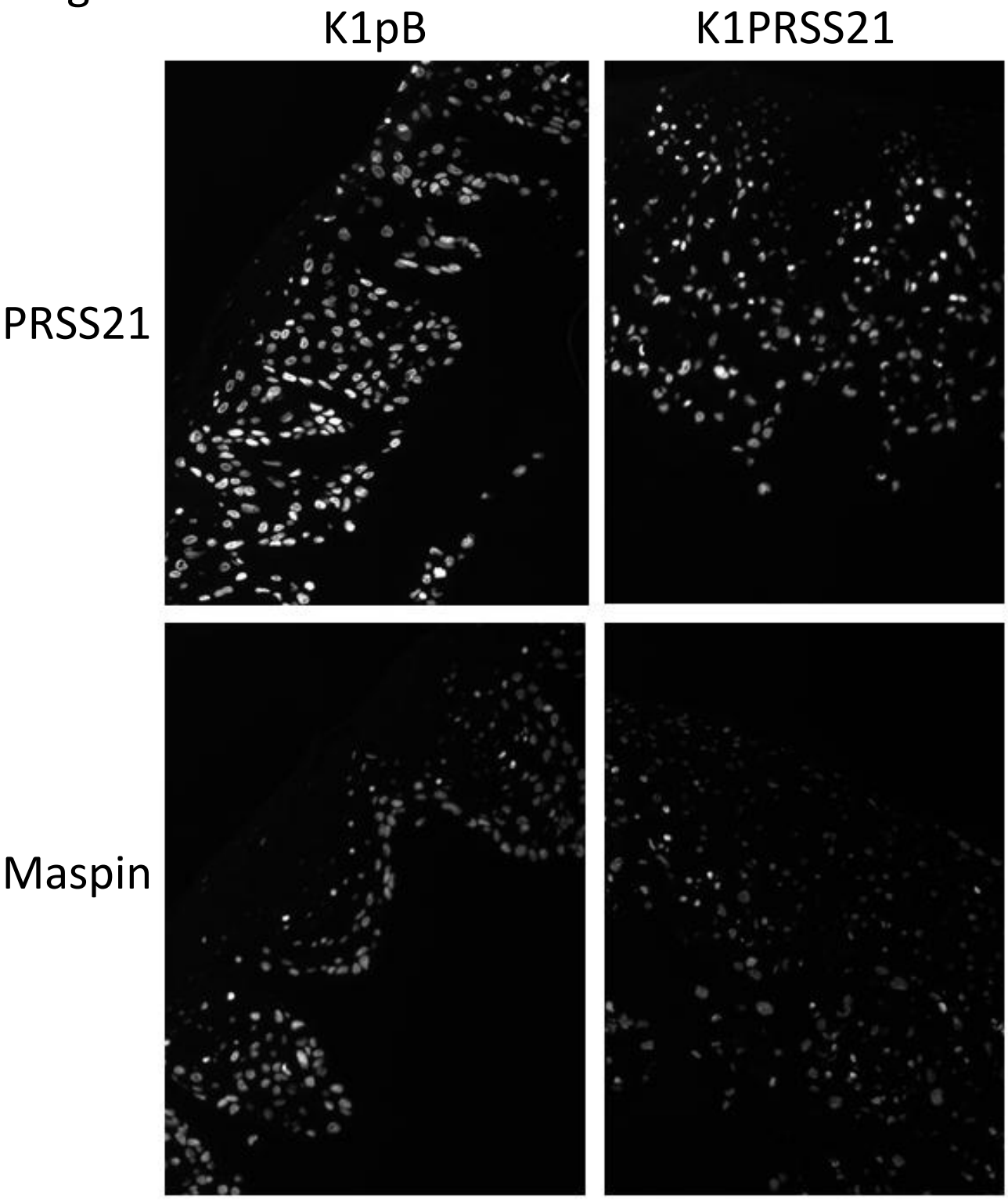

Figure 4.11B DAPI for collagen:matrigels in figure 4.11A

The top panel shows DAPI staining for PRSS21 staining in K1PRSS21 collagen:matrigel organotypics in figure 4.8A. The lower panel shows the DAPI staining for maspin staining in K1pB collagen matrigel organotypic s in figure 4.8A. Images taken at 16x magnification.

4.2.10 Retroviral Over-expression of PRSS21 Reduces Involucrin Expression

Previous work on maspin expression has shown its expression in skin and cutaneous carcinomas to be associated with differentiation status (Reis-Filoh et al 2002). Involucrin is marker of terminal differentiation and contributes to the cornified envelope of the skin (Eckrt & Green et al 1986). Haematoxylin and Eosin staining of 3D organotypic gels with cultured K1PRSS21 or K1pB cells, indicated that there was a decrease in keratin and the cornified envelope in the K1PRSS21 cells compared to K1pB (figure 4.6), indicative of a decrease in differentiation in this cell type. Using involucrin as a marker of differentiation, retroviral over-expression of PRSS21 in K1 cells reduces the expression of involucrin compared to the empty vector control after 7 days and 14 days (figure 4.12A and B. respectively).

Figure 4.12A

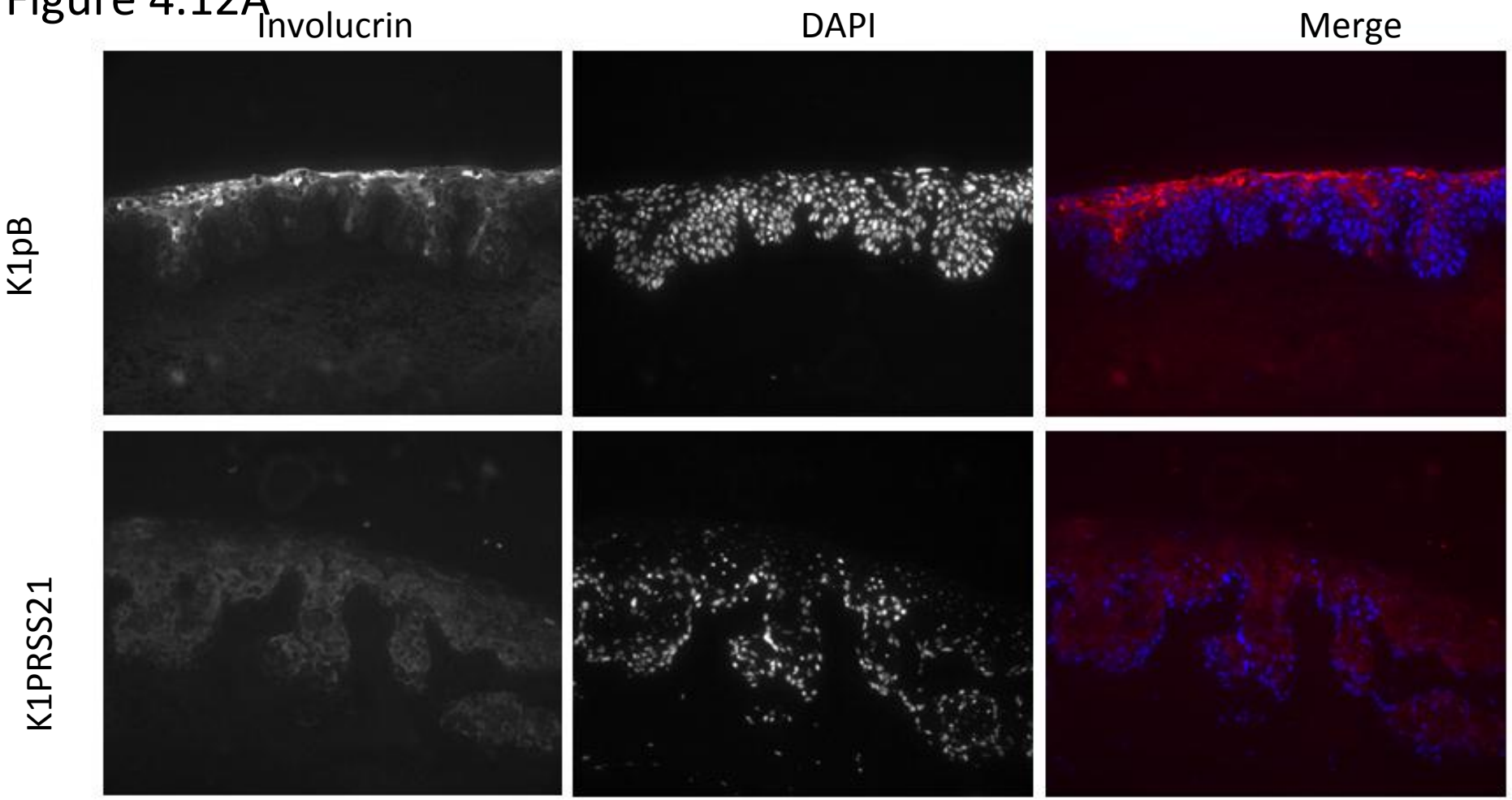

Figure 4.12A K1PRSS21 Collagen:matrigels Have a Lower Expression of Involucrin After 7 days Compared to K1pB gels.

Collagen:matrigels with either KIpB cells (top panel) or K1PRSS21 (lower panel) were stained with involucrin, 7 days after the gels were raised above the air:liquid interface. DAPI was used as a nuclear counter stain. Images taken at 16x magnification , n=2.

Figure 4.11B

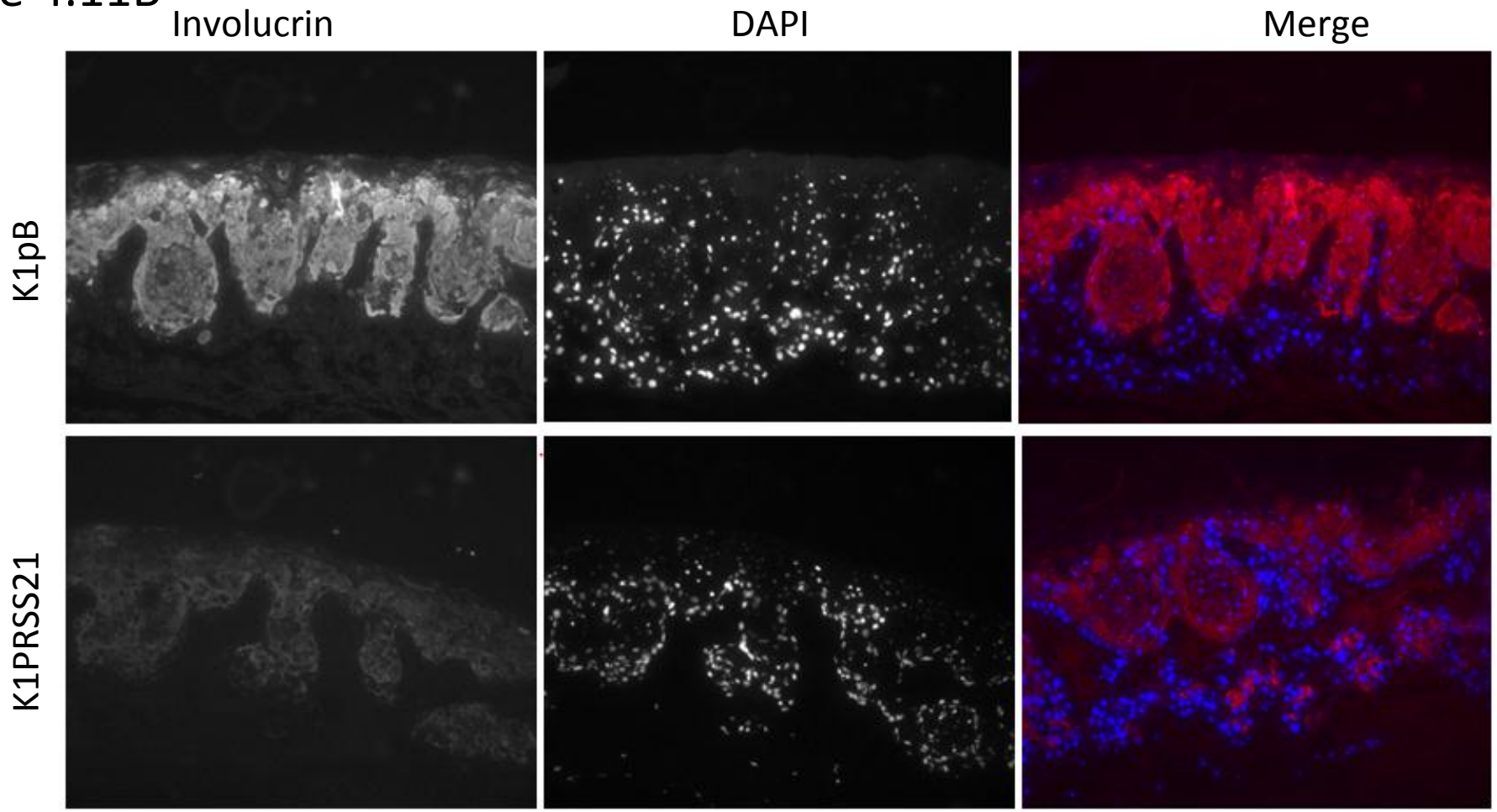

Figure 4.12B K1PRSS21 collagen:matrigels Have a Lower Expression of Involucrin After 14 Days compared to K1pB control collagen:matrigels

Collagen:matrigels with either KIpB cells (top panel) or K1PRSS21 (lower panel) were stained with involucrin, 7 days after the gels were raised above the air:liquid interface. DAPI was used as a nuclear counter stain. Images taken at 16x magnification, n=2.

Figure 4.12C

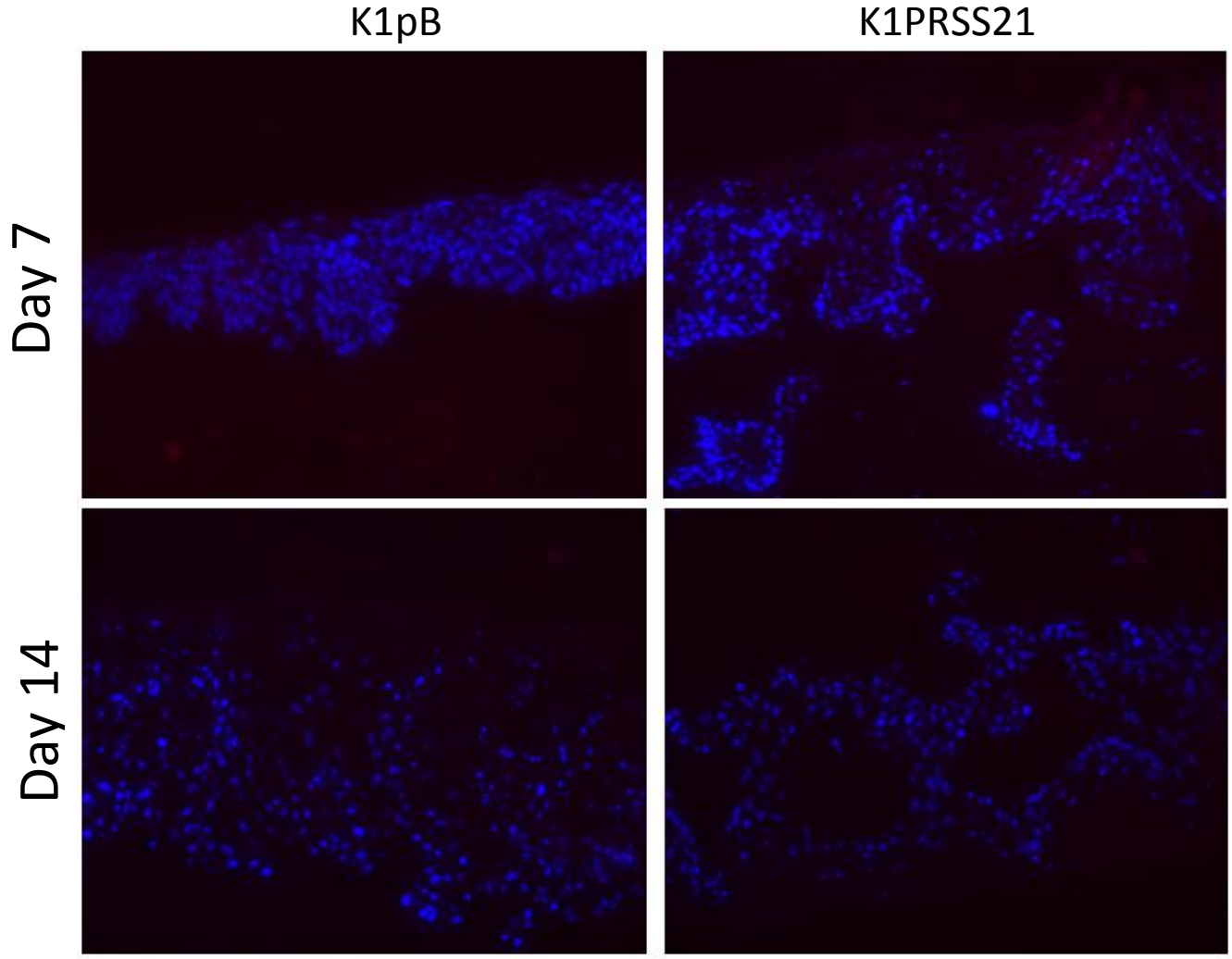

Figure 4.12C No Primary Antibody Control For Figures 4.12A, B

Collagen:matrigels with either KIpB cells (top panel) or K1PRSS21 (lower panel) were stained without the primary antibodies, to control for background staining caused by the secondary antibody. Images represent the secondary antibody staining and DAPI counter stain control merged together to show that there is very little background staining with this antibody. Images taken at 16x magnification, n=2.

4.2.11 PRSS21 depletion induced caspase activity is dependent on maspin

Previous work has shown that maspin is able to sensitise cancer cells to apoptosis (Liu, Shi et al. 2013). To analyse whether the PRSS21 siRNA induced caspase mediated cell death (figure 3.15A) could be regulated by maspin, a double knockdown strategy was employed by depleting both PRSS21 and maspin simultaneously. This showed a clear attenuation of PRSS21 depletion induced caspase activation, when maspin levels were reduced (figure 4.13). Hence PRSS21 depletion induced caspase activity is dependent on maspin.

Figure 4.13

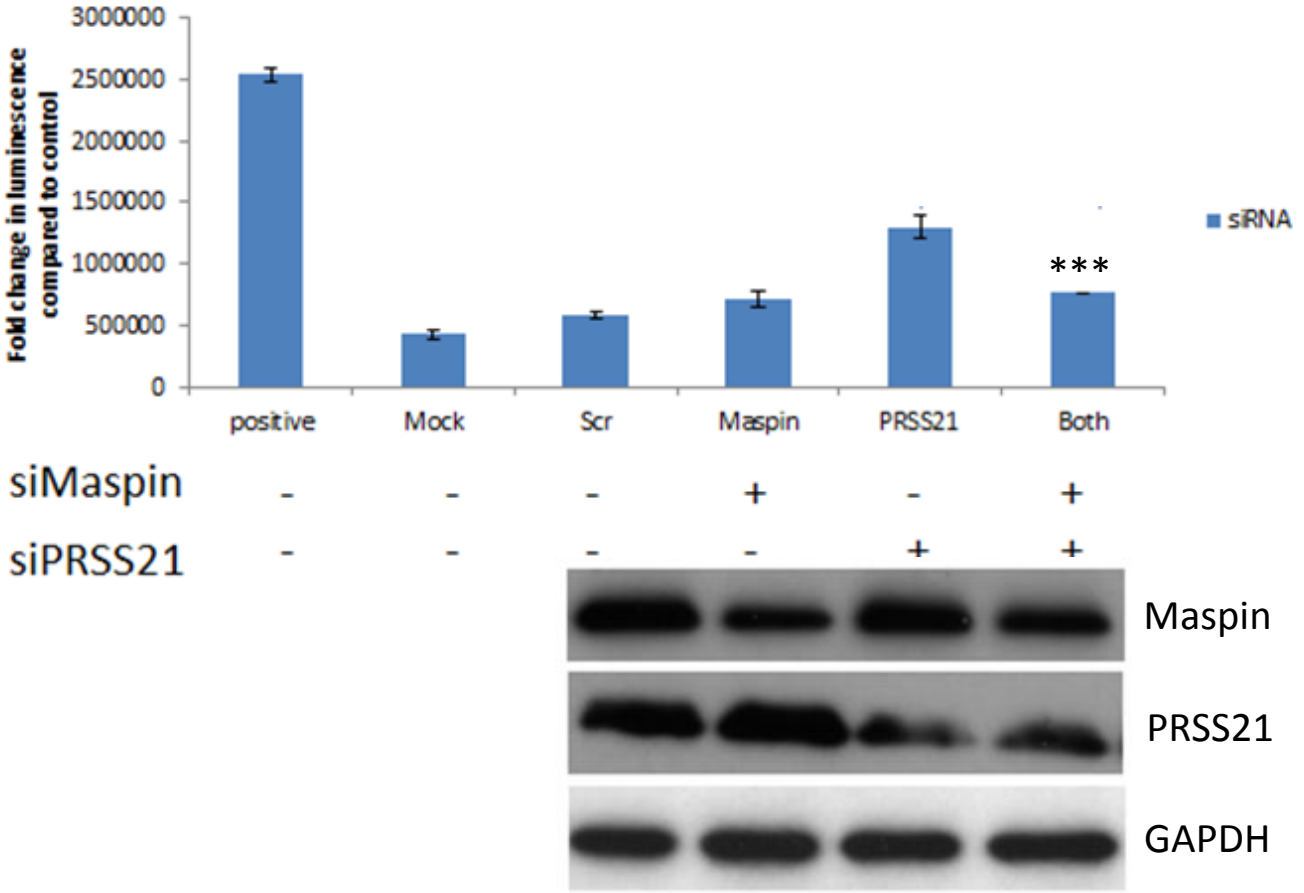

Figure 4.13 PRSS21 Depletion Induces Caspase 3/7 Activation Which Can be Attenuated Upon Depletion of Maspin

Using a siRNA knockdown strategy PRSS21 knockdown is shown to block maspin-induced caspase 3/7 activity. Positive cell death siRNA control (PC) siRNA was used as a positive control for caspase activation; "Mock" is a lipofectamine alone. All results show the mean ± SD,n=3, ***P<0.001. GAPDH was used as a loading control.

4.3 DISCUSSION

Previous work in our lab identified PRSS21 as being over-expressed in cSCC compared to normal human keratinocytes. This fits with a number of other publications showing that PRSS21 is over-expressed in a number of other cancers including ovarian, cervical, melanoma and lymphoma (Hooper, Nicol et al. 1999; Hooper, Bowen et al. 2000; Honda, Yamagata et al. 2002; Tang, Kmet et al. 2005). Subsequently, it was shown to induce colony formation and promote malignant transformation in ovarian cancer cells (Tang, Kmet et al. 2005). Gene expression analysis identified PRSS21 to be over-expressed in cSCC *in-vivo* (average fold change of 1.5 over three independent data sets) compared with normal skin and *in-vitro* (7.4 fold, $p<0.0005$, $n=8$) compared to normal keratinocytes (Watt 2011). In the previous chapter 3, PRSS21 was shown to be important for cSCC cell survival. RNAi knockdown of PRSS21 decreases cell viability (figure 3.13), through increased cytotoxicity (figure 3.2). Normal primary keratinocytes are unaffected. Cell death is via apoptosis as detected by an increase in cytoplasmic nucleosomes (figure 3.14), caspase activity (figure 3.16A) and Annexin V/7AAD positive cells (figure 3.16B). In this chapter, to explore the function of PRSS21 in cSCC keratinocytes, PRSS21 was over-expressed in a HPV immortalised normal human cell line, K1. K1 cells were chosen as they have low levels of endogenous PRSS21, which allows unequivocal exploration of its function and to observe if expression of PRSS21 transforms the behaviour of this keratinocyte cell line. Primary keratinocytes were not used as they cannot be split for successive rounds, as they tend to differentiate after three or more passages.

Degradation of ECM is an important pre-requisite of local invasion and distant metastasis of tumour cells. Organotypic cultures on collagen:matrigel gels have previously been utilised to

study tumour invasion as they are a good 3D model of the skin tumour invasion. Developed by Fusenig and colleagues, these gels allow the user to assess the "invasion index" of tumour cells and highlight the importance of the underlying communicators – the stromal cells in modulating the ability of tumour cells to invade (Fusenig et al 1983). Additionally, they enable a 3D model which recapitulates the *in-vivo* situation more closely than 2D cell culture. Using this 3D method, cells over-expressing PRSS21 (K1PRSS21) invade deeper into the gel than those expressing the empty vector as a control. Additionally, even after 14 days an intact dermal-epidermal junction is present in the K1pB cells and they closely resemble an organotypic formed by normal keratinocytes with proper stratification. It would be useful to stain for basement membrane proteins to illustrate an intact dermal epidermal junction.

Using a yeast two-hybrid system to identify an intracellular target of PRSS21, maspin was first shown to interact with PRSS21 in human HeLa cells – a cervical cancer cell line (Yeom, Jang et al. 2010). The authors show that the ratio of maspin and PRSS21 expression determines the invasiveness of two cervical cancer cells using transwell inserts coated with matrigel. siRNA knockdown of PRSS21 and maspin modulates the invasiveness of these cervical cancer cells, where siRNA depletion of maspin, increases the number of cells that have moved from the upper chamber to the lower chamber of the transwell insert, indicating an increase in invasion in the presence of PRSS21. Furthermore, maspin expression decreased the invasiveness of cervical cancer cells, and invasiveness was restored through expression of PRSS21 (Yeom, Jang et al. 2010). In this thesis, antibody staining of organotypic cultures with K1PRSS21 or K1pB cells demonstrates that maspin expression is reduced when PRSS21 is over-expressed in K1 cells. This reduction in maspin in addition to the expression of PRSS21 could aid the invasive phenotype of the K1PRSS21

cells. It is thought that maspin's ability to bind to the surface is key to its ability in decrease invasion and motility in breast and prostate cancer cells. Perhaps what might be happening is that the over-expression of PRSS21 results in maspin being secreted out of the cell to act at the cell membrane to inhibit invasion. Also of striking appearance, is that the over-expression of PRSS21 is highest at the leading edge of the tumour, which would be most important for its protease activity involved in invasion. One key experiment in follow up to these results would be to carry out site-directed mutagenesis on the essential serine in the catalytic domain of PRSS21 so that it loses its protease function and observe if this changes the amount of invasion. Unfortunately, due to time constraints this was not possible.

Haematoxylin and eosin staining of collagen matrigels with K1PRSS21 and K1pB shows noticeable differences in cellular differentiation. K1pB organotypics have a much larger cornifed layer than that of the K1PRSS21. Following this observation, the organotypics were stained with the terminal differentiation marker involucrin. This showed that there was a significant decrease in involucrin upon PRSS21 over-expression thereby indicating a decrease in differentiation. The expression of maspin is associated with differentiation status in lung adenocarcinoma and oral cSCC and is therefore indicative of good prognosis (Xia et al. 2000, Lonardo et al 2005). Furthermore, two studies have shown that maspin is more likely expressed in well-differentiated subtypes; especially in keratinous pearls which are swirl shaped accumulations of keratin made by malignant squamous cells (Yasumatsu et al. 2001, Reis-Filho et al 2002). Hence, perhaps the expression of maspin in cSCC is responsible for increasing differentiation and this function contributes to its tumour suppressive mechanism in normal keratinocytes and early stage cSCCs.

To summarise the data on PRSS21 the following hypothetical model has been developed to show that the ratio of PRSS21 and maspin may be important for cSCC cancer progression (figure 4.11). In normal cells maspin is highly expressed and its localisation has been demonstrated to be not only cytoplasmic, but nuclear, membrane bound and secreted into extracellular compartment (Zou, Anisowicz et al. 1994; Khalkhali-Ellis 2006). However PRSS21 is expressed at low levels in normal keratinocytes perhaps due to the high levels of maspin acting as a tumour suppressor in normal cells. In cSCC tumour cells a significant over-expression of PRSS21 reduces the expression of maspin perhaps through negative regulation. The ability of PRSS21 to increase proliferation and simultaneously increase invasion helps tumour cells to break away to colonise in other parts of the body. However maspin plays an opposing role as an important tumour suppressor which modulates tumour motility, inhibiting invasion and cellular migration. Maspin has been shown to affect cell adhesion through cytoskeletal reorganisation and integrin signalling transduction pathway. Additionally work here and in previous publications would suggest it also does this by contributing to differentiation.

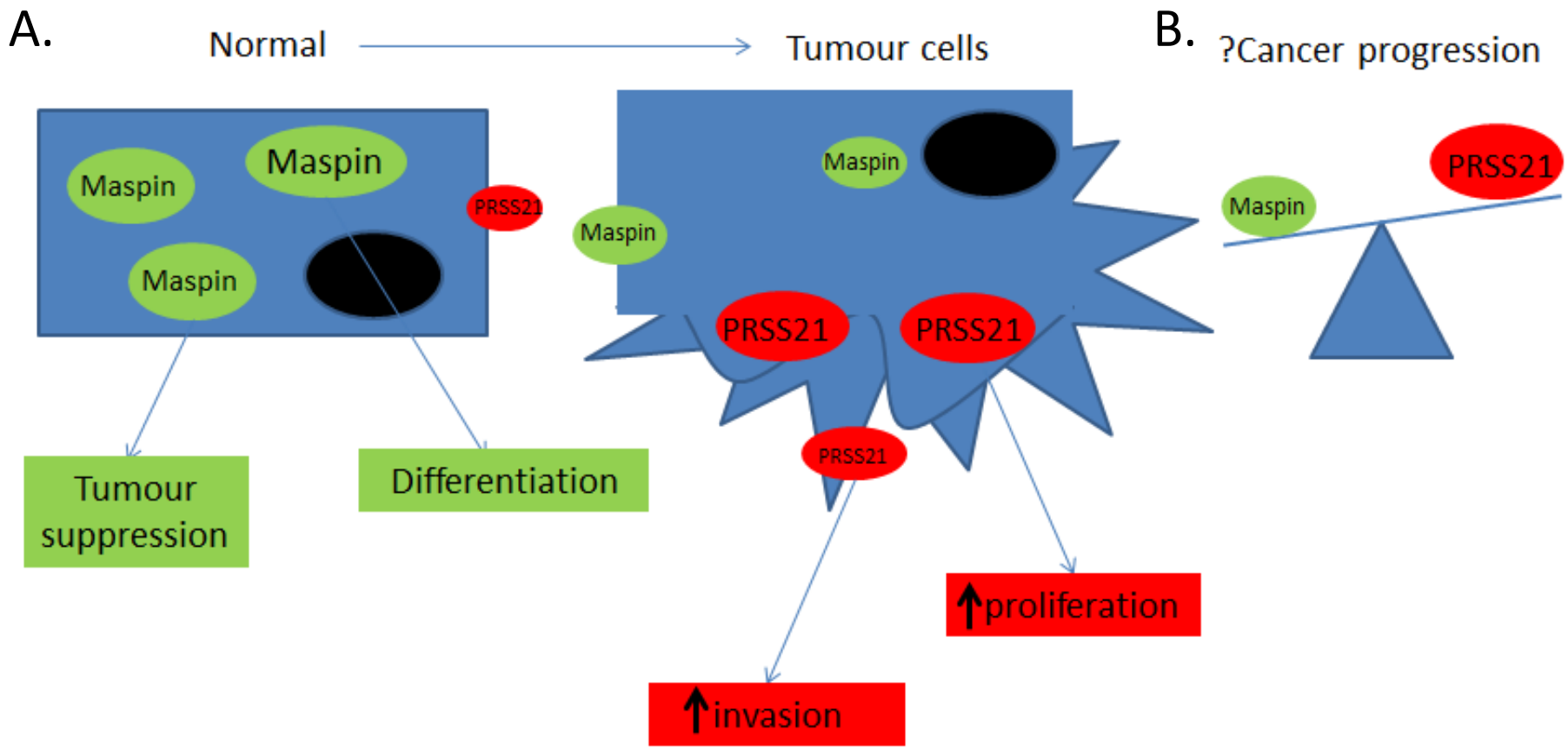

Figure 4.11 PRSS21 cSCC Hypothesis

(A) In normal tissues maspin is expressed at high levels to act as a tumour suppressor whereas PRSS21 is expressed at low levels in normal tissues. Following transformation of a normal cell into a tumour cell PRSS21 is substantially increased aiding tumour cell proliferation and invasion which helps it colonise new organs. Subsequently maspin expression is reduced, possibly through negative regulation by PRSS21 (B) Possible importance of the ration of maspin:PRSS21 in cancer progression, where a higher ratio of PRSS21 favours cancer progression.

Previous studies have shown that knockdown of PRSS21 expression leads to apoptosis (Tang, Kmet et al. 2005; Yeom, Jang et al. 2010). Using a caspase 3/7 assay and a double knockdown strategy it would appear that PRSS21 induced caspase activity is maspin dependant. Although it was shown that maspin does not directly regulate the activity of caspase-3 it appears to facilitate an upstream event that leads to its activation (Jiang, Meng et al. 2002). Figure 4.12 summarises the contribution of PRSS21 depletion and hence acts as a hypothetical model for cSCC therapy through PRSS21 inhibition. Chapter 3 showed that depletion of PRSS21 using siRNA lead to a significant reduction in cell viability, through increased cytotoxicity and cell death. The function of PRSS21 has been further explored in chapter 4 and shows that retroviral over-expression leads to a significant increase in invasion of keratinocytes. This would suggest that depletion of PRSS21 may reduce invasion, possibly by increasing maspin expression. This data together with existing literature suggests that PRSS21 may act to negatively regulate maspin expression and that small molecular inhibitors of PRSS21 may be useful for cSCC therapy either alone or in combination with another therapeutic target for cSCC.

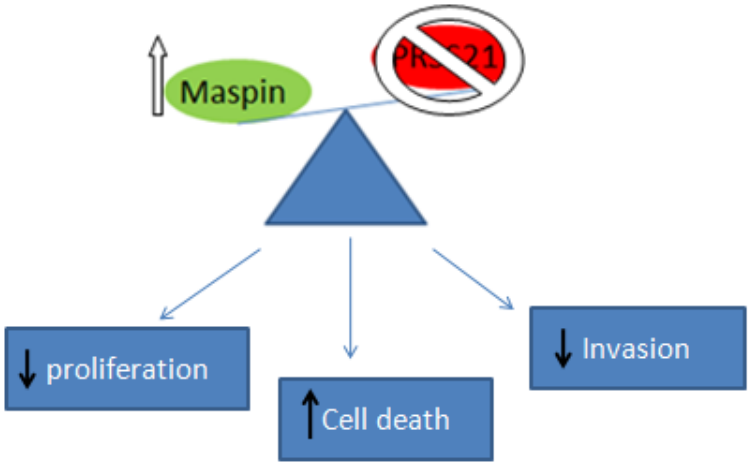

Figure 4.12 Hypothetical Model for cSCC therapy through PRSS21 Inhibition

Inhibition of PRSS21 may release its negative inhibition on maspin causing it to be upregulated. Work in this thesis has demonstrated that depletion of PRSS21 reduces proliferation and increases cell death through caspase activation.

Chapter 5 Assessing the Contribution of Notch Signalling to Differentiation in Cutaneous Squamous Cell Carcinoma

5.1 INTRODUCTION

5.1.1 Identification of loss of function mutations in notch receptors (Wang 2011)

Exome level sequencing identified at least one *notch1/notch2* mutation in 9/11 cSCC samples. Additionally, Sanger sequencing in one further cSCC and 14 cSCC cell lines, gave an overall mutation rate of ~75% (19/26) (Wang, Sanborn et al. 2011). Most of the mutations identified were truncations and a number of other mutations resulted in loss of function through point substitutions within the domains necessary for function. Of great importance to this project is the isolation and establishment of three *notch1* null cSCC cell lines, which using Sanger sequencing have been identified to have a homozygous stop codon mutation. South and colleagues also undertook whole exome sequencing, in addition to targeted deep sequencing on a total of 102 cSCC tumour samples giving an overall frequency of 84%, thus confirming the importance of loss of function of notch in cSCC (South, unpublished).

Additionally, eight BCCs were also Sanger sequenced, yet no *notch1* and *notch2* mutations were identified in this cell type (Wang, Sanborn et al. 2011). However, more recent work using a genome wide mutagenesis approach identified a role of notch1 as a potential driver in BCC suggesting that perhaps a larger *n* number may yield a higher number of mutations (Quintana et al 2013). In addition to the sequencing of these skin tumours, Wang and colleagues also describe a small number of loss of function *notch1* and *notch2* mutations in

lung SCC. However currently, the function of notch in this tumour type is debatable; gain-of-function *notch1* mutations have also been previously described in this tumour type (Westhoff, Colaluca et al. 2009). In parallel, two independent groups published back-to-back studies in Science identifying loss of function notch mutations in 15-20% of head and neck SCC, further endorsing a role for notch in SCC (Agrawal, Frederick et al. 2011). The recent identification of such mutations has arisen as, due to the notch genes being so large, conventional screening of entire ORF by Sanger sequencing was generally prohibited by cost and it was only the advent of next generation sequencing technologies where such mutations were identified. For an introduction to the notch pathway please see the section 1.1.2, p31.

5.1.1.1 Sanger sequencing

Fred Sanger's method of DNA sequencing was based on the earlier work of Arthur Kornberg on DNA replication, where a new DNA strand is synthesised using an existing strand as a DNA template (Sanger, Nicklen et al. 1977). To begin the sequencing process the DNA is amplified, usually by PCR. Following amplification the next major step is to expose the target sequence to DNA polymerase; polymerisation is driven in a sequence specific manner to construct a new DNA strand. The method also known as chain termination sequencing is based on the use of modified nucleotides, which when integrated into the DNA sequence prevent further addition of nucleotides thus terminating the chain. Following the termination step, these chained fragments remain bound to the DNA template strand. These strands are then heated and separated using high resolution denaturing gel electrophoresis. The sequence of the original strand is then deduced from the relative positions on the gel due to the terminators being labelled (Smith, Sanders et al. 1986).

The concept of next generation sequencing is similar to Sanger sequencing, in that the bases if a small fragment of DNA are sequentially identified from signals emitted as each fragment is re-synthesised from DNA template strand. However next generation sequencing extends this process across millions of reactions in a massively parallel fashion rather than being limited to a single/few DNA fragments (Mardis 2008).

5.1.2 Notch as an Oncogene

Although the focus of this thesis is regarding notch as a tumour suppressor, it must be noted that notch can also serve as an oncogene in some cellular contexts. Notch was first identified as an oncogene in the early 90's following the finding of a balanced translocation involving *notch1* gene and the TCRβ locus in a subset of acute lymphoblastic leukaemia, which lead to a constitutively active truncated notch (Ellisen, Bird et al. 1991). This translocation was observed in mice, however rarely occurred in humans, occurring in less than 1% of the population of human T-cell acute lymphoblastic leukaemia/lymphoma (T-ALL). Although this specific translocation has rarely been seen, notch1 gain-of-function mutations have been identified in almost 60% of primary T-ALL patients. Activating mutations in human T-ALL are mainly confined to *notch1* with the most common mutations falling within the trans-membrane domain that allow ligand independent activation or within the PEST domain which result in persistence in activation signal for notch (For a detailed review of oncogenic notch mutations in T-ALL see Aster et al 2008).

5.1.3 Notch as a Tumour Suppressor

On the contrary, loss of function signalling has been seen in a number of tumour types such as skin cancer, small-cell lung cancer, head and neck cancer and cervical cancer (Wang et al 2011, The Cancer Genome Research Network 2012, Agrwal et al 2011, Maliekal et al 2008). The focus of this chapter is on the function of notch in the skin/keratinocyte system. Radtke's group were the first to describe notch as a tumour suppressor through the increased incidence in skin cancers in conditional notch1 knockout mice which formed a number of BCC and papallomas in mice at 8-12 months of age. However, using a specific inhibitor of the Notch transcription complex, dominant~~uble~~ negative MAML1, led to the

development of cSCC in murine skin (Proweller, Tu et al. 2006). The differences observed by these two groups have been attributed to increased severity when knocking down all four receptors with DN-MAML. Notch1 deficient mice are also more susceptible to development of skin cancer in oncogenic RAS background (Lefort, Mandinova et al. 2007). This work suggests that notch may be required for ras-induced clonal expansion and fits with data from our lab that 60% of HRAS-driven lesions have notch mutations (South et al submitted). The genetic studies above demonstrate a role for notch, particularly notch1 as a potent tumour suppressor in skin. Notch1 is expressed in the suprabasal layers of the epidermis and is a direct transcriptional target of p53 (Lefort, Mandinova et al. 2007), Notch2 is expressed in the basal layer and its contribution to tumour suppression is less clear (Dotto 2008). While the timing of these Notch lesions thoroughout cancer progression is not known, data supports the role of notch in cSCC progression rather than in initiation. Wang and colleagues described a high frequency of G>A transitions induced by UV after homozygous p53 loss (85% of notch mutations) (Wang, Sanborn et al. 2011).

A number of tumour suppressive mechanisms have been proposed for notch in the skin (for review see (Dotto 2008, South 2012). *In-vitro* work carried out by Dotto's group show that notch activation induces differentiation through interferon regulatory factor 6 (IRF6) (Restivo, Nguyen et al. 2011) and an important role for p21 as a mediator of notch1 induced cell cycle arrest suggesting that loss of notch function in cSCC enables tumours to continue growing (Rangarajan, Talora et al. 2001). Besides cell cycle withdrawal, keratinocyte differentiation is elicited by induction of differentiation markers of the suprabasal layers (keratin 1/10, involucrin; (Rangarajan, Talora et al. 2001), (Nickoloff, Qin et al. 2002)). Cross talk between a number of pathways linked to skin carcinogenesis including RAS, NFκB, Wnt

and Hedgehog have also been described to contribute to tumour suppressive activity. Kopan's group conversely suggest that the loss of function of notch produces a chronic inflammatory state that promotes tumour growth through factors released by the fibroblasts creating a tumour micro-environment through increased inflammation (Demehri, Turkoz et al. 2009). However, the downstream molecular mechanisms remain to be defined and currently discrepancies between mouse and human models are evident. For instance, notch induced up-regulation of p21 is associated with suppression of Wnt (Devgan, Mammucari et al. 2005) in mouse keratinocytes but in human keratinocytes notch activation leads to suppression of growth and induction of differentiation related, in part due to reduced p63 expression rather than increased p21 (Nguyen, Lefort et al. 2006).

5.1.4 Targeting Notch for Cancer Treatment

Notch can act as either an oncogene or a tumour suppressor, suggesting that notch signalling is highly context and cell type dependant which has complications for targeted therapy. One current approach to inactivate notch signalling in an oncogenic setting is via the inhibition of the gamma secretase complex. At present there are a number of gamma secretase inhibitors (GSI) available which were originally formulated for the treatment of Alzheimer's disease. Gamma secretase is implicated in the pathogenesis of Alzheimer's as it cleaves amyloid β peptide- the principle component of the characteristic cerebral plaques found in Alzheimer's. The use of GSIs for this disease resulted in the formation of skin tumours without improvement of the disease itself and hence termination of the clinical trial. Following termination of the trial it was discovered that the tumour formation was a result of loss of notch signalling in brain tissue. Currently GSIs which don't inhibit notch signalling are being developed (Tang, Kmet et al. 2005). However a new niche for these compounds is being explored, in tumours where notch is oncogenic. Phase I and II clinical

trials are being carried out for various malignancies including breast, advanced solid tumours and pancreatic (Tolcher et al 2012, Krop et al 2012). However these ~~trails~~ trials aim to carefully modulate notch expression to prevent any secondary cancers forming that may outweigh the treatment benefits.

On the flip-side agents which interfere with the epigenetic silencing of notch are currently in investigation for tumours with loss of notch function. Histone deacetylase inhibitors inhibitors have previously been reported to reduce tumours through reduction of notch in pre-clinical models (Pinchot et al 2011). Additionally a phase II study using Valporic acid showed that notch1 expression significantly increased after treatment (Mohammed et al 2011). However a more context and functional understanding of the notch pathway in the context of each cancer is required.

5.2 RESULTS

5.2.1 Activated ICN1 is reduced in cSCC compared to normal human keratinocytes

In order to confirm that notch1 is reduced in cSCC a panel of cSCC cells were assessed for protein expression of the activated form of notch1 (activated ICN1). Western blot of a panel of cell lines showed that in all of the cSCC lines tested, cleaved notch1 (ICN1) is reduced compared to normal human keratinocytes (figure 5.1A). The addition of 1μM GSI inhibited the expression of ICN1 however in cSCC cell lines the expression of ICN1 was not completely inhibited by this concentration, suggesting that these cells harbour a resistance mechanism to the concentration of GSI used. A dose response curve may be required to elucidate the appropriate concentration. Additionally below the protein data is a table showing the mutational status of notch1 in these lines which has been identified using Sanger sequencing ((Wang, Sanborn et al. 2011), figure 5.1B). Even in the T8 cells, which have wild type expression of notch1 the expression at protein level is reduced suggesting that that other mechanisms may be acting on the signalling pathway to reduce the expression of notch signalling in these cells. Additionally immunoblot confirms that the SCCIC15 cells, which contain a stop codon mutation, have no protein expression of ICN1 which is as expected.

Figure 5.1

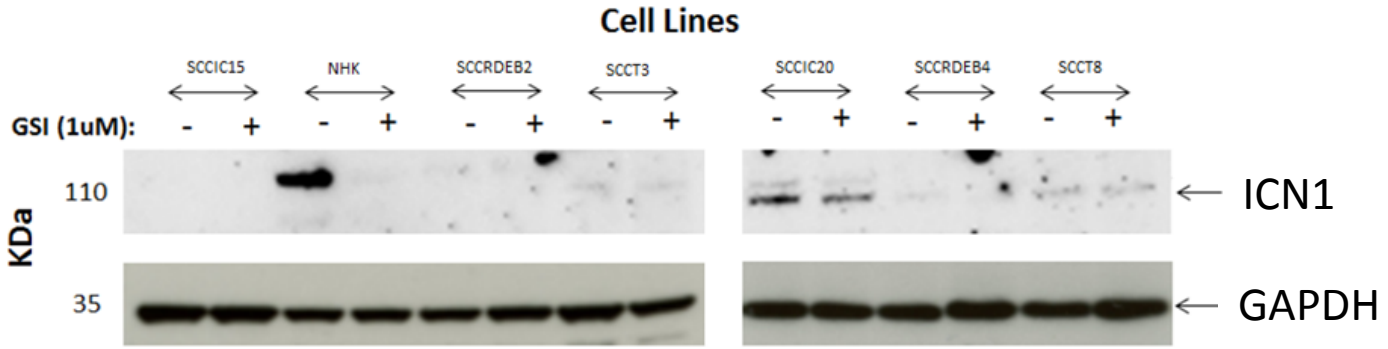

B.

Cell Line	Notch1 mutation
SCCIC15	Q1687*, Q1864R
NHK	Wild type
SCCRDEB2	T1090S
SCCT3	D910G
SCCIC20	Awaiting data
SCCRDEB4	D1517N
SCCT8	Wild type

Figure 5.1 The Expression of Notch is Reduced in cSCC Compared to Normal Human Keratinocytes (NHK)

(A) Protein expression of activated notch (ICN1) was explored in a panel of cSCC cell lines compared to normal human keratinocytes, with and without gamma secretase inhibitor (1µM, GSI). Protein expression of ICN1 is significantly reduced in cSCC compared to normal human keratinocytes. Results represent two experiments. (B) Table shows the mutational status of the panel of cell lines selected above for ICN1 protein expression. RDEB; recessive dystrophic epidermolysis bullosa, T; transplant, IC; immunocompetant (Wang et al 2011).

5.2.2 The Effect of GSI in Normal and cSCC Keratinocytes on Cell Viability

Previously notch signalling has been shown to reduce proliferation in keratinocytes through increased differentiation and cell death (Rangarajan, Talora et al. 2001). Therefore in order to confirm these data and to assess whether GSI had an effect on cSCC cells were seeded into 96 well plates and treated with different concentrations of GSI, ranging from 0.1-100μM and the impact of GSI on percentage cell viability assessed using the MTS assay (figure 5.4). The human telomerase reverse transcriptase (hTERT) cell line and the K17 cell line are both immortalised normal human cell lines. It has been shown that HPV16 interacts with MAML, one of notch's targets and has been shown to subsequently upregulate notch expression and activity. Therefore notch signalling may be dysregulated in cells with positive HPV status (Tan et al 2012). GSI slightly increases cell viability in the hTERT (figure 5.2A) after 72h, apart from at the highest dose, 100μM which reduces cell viability. However, in the K17 (figure 5.2B) cell line GSI slightly reduces the percentage cell viability which is similar to the effect seen in the cSCC notch null cell lines. In both SCC1C15 (figure 5.4C) and SCCIC8 (figure 5.4D) a slight reduction in cell viability is seen after 72 hours. The greatest reduction is using the 100μM concentration.

Figure 5.2

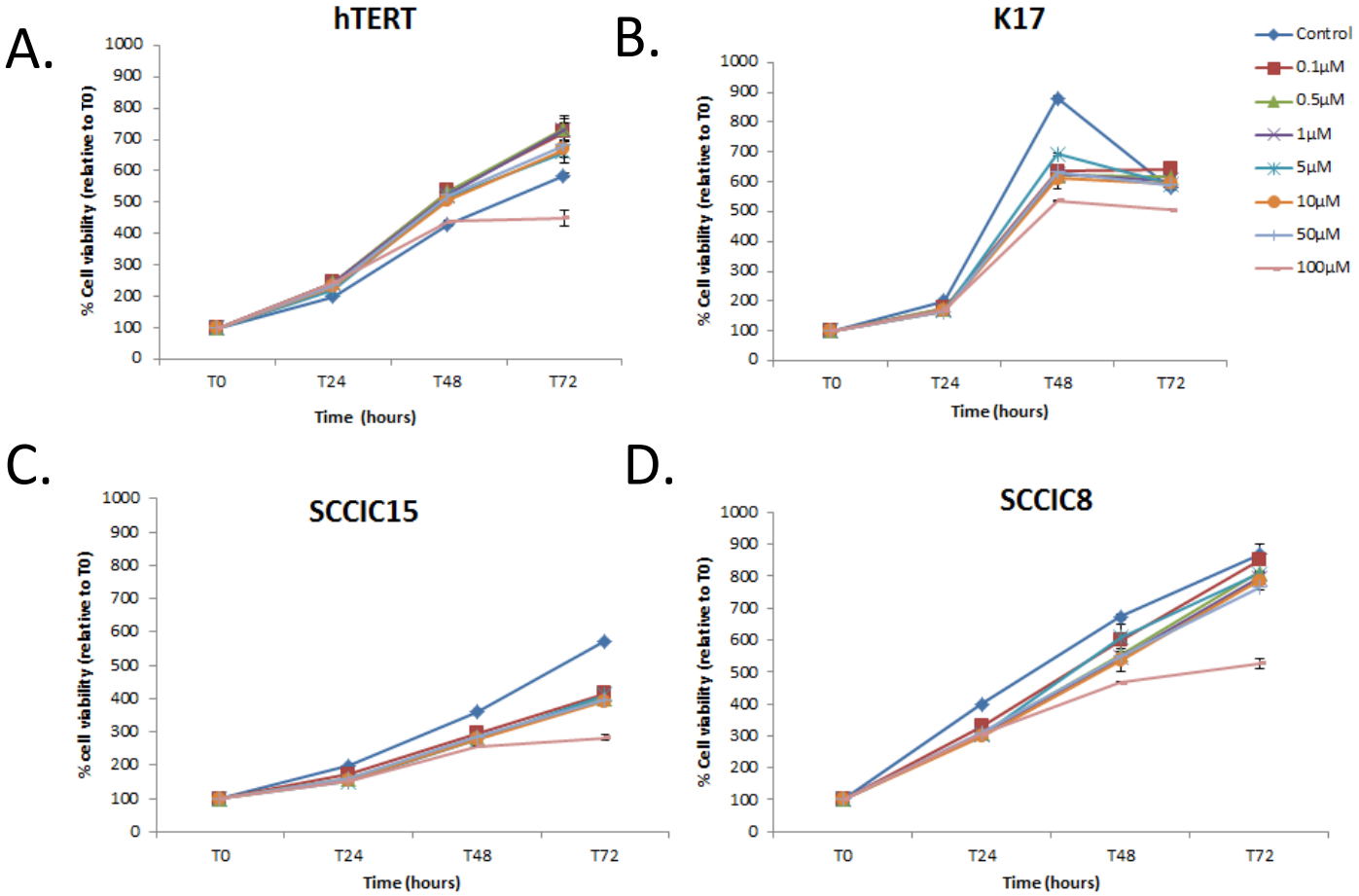

Figure 5.2 The Effect of GSI in Normal and Notch Null cSCC Keratinocytes

Percentage cell viability was assessed using the MTS assay. Immortalised normal keratinocytes, either the (A) hTERT or the (B) K17 which has been immortalised using either human telomerase reverse transcriptase or papilloma virus, respectively were assessed along with notch null cSCC keratinocytes (C) SCCIC15 and (D) SCCIC8. Results show that GSI slightly increases % cell viability in the hTERTS following 72h incubation with GSI compared to control. However in the K17, SCCIC15 and SCC1C8 cell lines GSI causes a slight reduction in proliferation. Results represent n=4±SD

5.2.3 There is a correlation between mutational status of notch1, and protein expression of ICN1 in SCCIC12, SCCT2 and SCCIC8 cells

Currently the tumour suppressive mechanism behind notch is unknown. One theory is that it functions as a tumour suppressor through mediation of pro-differentiation signals (Restivo, Nguyen et al. 2011; Rangarajan, Talora et al. 2001). The mutational status of these three lines was confirmed using western blot and immunohistochemistry (figure 5.3). The mutational status of the cSCC cell lines was identified using Sanger and exome sequencing of which three lines were chosen for study, the immunocompetent cell lines SCCIC12, SCCIC8 and SCCT2 which is an cSCC derived from a transplant patient (figure 5.3A). The SCCIC12 cell line was found to be wild type for notch1. The SCCT2 cell line was found to be loss of function (LOF) which has a number of mutations E415D, C409F, D469G. Of note the E415D and the D469G lie within the N-terminal ex~~in~~tracellular portion, of which functional study of the E415D mutation suggests that this mutation causes LOF by disrupting the structure of EGF repeats required for ligand binding (Wang, Sanborn et al. 2011). The effects of the notch1 mutations on protein were confirmed using an antibody raised against full length notch (NOTCH1 total) which was a kind gift from Jon Aster and NICD (figure 5.3B). SCCIC12 and SCCT2 both have immune-reactivity at 300KDa, indicating the presence of full length notch however SCCIC8, which is a notch null cell line, has no identifiable protein expression as determined by immunoblotting which is expected. Using an antibody raised against activated notch SCCIC12 which is wild type for notch is the only cell line to display a band at 100KDa indicating NICD, again as expected.

Additionally the mutational status was confirmed using immunohistochemistry of xenograft tumours (figure 5.3C). These sections were stained using an immunohistochemistry protocol

optimised by Jon Aster's group for the Ventana auto-stainer and were kindly performed by Tayside Tissue Bank (Kluk et al 2013, Tayside Tissue Bank, Dundee). Using this method with the monoclonal cleaved notch1 antibody (ab4147), the SCCIC12 showed positive nuclear staining which was absent in the SCCT2 and SCCIC8 cell lines. The positive staining in the SCCT2 section is fibroblast staining, thus providing a robust internal control. Together the immunoblot and immunohistochemistry results confirm the mutational status of these cSCC cell lines.

Figure 5.3

A.

Cell line	Mutation status
SCCIC12	Wild type
SCCT2	LOF mutation
SCCIC8	Notch Null

B.

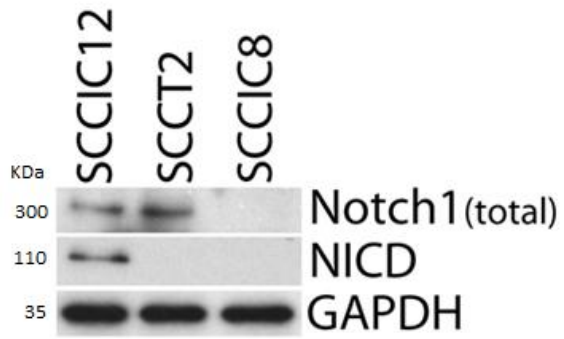

C.

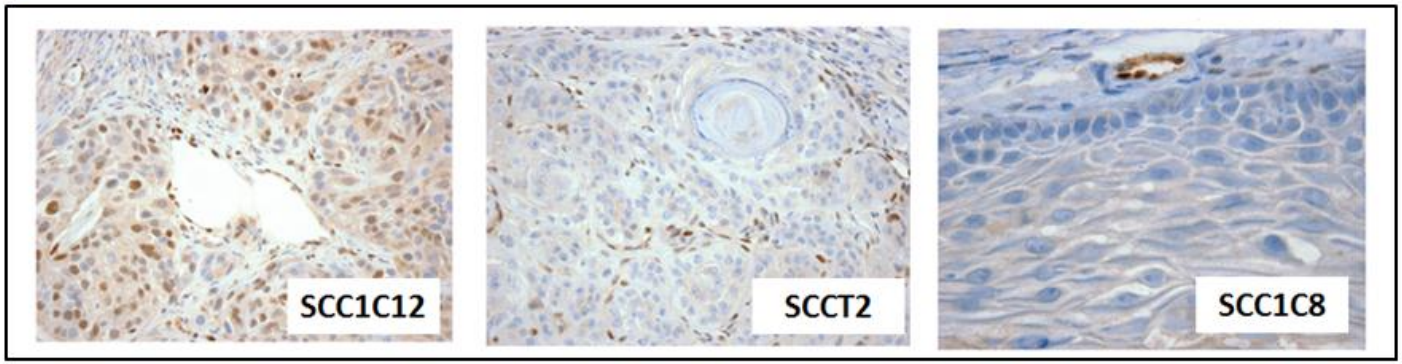

Figure 5.3 Correlation Between Notch Mutational Status, Protein and IHC in cSCC

(A) Mutational status of SCCIC12, SCCT2 & SCCIC8 as obtained from the Sanger and Exome sequencing study (Wang et al 2011, South et al submitted). (B) Protein expression of SCCIC12, SCCT2 & SCCIC8 was assessed using full length notch1 Ab (notch1, kind gift from Jon Aster), cleaved notch (NICD, Val1447) and GAPDH as a loading control. Data confirms the mutational status wild type SCCIC12 has both full length and activated notch protein expression, SCCT2 has only full length confirming its loss of function of notch. SCCIC8 has no bands for either full length NOTCH1 or NCID indicating its NOTCH1 null status. (C) Immunohistochmistry staining using JC Aster's method (Kluck et al 2013) kindly performed by Tayside Tissue Bank, Dundee. Staining was performed using a monoclonal, cleaved notch1 antibody (ab4147). Where positive staining is seen in the nucleus of SCC1C12 however, no positive keratinocyte staining is seen in the SCCT2 and SCCIC8 cell lines.

5.2.4 Involucrin and Keratin 10 staining of NHK, SCCIC12, SCCT2 and SCCIC8 cells is Affected by Notch Inhibition Using a Gamma Secretase Inhibitor

In order to understand the relationship between differentiation and mutational status fibrin gels with either normal human keratinocytes, SCCIC12, SCCT2 and SCCIC8 were grown either without or in the presence of GSI to inhibit expression in the cell types with notch expression. Fibrin gels are a form of 3 dimensional cultures, prepared from fibrinogen and thrombin, which are key proteins involved in blood clotting and its unique polymerisation mechanism of fibrin allows the formation of a dense network of fibres. Fibrin gels were chosen to study differentiation as they provide a stronger base than the collagen matrigel system to support differentiation. To begin the expression of ICN1 was confirmed using imunohistochemistry using an antibody raised against cleaved notch1. Both NHK and SCCIC12, which have wild type notch, showed positive nuclear staining (figure 5.6A). However the expression of ICN1 in the NHK is localised in the supra-basal layer whereas in the SCCIC12 cell line it is distributed throughout the epidermis – perhaps suggesting a change in function. No positive nuclear staining is seen in the SCCT2 and SCCIC8 cell lines, which have a loss of function notch1 mutation and notch1 null, respectively. Additionally, no positive staining is seen in fibroblasts suggesting that they do not express ICN1 (figure 5.4B). These gels were then stained using involucrin or K10, which are known markers of keratinocyte differentiation to identify if the notch1 status affected terminal differentiation. In the gels cultured with normal human keratinocytes (figure 5.4A) and SCCIC12 (figure 5.7B) which have wild type notch1, the addition of GSI reduced the expression of involucrin in these keratinocytes however in the T2 (figure 5.4C) cell line which has a LOF notch1 mutation, the reduction in the expression of involucrin was not as great following GSI inhibition. Immunofluoresecent staining of the SCCIC8 (figure 5.4D) cells with an antibody

raised against involucrin showed a significant reduction in immune-reactivity compared to normal human keratinocytes suggesting that terminal differentiation is reduced in this cell type. The addition of GSI to the media of SCCIC8 cells did not have an effect on involucrin expression in this cell type.

Immunofluorescent staining using an antibody raised against keratin 10 (K10) yielded similar results to the involucrin staining, incubation of both NHK (figure 5.5E) and the SCCIC12 (figure 5.5F) with the K10 antibody, resulted in a reduction in K10 expression indicating the importance of notch for differentiation in both cell types. Compared to the normal human keratinocytes all three of the cSCC cell lines have reduced K10 expression, with the SCCT2 (figure 5.5G) expressing the least amount of K10. Surprisingly, SCCIC8 cells (figure 5.5H) which are Notch null, show positive K10 expression which is not reduced following incubation of GSI. It would seem that differentiation is under tight control by notch in the NHK cells however in the cSCC cells, which presumably contain a whole host of mutations which influence other differentiation pathways other than notch – differentiation cannot be controlled as regimentally.

Figure 5.4A

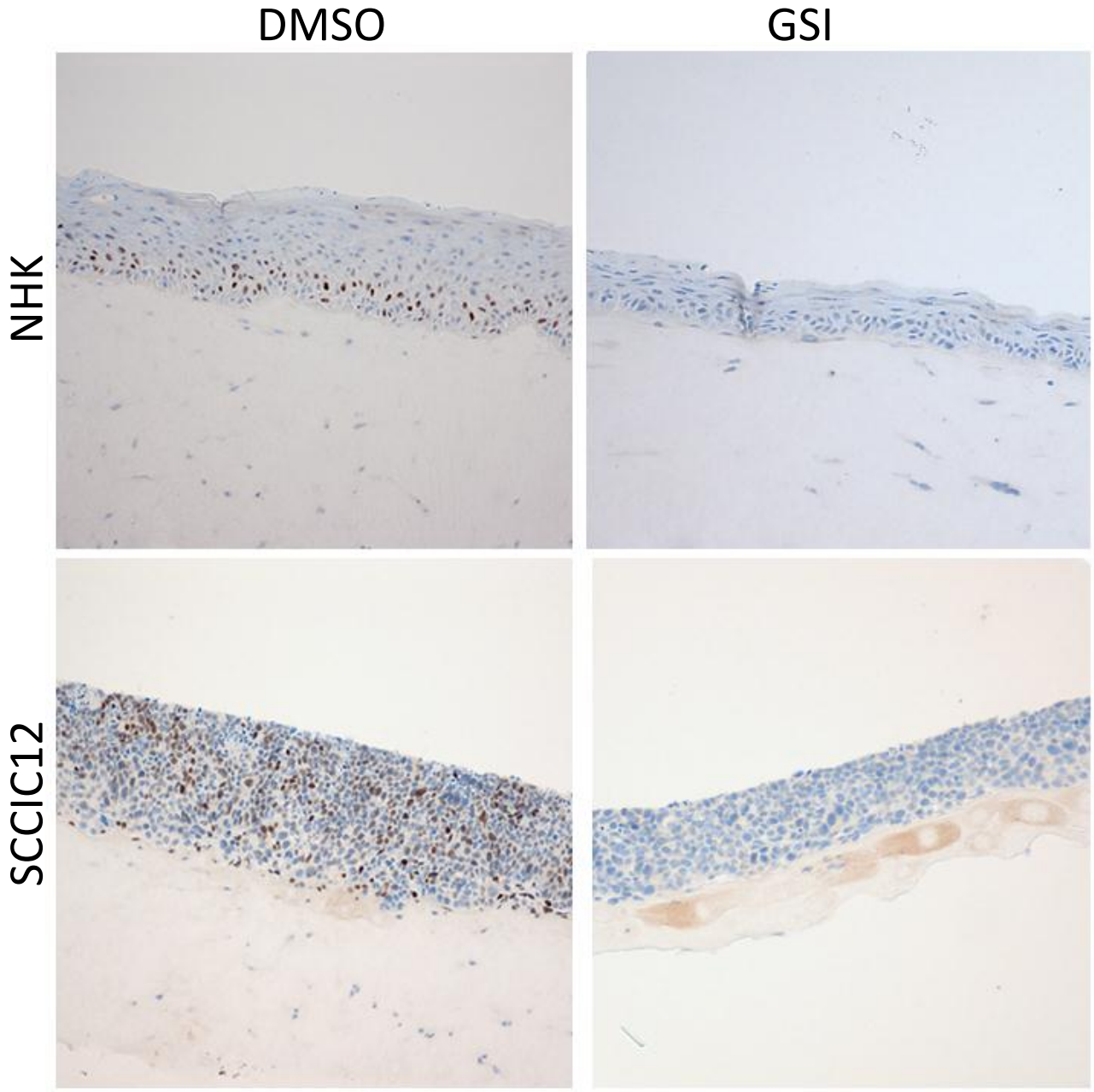

Figure 5.4A Immunohistochemistry Shows GSI Regulatable Positive Nuclear Staining in Both NHK and SCCIC12 Which Express Wild Type Notch1

Immunohistochemistry staining of fibrin gels, fixed 7 days after being raised. Staining was performed using JC Aster's method (Kluck et al 2013) and was kindly performed by Tayside Tissue Bank, Dundee using a monoclonal, cleaved notch1 antibody (ab4147). Positive nuclear staining in the suprabasal layer is seen in the normal human keratinocytes (NHK, Top, LHS panel) in the presence of DMSO. This nuclear expression is lost following the addition of 1µM GSI in the top, RHS panel. Similarly, SCCIC12 which also expresses wild type notch expresses positive nuclear staining throughout the epidermal layers. This expression is GSI regulatable.

Figure 5.4B

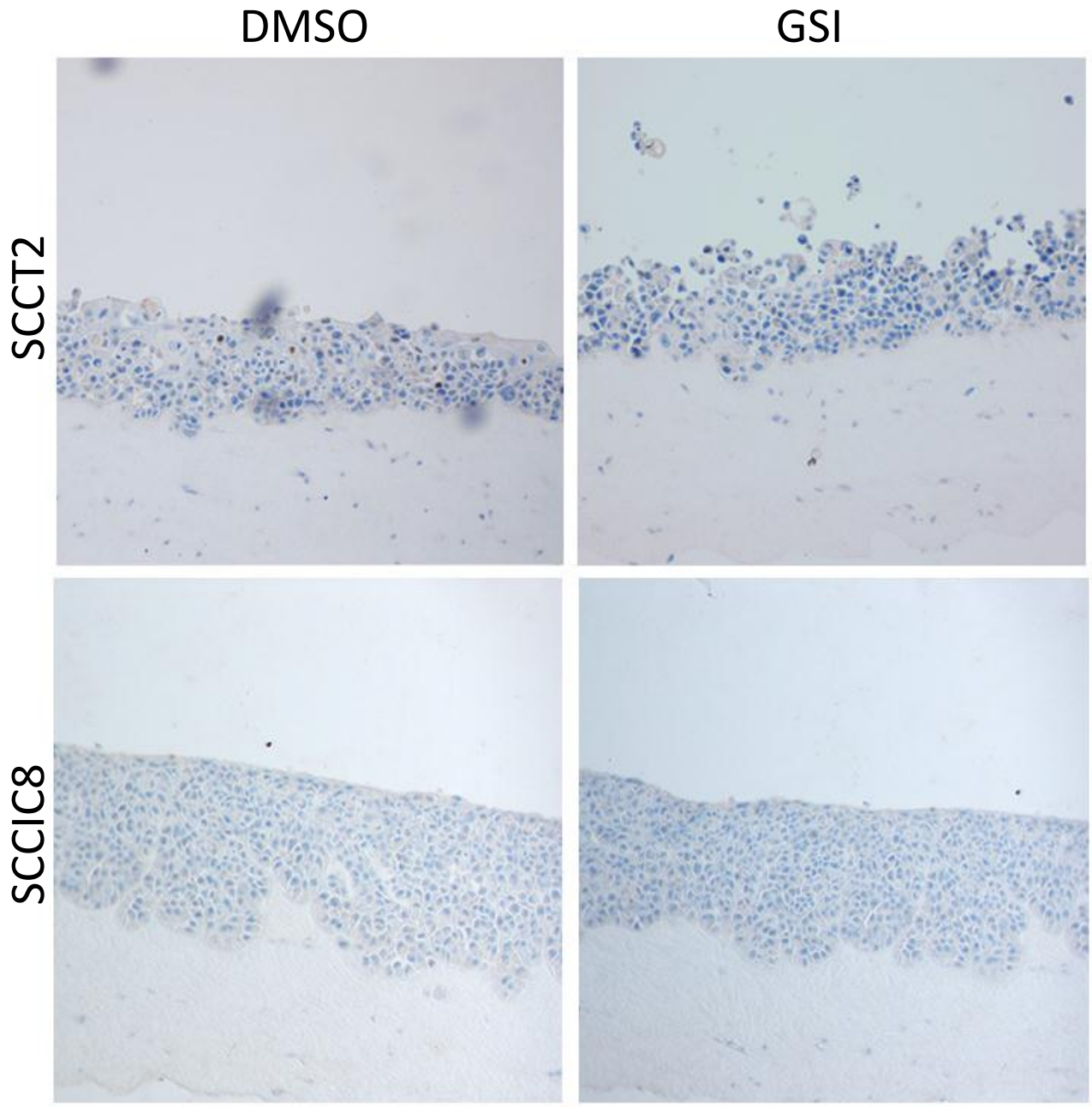

Figure 5.4B Immunohistochemistry Shows No Positive Nuclear Staining i~~n the~~ SCCT2 or SCCIC8 Keratinocytes Which Are Notch Mutant

Immunohistochemistry staining of fibrin gels, fixed 7 days after being raised. Staining was performed using JC Aster's method (M.Kluk et al 2013) and was kindly performed by Tayside Tissue Bank, Dundee using a monoclonal, cleaved notch1 antibody (ab4147). No positive nuclear staining is seen in either the SCCT2 which has a loss of function notch mutation (top panel, LHS) or the SCCIC8 cells which is notch null (bottom panel, RHS). The addition of 1µM GSI does not alter this result in either cell line (RHS panel).

Figure 5.5A

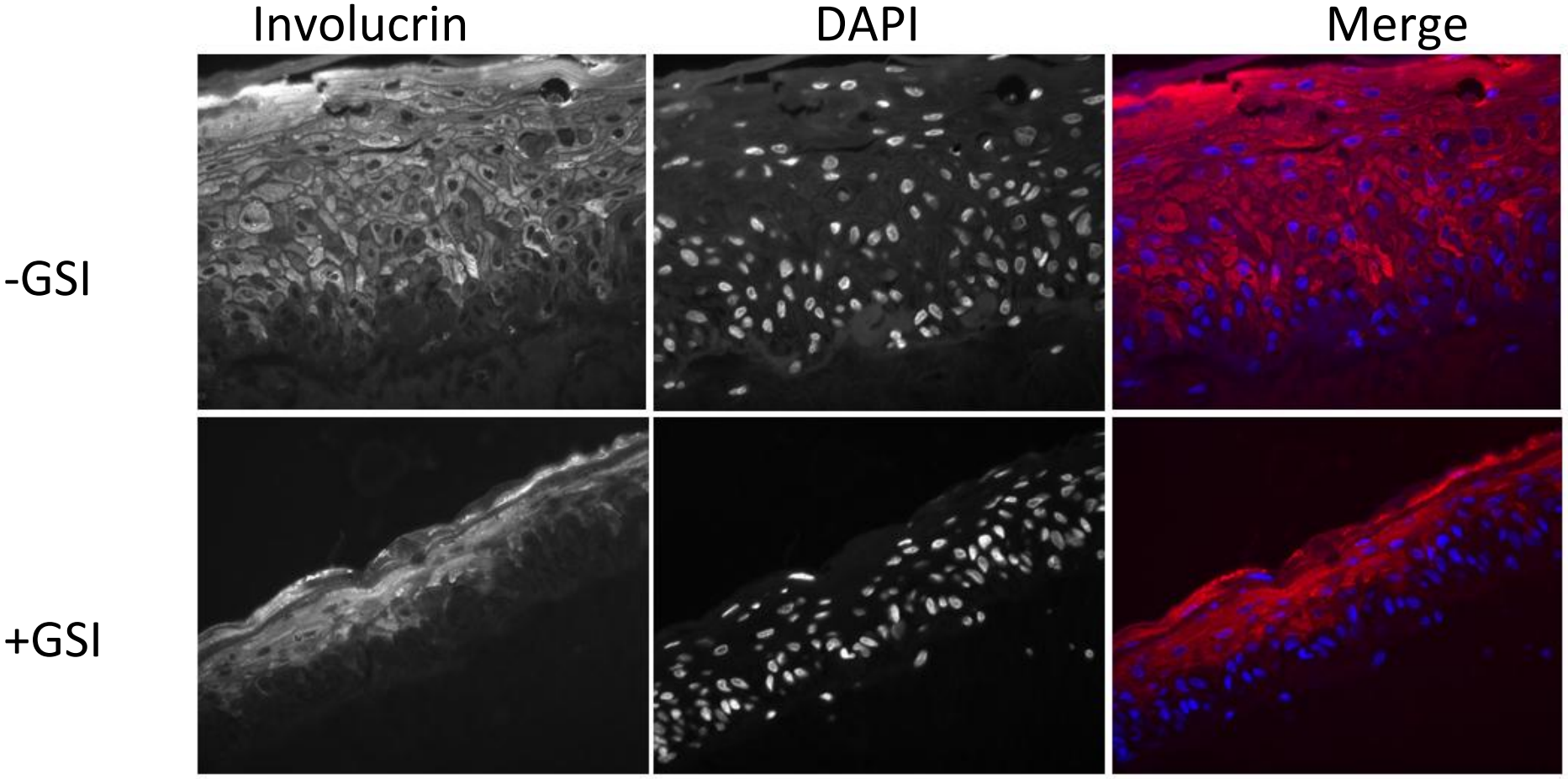

Figure 5.5A GSI Reduces Involucrin Expression in Normal Human Keratinocytes

Fibrin gels cultured with normal human keratinocytes with/without a gamma secretase inhibitor (GSI) and stained for the terminal differentiation marker, involucrin. LHS panel is the black and white image for involucrin staining only, middle is the corresponding DAPI for this image and the RHS images are the involucrin staining (RED) and DAPI (BLUE) images merged together in colour. The top set is grown without (1µM) GSI in DMSO and the bottom is in the presence of GSI. There is a reduction in involucrin staining in the presence of GSI. These images show that there is a reduction in involucrin following addition of GSI. Images are taken under 43 x objective.

Figure 5.5B

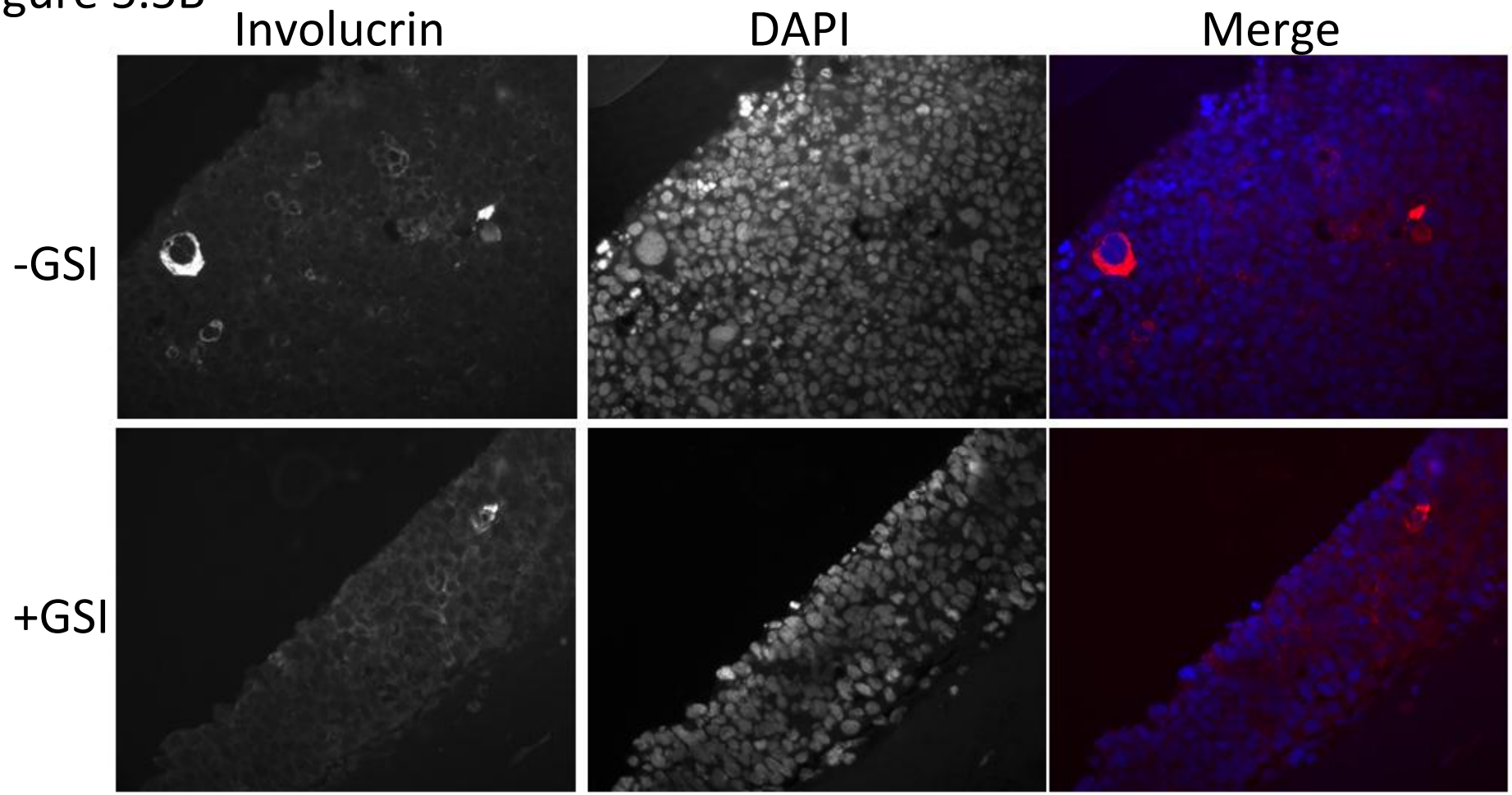

Figure 5.5B GSI has no effect on involucrin expression in SCCIC12

Fibrin gels cultured with SCCIC12 with/without a gamma secretase inhibitor (GSI) and stained for the terminal differentiation marker, involucrin. LHS panel is the black and white image for involucrin staining only, middle is the corresponding DAPI for this image and the RHS images are the involucrin staining (RED) and DAPI (BLUE) images merged together in colour. The top set is grown without (1µM) GSI in DMSO only and the bottom is in the presence of GSI. There is a reduction in involucrin staining in the presence of GSI. These images show that there is a reduction in involucrin following addition of GSI. Images are taken under 43 x objective.

Figure 5.5C

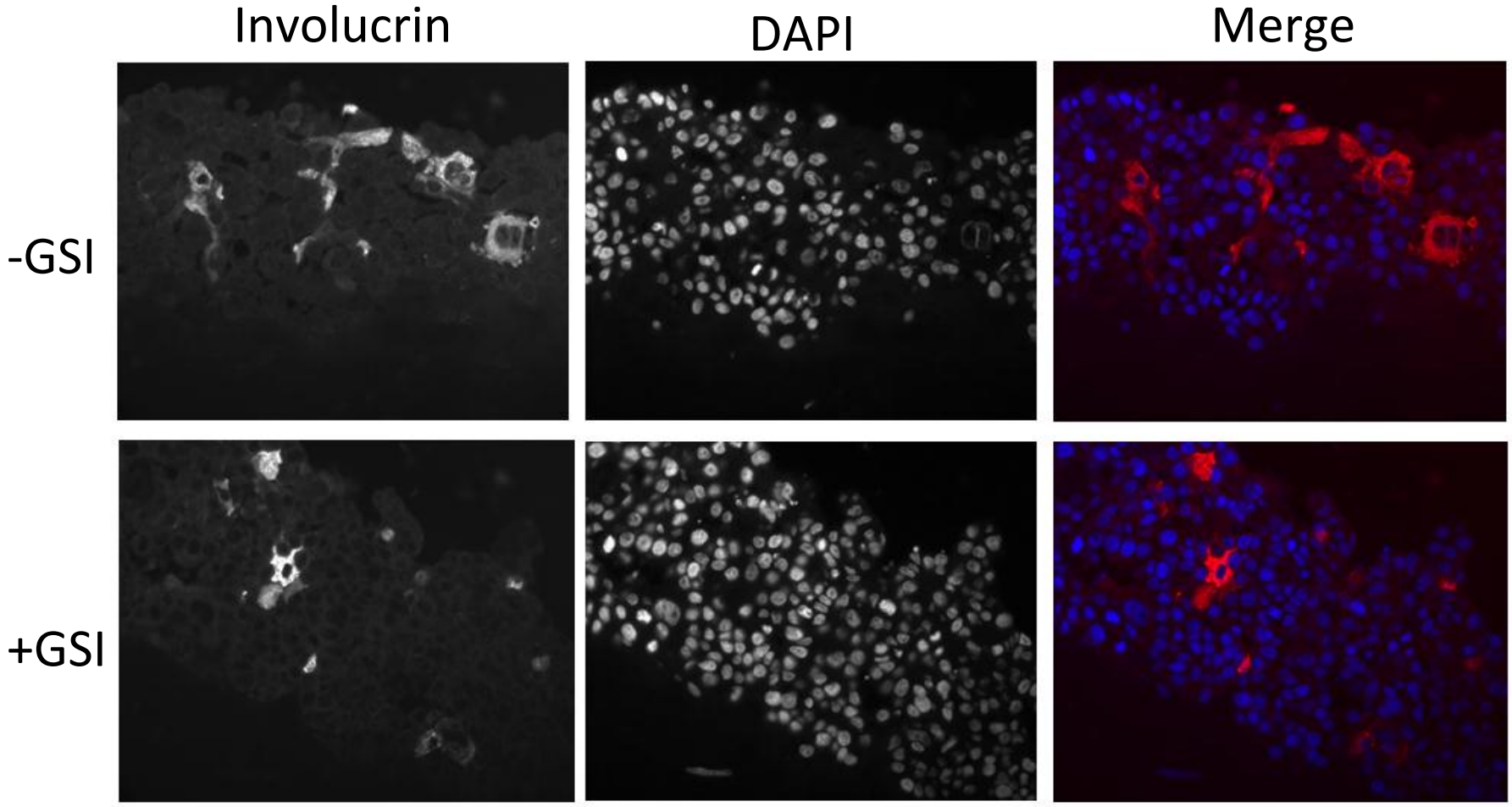

Figure 5.5C GSI has no effect on Involucrin Expression in SCCT2

Fibrin gels cultured with SCCT2 with/without a gamma secretase inhibitor (GSI) and stained for the terminal differentiation marker, involucrin. LHS panel is the black and white image for involucrin staining only, middle is the corresponding DAPI for this image and the RHS images are the involucrin staining (RED) and DAPI (BLUE) images merged together in colour. The top set is grown without (1µM) GSI in DMSO only and the bottom is in the presence of GSI. There is a reduction in involucrin staining in the presence of GSI. These images show that there is a reduction in involucrin following addition of GSI. Images are taken under 43 x objective.

Figure 5.5D

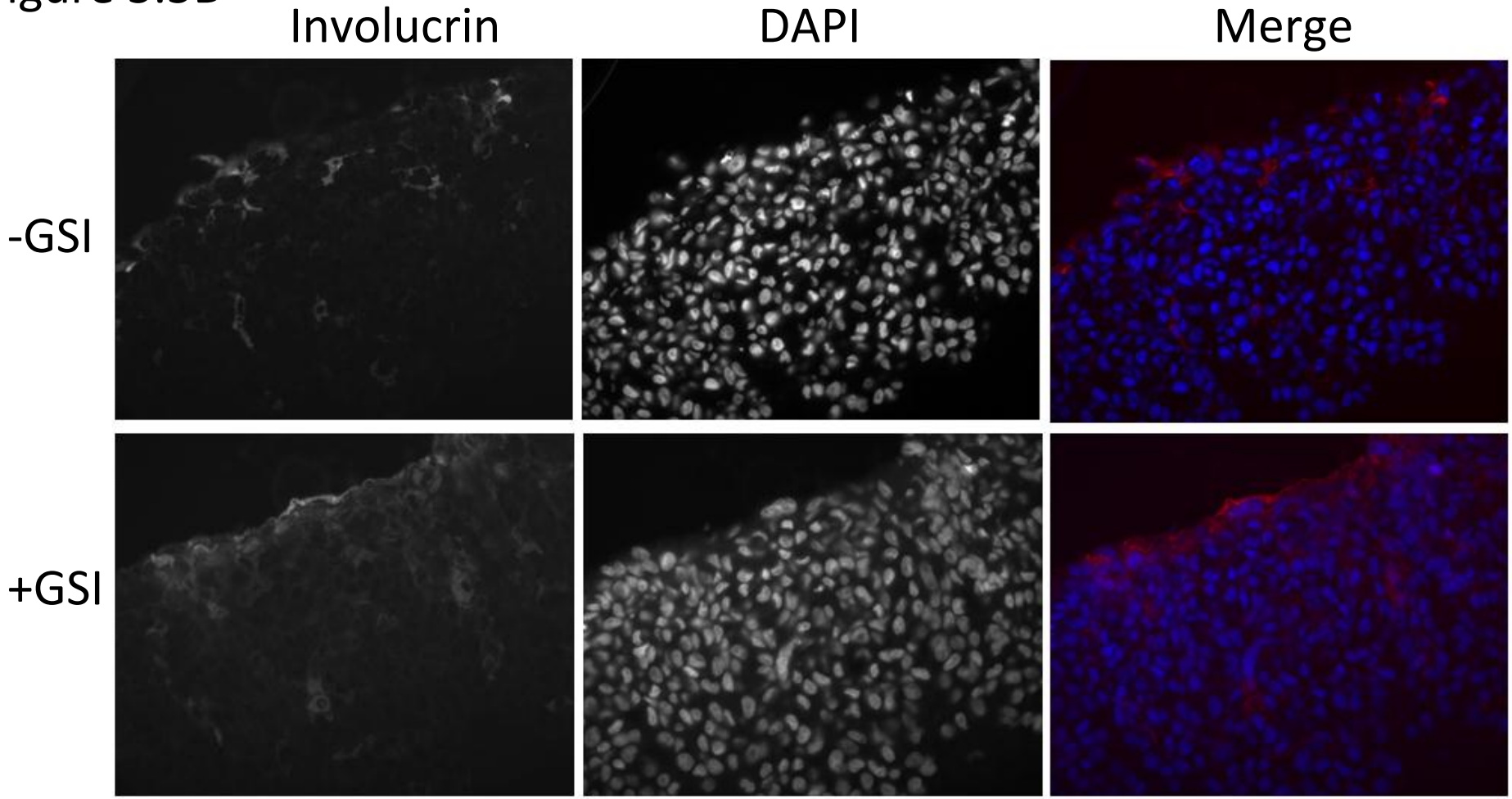

Figure 5.5D GSI has no effect on Involucrin Expression in SCCIC8

Fibrin gels cultured with SCCIC8 with/without the gamma secretase inhibitor and stained for the terminal differentiation marker, involucrin. LHS panel is the black and white involucrin staining only, middle is the corresponding DAPI for this image and the RHS images are the involucrin staining (RED) and DAPI (BLUE) images merged together. The top set is grown without (1µM) GSI in DMSO only and the bottom is in the presence of GSI. There is a reduction in involucrin staining in the presence of GSI. Images are taken under 43 x objective.

Figure 5.5E

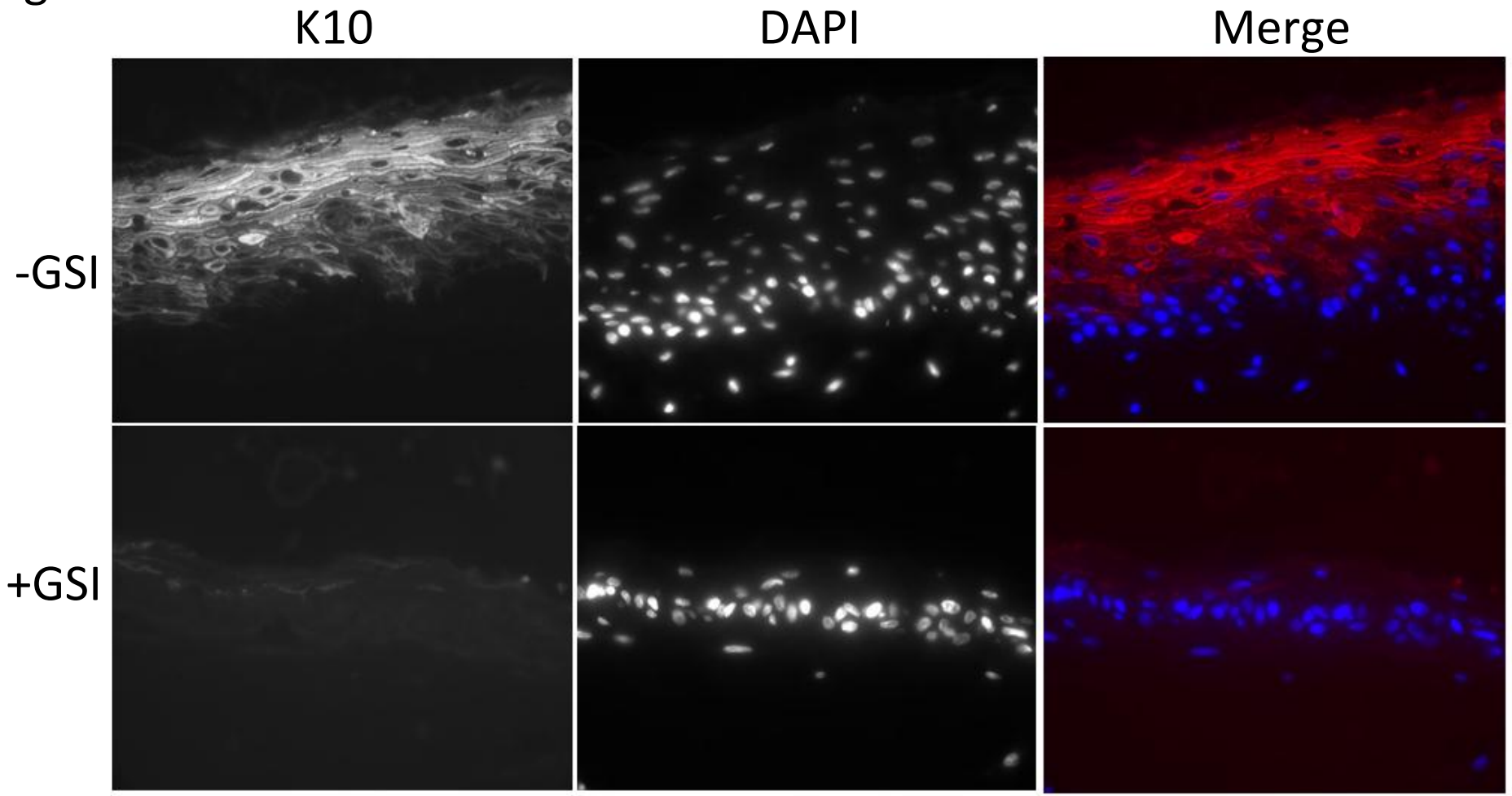

Figure 5.5E GSI Reduces K10 Expression in NHK

Fibrin gels cultured with NHK with/without the gamma secretase inhibitor and stained for the terminal differentiation marker, K10. LHS panel is the black and white K10 staining only, middle is the corresponding DAPI for this image and the RHS images are the K10 staining (RED) and DAPI (BLUE) images merged together. The top set is grown without (1µM) GSI in DMSO only and the bottom is in the presence of GSI. There is a reduction in K10 staining in the presence of GSI. Images are taken under 43 x objective.

Figure 5.5F

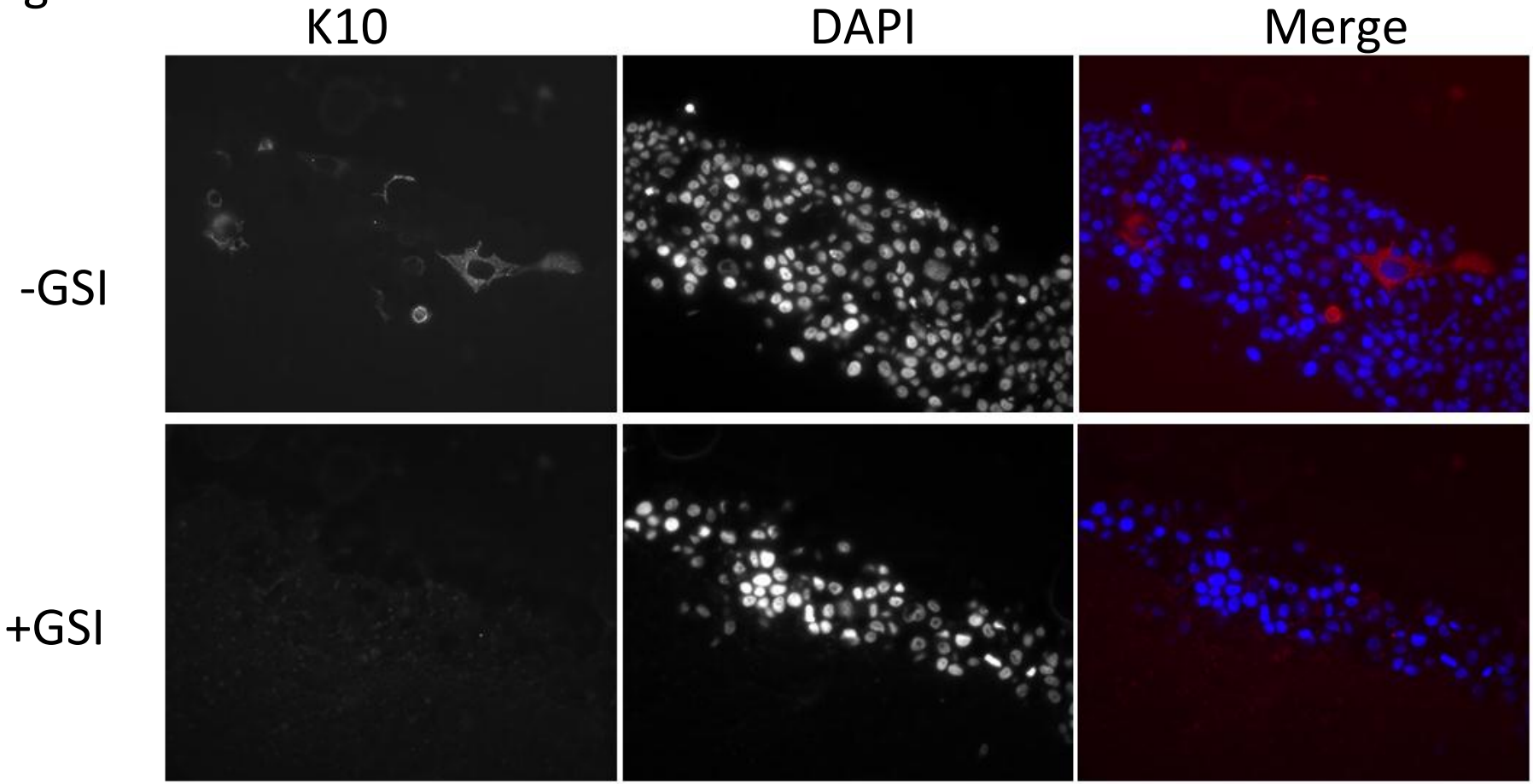

Figure 5.5F GSI Reduces K10 Expression in SCCIC12

Fibrin gels cultured with ~~SCCIC8~~ SCCIC12 with/without the gamma secretase inhibitor and stained for the terminal differentiation marker, K10. LHS panel is the black and white K10 staining only, middle is the corresponding DAPI for this image and the RHS images are the K10 staining (RED) and DAPI (BLUE) images merged together. The top set is grown without (1µM) GSI and the bottom is in the presence of GSI. There is a reduction in K10 staining in the presence of GSI. Images are taken under 43 x objective.

Figure 5.5G

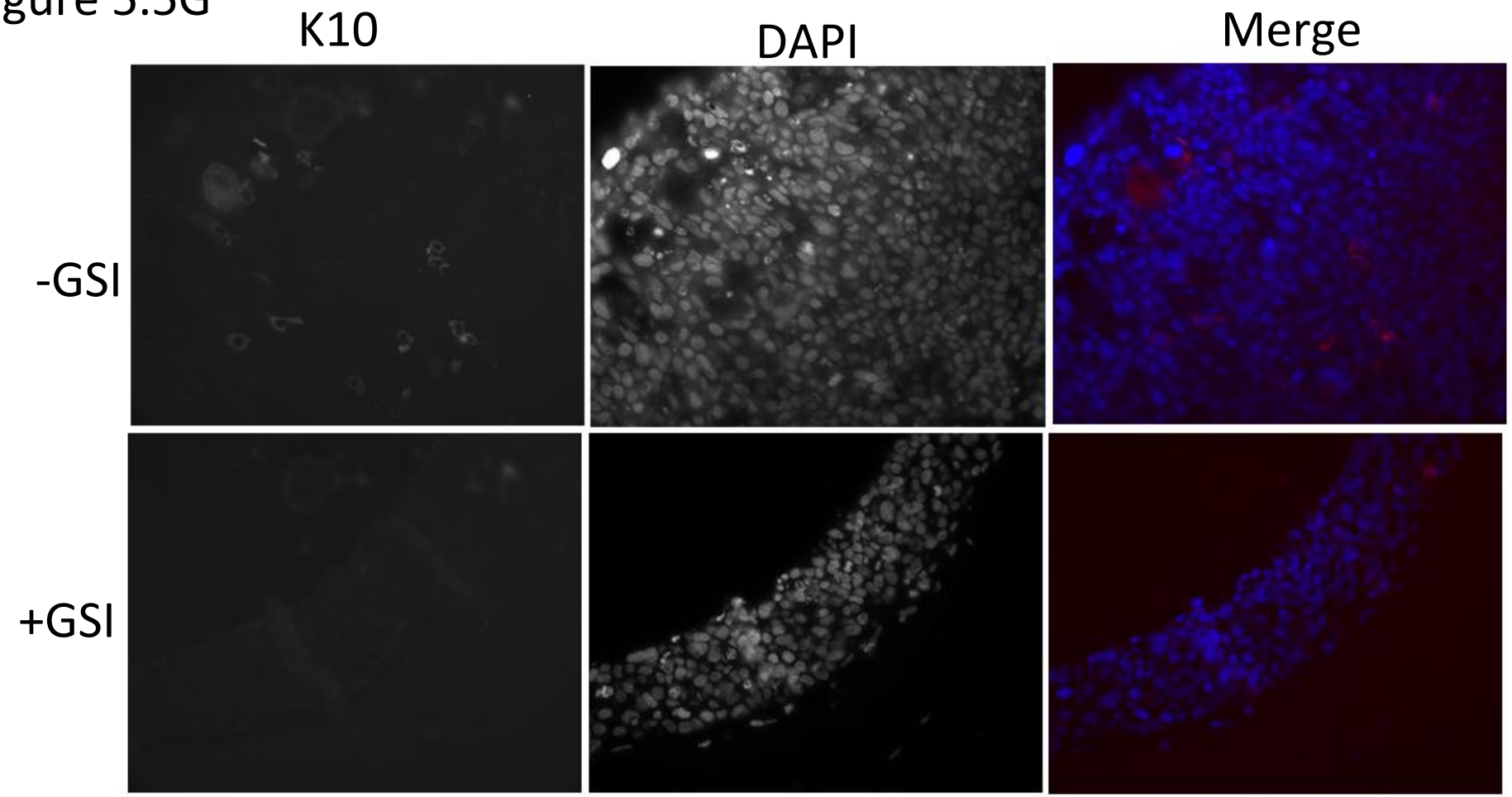

Figure 5.5G GSI Reduces K10 Expression in SCCT2

Fibrin gels cultured with SCCIC8 with/without the gamma secretase inhibitor and stained for the terminal differentiation marker, K10. LHS panel is the black and white K10 staining only, middle is the corresponding DAPI for this image and the RHS images are the K10 staining (RED) and DAPI (BLUE) images merged together. The top set is grown without (1µM) GSI in DMSO only and the bottom is in the presence of GSI. There is a reduction in K10 staining in the presence of GSI. Images are taken under 43 x objective.

Figure 5.5H

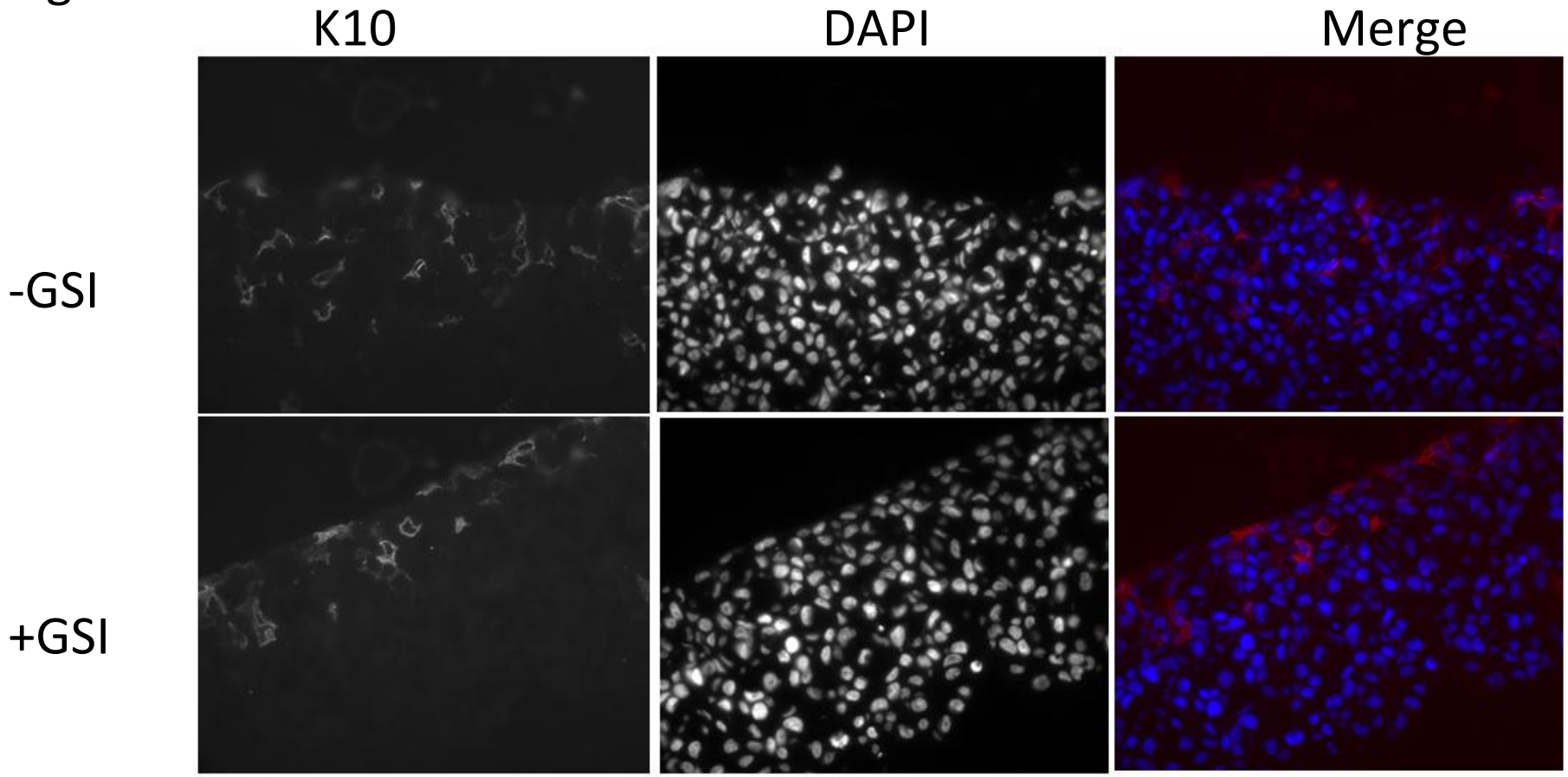

Figure 5.5H GSI has no effect on K10 Expression in SCCIC8

Fibrin gels cultured with SCCIC8 with/without the gamma secretase inhibitor and stained for the terminal differentiation marker, K10. LHS panel is the black and white K10 staining only, middle is the corresponding DAPI for this image and the RHS images are the K10 staining (RED) and DAPI (BLUE) images merged together. The top set is grown without (1µM) GSI and the bottom is in the presence of GSI. There is a reduction in K10 staining in the presence of GSI. Images are taken under 43 x objective.

5.2.5 Transduction of SCCIC8 Notch1 Null keratinocytes with a GSI Regulatable Notch construct dE to Allow Expression of Notch in This Cell Type

Jon Aster kindly sent a notch1 vector "dE" which when over-expressed in cells does not require notch ligand stimulation for notch signalling to be switched on but only requires GSI to be activated (see below for representative image of construct compared to full length notch).

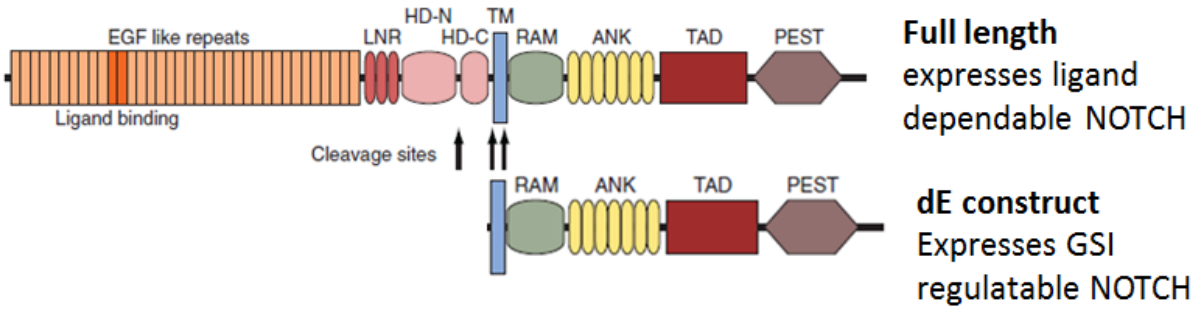

SCCIC8 cells were then retrovirally transduced with the dE vector (figure 5.6). The cells transduced with dE notch construct (SCCIC8dE), not in the presence of GSI, are morphologically different from those in the presence of GSI and the SCCIC8pB control. These cells appeared rounded, phase bright and were growing on-top of one another. The SCCIC8dE cells in the presence of the GSI, did not have the same morphology, however did have areas of cells which were more stacked on-top. SCCIC8pB cells which had been transduced with the pB empty vector control did not show any morphological differences – either with or without GSI.

Figure 5.6

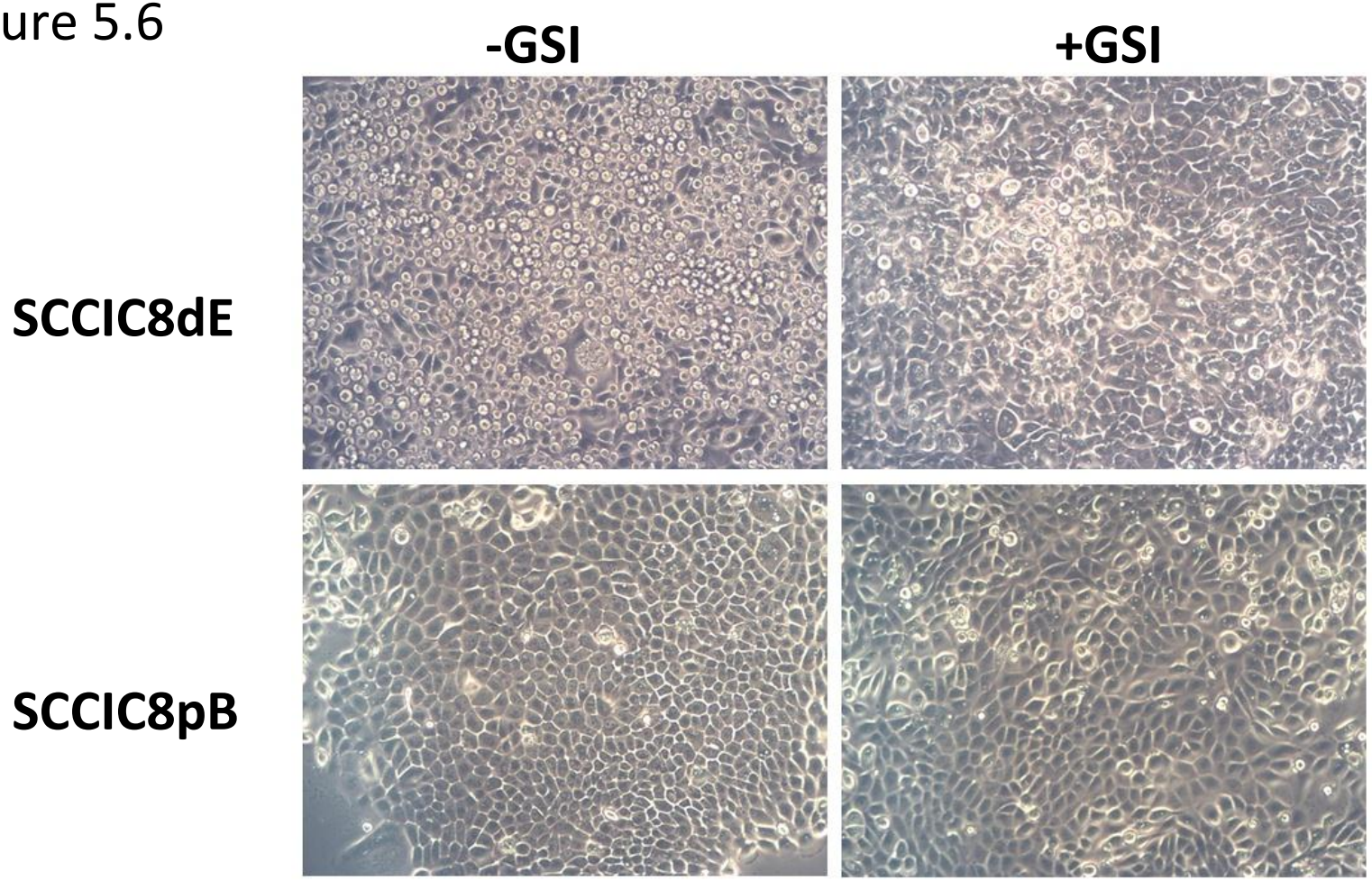

Figure 5.6 Transduction of SCCIC8 with dE Vector

SCCIC8 notch null cSCC cells were transduced with the dE construct, in the presence of 1µM GSI or DMSO. Cells transduced without GSI appeared more rounded and growing on-top of each other compared to those transduced in the presence of GSI. No morphological difference was noted between the SCCIC8pB cells wither with or without GSI. Results represent 3 experiments.

5.2.6 Washout Strategy Shows That dE Can Be Controlled By GSI

Previous work by Jon Aster and colleagues suggested that following removal of GSI from the media re-expression of activated notch occurred after 24h in lymphocytes. Using this strategy in keratinocytes to “switch on” notch expression as shown in figure 5.9, activated notch can be switched on in the SCCIC8 cells that have been transduced with the dE vector. Western blot looking at the expression of full length notch1 (notch1) and ICN1 in cells transduced with the empty vector control (SCCIC8pB) do not show any expression of Notch1 or activated notch as expected even following washout of GSI. However IC8 cells transduced with the GSI regulatable vector (SCCIC8dE) in the presence of GSI have a band a 150KDa indicating expression of dE however this band disappears following washout of GSI and a band appears at 110KDa indicating that notch has been activated in these cells.

Figure 5.7

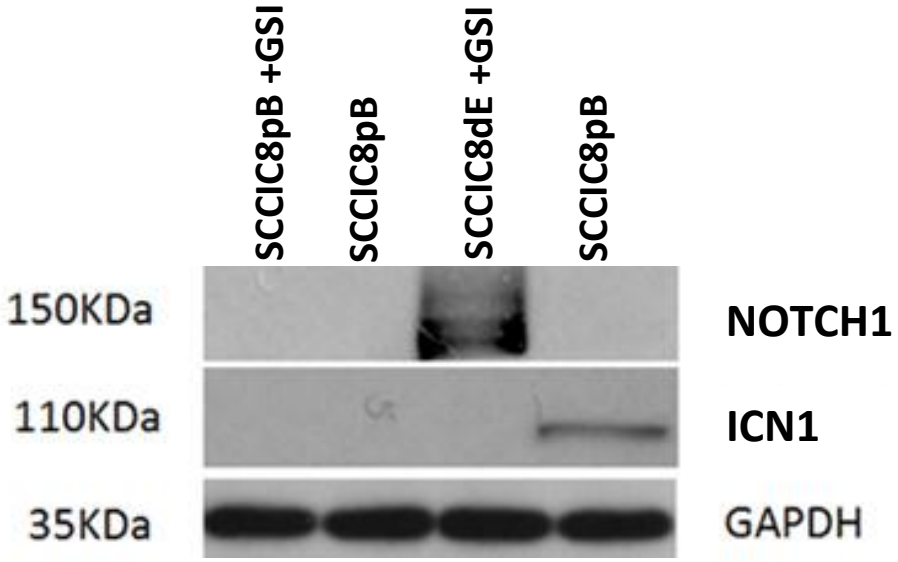

Figure 5.7 Washout Strategy Shows That dE Can Be Switched On Following GSI Removal

Western blot using a GSI washout strategy were cells (either SCCIC8dE/SCCIC8pB) were cultured in the presence of GSI and GSI is then removed. Removal of GSI from the SCCIC8dE cells switches on activated notch (ICN1). GAPDH was used as a loading control. Immunoblot represents n=3.

5.2.7 Washout of GSI leads to nuclear localisation of ICN1 signal in SCCIC8dE cells as determined by immunofluorescence

Immunofluorescence staining of SCCIC8dE cells shows that in the presence of GSI (Figure 5.8A, panel 1) full length notch is located in the endoplasmic reticulum (ER) whereas ICN1 expression is located perinuclear. Washout of GSI from the SCCIC8dE notch cells leads to a change in localisation of ICN1 from cytoplasmic to nuclear with the localisation of the full length notch (notch1) being unaffected, as expected (figure 5.8A, panel 1). These data further confirms that it is possible to washout the GSI in order to switch on the expression of notch. Staining of SCCIC8pB cells with notch1 or ICN1 shows no positive staining either in the presence of GSI (figure 5.8A & 5.8B, Panel 2).

Figure 5.8A

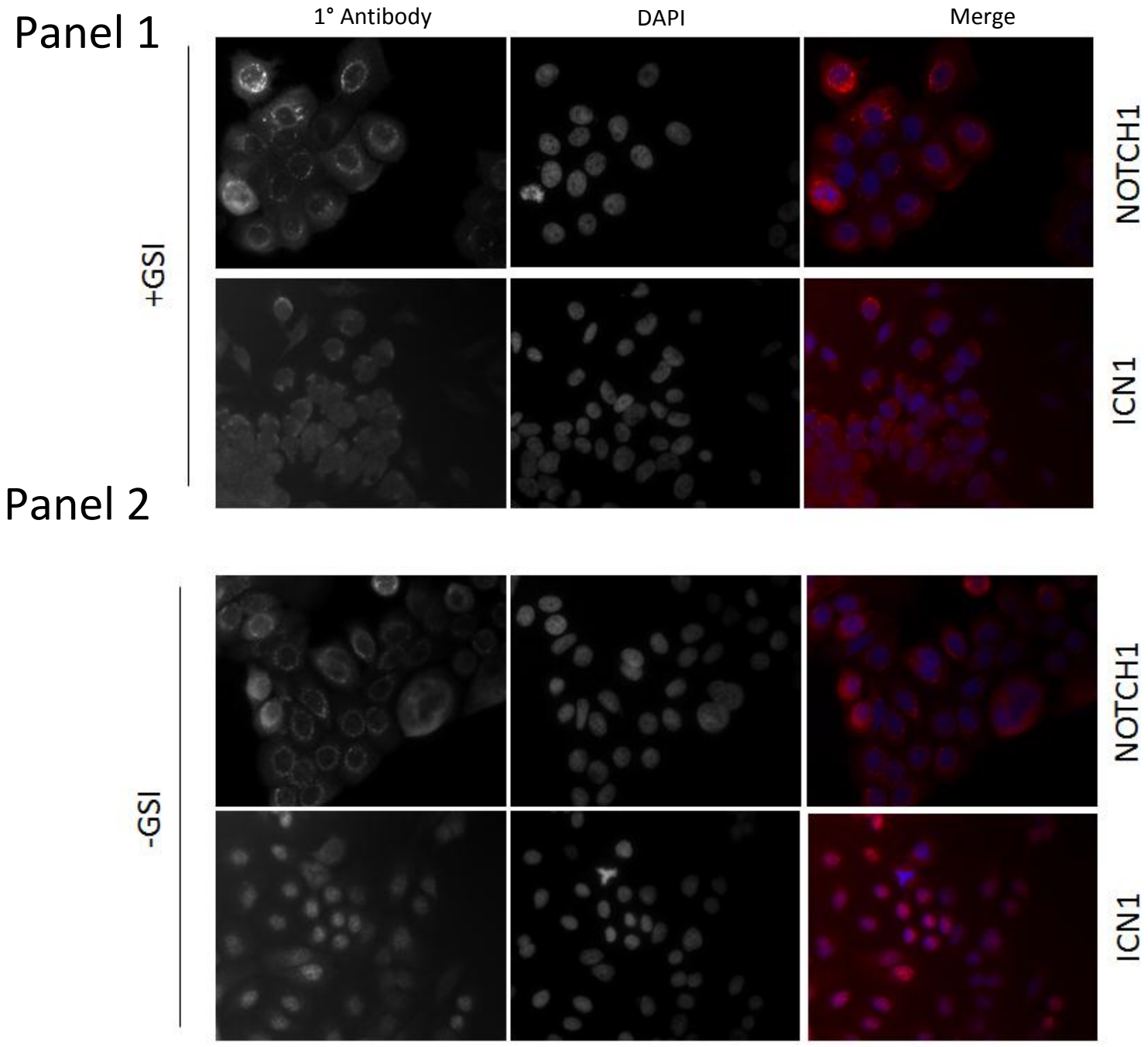

Figure 5.8A Washout of GSI Leads to Nuclear Localisation of ICN1 Signal in SCCIC8dE Cells as Determined By Immunofluorescence.

SCCIC8dE cells were grown on cover-slips in the presence of GSI and 24h before fixation GSI was removed from the cells in panel 1. Following fixation cells were stained using the staining method in (2.7.1) using 2 primary antibodies – full length NOTCH1 (NOTCH1) or activated NOTCH1 (ICN1). Staining shows that on removal of GSI, ICN1 is localised to the nucleus however NOTCH1 is unchanged. Results represent two independent experiments. Images taken with 43x objective.

Figure 5.8B

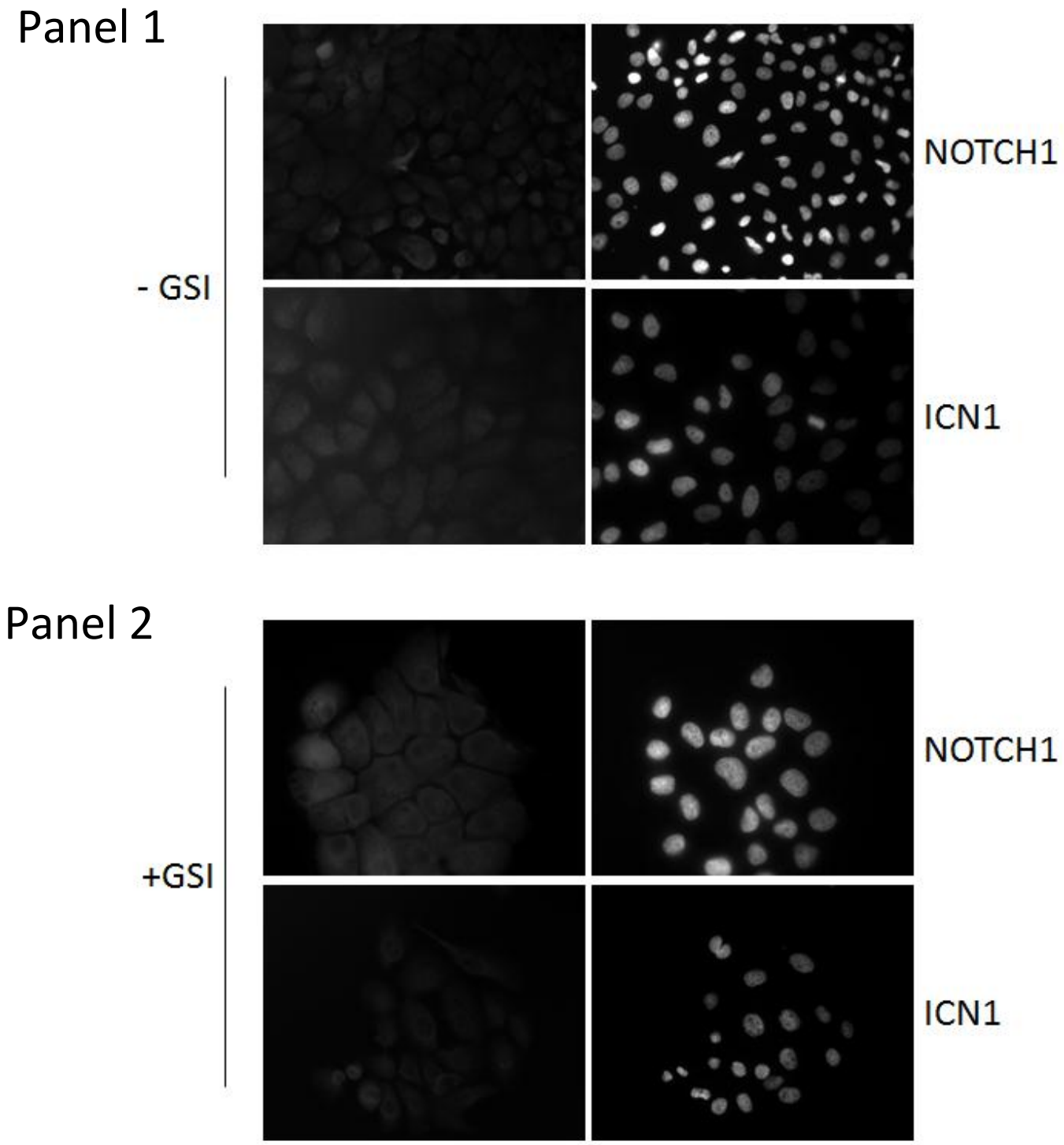

Figure 5.8B Immunofluorescence of SCCIC8pB Cells Following GSI Washout

SCCIC8pB cells were grown on cover-slips in the presence of GSI and 24h before fixation GSI was removed from the cells in panel 1. Following fixation cells were stained using the staining method in (2.7.1) using 2 primary antibodies – full length NOTCH1 (NOTCH1) or activated NOTCH1 (ICN1). No positive staining is seen with either antibody. Results represent two independent experiments. Images taken with 43x objective.

5.2.8 Overexpression of dE Notch Increases Involucrin Expression With a Reduction in c-Myc

Compared to the cells which express the empty vector pB control, SCCIC8pB there is an up-regulation of involucrin in the cells which express the construct SCCIC8dE (figure 5.9). This expression was reduced with the addition of GSI which reduces notch expression. This increase in involucrin suggests an increase in differentiation, which is greater in the presence of activated notch, and can be reduced through the removal of GSI. In addition to the rise in involucrin is a simultaneous decrease in c-Myc in the SCCIC8dE cells. This decrease in c-Myc is reverincreased with the addition of GSI to a protein level to a similar level seen in the SCCIC8pB lysates.

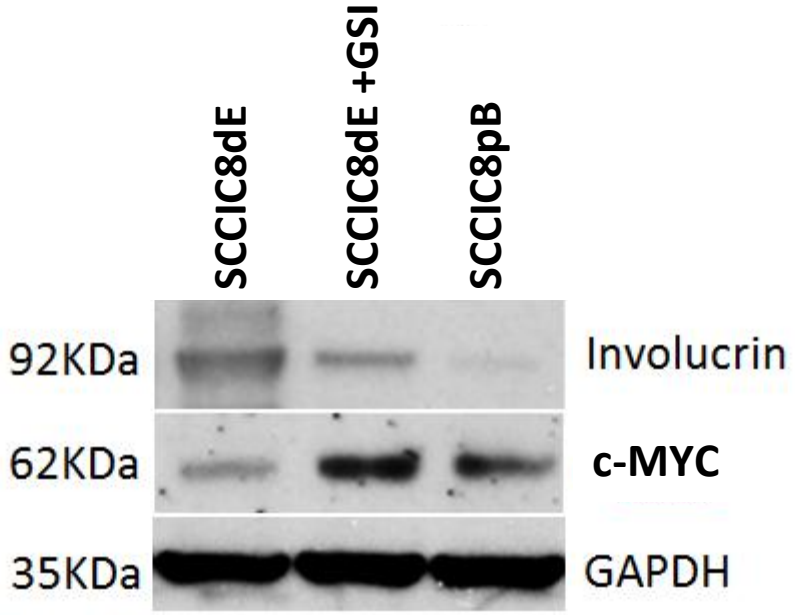

Figure 5.9 The Expression of Notch in the SCCIC8 cells Increases Involucrin While Reducing c-myc.

Western blot shows increased expression of involucrin in the SCCIC8dE cell line which overexpress a GSI regulatable form of notch, dE. This expression is reduced following the addition of GSIinvolucrin. Cells which express the empty vector control, SCCIC8pB, shows much less involucrin expression. Additionally the results show a simultaneous reduction in c-myc expression. SCCIC8dE cells have reduced c-myc expression which is increased with the addition of GSI. A similar level of c-myc is seen in the SCCIC8pB, pBABE empty vector control. Additionally, the expression of c-Myc is restored with the addition of GSI. Results represent three independent experiments.

5.2.9 MTS Shows a Reduction in Proliferation Following Washout of GSI in the SCCIC8dE Cells

Following washout of GSI from the SCCIC8dE cells there was a reduction in proliferation over 96h (figure 5.10) as determined by the MTS assay. This was not seen in the SCCIC8pB cells suggesting that inhibition of notch signalling with GSI was the cause of the effect.

Figure 5.10

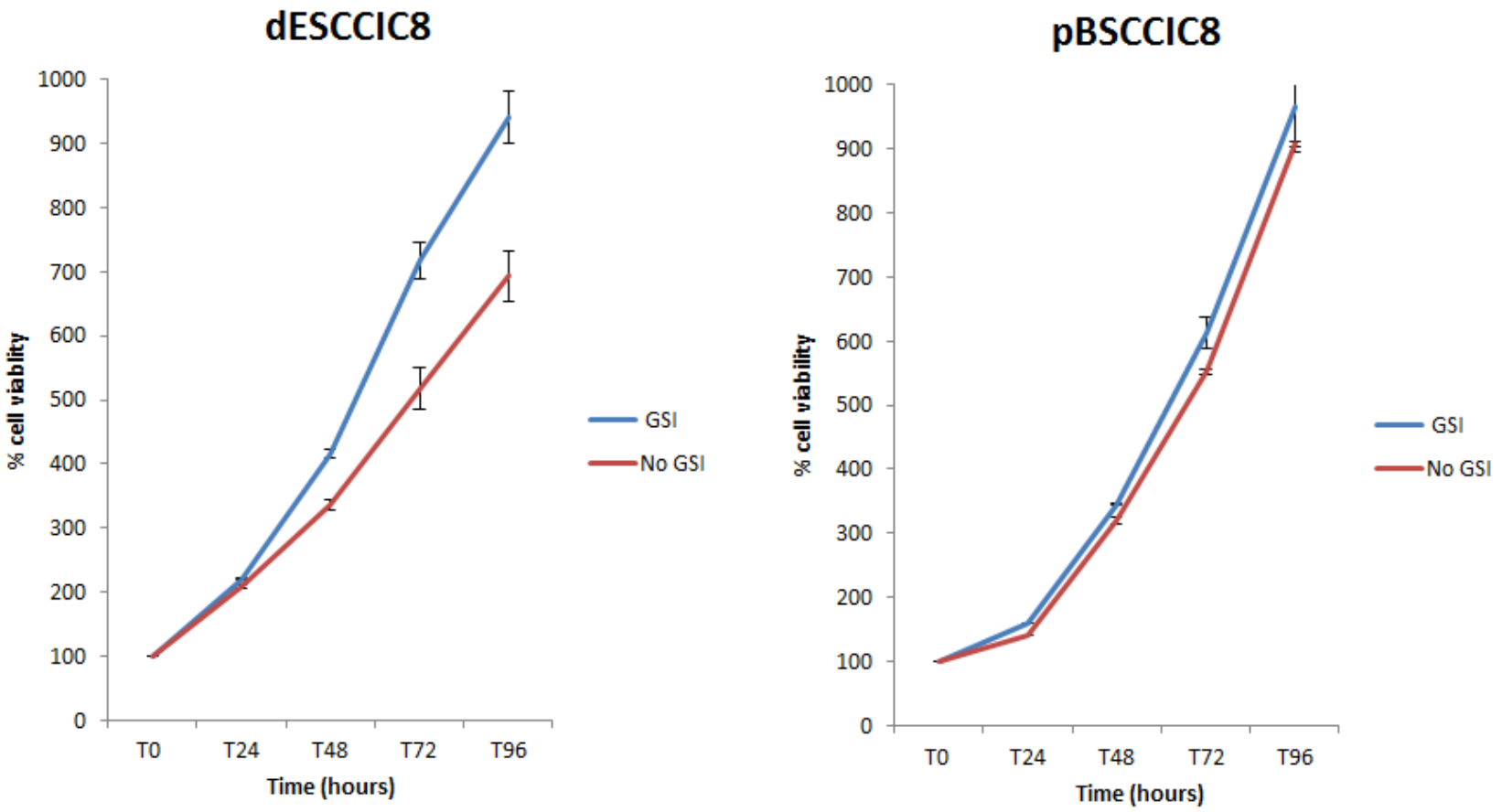

Figure 5.10 MTS Shows a Reduction in Proliferation Following Washout of GSI in SCCIC8dE Cells

Assessment of proliferation, using the MTS assay in the SCCIC8dE cells showed a slight reduction in proliferation following washout of GSI. This reduction in proliferation is not seen in the pBABE empty vector control cells, SCCIC8pB. Results expressed are the mean of 3 experiments ±SD.

5.2.10 The use of 3D organotypic confirms notch over-expression but Identifies Leaky Expression in SCCIC8dE cells

SCCIC8dE cells were grown on fibrin gels as previously described in the material and methods chapter (2.6.1.2). These gels were then kept in the presence of GSI or without and fixed after 7 days and stained for cleaved notch. The images show that in the absence of GSI, notch is activated and present in the nucleus (figure 5.11). However, with the addition of GSI ~~which is to prevented notch activation and hence cleaved~~ notch staining is not entirely switched off. Fibrin gels were also fixed following 42 days after they had been raised above the liquid interface (figure 5.12). This showed similar results in that the expression of the dE notch in the SCCIC8dE cells is reduced however some expression is still retained in the basal layer. This means that the current concentration of GSI is not switching off notch expression completely, which is also observed after 7 days.

Figure 5.11

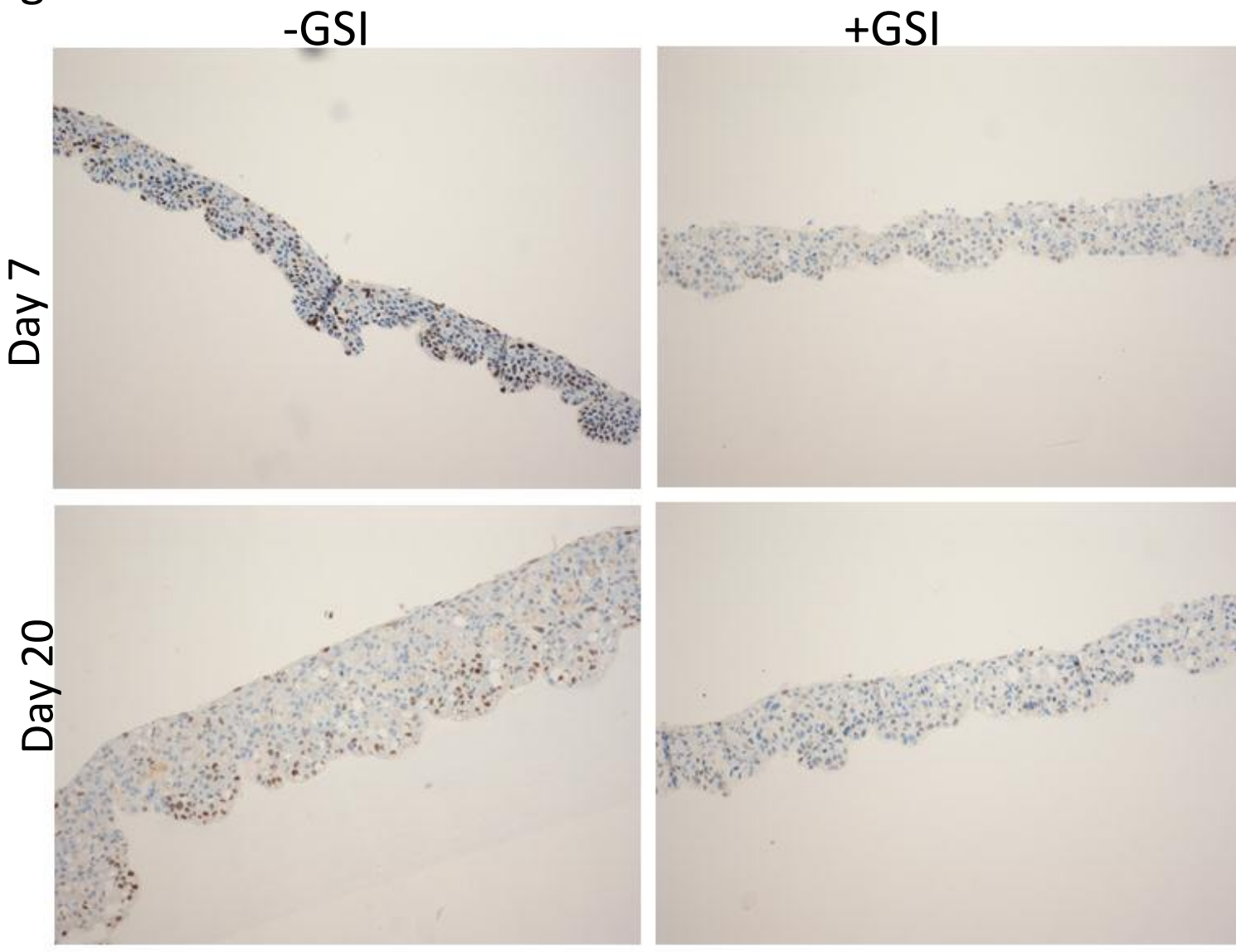

Figure 5.13 GSI Reduces the Expression of ICN1 7 Days After Being Lifted

Fibrin gels with SCCIC8dE keratinocytes grown on-top were grown either in the presence of GSI or without and then fixed after 7 days. They were then stained with cleaved notch to detect the presence of activated intracellular notch. Without GSI ICN1 was present in the nucleus however GSI reduces the expression of notch in this cell type. Staining was performed using Jon Aster's groups staining protocol (M.Kluk 2013) by the Tayside Tissue Bank Dundee.

Figure 5.12

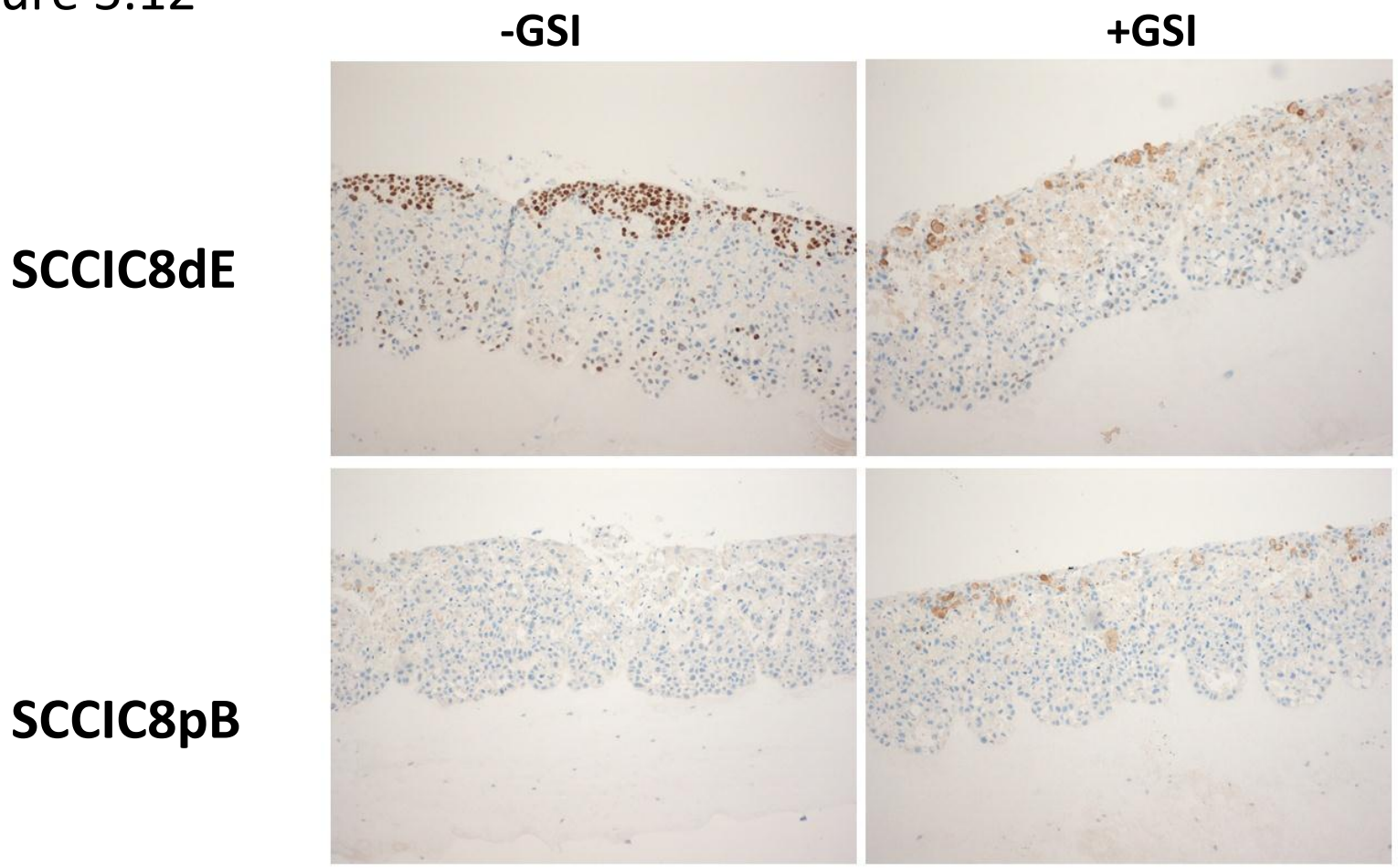

Figure 5.12 GSI Reduces the Expression of ICN1 Expression 42 Days After Being Lifted

Fibrin gels with SCCIC8dE keratinocytes grown on-top were grown either in the presence of GSI or without and then fixed after 7 days. They were then stained with cleaved notch to detect the presence of activated intracellular notch. Without GSI ICN1 was present in the nucleus however GSI reduces the expression of notch in this cell type. Staining was performed using Jon Aster's groups staining protocol (M.Kluk 2013) by the Tayside Tissue Bank Dundee.

5.2.11 SCCIC8dE Increases Involucrin in 3D Organotypics

Over-expression of the dE construct in SCCIC8 cells increases involucrin staining in 3D organotypic cultures which confirms the western blot data shown in figure 5.9 (figure 5.13A). Additionally this expression of involucrin can be reduced with the addition of 1µM GSI. However involucrin staining is still evident suggesting that the dose of GSI may not completely switch the expression of involucrin off. Comparatively, the SCCIC8pB cells show a much lower expression of involucrin, both in the presence of GSI and without, suggesting that the increase in involucrin staining is due to the expression of the dE construct (figure 5.13B).

Figure 5.13A

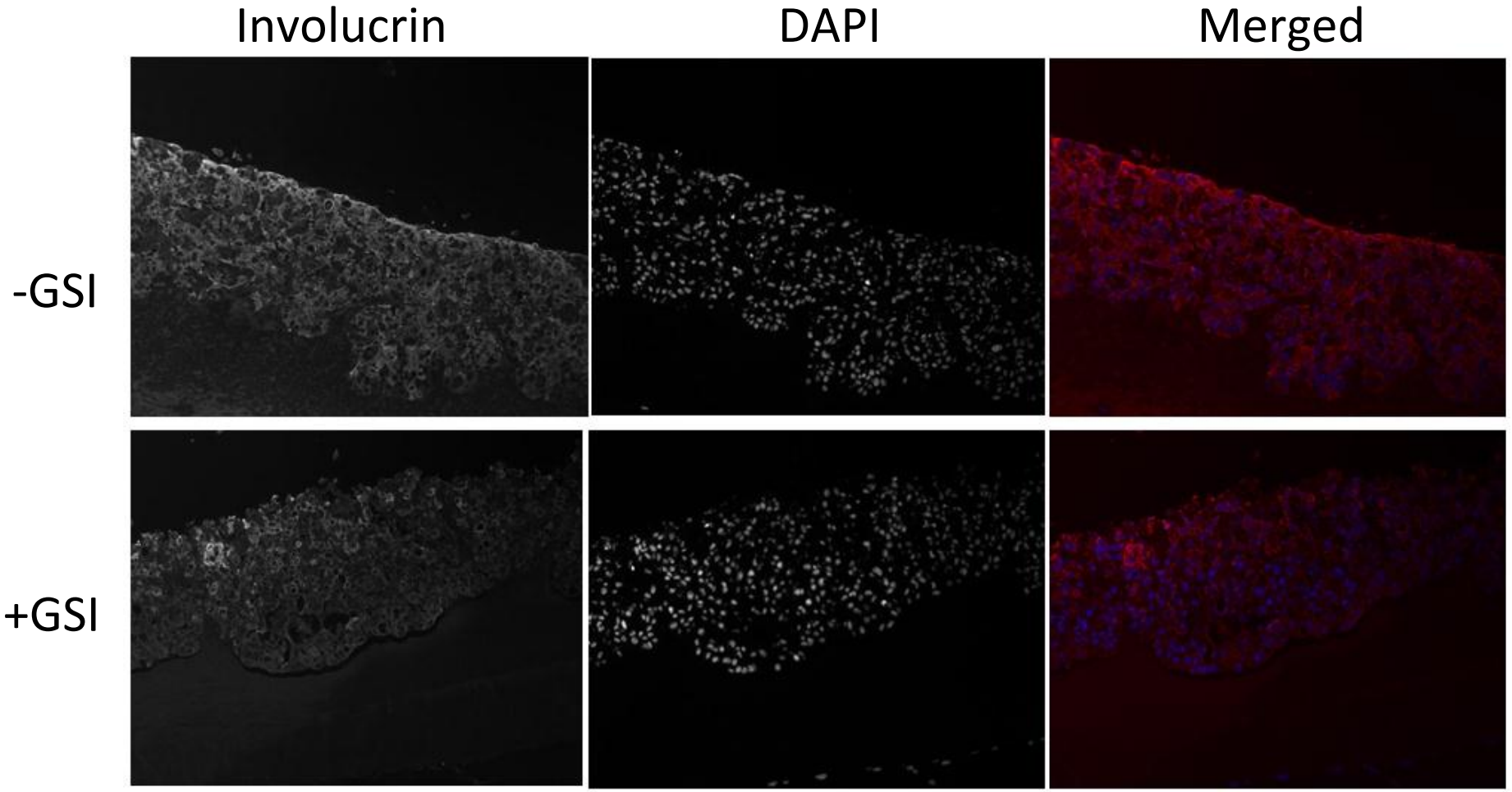

Figure.15A SCCIC8dE Cells Have Increased Involucrin Immunofluorescence Staining Which is Reduced Following Incubation With GSI

Fibrin gels cultured with normal human keratinocytes with/without the gamma secretase inhibitor and stained for the terminal differentiation marker, involucrin. LHS panel is the black and white involucrin staining only, middle is the corresponding DAPI for this image and the RHS images are the involucrin staining (RED) and DAPI (BLUE) images merged together. The top set is grown without GSI and the bottom is in the presence of GSI. There is a reduction in Involucrin staining in the presence of GSI. Images obtained using the 16x objective.

Figure 5.13B

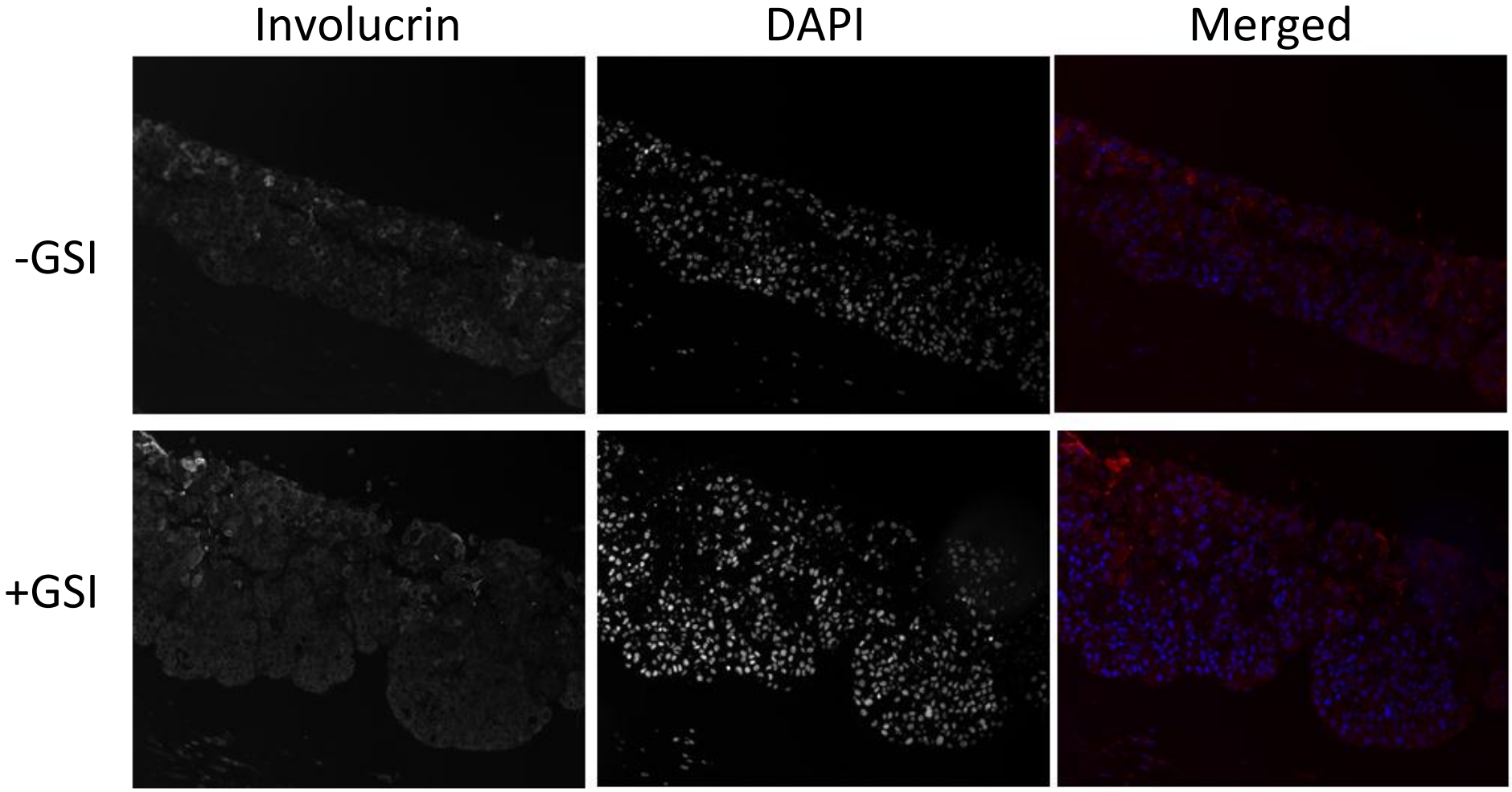

Figure 5.15B SCCIC8pB Has Reduced Involucrin Staining Compared to SCCIC8dE

Fibrin gels cultured with normal human keratinocytes with/without the gamma secretase inhibitor and stained for the terminal differentiation marker, involucrin. LHS panel is the black and white involucrin staining only, middle is the corresponding DAPI for this image and the RHS images are the involucrin staining (RED) and DAPI (BLUE) images merged together. The top set is grown without GSI and the bottom is in the presence of GSI. There is a reduction in Involucrin staining in the presence of GSI. Images obtained using the 16x objective.

5.3 DISCUSSION

The sequencing data produced from our lab identified a high prevalence of biallelic inactivation of *notch1* and *notch2* genes, which as with the tumour suppressor *p53*, appear to act as critical tumour suppressors in cSCC. Notch receptors participate in a highly conserved signalling pathway, which elicits a duality of critical cellular functions including, differentiation, survival, growth and death occurring in a context dependant manner. In many tissue lineages, notch signalling can enhance stem cell potential and suppress differentiation while in keratinocytes it exerts an opposite effect (Artavanis-Tsakonas et al 1999). It is well established that in haematological malignancies Notch1 functions as an oncogene (for a review see Aster 2008) (Di Ianni et al 2009, Fabbri et al 2011, Kridel 2012). However in the skin, loss of function experiments has unequivocally demonstrated Notch1 tumour suppressing ability (Nicolas et al 2003, Proweller et al 2006, Lefort et al 2007). This dichotomy between tumour promoting and suppressing function remains to be investigated but undoubtedly has implications on notch as a target for cancer therapy. Furthermore, this apparent dichotomy is convoluted by the novel finding thatt ~~in~~ a small population of patients with myeloid leukaemia have inactivating notch mutations- suggesting a tumour suppressive and tumour promoting role within the same tumour (Klinakis et al 2011). A similar situation has been unveiled in pancreatic cancer where mouse models have used to reveal that notch receptors can either promote or inhibit pancreatic neoplasia depending on cellular context (Avila and Kissil et al 2013).

This chapter has focused on the role of notch1 as a tumour suppressor in the skin/keratinocyte system. Previous reports have suggested a pro-differentiation role for notch activation in normal keratinocytes (Lowell et al 2000, Rangarajan et al 2001, Nickoloff

et al 2002a, Nguyen et al 2006, Letfort et al 2007) which has been further disseminated in this chapter using two approaches. Firstly, through immunohistochemistry staining of three cell lines of known genotype and secondly, through over-expression of a GSI regulatable notch in a notch null cSCC cell line. Following the sequencing data, which identified loss-of function of notch in cSCC, protein expression analysis in a panel of cSCC confirmed that the expression of notch was markedly reduced in all six of the cSCC cell lines tested. Surprisingly, even in the SCCT8 cell line which expressed wild type Notch. This may suggest that notch signalling is reduced in all cSCC in one way or another irrespective ofdespite the mutational status. Further work needs to be done to establish exactly how notch synthesis is activated and inhibited. Notch signalling is under tight control by a number of complex mechanisms. One mechanism is through membrane trafficking – where several factors modulate notch signal perception at the membrane (Struhlhul and Greenwald 1999, Seugnet 1997, Wilkin et al 2008). Studies, mainly in *Drosophila*, have identified a number of proteins that are involved in endocytosis such as Dynamin a GTPase at the cell surface; numb a cytoplasmic protein and Sanpodo a multipass transmembrane protein which is localised to the cell membrane (Fortini 2009). Additionally, ubiquitination of notch using E3 ligaagses is an important regulatory mechanism of notch signalling (Wwilkin et al 2004). DSL endocytosis and endosomal trafficking within the signal sending cell, using other E3 ligases such as Neutralised (Neur) and Mindbomb (Mib) can also alter Notch activation through ubiquitination (Wang and Struhl 2005). Finally, a second endocytotic event to further activate notch proteolytic cleavages has been proposed - a “pulling force” which triggers trans-endocytosis of the NICD (Meloty-Kapella 2012). Once activated nuclear events can occur in order to switching off Notch signalling. Nuclear kinases can phosphorylate NICD, which is thought to be important for the stability of NICD and hence it is activity (Espinosa et

al 2003, Fryer et al 2004). Furthermore, E3 ubiquitin ligases FBXW7, modifies NICD and targets it for proteosomal degradation (Gupta-Rossi et al 2001). These few processes mentioned above are but a small proportion of the control mechanisms on notch's complex pathway. Further to this complexity our group have also identified a number of mutations in genes within the notch pathway which would undoubtedly have an effect activation or inactivation of the pathway. Genome-scale studies in *Drosophila* have revealed an extraordinarily complex network of genes that control this highly conserved pathway (Giot L, 2003). This means we are faced with serious challenges in understanding the control mechanisms for notch signalling in human disease. Currently our collaborators are performing RNAseq analysis of one of our notch null cell lines that over-express a GSI regulatable form of notch and comparing it to these cells expressing the empty vector control. This experiment will hopefully provide valuable global insights into biological networks following the expression of notch in these cells and hopefully, with the use of GSI help our understanding of the implications of switching notch signalling off in cSCC cells.

Inhibition of notch activation using GSI at a concentration of 1µM was enough to inhibit notch activation in normal human keratinocytes but not in cSCC keratinocytes. This concentration of GSI was chosen, as Jon Aster, our collaborator was able to inhibit notch expression in Jurkat cells, a T cell leukaemia cell line with activated notch expression. Perhaps the cSCC cell lines tested have mutations in the gamma secretase complex, which reduces its sensitivity to GSI. It has been previously reported that knockout of nicastrin, a component of the gamma secretase complex, produces myeloproliferative disorder in mice (Klinakis et al 2011). Additionally gamma secretase interacts with a number of other substrates including E-Cadherin and CD44 which are important for cell-cell adhesion and

have been reported to be down regulated in cSCC perhaps a reduction in the~~n~~ is related to GSI sensitivity (Lyakhovitsky et al 2004). Additionally this concentration of GSI was unable to switch off notch expression following stable retroviral over-expression of the dE notch construct. This was only evident when carrying out immunohistochemistry staining on organotypic cultures and could not be confirmed by western blot which is much quicker and less labour intensive than the former. This was also confirmed by our collaborators whom were unable to switch off notch signalling at mRNA level using GSI. They also tried switching the dE notch off using a dose response and were still unable to switch off the expression. Further to this our collaborators have developed 3 other constructs and expressed one of these in the notch null cSCC cells and are now performing RNAseq on these cells.

Using three cell lines of known genotype the SCC1C12 cells with wild type notch, the SCCT2 cells with loss of function notch and the notch null SCCIC8 cell line, the function of notch in differentiation was explored. Using the 1µM concentration to inhibit notch expression in these cell types fibrin gels were grown and fixed after 7 days and stained with involucrin or K10, which are markers of differentiation in the suprabasal layers which have been previously shown to be elicited by notch activation (Rangarajan et al 2001, Nickoloff et al 2002). The expression of both involucrin and K10 was reduced in the presence of GSI, in the normal human keratinocytes and the SCCIC12 cell line which both express wild type notch,

This would suggest that notch contributes to differentiation in normal but also tumour keratinocytes. Of note the involucrin expression is not completely obliterated with 1µM GSI possibly due to involucrin being already expressed in a small fraction of keratinocytes undergoing spontaneous differentiation under low calcium conditions (Brissette et al 1996). Although there is evidence to suggest that notch signals non-autonomously within the

epidermis to regulate differentiation there is still much to be learned about notch's complex interaction with other pathways. Additionally it is important to explore the possibility that different levels of notch have different outcomes through investigating cell lines with different mutational statuses. Furthermore the organotypic system allows the user to explore the contribution of fibroblasts autonomous induction of differentiation.

In addition to this, looking at the DAPI counterstaining for both the normal human keratinocytes and the SCCIC12 cells shows that there are significant differences in the numbers of cells in the presence of GSI in the SCCIC12 cells but not the normal human keratinocytes. This would suggest that the function of notch is different in normal human keratinocytes and cSCC. Additionally, these data suggests that differentiation is markedly decreased in the cSCC cells compared to normal human keratinocytes, with the notch null SCCIC8 cells expressing the least.

In conclusion these data suggests that notch contributes to carcinogenesis through a reduction in differentiation. Keratinocyte specific re-activation of notch would therefore be a potential therapy for cSCC. Possible methods of reactivation include re-expression of notch using a targeted antibody or through inhibition of the co-repressor complex CSL. However in cancers which are harboured with notch mutations re-expression may prove more difficult. Hence determination of networks and pathways associated with notch activation in both normal and mutated cell lines is essential. RNAseq would be crucial for elucidating these associated networks.

Chapter 6 Final Conclusions and Future Work

Carcinogenesis results from the accumulation of genetic and epigenetic events. Studies to understand these changes are paramount in finding a treatment for this disease of which emerging genomic technologies will no doubt, facilitate this pursuit. Dr South's group have utilised two methods; microarray technology and Sanger sequencing which has yielded a number of potential molecular targets for cSCC, some of which are demonstrated within this thesis.

6.1 VALIDATION OF MOLECULAR TARGETS FOR CSCC

Genetic screens have previously been used to further validate molecular targets and identify the gene function within that cell type. Within this thesis, the original screen performed by Watt and colleagues was repeated, however using cytotoxicty as an endpoint. Although a further three targets PARP1, FUCA2 and PSMG3 were identified using this method, these targets were not pursed due to time constraints and the desire to further study a target which showed potential in a number of different assays and cell lines. Furthermore, this cytotoxicty screen highlighted the target PRSS21 which had also been highlighted in the previous screen by Watt et al 2011, making it a good candidate as a molecular target in cSCC.

In follow up of the screen performed by Watt and colleagues, three genes, BDKRB1, GSG2 and PRSS21 were explored as potential molecular targets for cSCC. A number of functional assays of cell viability and cell death were utilised to determine if these genes were

important for cSCC cell survival. Using this method PRSS21 showed most promise as a molecular target using a series of different assays.

6.2 IDENTIFICATION OF PRSS21 AS A POTENTIAL MOLECULAR TARGET FOR CSCC

PRSS21 was identified as being a potential molecular target for cSCC being able to significantly reduce cell viability and induce cytotoxicity through an increase of apoptosis, leading to the conclusion that PRSS21 over-expression is essential for cSCC cell survival. Using cell migratory and collagen matrigel assays, retroviral over-expression of PRSS21 in K1 keratinocytes resulted in significantly increased migration and invasion into the gel compared to the empty vector control. Following on from this result it would be useful to further identify if the protease function of PRSS21 was required for invasion, using site directed mutagenesis of PRSS21's catalytic activity. Furthermore, this retroviral over-expression of PRSS21 led to the reduction in the expression of the tumour suppressor maspin, which is frequently down-regulated in cancer. Interestingly maspin, has been shown to inhibit tumour growth and suppress metastasis in a number of malignancies however the underlying mechanisms of maspin's tumour suppressing ability are currently unclear. This thesis shows that PRSS21 potentially negatively regulates maspin over-expression in cSCC. Suggesting that inhibition of PRSS21 may not only reduce PRSS21 levels but re-introduce maspin expression in cSCC. Primarily, further work to evaluate the function of maspin in both NHK and cSCC is necessary. Information as to wither RNAi depletion of maspin affects proliferation and cell death in NHK would also be useful for our understanding in cSCC. Furthermore, retroviral over-expression of maspin in cSCC and exploration of its effects on cell migration and matrigel invasion, compared to the empty vector control, would determine~~support~~ if~~wither~~ re-introducing maspin would be a potential therapy. Additionally

the potential of both PRSS21 and maspin to serve as biomarkers for disease progression, where PRSS21 may indicate invasive tumour potential and maspin act as a indicator of good prognosis, further reinforces them to pave the way for the development of improved diagnostics and therapies for cSCC.

Overall, the data show that PRSS21 would be a promising molecular target for cSCC and that development of inhibitors to PRSS21 may have clinical use. Although having high affinities, previous studies have shown that small molecular inhibitors to proteases often lack specificity. However PRSS21 is predominantly expressed in the testis, which would reduce any non-specific effects on normal tissue.

6.3 THE CONTRIBUTION OF NOTCH LOSS OF FUNCTION TO CSCC

Loss-of-function mutations were found in ~75% of cSCC, suggesting that Notch is an important tumour suppressor within this tumour type. The mechanism of this loss-of-function remains undefined, so exploration of the regulation and function of this gene network in the skin is important. Culture of keratinocytes in 3D cultures at the air-liquid inter-phase allows the production of a cornified layer and hence allows the user to study the differentiation program at the level of the granular and cornified layer which is important for notch function. Using this method a reduction in differentiation is seen following incubation with GSI in both NHK and cSCC cells. Additionally, differentiation is reduced overall in cSCC compared to the NHK and is not as responsive to GSI regulation of notch regardless of the genotype. In parallel to these differentiation experiments, it would have been interesting to identify if proliferation was also being regulated through notch expression. Using an antibody raised against Ki67 which is a marker of keratinocyte proliferation would be one quick method of identifying this. Using this 3D organotypic

model it would be useful to explore the function of the fibroblasts to notch differentiation, as recently Dotto's group have demonstrated a role for rbpjk-/- fibroblasts to increase proliferation and suppress differentiation of the overlying keratinocytes (Hu 2012). However, interestingly staining of 3D organotypic gels for activated notch, in this thesis showed no positive staining in the fibroblasts of these gels (figure 5.6). Overall the data suggests that notch contributes to differentiation however this still remains to be resolved mechanistically in addition to working towards the development of a drug which could re-express it.

6.4 CONCLUSION

To conclude, three potential molecular targets have been identified by the work in this thesis. The over-expression of PRSS21 provides a mechanism by which cSCC cells can migrate and invade into the surrounding extracellular matrix, thus potentially contributing to tumour progression. Furthermore, the over-expression reduces the TS maspin suggesting that inhibition of PRSS21 would simultaneously re-express maspin in addition to inhibition of PRSS21 expression, and may be effective for cSCC therapeutic intervention. Additionally notch is a potential molecular target for cSCC due to large number of LOF mutations that occur within this cell type. This thesis demonstrates that loss of notch functions to decreases epidermal differentiation in cSCC, suggesting that re-expression of notch would reduce tumour progression.

References

(4th May 2011). "Cancer Research UK." Retrieved 20th May 2011, from http://info.cancerresearchuk.org/cancerstats/incidence/commoncancers/.

(2011, 5th October 2013). "ISD Scotland." from www.isdscotland.org/Health/Cancer/Cancer-Statistics/.

Agrawal, N., M. J. Frederick, et al. (2011). "Exome sequencing of head and neck squamous cell carcinoma reveals inactivating mutations in NOTCH1." Science 333(6046): 1154-1157.

Alam, M. and D. Ratner (2001). "Cutaneous squamous-cell carcinoma." N Engl J Med 344(13): 975-983.

Altschul, S. F., T. L. Madden, et al. (1997). "Gapped BLAST and PSI-BLAST: a new generation of protein database search programs." Nucleic Acids Res 25(17): 3389-3402.

Andersson, E. R. (2012). "The role of endocytosis in activating and regulating signal transduction." Cell Mol Life Sci 69(11):1755-71.

Arnault, J. P., J. Wechsler, et al. (2009). "Keratoacanthomas and squamous cell carcinomas in patients receiving sorafenib." J Clin Oncol 27(23): e59-61.

Artavanis-Tsakonas, S., (1999). "Notch signalling: cell fate control and signal integration in development." Science 30;284(5415):770-6.

Aster, J. C., S. C. Blacklow, et al. (2011). "Notch signalling in T-cell lymphoblastic leukaemia/lymphoma and other haematological malignancies." J Pathol 223(2): 262-273.

Aster, J. C., et al (2008). "Notch signalling in leukemia." Annu Rev Pathol3:587-613

Avila, J.L. and Kissil, J.L. (2013). "Notch signalling in pancreatic cancer:oncogene or tumour suppressor." Trends mol Med 19(5):320-7.

Balmain, A., M. Ramsden, et al. (1984). "Activation of the mouse cellular Harvey-ras gene in chemically induced benign skin papillomas." Nature 307(5952): 658-660.

Bamford, S., E. Dawson, et al. (2004). "The COSMIC (Catalogue of Somatic Mutations in Cancer) database and website." Br J Cancer 91(2): 355-358.

Barki-Harrington, L., A. L. Bookout, et al. (2003). "Requirement for direct cross-talk between B1 and B2 kinin receptors for the proliferation of androgen-insensitive prostate cancer PC3 cells." Biochem J 371(Pt 2): 581-587.

Beeram, M., A. Patnaik, et al. (2003). "Regulation of c-Raf-1: therapeutic implications." Clin Adv Hematol Oncol 1(8): 476-481.

Beliveau, F., A. Desilets, et al. (2009). "Probing the substrate specificities of matriptase, matriptase-2, hepsin and DESC1 with internally quenched fluorescent peptides." Febs J 276(8): 2213-2226.

Benhamou, S. and A. Sarasin (2000). "Variability in nucleotide excision repair and cancer risk: a review." Mutat Res 462(2-3): 149-158.

Bernal, F., M. Wade, et al. (2010). "A stapled p53 helix overcomes HDMX-mediated suppression of p53." Cancer Cell 18(5): 411-422.

Bouwes Bavinck, J. N., S. Euvrard, et al. (2007). "Keratotic skin lesions and other risk factors are associated with skin cancer in organ-transplant recipients: a case-control study in The Netherlands, United Kingdom, Germany, France, and Italy." J Invest Dermatol 127(7): 1647-1656.

Brash, D. E. (2006). "Roles of the transcription factor p53 in keratinocyte carcinomas." Br J Dermatol 154 Suppl 1: 8-10.

Brown, V.D., Philips, R.A. et al. (1999) "Cumulative effect of phosphorylation of pRB on regulation of E2F activity" Mol Cell Biol19(5):3246-56.

Brissette, J.L. et al (1996) "The product of the mouse locus,Whn, regulates the balance between epithelial cell growth and differentiation." Genes Dev 1;10(17):2212-21.

Burgeson, R. E. and A. M. Christiano (1997). "The dermal-epidermal junction." Curr Opin Cell Biol 9(5): 651-658.

Calixto, J. B., R. Medeiros, et al. (2004). "Kinin B1 receptors: key G-protein-coupled receptors and their role in inflammatory and painful processes." Br J Pharmacol 143(7): 803-818.

Carrell, R. and Travis, J. (1985). "α1-Antitrypsin and the serpins:Variation and countervariation." Trends Biochem. Sci. 10: 20-24.

Cartlidge, P. H. T. and N. Rutter (1992). Skin Barrier Function. Fetal & Neonatal Physiology. R. Polin and W. Fox. Philadelphia, Saunders, WB: pp569-585.

Cella, N., A. Contreras, et al. (2006). "Maspin is physically associated with [beta]1 integrin regulating cell adhesion in mammary epithelial cells." Faseb J 20(9): 1510-1512.

Chambers, A. F. and L. M. Matrisian (1997). "Changing views of the role of matrix metalloproteinases in metastasis." J Natl Cancer Inst 89(17): 1260-1270.

Chen, E. I., L. Florens, et al. (2005). "Maspin alters the carcinoma proteome." Faseb J 19(9): 1123-1124.

Christiano, A. M. (1997). "Frontiers in keratodermas: pushing the envelope." Trends Genet 13(6): 227-233.

Chuang, T. Y., L. A. Heinrich, et al. (1992). "PUVA and skin cancer. A historical cohort study on 492 patients." J Am Acad Dermatol 26(2 Pt 1): 173-177.

Clayman, G. L., J. J. Lee, et al. (2005). "Mortality risk from squamous cell skin cancer." J Clin Oncol 23(4): 759-765.

Cobleigh, M. A., C. L. Vogel, et al. (1999). "Multinational study of the efficacy and safety of humanized anti-HER2 monoclonal antibody in women who have HER2-overexpressing metastatic breast cancer that has progressed after chemotherapy for metastatic disease." J Clin Oncol 17(9): 2639-2648.

Connolly, K., P. Manders, et al. (2013). "Papillomavirus-associated squamous skin cancers following transplant immunosuppression: one Notch closer to control." Cancer Treat Rev.

Cory, A.H., et al. (1991). "Use of an aqueous soluable tetrazolium/formazan assay for cell growth assays in culture." Cancer commun 3,207-201.

da Rocha Dias, S., T. Salmonson, et al. (2013). "The European Medicines Agency review of vemurafenib (Zelboraf(R)) for the treatment of adult patients with BRAF V600 mutation-positive unresectable or metastatic melanoma: summary of the scientific assessment of the Committee for Medicinal Products for Human Use." Eur J Cancer 49(7): 1654-1661.

Dai, J. and J. M. Higgins (2005). "Haspin: a mitotic histone kinase required for metaphase chromosome alignment." Cell Cycle 4(5): 665-668.

Dai, J., B. A. Sullivan, et al. (2006). "Regulation of mitotic chromosome cohesion by Haspin and Aurora B." Dev Cell 11(5): 741-750.

Dajee, M., M. Lazarov, et al. (2003). "NF-kappaB blockade and oncogenic Ras trigger invasive human epidermal neoplasia." Nature 421(6923): 639-643.

Dano, K., J. Romer, et al. (1999). "Cancer invasion and tissue remodeling--cooperation of protease systems and cell types." Apmis 107(1): 120-127.
Dave, S. S., K. Fu, et al. (2006). "Molecular diagnosis of Burkitt's lymphoma." N Engl J Med 354(23): 2431-2442.
Davie, E. W., K. Fujikawa, et al. (1991). "The coagulation cascade: initiation, maintenance, and regulation." Biochemistry 30(43): 10363-10370.
Davies, B. J., B. S. Pickard, et al. (1998). "Serine proteases in rodent hippocampus." J Biol Chem 273(36): 23004-23011.
Dazard, J. E., H. Gal, et al. (2003). "Genome-wide comparison of human keratinocyte and squamous cell carcinoma responses to UVB irradiation: implications for skin and epithelial cancer." Oncogene 22(19): 2993-3006.
de Gruijl, F. R., J. Longstreth, et al. (2003). "Health effects from stratospheric ozone depletion and interactions with climate change." Photochem Photobiol Sci 2(1): 16-28.
Demehri, S., A. Turkoz, et al. (2009). "Epidermal Notch1 loss promotes skin tumorigenesis by impacting the stromal microenvironment." Cancer Cell 16(1): 55-66.
Deu, E., M. Verdoes, et al. (2012). "New approaches for dissecting protease functions to improve probe development and drug discovery." Nat Struct Mol Biol 19(1): 9-16.
Devgan, V., C. Mammucari, et al. (2005). "p21WAF1/Cip1 is a negative transcriptional regulator of Wnt4 expression downstream of Notch1 activation." Genes Dev 19(12): 1485-1495.
Di Cera, E. (2009). "Serine proteases." IUBMB Life 61(5): 510-515.
Dixit, V. and T. W. Mak (2002). "NF-kappaB signaling. Many roads lead to madrid." Cell 111(5): 615-619.
Dodson, J. M., J. DeSpain, et al. (1991). "Malignant potential of actinic keratoses and the controversy over treatment. A patient-oriented perspective." Arch Dermatol 127(7): 1029-1031.
Donehower, L. A., M. Harvey, et al. (1992). "Mice deficient for p53 are developmentally normal but susceptible to spontaneous tumours." Nature 356(6366): 215-221.
Dotto, G. P. (2008). "Notch tumor suppressor function." Oncogene 27(38): 5115-5123.
Druker, B. J., M. Talpaz, et al. (2001). "Efficacy and safety of a specific inhibitor of the BCR-ABL tyrosine kinase in chronic myeloid leukemia." N Engl J Med 344(14): 1031-1037.
Eady, R. A., J. D. Fine, et al. (2004). Genetic Blistering Diseases. Textbook of Dermatology. T. Burns, S. Brreathnach, N. Cox and C. Griffiths, Oxford: Wiley-Blackwell.
Eckert, R.L., Green, H. (1986). "Structure and evolution of the human involucrin gene." Cell 15;46(4):583-9
Einspahr, J. G., V. Calvert, et al. (2012). "Functional protein pathway activation mapping of the progression of normal skin to squamous cell carcinoma." Cancer Prev Res (Phila) 5(3): 403-413.
Ellisen, L. W., J. Bird, et al. (1991). "TAN-1, the human homolog of the Drosophila notch gene, is broken by chromosomal translocations in T lymphoblastic neoplasms." Cell 66(4): 649-661.
Espinosa, L., et al. (2003). "Phosphorylation by glycogen synthase kinase-3β down regulates notch activity, a link for notch and wnt pathways." J Bio Chem 287,32227-32235.
Esseghir, S., J. S. Reis-Filho, et al. (2006). "Identification of transmembrane proteins as potential prognostic markers and therapeutic targets in breast cancer by a screen for signal sequence encoding transcripts." J Pathol 210(4): 420-430.

Fabbri, G., et al (2011). "Analysis o the chronic lymphocytic leukemia coding geneome: role of NOTCH1 mutational activation." 4;208(7):1389-401.

Fine, J. D. (1999). The Clasification of Inherited Epidermolyosis Bullosa. Epidermolysis Bullosa:Clinical, Epidemiologic & Laboratory Advances and Findings of the National epidermolysis Bullosa Registary. J. D. Fine, E. Bauer, J. McGuire and A. Moshell, Baltimore: The John Hopkins University Press: 101-113.

Fine, J. D., L. B. Johnson, et al. (2009). "Epidermolysis bullosa and the risk of life-threatening cancers: the National EB Registry experience, 1986-2006." J Am Acad Dermatol 60(2): 203-211.

Fior, R. and D. Henrique (2009). ""Notch-Off": a perspective on the termination of Notch signalling." Int J Dev Biol 53(8-10): 1379-1384.

Fire, A. (1999). "RNA-triggered gene silencing." Trends Genet 15(9): 358-363.

Fortina, A. B., S. Piaserico, et al. (2004). "Immunosuppressive level and other risk factors for basal cell carcinoma and squamous cell carcinoma in heart transplant recipients." Arch Dermatol 140(9): 1079-1085.

Fortini , M.E. and Bilde, D. (2009) "Endocytic regulation of notch signaling." Curr Opin Genet Dev 19(4):323-8.

Fuchs, E. and V. Horsley (2008). "More than one way to skin." Genes Dev 22(8): 976-985.

Fusenig, N. E., et al. (1983). "Growth and differentiaition characteristics of transformed keratinocytes form mouse and human skin in vitro and in vivo." J invest Dermatol 81(1 Suppl):168s-75s

Futshcher, B.W. et al. (2002). "Role of DNA methylation in the control of cell type specific maspin expression." Nat Genet 31(2):175-9.

Froeling, F. M. et al. (2010). "Pancreatic cancer organotypic cultures." J Biotechnol 1;148(1):16-23.

Fryer, C.J., et al., (2004) " Mastermind recruits CycC:CDK8 to phosphorylate the notch ICD and Coordinate Activation with Turnover." Mol Cell 16(4)509-520.

Gambardella, L. and Y. Barrandon (2003). "The multifaceted adult epidermal stem cell." Curr Opin Cell Biol 15(6): 771-777.

Gera, L., J. P. Fortin, et al. (2006). "Discovery of a dual-function peptide that combines aminopeptidase N inhibition and kinin B1 receptor antagonism." J Pharmacol Exp Ther 317(1): 300-308.

Getting, S. J. (2002). "Melanocortin peptides and their receptors: new targets for anti-inflammatory therapy." Trends Pharmacol Sci 23(10): 447-449.

Girdler, F., K. E. Gascoigne, et al. (2006). "Validating Aurora B as an anti-cancer drug target." J Cell Sci 119(Pt 17): 3664-3675.

Giot, L., et al (2003). "A protien interaction map of drosophila melanogaster." Science 302,1727.

Gleason, D. F. and G. T. Mellinger (1974). "Prediction of prognosis for prostatic adenocarcinoma by combined histological grading and clinical staging." J Urol 111(1): 58-64.

Gleixner, K. V., V. Ferenc, et al. (2010). "Polo-like kinase 1 (Plk1) as a novel drug target in chronic myeloid leukemia: overriding imatinib resistance with the Plk1 inhibitor BI 2536." Cancer Res 70(4): 1513-1523.

Glover, M. T., N. Niranjan, et al. (1994). "Non-melanoma skin cancer in renal transplant recipients: the extent of the problem and a strategy for management." Br J Plast Surg 47(2): 86-89.

Greenhalgh, D. A., X. J. Wang, et al. (1996). "Paradoxical tumor inhibitory effect of p53 loss in transgenic mice expressing epidermal-targeted v-rasHa, v-fos, or human transforming growth factor alpha." Cancer Res 56(19): 4413-4423.

Greenhalgh, D. A., X. J. Wang, et al. (1995). "12-O-tetradecanoylphorbol-13-acetate promotion of transgenic mice expressing epidermal-targeted v-fos induces rasHA-activated papillomas and carcinomas without p53 mutation: association of v-fos expression with promotion and tumor autonomy." Cell Growth Differ 6(5): 579-586.

Gupta-Rossi, N., et al (2001). "Functional interaction between SEL-10, an F-box protein, and the nuclear form of activated notch1 receptor." J Biol Chem 14;276(37):34371-8.

Hameetman, L., S. Commandeur, et al. (2013). "Molecular profiling of cutaneous squamous cell carcinomas and actinic keratoses from organ transplant recipients." BMC Cancer 13: 58.

Hamilton, A. J. and D. C. Baulcombe (1999). "A species of small antisense RNA in posttranscriptional gene silencing in plants." Science 286(5441): 950-952.

Hanahan, D. and R. A. Weinberg (2000). "The hallmarks of cancer." Cell 100(1): 57-70.

Hanahan, D. and R. A. Weinberg (2011). "Hallmarks of cancer: the next generation." Cell 144(5): 646-674.

Harrington, E. A., D. Bebbington, et al. (2004). "VX-680, a potent and selective small-molecule inhibitor of the Aurora kinases, suppresses tumor growth in vivo." Nat Med 10(3): 262-267.

Herter, S., D. E. Piper, et al. (2005). "Hepatocyte growth factor is a preferred in vitro substrate for human hepsin, a membrane-anchored serine protease implicated in prostate and ovarian cancers." Biochem J 390(Pt 1): 125-136.

Higgins, J. M. (2001). "The Haspin gene: location in an intron of the integrin alphaE gene, associated transcription of an integrin alphaE-derived RNA and expression in diploid as well as haploid cells." Gene 267(1): 55-69.

Higgins, J. M. (2010). "Haspin: a newly discovered regulator of mitotic chromosome behavior." Chromosoma 119(2): 137-147.

Honda, A., K. Yamagata, et al. (2002). "A mouse serine protease TESP5 is selectively included into lipid rafts of sperm membrane presumably as a glycosylphosphatidylinositol-anchored protein." J Biol Chem 277(19): 16976-16984.

Hooper, J. D., N. Bowen, et al. (2000). "Localization, expression and genomic structure of the gene encoding the human serine protease testisin." Biochim Biophys Acta 1492(1): 63-71.

Hooper, J. D., D. L. Nicol, et al. (1999). "Testisin, a new human serine proteinase expressed by premeiotic testicular germ cells and lost in testicular germ cell tumors." Cancer Res 59(13): 3199-3205.

Hopkins, P. C. and J. Whisstock (1994). "Function of maspin." Science 265(5180): 1893-1894.

Huertas, D., M. Soler, et al. (2012). "Antitumor activity of a small-molecule inhibitor of the histone kinase Haspin." Oncogene 31(11): 1408-1418.

Huntington, J. A. (2011). "Serpin structure, function and dysfunction." J Thromb Haemost 9 Suppl 1: 26-34.

Irving, J. A., P. J. Steenbakkers, et al. (2002). "Serpins in prokaryotes." Mol Biol Evol 19(11): 1881-1890.

Iso, T. et al. (2003). "HES and HERP families: multiple effectors of the Notch signalling pathway." J Cell Physiol 194(3):237-55.

Jensen, P., S. Hansen, et al. (1999). "Skin cancer in kidney and heart transplant recipients and different long-term immunosuppressive therapy regimens." J Am Acad Dermatol 40(2 Pt 1): 177-186.

Jerant, A. F., J. T. Johnson, et al. (2000). "Early detection and treatment of skin cancer." Am Fam Physician 62(2): 357-368, 375-356, 381-352.

Jiang, N., Y. Meng, et al. (2002). "Maspin sensitizes breast carcinoma cells to induced apoptosis." Oncogene 21(26): 4089-4098.

Jiang, W., H. N. Ananthaswamy, et al. (1999). "p53 protects against skin cancer induction by UV-B radiation." Oncogene 18(29): 4247-4253.

Kaplan, A. L. and J. L. Cook (2005). "Cutaneous squamous cell carcinoma in patients with chronic lymphocytic leukemia." Skinmed 4(5): 300-304.

Karagas, M. R., V. A. Stannard, et al. (2002). "Use of tanning devices and risk of basal cell and squamous cell skin cancers." J Natl Cancer Inst 94(3): 224-226.

Karagas MR, et al "Genus β human papillomaviruses and incidence of basal cell and squamous cell carcinomas of skin: population based case-control study" *BMJ* 2010; 341: c2986.

Khalkhali-Ellis, Z. (2006). "Maspin: the new frontier." Clin Cancer Res 12(24): 7279-7283.

Khoury, M. P. and J. C. Bourdon (2010). "The isoforms of the p53 protein." Cold Spring Harb Perspect Biol 2(3): a000927.

Kim, T. K. and J. H. Eberwine (2010). "Mammalian cell transfection: the present and the future." Anal Bioanal Chem 397(8): 3173-3178.

Klasa-Mazurkiewicz, D., J. Narkiewicz, et al. (2009). "Maspin overexpression correlates with positive response to primary chemotherapy in ovarian cancer patients." Gynecol Oncol 113(1): 91-98.

Kleinman, H.K. And Martin, G.R. (2005). "Matrigel: basement membrane matrix with biological activity." Semin Cancer Biol 15(5):378-86.

Klinakis, A., et al. (2011). "A novel tumour suppressor function for the notch pathway in myeloid leukaemia." Nature 12;473(7346):230-3.

Kluk M.J. et al., (2013). "Gauging NOTCH1 activation in cancer using immunohistochmistry." PLOS one 18;8(6):e67306.

Kohn, E.C. and Liotta, L.A. (1995). "Molecular insights into cancer invasion:strateggies for prevention and intervention."1;55(9):1856-62.

Kopan, R. and M. X. Ilagan (2009). "The canonical Notch signaling pathway: unfolding the activation mechanism." Cell 137(2): 216-233.

Koshikawa, N., S. Hasegawa, et al. (1998). "Expression of trypsin by epithelial cells of various tissues, leukocytes, and neurons in human and mouse." Am J Pathol 153(3): 937-944.

Kraemer, K. H., M. M. Lee, et al. (1994). "The role of sunlight and DNA repair in melanoma and nonmelanoma skin cancer. The xeroderma pigmentosum paradigm." Arch Dermatol 130(8): 1018-1021.

Kraemer, K. H., M. M. Lee, et al. (1987). "Xeroderma pigmentosum. Cutaneous, ocular, and neurologic abnormalities in 830 published cases." Arch Dermatol 123(2): 241-250.

Kridel, R., et al (2012). "Whole transcriptome sequencing reveals recurrent NOTCH1 mutations in mantle cell lymphoma."Blood1;119(9):1963-71.

Krop, I. et al. (2012). "Phase I phamacologic and phamacodynamic study of the gamma secretase (notch) inhibitor MK-0752 in adult patients with advanced solid tumors." J Clin Oncol. 2012 1;30(19):2307-13.

Kudchadkar, R. R., K. S. Smalley, et al. (2013). "Targeted therapy in melanoma." Clin Dermatol 31(2): 200-208.

Kwa, R. E., K. Campana, et al. (1992). "Biology of cutaneous squamous cell carcinoma." J Am Acad Dermatol 26(1): 1-26.

Lane, D. P. (1992). "Cancer. p53, guardian of the genome." Nature 358(6381): 15-16.

Lane, E. B., E. L. Rugg, et al. (1992). "A mutation in the conserved helix termination peptide of keratin 5 in hereditary skin blistering." Nature 356(6366): 244-246.

Lanssens, S. and K. Ongenae (2011) "Dermatologic lesions and risk for cancer." Acta Clin Belg 66(3): 177-185.

Lazarov, M., Y. Kubo, et al. (2002). "CDK4 coexpression with Ras generates malignant human epidermal tumorigenesis." Nat Med 8(10): 1105-1114.

Leeb-Lundberg, L. M., F. Marceau, et al. (2005). "International union of pharmacology. XLV. Classification of the kinin receptor family: from molecular mechanisms to pathophysiological consequences." Pharmacol Rev 57(1): 27-77.

Lefort, K., A. Mandinova, et al. (2007). "Notch1 is a p53 target gene involved in human keratinocyte tumor suppression through negative regulation of ROCK1/2 and MRCKalpha kinases." Genes Dev 21(5): 562-577.

LeVee, G. J., L. Oberhelman, et al. (1997). "UVA II exposure of human skin results in decreased immunization capacity, increased induction of tolerance and a unique pattern of epidermal antigen-presenting cell alteration." Photochem Photobiol 65(4): 622-629.

Liotta, L. A., C. W. Lee, et al. (1980). "New method for preparing large surfaces of intact human basement membrane for tumor invasion studies." Cancer Lett 11(2): 141-152.

Liu, Z., Y. Shi, et al. (2013). "Expression and localization of maspin in cervical cancer and its role in tumor progression and lymphangiogenesis." Arch Gynecol Obstet.

Livak, K. J. and T. D. Schmittgen (2001). "Analysis of relative gene expression data using real-time quantitative PCR and the 2(-Delta Delta C(T)) Method." Methods 25(4): 402-408.

Lochter, A., S. Galosy, et al. (1997). "Matrix metalloproteinase stromelysin-1 triggers a cascade of molecular alterations that leads to stable epithelial-to-mesenchymal conversion and a premalignant phenotype in mammary epithelial cells." J Cell Biol 139(7): 1861-1872.

Lockett, J., S. Yin, et al. (2006). "Tumor suppressive maspin and epithelial homeostasis." J Cell Biochem 97(4): 651-660.

Lonkar, P. and P. C. Dedon (1999). "Reactive species and DNA damage in chronic inflammation: reconciling chemical mechanisms and biological fates." Int J Cancer 128(9): 1999-2009.

Lowe, S. W. and H. E. Ruley (1993). "Stabilization of the p53 tumor suppressor is induced by adenovirus 5 E1A and accompanies apoptosis." Genes Dev 7(4): 535-545.

Lozano, G. (2010). "Mouse models of p53 functions." Cold Spring Harb Perspect Biol 2(4): a001115.

Lucas, J. M., et al. "The androgen-regulated type II serine protease TMPRSS2 is differentially expressed and mislocalised in prostate adenocarcinoma." J.Pathol. 215 118-125.

Maliekal M (2008). "The role of notch signalling in human cervical cancer:implications for solid tumours." Oncogene 27(38):5110-4.

Malkin, D. (1994). "p53 and the Li-Fraumeni syndrome." Biochim Biophys Acta 1198(2-3): 197-213.
Malumbres, M., P. Pevarello, et al. (2008). "CDK inhibitors in cancer therapy: what is next?" Trends Pharmacol Sci 29(1): 16-21.
Marioni, G., C. Staffieri, et al. (2009). "MASPIN tumour-suppressing activity in head and neck squamous cell carcinoma: emerging evidence and therapeutic perspectives." Acta Otolaryngol 129(5): 476-480.
Marioni, G., E. Zanoletti, et al. (2013). "Expression of the tumour-suppressor maspin in temporal bone carcinoma." Histopathology 63(2): 242-249.
Markaki, Y., A. Christogianni, et al. (2009). "Phosphorylation of histone H3 at Thr3 is part of a combinatorial pattern that marks and configures mitotic chromatin." J Cell Sci 122(Pt 16): 2809-2819.
Marks, R., P. Foley, et al. (1986). "Spontaneous remission of solar keratoses: the case for conservative management." Br J Dermatol 115(6): 649-655.
Martins, V. L. et al (2009). "Increased invasive behaviour in cutaneous squamous cell carcinoma with loss of basement-membrane type VII collagen." J Cell Sci 1;122(11):1788-1799.
Martinez, J. C. and C. C. Otley (2001). "The management of melanoma and nonmelanoma skin cancer: a review for the primary care physician." Mayo Clin Proc 76(12): 1253-1265.
Masini, C., P. G. Fuchs, et al. (2003). "Evidence for the association of human papillomavirus infection and cutaneous squamous cell carcinoma in immunocompetent individuals." Arch Dermatol 139(7): 890-894.
McGowen, R., H. Biliran, Jr., et al. (2000). "The surface of prostate carcinoma DU145 cells mediates the inhibition of urokinase-type plasminogen activator by maspin." Cancer Res 60(17): 4771-4778.
McGrath, J. A. (2004). "Translational benefits from research on rare genodermatoses." Australas J Dermatol 45(2): 89-93.
McGrath, J. A., R. A. Eady, et al. (2004). Anatomy & Organisation of Human Skin. Rook's Textbook of Dermatology. T. Burns, S. Breathnach, N. Cox and C. Griffiths, Oxford: Blackwell Science. Vol 1.
Meek, D. W. and C. W. Anderson (2009). "Posttranslational modification of p53: cooperative integrators of function." Cold Spring Harb Perspect Biol 1(6): a000950.
Meltzer, P. S. (2001). "Spotting the target: microarrays for disease gene discovery." Curr Opin Genet Dev 11(3): 258-263.
Meloty-Kapella, L., et al. (2012) "Notch ligand endocytosis generates mechanical pulling force dependant on dynamin, epsins and actin." Dev Cell 12;22(6):1299-312.
Mohammed, T.A. , et al (2011). "A pilot phase II study of valporic acid treatment of low grade neuroendocrine carcinoma." Oncologist 16(6):835-43.
Mohr, S., G. D. Leikauf, et al. (2002). "Microarrays as cancer keys: an array of possibilities." J Clin Oncol 20(14): 3165-3175.
Moll, I., M. Roessler, et al. (2005). "Human Merkel cells--aspects of cell biology, distribution and functions." Eur J Cell Biol 84(2-3): 259-271.
Mook, O. R., W. M. Frederiks, et al. (2004). "The role of gelatinases in colorectal cancer progression and metastasis." Biochim Biophys Acta 1705(2): 69-89.
Morgan, T.H. (1917). "The theory of the gene." Am Naturalist 51(609):513-544.

Morris, R. J., S. M. Fischer, et al. (1985). "Evidence that the centrally and peripherally located cells in the murine epidermal proliferative unit are two distinct cell populations." J Invest Dermatol 84(4): 277-281.

Motley, R. J., P. W. Preston, et al. (2009). "Multi-professional Guidelines for the Patient with Primary Cutaneous Squamous Cell Carcinoma."

Moulder, S. L., F. M. Yakes, et al. (2001). "Epidermal growth factor receptor (HER1) tyrosine kinase inhibitor ZD1839 (Iressa) inhibits HER2/neu (erbB2)-overexpressing breast cancer cells in vitro and in vivo." Cancer Res 61(24): 8887-8895.

Moyal, D. D. and A. M. Fourtanier (2001). "Broad-spectrum sunscreens provide better protection from the suppression of the elicitation phase of delayed-type hypersensitivity response in humans." J Invest Dermatol 117(5): 1186-1192.

Netzel-Arnett, S., T. H. Bugge, et al. (2009). "The glycosylphosphatidylinositol-anchored serine protease PRSS21 (testisin) imparts murine epididymal sperm cell maturation and fertilizing ability." Biol Reprod 81(5): 921-932.

Neurath, H. and K. A. Walsh (1976). "Role of proteolytic enzymes in biological regulation (a review)." Proc Natl Acad Sci U S A 73(11): 3825-3832.

Ng, Y. Z., C. Pourreyron, et al. (2012). "Fibroblast-derived dermal matrix drives development of aggressive cutaneous squamous cell carcinoma in patients with recessive dystrophic epidermolysis bullosa." Cancer Res 72(14): 3522-3534.

Ng, Y. Z., Dayal, J.HS and South,A.P (2011). Genetic Predisposition to Cutaneous Squamous Cell Carcinoma, Skin Cancers - Risk Factors, Prevention and Therapy, Prof. Caterina La Porta (Ed.), ISBN: 978-953-307-722-2, InTech, DOI: 10.5772/26714. Available from: http://www.intechopen.com/books/skin-cancers-risk-factors-prevention-and-therapy/genetic-predisposition-to-cutaneous-squamous-cell-carcinoma

Nguyen, B. C., K. Lefort, et al. (2006). "Cross-regulation between Notch and p63 in keratinocyte commitment to differentiation." Genes Dev 20(8): 1028-1042.

Nicolas, M. et al. (2003). "Notch1 functions as a tumour suppresor in mouse skin." Nat Genet 33(3):416-21.

Nickoloff, B. J., J. Z. Qin, et al. (2002). "Life and death signaling pathways contributing to skin cancer." J Investig Dermatol Symp Proc 7(1): 27-35.

Nindl, I., C. Dang, et al. (2006). "Identification of differentially expressed genes in cutaneous squamous cell carcinoma by microarray expression profiling." Mol Cancer 5: 30.

Nomura, T., H. Nakajima, et al. (1997). "Induction of cancer, actinic keratosis, and specific p53 mutations by UVB light in human skin maintained in severe combined immunodeficient mice." Cancer Res 57(11): 2081-2084.

Nystrom, M.L. et al. (2005). "Development of a quantitive method to analyse tumor cell invasion in organotypic culture." J. Pathol. 205, 468-475.

Ohnstad, H. O., E. B. Paulsen, et al. (2011). "MDM2 antagonist Nutlin-3a potentiates antitumour activity of cytotoxic drugs in sarcoma cell lines." BMC Cancer 11: 211:211-211.

Olivier, M., M. Hollstein, et al. (2010). "TP53 mutations in human cancers: origins, consequences, and clinical use." Cold Spring Harb Perspect Biol 2(1): a001008.

Owens, D. M. and F. M. Watt (2003). "Contribution of stem cells and differentiated cells to epidermal tumours." Nat Rev Cancer 3(6): 444-451.

Park, W. S., H. K. Lee, et al. (1996). "p53 mutations in solar keratoses." Hum Pathol 27(11): 1180-1184.

Pear, W. S., G. P. Nolan, et al. (1993). "Production of high-titer helper-free retroviruses by transient transfection." Proc Natl Acad Sci U S A 90(18): 8392-8396.

Pemberton, P. A., D. T. Wong, et al. (1995). "The tumor suppressor maspin does not undergo the stressed to relaxed transition or inhibit trypsin-like serine proteases. Evidence that maspin is not a protease inhibitory serpin." J Biol Chem 270(26): 15832-15837.

Penn, I. and T. E. Starzl (1972). "Malignant tumors arising de novo in immunosuppressed organ transplant recipients." Transplantation 14(4): 407-417.

Pierceall, W. E., L. H. Goldberg, et al. (1991). "Ras gene mutation and amplification in human nonmelanoma skin cancers." Mol Carcinog 4(3): 196-202.

Pinchot, S.N., et al (2011). "Identification and validation of notch pathway activating compounds through a novel high throughput screening method." Cancer 1;117(7):1386-98.

Potten, C. S. and J. C. Bullock (1983). "Cell kinetic studies in the epidermis of the mouse. I. Changes in labeling index with time after tritiated thymidine administration." Experientia 39(10): 1125-1129.

Poumay, Y. and A. Coquette (2007). "Modelling the human epidermis in vitro: tools for basic and applied research." Arch Dermatol Res 298(8): 361-369.

Prendergast, G. C. and W. Du (1999). "Targeting farnesyltransferase: is Ras relevant?" Drug Resist Updat 2(2): 81-84.

Proweller, A., L. Tu, et al. (2006). "Impaired notch signaling promotes de novo squamous cell carcinoma formation." Cancer Res 66(15): 7438-7444.

Prunieras, M., M. Regnier, et al. (1983). "Methods for cultivation of keratinocytes with an air-liquid interface." J Invest Dermatol 81(1 Suppl): 28s-33s.

Puente, X. S., L. M. Sanchez, et al. (2003). "Human and mouse proteases: a comparative genomic approach." Nat Rev Genet 4(7): 544-558.

Purdie, K. J., C. Pourreyron, et al. (2011). Isolation and Culture of Squamous Cell Carcinoma Lines Cancer Cell Culture: Methods and Protocols, Second Edition, Methods in Molecular Biology. I. A. Cree. Portsmouth, UK, Springer Science+Business Media. 731.

Quinn, A. G., C. Campbell, et al. (1994). "Chromosome 9 allele loss occurs in both basal and squamous cell carcinomas of the skin." J Invest Dermatol 102(3): 300-303.

Quintana, R.M. et al. (2013). "A transposon-based analysis of gene muations related to skin cancer development." J Invest Dermatol 133(1):239-48.

Rangarajan, A., C. Talora, et al. (2001). "Notch signaling is a direct determinant of keratinocyte growth arrest and entry into differentiation." Embo J 20(13): 3427-3436.

Ratushny, V.,Gober, M. D. Hick, R., Ridky, T.W., Seykora, J.T., (2012). From keratinocyte to cancer: the pathogenesis and modeling of cutaneous squamous cell carcinoma." J Clin Invest 1;122(2):464-72.

Rawlings, N. D., D. P. Tolle, et al. (2004). "Evolutionary families of peptidase inhibitors." Biochem J 378(Pt 3): 705-716.

Reis-Filho, J.S. et al (2002). "Maspin expression in normal skin and usual cutaneous carcinomas." Virchows Arch 441(6):551-8.

Restivo, G., B. C. Nguyen, et al. (2011). "IRF6 is a mediator of Notch pro-differentiation and tumour suppressive function in keratinocytes." Embo J 30(22): 4571-4585.

Rheinwald, J. G. and M. A. Beckett (1980). "Defective terminal differentiation in culture as a consistent and selectable character of malignant human keratinocytes." Cell 22(2 Pt 2): 629-632.

Rheinwald, J. G. and M. A. Beckett (1981). "Tumorigenic keratinocyte lines requiring anchorage and fibroblast support cultures from human squamous cell carcinomas." Cancer Res 41(5): 1657-1663.

Rheinwald, J. G. and H. Green (1975). "Serial cultivation of strains of human epidermal keratinocytes: the formation of keratinizing colonies from single cells." Cell 6(3): 331-343.

Ridky, T. W. and P. A. Khavari (2004). "Pathways sufficient to induce epidermal carcinogenesis." Cell Cycle 3(5): 621-624.

Riker, A. L. et al. (2008). "The gene expression profiles of primary and metastatic melanoma yields a transition point of tumour pogression and metastasis." BMC Med Genomics 1:13

Robles, A. I. and C. C. Harris (2010). "Clinical outcomes and correlates of TP53 mutations and cancer." Cold Spring Harb Perspect Biol 2(3): a001016.

Romanowska, M., L. Reilly, et al. (2010). "Activation of PPARbeta/delta causes a psoriasis-like skin disease in vivo." PLoS One 5(3): e9701.

Rosenwald, A., A. A. Alizadeh, et al. (2001). "Relation of gene expression phenotype to immunoglobulin mutation genotype in B cell chronic lymphocytic leukemia." J Exp Med 194(11): 1639-1647.

Rowe, D. E., R. J. Carroll, et al. (1992). "Prognostic factors for local recurrence, metastasis, and survival rates in squamous cell carcinoma of the skin, ear, and lip. Implications for treatment modality selection." J Am Acad Dermatol 26(6): 976-990.

Ryther, R.C., et al. (2005). "siRNA theraputics: big potential from small RNAs." Gene Ther 12(1):5-11.

Saltz, L. B., N. J. Meropol, et al. (2004). "Phase II trial of cetuximab in patients with refractory colorectal cancer that expresses the epidermal growth factor receptor." J Clin Oncol 22(7): 1201-1208.

Sanger, F., S. Nicklen, et al. (1977). "DNA sequencing with chain-terminating inhibitors." Proc Natl Acad Sci U S A 74(12): 5463-5467.

Schallreuter, K. U. and J. M. Wood (1995). "The human epidermis." Proc Nutr Soc 54(1): 191-195.

Schneider, S. S., C. Schick, et al. (1995). "A serine proteinase inhibitor locus at 18q21.3 contains a tandem duplication of the human squamous cell carcinoma antigen gene." Proc Natl Acad Sci U S A 92(8): 3147-3151.

Scholl, F. A., P. A. Dumesic, et al. (2004). "Mek1 alters epidermal growth and differentiation." Cancer Res 64(17): 6035-6040.

Schwartz, R. A. (1997). "The actinic keratosis. A perspective and update." Dermatol Surg 23(11): 1009-1019; quiz 1020-1001.

Seftor, R. E., E. A. Seftor, et al. (1998). "maspin suppresses the invasive phenotype of human breast carcinoma." Cancer Res 58(24): 5681-5685.

Seugnet, L., et al. (1997). "Requirement for dynamin during notch signalling in drosophila neurogenesis." Dev Biol 15;192(2):585-98.

Shalon, D., S. J. Smith, et al. (1996). "A DNA microarray system for analyzing complex DNA samples using two-color fluorescent probe hybridization." Genome Res 6(7): 639-645.

Sheng, S., J. Carey, et al. (1996). "Maspin acts at the cell membrane to inhibit invasion and motility of mammary and prostatic cancer cells." Proc Natl Acad Sci U S A 93(21): 11669-11674.

Sherr, C. J. (2001). "The INK4a/ARF network in tumour suppression." Nat Rev Mol Cell Biol 2(10): 731-737.

Sluyter, R. and G. M. Halliday (2001). "Infiltration by inflammatory cells required for solar-simulated ultraviolet radiation enhancement of skin tumor growth." Cancer Immunol Immunother 50(3): 151-156.

Smith, L. M., J. Z. Sanders, et al. (1986). "Fluorescence detection in automated DNA sequence analysis." Nature 321(6071): 674-679.

Smith, M. L. and A. J. Fornace, Jr. (1997). "p53-mediated protective responses to UV irradiation." Proc Natl Acad Sci U S A 94(23): 12255-12257.

Sorrell, J. M. and A. I. Caplan (2004). "Fibroblast heterogeneity: more than skin deep." J Cell Sci 117(Pt 5): 667-675.

South, A. P. Unpublished

South, A. P. et al (2012). "The double-edged sword of notch signalling in cancer." Sem Cell Dev Biol 23(4):458-464.

Southern, E. M., U. Maskos, et al. (1992). "Analyzing and comparing nucleic acid sequences by hybridization to arrays of oligonucleotides: evaluation using experimental models." Genomics 13(4): 1008-1017.

Stetler-Stevenson, W. G., S. Aznavoorian, et al. (1993). "Tumor cell interactions with the extracellular matrix during invasion and metastasis." Annu Rev Cell Biol 9: 541-573.

Struhl, G. and Greenwald, I. (1999) "Presenilin is required for acivity and nuclear acess of notch in drosophila." Nature 8;398(6727):522-5.

Suchniak, J. M., S. Baer, et al. (1997). "High rate of malignant transformation in hyperkeratotic actinic keratoses." J Am Acad Dermatol 37(3 Pt 1): 392-394.

Sylven, B. and H. Malmgren (1957). "The histological distribution of proteinase and peptidase activity in solid tumor transplants; a histochemical study on the enzymic characteristics of the different tumor cell types." Acta Radiol Suppl(154): 1-124.

Tan, M.J., et al. (2012). "Cutaneous β-human papillomavirus E6 protiens bind mastermind-like coactivators and repree notch signalling." PNAS 109(23):E14733-E1480.

Tang, T., M. Kmet, et al. (2005). "Testisin, a glycosyl-phosphatidylinositol-linked serine protease, promotes malignant transformation in vitro and in vivo." Cancer Res 65(3): 868-878.

Taub, J. S., R. Guo, et al. (2003). "Bradykinin receptor subtype 1 expression and function in prostate cancer." Cancer Res 63(9): 2037-2041.

The Cancer Genome Atlas Research Network (2012). "Comprehensive genomic characterization of squamous cell lung cancers." Nature 489, 519-525.

Todaro, G. J. and H. Green (1963). "Quantitative studies of the growth of mouse embryo cells in culture and their development into established lines." J Cell Biol 17: 299-313.

Tolcher, A.W. et al. (2012). "Phase I study of RO4929097, a gamma secretase inhibitor of notch signalling, in patients with refractory metastatic or locally advanced solid tumours." J Clin Onco 30(19) 2348-2353.

Toogood, P. L. (2001). "Cyclin-dependent kinase inhibitors for treating cancer." Med Res Rev 21(6): 487-498.

Torrora, G. J. and B. H. Derrickson (2006), Eds. Principles of Anatomy & Physiology, John Wiley & Sons Inc.

van Hogerlinden, M., B. L. Rozell, et al. (1999). "Squamous cell carcinomas and increased apoptosis in skin with inhibited Rel/nuclear factor-kappaB signaling." Cancer Res 59(14): 3299-3303.

Vassilev, L. T., C. Tovar, et al. (2006). "Selective small-molecule inhibitor reveals critical mitotic functions of human CDK1." Proc Natl Acad Sci U S A 103(28): 10660-10665.

Veness, M. J., S. Porceddu, et al. (2007). "Cutaneous head and neck squamous cell carcinoma metastatic to parotid and cervical lymph nodes." Head Neck 29(7): 621-631.

Vogelstein, B., D. Lane, et al. (2000). "Surfing the p53 network." Nature 408(6810): 307-310.

Wall, N. R. and Y. Shi (2003). "Small RNA: can RNA interference be exploited for therapy?" Lancet 362(9393): 1401-1403.

Wang, F., J. Dai, et al. "Histone H3 Thr-3 phosphorylation by Haspin positions Aurora B at centromeres in mitosis." Science 330(6001): 231-235.

Wang, N. J., Z. Sanborn, et al. (2011). "Loss-of-function mutations in Notch receptors in cutaneous and lung squamous cell carcinoma." Proc Natl Acad Sci U S A 108(43): 17761-17766.

Wang, W. and Struhl, G., (2005). "Distinct roles for mind bomb, neutralised and epsin in mediating DSL endocytosis and signalling in drosphila." Development 132(12):2883-94.

Wassenegger, M., S. Heimes, et al. (1994). "An infectious viroid RNA replicon evolved from an in vitro-generated non-infectious viroid deletion mutant via a complementary deletion in vivo." Embo J 13(24): 6172-6177.

Watt (2011). "Integrative mRNa profiling comparing cultured primary cells with clinical samples reveals PLK1 and C20orf20 as a theraputic targets in cutaneous squamous cell carcinoma." Oncogene.

Watt, F. M. (1989). "Terminal differentiation of epidermal keratinocytes." Curr Opin Cell Biol 1(6): 1107-1115.

Weinberg, R. A. (1995). "The retinoblastoma protein and cell cycle control." Cell 81(3): 323-330.

Westhoff, B., I. N. Colaluca, et al. (2009). "Alterations of the Notch pathway in lung cancer." Proc Natl Acad Sci U S A 106(52): 22293-22298.

Wharton, K. A., K. M. Johansen, et al. (1985). "Nucleotide sequence from the neurogenic locus notch implies a gene product that shares homology with proteins containing EGF-like repeats." Cell 43(3 Pt 2): 567-581.

Wilkin, M., et al., (2004). "Regulation f notch endosomal sorting and signalling by drosophila Nedd4 family protiens." Curr Biol 29;14(24):2237-44.

Wilkin, M., et al ., (2008). "Drosophila HOPS and AP-3 complex genes are required for deltex-regulated activation of notch endosomal trafficking pathway." Dev Cell 15(5):762-72.

Wiseman, H. and B. Halliwell (1996). "Damage to DNA by reactive oxygen and nitrogen species: role in inflammatory disease and progression to cancer." Biochem J 313 (Pt 1)(Pt 1): 17-29.

Xia, W., Y. K. Lau, et al. (2000). "High tumoral maspin expression is associated with improved survival of patients with oral squamous cell carcinoma." Oncogene 19(20): 2398-2403.

Yasumatsu, R. et al. (2001). "Maspin expression in stage I and II oral tounge squamous cell carcinoma." Head and Neck 23(11):962-6.

Yamagishi, Y., T. Honda, et al. "Two histone marks establish the inner centromere and chromosome bi-orientation." Science 330(6001): 239-243.

Yeom, S. Y., H. L. Jang, et al. (2010). "Interaction of testisin with maspin and its impact on invasion and cell death resistance of cervical cancer cells." FEBS Lett 584(8): 1469-1475.

Yin, S., J. Lockett, et al. (2006). "Maspin retards cell detachment via a novel interaction with the urokinase-type plasminogen activator/urokinase-type plasminogen activator receptor system." Cancer Res 66(8): 4173-4181.

Yochem, J., K. Weston, et al. (1988). "The Caenorhabditis elegans lin-12 gene encodes a transmembrane protein with overall similarity to Drosophila Notch." Nature 335(6190): 547-550.

Yuspa, S. H. and D. L. Morgan (1981). "Mouse skin cells resistant to terminal differentiation associated with initiation of carcinogenesis." Nature 293(5827): 72-74.

Zhang, J., B. Shen, et al. (2007). "Novel strategies for inhibition of the p38 MAPK pathway." Trends Pharmacol Sci 28(6): 286-295.

Zhang, Y. and D. Reinberg (2001). "Transcription regulation by histone methylation interplay between different covalent modification of the core histone tails." Gen Dev 15:2343-2360.

Zhu, K., A. D. Hamilton, et al. (2003). "Farnesyltransferase inhibitors as anticancer agents: current status." Curr Opin Investig Drugs 4(12): 1428-1435.

Zou, Z., A. Anisowicz, et al. (1994). "Maspin, a serpin with tumor-suppressing activity in human mammary epithelial cells." Science 263(5146): 526-529.

Zucker, S., J. Cao, et al. (2000). "Critical appraisal of the use of matrix metalloproteinase inhibitors in cancer treatment." Oncogene 19(56): 6642-6650.